Innate immunity in HIV, helminth and malaria co-infections: effects on experimental TB vaccination and clinical malaria presentation

INAUGURALDISSERTATION

zur

Erlangung der Würde einer Doktorin der Philosophie

vorgelegt der

Philosophisch-Naturwissenschaftlichen Fakultät

der Universität Basel

von **Nicole Lenz**

aus Uesslingen-Buch (Thurgau)

Basel, 2016

Genehmigt von der Philosophisch-Naturwissenschaftlichen Fakultät

auf Antrag von:

Prof. Dr. Marcel Tanner

Fakultätsverantwortlicher

PD Dr. Claudia Daubenberger

Dissertationsleiterin

Prof. Dr. Ulrich Certa

Korreferent

Basel, den 21.04.2015

Prof. Dr. Jörg Schibler

Dekan

Abstract

Tuberculosis (TB), malaria and helminthiasis are a major challenge for the global public health in the 21^{st} century. The HIV-associated TB epidemic, occurrence of drug-resistant strains of *Mycobacterium tuberculosis* (*M.tb*) and the limited efficacy of the Bacille Calmette Guérin (BCG) vaccine are important obstacles of reducing TB morbidity and mortality. An estimated 1.5 million people died from TB in 2013, of these approximately one quarter were HIV positive. A new TB vaccine should be safe and efficacious in all populations, including HIV positives. In Sub-Saharan Africa, there is substantial geographical overlap of malaria tropica and soil-transmitted helminth infections and co-infections are common. Intervention strategies mostly neglect co-morbidity, although there is evidence that helminths impact on clinical malaria. The human gut microbiota has an extensive role in nutrition and host health. Gastrointestinal helminths and the gut microbiota share the same niche and close interactions are likely.

Chapter 2 documents the clinical trial testing the safety and immunogenicity of the TB vaccine H1/IC31® in HIV infected volunteers. The trial was designed as a phase II, multi-centre, double-blind, placebo-controlled trial and volunteers with a $CD4^+$ lymphocyte count above $350/mm^3$ and no evidence of active TB were included. H1/IC31® consists of a fusion protein of Ag85B and ESAT-6, both secreted, immuno-dominant proteins isolated from *M.tb* culture supernatants. Safety was assessed based on medical history, clinical examinations, and blood and urine

testing. Immunogenicity was tested using whole blood stimulation followed by intracellular cytokine staining and flow cytometry. The vaccine was safe and well tolerated in HIV infected individuals and $CD4^+$ lymphocyte counts and viral loads remained constant. H1/IC31® was observed to be immunogenic and induced specific Th1 responses with bi-functionl $CD4^+$ T cells expressing IL-2 and TNF-α and polyfunctional $CD4^+$ T cells expressing IFNγ, IL-2 and TNF-α.

The ancillary study in chapter 3 investigates the induction and maintenance of $CD4^+$ memory T cells following vaccination with H1/IC31®. Induction of vaccine specific central (T_{CM}) and effector (T_{EM}) memory $CD4^+$ T cells was detected. The magnitude was highly heterogeneous and the volunteers were grouped into non-, intermediate and high-responder based on maintenance of vaccine specific T_{CM} or T_{EM} until 6 months after initial vaccination. Amplicon based transcript quantification of peripheral whole blood using next generation sequencing was performed to identify differentially expressed genes either induced by vaccination or present at baseline. Higher expression of genes implicated in resolution of inflammation were detected in high responder three days after the first vaccination. At baseline, high expression of genes involved in antiviral innate immunity was observed in non-responders and correlated with impaired vaccine specific maintenance of T_{CM} and T_{EM}. A functional variant of TLR-8 was present in a subgroup of T_{EM} high responder, that was previously reported to result in slower disease progression in HIV infected individuals. Summarizing, HIV infected individuals with high expression levels of genes involved in antiviral innate immunity were found to have an affected long-term maintenance of H1/IC31® induced cellular memory response.

In chapter 4 co-infections of *Plasmodium falciparum* (*P. falciparum*) and soil-transmitted helminths and the effect on clinical presentation of malaria are investigated in children aged 2 months to 9 years from the coastal region of Tanzania. Opposite to Hookworm infections, children co-infected with *P. falciparum*

and *Enterobius vermicularis* (*E. vermicularis*) showed a significant reduction of clinical malaria cases. Expression of IL-6 and TNF-α by monocytes and conventional dendritic cells from peripheral blood after stimulation of toll-like receptors with known agonists was reduced in children infected with *E. vermicularis*. Transcriptome analysis of whole blood revealed lower expression of genes implicated in Th1 responses, pro-inflammation and IFN inducible genes in children with *E. vermicularis*. The gut microbiome from children with *E. vermicularis* showed a higher diversity and a function towards an anti-inflammatory enterotype. For the first time it was demonstrated, that *E. vermicularis* reduces the risk of clinical malaria by suppression of pro-inflammatory cytokine expression at the level of the systemic innate immune system.

Contents

Abstract **3**

1 Introduction **13**

1.1 Experimental vaccination outcome of the *Mycobacterium tuberculosis* vaccine H1/IC31® in HIV infected individuals 14

1.1.1 Tuberculosis epidemiology 14

1.1.2 General features of *Mycobacterium tuberculosis* 14

1.1.3 Clinical manifestations of TB 16

1.1.4 TB diagnosis 16

1.1.5 TB chemotherapy 17

1.1.6 The immune response against *Mycobacterium tuberculosis* . 18

1.1.7 Natural protective cellular immune mechanisms against *Mycobacterium tuberculosis* 21

1.1.8 Impairment of protective immunity 21

1.1.9 Tuberculosis and vaccine development 23

1.1.10 From H1/IC31®-vaccine induced innate immune responses to immunological memory 27

1.1.11 HIV infection and vaccination outcome 30

1.2 Interactions of Malaria, helminths and the microbiome 32
1.2.1 Malaria tropica 32
1.2.2 Soil-transmitted helminths 38
1.2.3 The human gastrointestinal microbiome 42
1.2.4 Interactions of *P. falciparum*, Helminths and GI microbiome 48
1.3 Aims of the thesis 52

2 Safety and Immunogenicity of H1/IC31® in HIV infected adults 55
2.1 Abstract 56
2.2 Introduction 57
2.3 Methods 58
2.3.1 Regulatory approval 58
2.3.2 Study design and sites 58
2.3.3 Randomisation and blinding 59
2.3.4 Investigational product and vaccination 59
2.3.5 Safety 60
2.3.6 IFN-γ release assay 60
2.3.7 Immunological assays 61
2.3.8 IFN-γ EliSpot assay 63
2.3.9 Statistical considerations 63
2.4 Results 64
2.4.1 Study population 64
2.4.2 Safety and reactogenicity 64
2.4.3 QuantiFERON status 69
2.4.4 Immunogenicity 70

2.4.5 Humoral response determined by Anti-Ag85B-ESAT-6 specific IgG antibody assay 74

2.5 Discussion 74

2.6 Supporting Information 80

2.7 Acknowledgments 81

3 Antiviral innate immune activation in HIV infected adults negatively affects H1/IC31® induced vaccine-specific memory CD4$^+$ T cells 83

3.1 Abstract 84

3.2 Introduction 85

3.3 Methods 87

3.3.1 Ethics statement 87

3.3.2 Participant enrolment and blood collection 87

3.3.3 Intracellular cytokine staining (ICS) and analysis by flow cytometry 88

3.3.4 Extraction of total RNA 89

3.3.5 AmpliSeq panels 90

3.3.6 Amplicon-based transcript quantification by semiconductor sequencing 90

3.3.7 Statistical analysis 91

3.4 Results 92

3.4.1 Cytokine producing memory CD4$^+$ T cell subsets 92

3.4.2 Definition of vaccine responder groups 95

3.4.3 Gene expression data 95

3.4.4 Vaccine-induced differential gene expression 97

3.4.5 Differential immune activation at baseline 99
3.4.6 Toll-like receptor 8 variant 103
3.5 Discussion 103
3.6 Acknowledgements 106

4 *Enterobius vermicularis* modifies human gut microbiome and suppresses pro-inflammatory immunity 109
4.1 Abstract 110
4.2 Introduction 110
4.3 Results 113
4.3.1 Impact of STH infection on malaria acquisition and progression to disease 113
4.3.2 Monocytes and dendritic cells in children with *E. vermicularis* and asymptomatic *P. falciparum*-malaria infection have reduced IL-6 and TNF-α production 116
4.3.3 Genes involved in Th1 and IFN signaling are lower expressed in peripheral whole blood of children that are infected with *E. vermicularis* 118
4.3.4 The gut microbiome diversity and function changes in *E. vermicularis* infected volunteers 121
4.4 Discussion 125
4.5 Funding 130
4.6 Competing interest 130
4.7 Materials and Methods 130
4.7.1 Ethics statement 130
4.7.2 Study Design 131

4.7.3 Participant recruitment and follow-up visits 132
4.7.4 Sample collection, diagnosis of Plasmodium and helminth infection 132
4.7.5 Clinical data management and statistical analysis 133
4.7.6 Blood collection for immunology assays 134
4.7.7 Toll-like receptor stimulation and whole blood culture 134
4.7.8 Intracellular cytokine staining 135
4.7.9 Data analysis of Flow Cytometry 136
4.7.10 DcRT-MLPA assay 136
4.7.11 Data analysis of dcRT-MLPA 137
4.7.12 Standardization 137
4.7.13 Amplification and sequencing of variable 3 (V3) region of 16S ribosomal RNA 138
4.7.14 Ion Torrent PGM 138

5 Conclusion and Outlook 147

5.1 Conclusion 147
5.2 Outlook 155

References 159

6 Appendix 221

6.1 MyFlowCyt Reporting standard for chapter 3 221
6.1.1 Experiment Overview 221
6.1.2 Flow Sample/Specimen Description 223
6.1.3 Instrument Details 227

6.1.4 Data Analysis Details 227

6.2 MyFlowCyt Reporting standard for chapter 4 231

6.2.1 Experiment Overview 231

6.2.2 Flow Sample/Specimen Description 233

6.2.3 Instrument Details 235

6.2.4 Data Analysis Details 237

Acknowledgments **241**

Curriculum vitae **244**

Chapter 1

Introduction

1.1 Experimental vaccination outcome of the *Mycobacterium tuberculosis* vaccine H1/IC31® in HIV infected individuals

1.1.1 Tuberculosis epidemiology

Approximately one third of the world's population is infected with *Mycobacterium tuberculosis* (*M.tb*), with new infections occurring at a rate of one per second. Tuberculosis (TB) is a major challenge to the global public health in the 21^{st} century. In 2013, there were an estimated 9 million people that developed active disease with 1.5 million deaths, of whom 360'000 where human immunodeficiency virus (HIV) positive. Compared to 2000, an estimated 37 million lives were saved during the following thirteen years, mainly accountable to effective diagnosis and treatment. The proportion of new cases of multi-drug resistant TB of 3.5% remained stable compared to recent years. One quarter of the 9 million new TB cases occurred in the African Region, where also the highest rates of cases and deaths relative to population were reported. An overview of the worldwide TB incidence rates is given in Figure 1.1.

1.1.2 General features of *Mycobacterium tuberculosis*

M.tb is a non-motile pathogen exclusively infecting humans without other known reservoirs. It is a rod-shaped bacterium that is a member of the family *Mycobacteriaceae* within the order *Actinomycetales*. *M.tb* is a weakly gram positive obligate aerobe. It is a slow-growing intracellular bacterium that is able to survive inside macrophages. *M.tb* is classified as 'acid-fast', because it is able to retain certain dyes and stains only after being treated with an acidic solution. The underlying

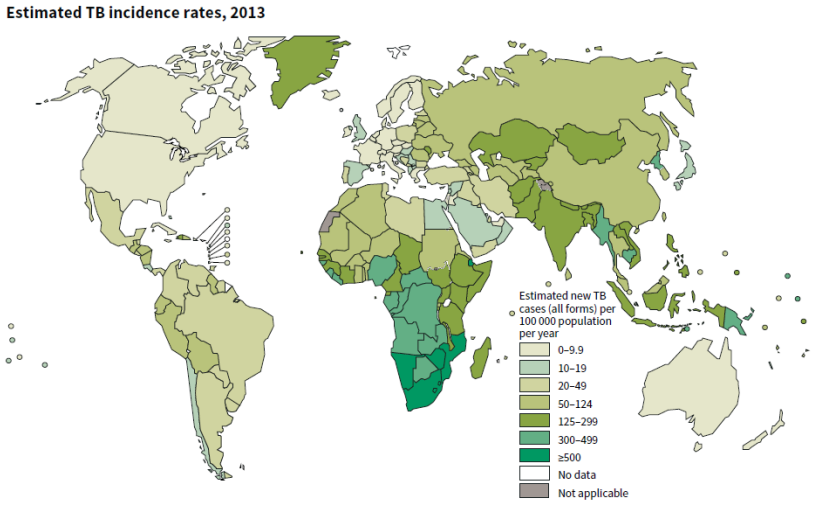

Figure 1.1: Estimated TB incidence rates in 2013 [1].

reason is the unusual composition of the bacterial cell wall, which mainly consists of hydrophobic mycolic acids. This component is uniquely found in the mycobacterial cell wall and makes up 50% of its dry weight. The mycolic acids are responsible for the slow growth of the bacterium, since entry of nutrients is impaired. It is also the cause of partial resistance to degradation by enzymes of the lysosomes [2]. Figure 1.2 comprises an overview of the mycobacterial cell wall components. Next to the high abundance of mycolic acids at the external part of the cell wall, external layers mostly consist of arabinogalactan, phosphatidyl-myo-inositol mannosides and peptidoglycans. Other components of the external part consist of mannose-containing biomolecules including mannose-capped lipoarabinomannan, the related lipomannan and mannoglycoproteins. The outer capsule of the bacterium is formed by mannan and arabinomannan [3, 4].

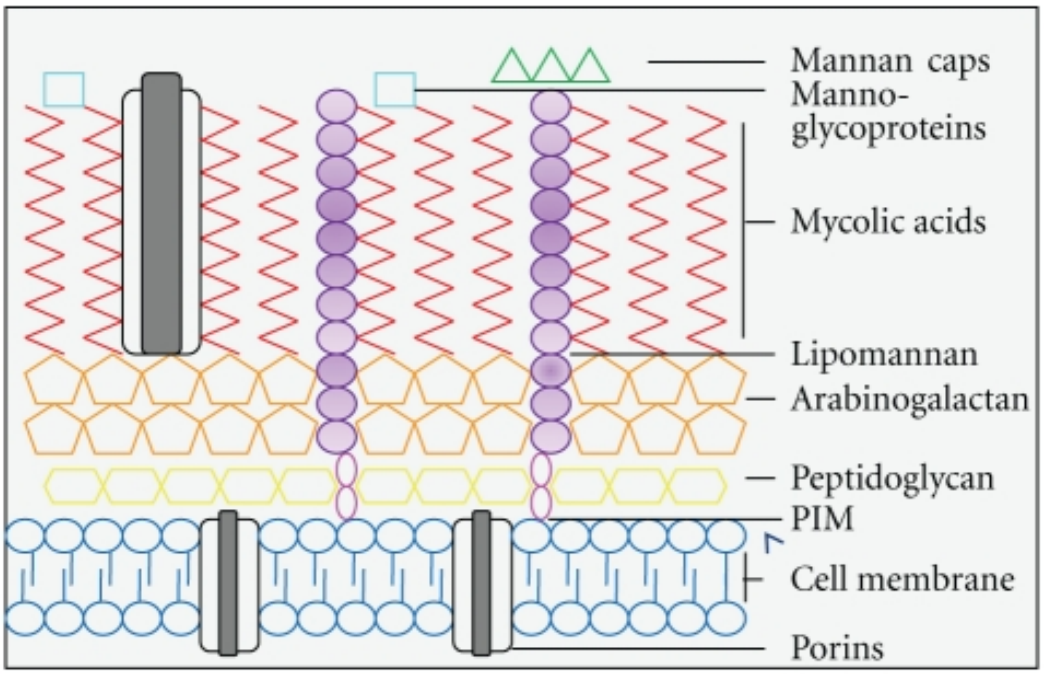

Figure 1.2: Structure and components of the *Mycobacterium tuberculosis* cell wall [4]. PIM = phosphatidyl-myo-inositol mannosides

1.1.3 Clinical manifestations of TB

The most common clinical manifestation of TB is pulmonary disease with chronic, productive cough, low-grade fever, night sweats, malaise, and weight loss. In rare cases, *M.tb* may also spread from the lungs, causing extrapulmonary manifestations including lymphadenitis, kidney, bone, or joint involvement, meningitis or disseminated (miliary) disease. Only 3-4% of infected people develop active disease upon initial infection, and 5-10% within 1 year [5].

1.1.4 TB diagnosis

One of the most common TB diagnostic tools is microscopic examination of sputum smear samples stained with Ziehl-Neelsen stain. Although inexpensive, this test has certain disadvantages, as other environmental mycobacteria are also acid

fast and thus are stained as well. Furthermore, sputum samples from patients with active pulmonary TB disease might not contain bacteria, particularly in individuals with HIV-TB co-infections [6]. Another method to diagnose active TB is sputum culture on specific medium such as Löwenstein-Jensen. The major disadvantage of the culture method is the 2 months time period until positivity can be determined. By making use of the polymerase chain reaction (PCR), recent advances have been made in developing rapid diagnostic tools, such as the GeneXpert® MTB/RIF (Cepheid, Sunnyvale USA). The GeneXpert® MTB/RIF tool in addition allows for screening of rifampicin resistance and is therefore recommended to use for monitoring multi-drug resistant TB cases [1,6]. Currently there are two tools available to test for latent (inactive) TB. The tuberculin skin test measures T cell activation following intracutaneous injection of PPD, a purified protein derivative of tuberculin. The test is read within 2-3 days and positivity is considered if the diameter of a resulting lesion is 10 mm or greater. This test has poor specificity as components of PPD are also expressed by environmental bacterial and - most importantly - also by the Bacille Calmette-Guérin (BCG), the only available vaccine against TB. Interferon-γ release assays, such as the QuantiFERON-TB Gold In-Tube assay (QFT), prove more sensitive to *M.tb* and can be used in BCG vaccinated individuals. It measures released interferon (IFN)-γ from T cells *ex vivo* following stimulation with ESAT-6 and CFP10, two *M.tb* specific antigens [7].

1.1.5 TB chemotherapy

TB treatment is based on a cocktail of antibiotics that are effective primarily against *Mycobacteria*. Therapy is usually concluded within 6-9 months. The most commonly used antibiotics (first-line) comprise rifampicin, isoniazid, pyrazinamide and ethambutol or streptomycin. Multidrug-resistant TB is defined as resistant to

more than one first-line drug and at least to isoniazid and rifampicin. In these cases adjusted treatment regimens are pursued with the course of therapy lasting up to 24 months [8]. Latent TB is cured with low doses of either isoniazid or rifampicin during a course of 3-9 months [9].

1.1.6 The immune response against *Mycobacterium tuberculosis*

An infection with *M.tb* begins with inhaling aerosols containing bacteria. Innate immune cells recognize *M.tb* specific pathogen associated molecular patterns (PAMPs) via pattern recognition receptors (PRRs). Of these, toll-like receptor (TLR) -2 located on the surface of the host cell has the largest number of identified *M.tb* encoded agonists. It senses *M.tb*-specific lipoproteins, phosphatidylinositol mannans and lipomannan [10]. Endosomal TLR-9 recognizes mycobacterial DNA [11]. Additional recognition is mediated by members of the C-type lectins, including DC-SIGN, dectin-1 and mannose receptos [12]. Cytosolic nucleotide-binding oligomerization domain protein (NOD) -2 and NOD-, leucin rich repeat (LRR)- and pyrin domain containing (NLRP) -3 ligate to the peptidoglycan subunit N-glycolyl muramyl dipeptide and one or more ESX1-secreted substrates (such as early secretory antigenic target (ESAT) -6) [13, 14]. ESX1 is a type VII secretion system, which promotes the necrotic death of infected cells [15]. This process provides a niche for bacterial spread, since necrotic cell death recruits new macrophages. Once *M.tb* are recognized, they are engulfed by alveolar macrophages. Inside the phagosome, mycobacteria evade phagocytosis via inhibition of ligation of the phagosome to the lysosome (which contains digestive enzymes) [16]. This mechanism is thought to be part of the major evasion strategy of *M.tb* - the delay of the onset of adaptive immunity. This process represents a critical bottleneck for disease control [17].

M.tb delays the transport to the draining lymphnode. Their primary target, alveolar macrophages, are not migratory cells and via inhibition of cell death and PRR-pathways, *M.tb* orchestrates its focal retention in this cell population. Most likely this restricts pro-inflammatory processes and ensures intracellular bacterial replication [18, 19]. About 8 days post infection, *M.tb* eventually are taken up by newly recruited phagocytes, such as neutrophils, inflammatory macrophages and dendritic cells (DCs). Infected DC home to the draining lymphnode, where via transfer of bacterial antigen to uninfected DC, effector T cell priming takes place [20]. At this stage, a highly suppressive population of *M.tb* specific Foxp3$^+$ positive regulatory T cells (Tregs) expand in parallel to effector T cells, further delaying priming of T cells (15-20 days post infection) [21]. By the time T cells arrive at the site of infection, they are exposed to many layers of immune regulation that avoids immunopathogenesis, but restricts the T cell's ability to control and kill *M.tb*. Multicellular granulomas are formed, that contain a high bacterial burden. They consist of a necrotic core with extracellular bacteria surrounded by a layer of infected phagocytes and an outer layer of T cells. The cytokine milieu is mainly anti-inflammatory including IL-10 and transforming growth factor (TGF)-β and immunosuppressive cells and lipids, therefore suppressing the effector T cell function [22,23]. Moreover, the high bacterial burden could lead to permanent antigenic stimulation and restrict the protective capacity of T cells [24].

At this stage, the bacteria are not eradicated but contained, also referred to as the latent phase of the infection. Upon specific alterations of the immune response, the clinical phase begins with the development of necrotic areas that trigger the granuloma to become caseous. Consequently, the granuloma rupture and release high numbers of living bacteria. They cause excessive damage to the lung and also spread to other organs [25]. At this stage exhaled droplets are infectious and able to remain in the atmosphere for several hours, while the minimum dose required

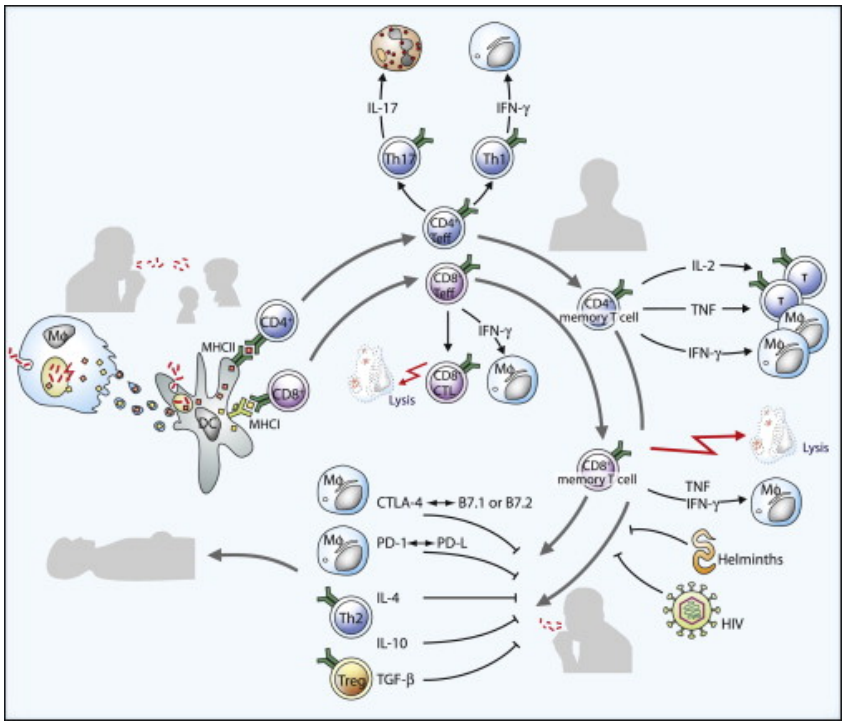

Figure 1.3: The protective and pathologic basis of the cellular host response during TB infection [25].

for another infection is estimated to be 1 bacterium [26].

The immune response against TB of animal models and humans are only partially similar. The assessment of the immune response against TB in humans has proven difficult, since there is no access to the focal immune response in the lungs and conclusions are made based on the analysis of human peripheral blood or urine [26]. Most adult TB cases result from a reactivation of pre-existing, chronic infections. Upon inhalation of infectious *M.tb*, the immune system is able to contain the bacteria. Natural protection resulting in latent infection is described in section 1.1.7 and Figure 1.3. The reactivation of bacteria contained in granuloma is coincident with a compromised immune system. Associated diseases like HIV, helminthiasis and diabetes mellitus (DM) are important drivers of the development of active TB (see section 1.1.8). Other factors are stress, old age, poor nutrition, pollution and tobacco smoke [27, 28].

1.1.7 Natural protective cellular immune mechanisms against *Mycobacterium tuberculosis*

The exact mechanisms underlying protective immunity against TB in humans has yet to be fully elucidated. Cellular immunity including $CD4^+$ and $CD8^+$ T cells is thought to be important for effective prevention of active disease following *M.tb* infection [29]. $CD8^+$ T cells can contribute to control *M.tb* by perforin-mediated cytolysis of infected macrophages or direct killing of the bacteria [25,30]. Another way to control infections in humans relies on activation of macrophages to eliminate the intracellular bacteria [26]. These T cell effector molecules are known to play central roles in *M.tb* control and activation of macrophages, including the T helper 1 (Th1) cytokines interferon-gamma (IFN-γ), tumor necrosis factor-α (TNF-α) and interleukin-2 (IL-2) [31–34]. IL-17 expressing Th17 cells contribute to control by facilitating recruitment of Th1 cells into the lung, a process important for accelerating the response and hence partially overcoming the delay of adaptive immunity [35].

Opposing to this, recent evidence from mouse studies suggests, that less differentiated $CD4^+$ T cells may provide a better correlate of protective immunity than terminally-differentiated Th1 cells. Less differentiated T-bet^{int} and $KLRG^-$ $CD4^+$ T cells were associated with less IFN-γ production but higher proliferative capacity and longer lived as compared to terminally-differentiated Th1 cells. Furthermore, the former $CD4^+$ T cells can migrate better to the lung parenchyma and adoptive transfer and vaccine studies also suggest they confer greater protection [36–38].

1.1.8 Impairment of protective immunity

As discussed in section 1.1.6 appearance of the cytokines IL-10 and TGF-β and the Tregs are indicators of an impaired natural protection. A skew towards a type

2 response by T helper 2 (Th2) cells secreting IL-4, -5, and -13 counter regulates protective Th1 cells. The surface molecules CTLA-4 and PD-1 are indicators of an exhaustion of T cells (see figure 1.3) [25,39]. Certain diseases have the ability to induce afore-stated alterations in the human immune system and during co-infection with *M.tb* could possibly lead to reactivation and the manifestation of clinical TB.

Impairment of protective immunity by HIV infection

Individuals harboring an HIV co-infection have a greater than ten fold risk of TB infection and subsequent progression to TB disease [40–42]. Largely due to the HIV epidemic, Sub-Saharan Africa has experienced massive increases in TB prevalence and incidence rates [43]. Diagnosis of active TB is more difficult in HIV infected individuals. The HIV associated immunosuppression makes it more difficult to diagnose active TB due to a higher likelihood of atypical and extra-pulmonary presentation and poorer performance of standard diagnostic tools [44]. TB diagnosis in the HIV infected is delayed and therefore causing increased morbidity and mortality with associated case fatality rates of up to 40%. The risk of TB disease in HIV co-infected individuals correlates with the decline of $CD4^+$ T cell counts. In South African groups of anti-retroviral therapy-naïve patients with $CD4^+$ cell counts of less than 200 cells/mm^3, between 200 - 350 cells/mm^3 and greater than 350 cells/mm^3, incidence rates of TB were at 17.5, 12.0 and 3.6 cases per 100 person-years, respectively [45].

Impairment of protective immunity by intestinal Helminthiasis

The immuno-modulatory effects during a chronic intestinal helminth infection are discussed in detail in section 1.2.2. Briefly, a chronic infection with helminths is

coincident with a skew towards a type 2 (Th2) immune response, induction of tissue healing processes and anti-inflammation. Evidence suggests, that helminth induced intestinal responses can affect the outcome of concurrent infections at different sites, including the lungs [46]. This could lead to reactivation of latent TB [47].

Impairment of protective immunity by Diabetes mellitus

Diabetes mellitus (DM) has been reported to increase the risk of active TB up to 3-fold [48]. Glucose control is regarded to be the unifying factor from epidemiological, clinical and immunological studies on prevention of TB and DM associated complications [49]. Little is known about the exact mechanism of how DM promotes TB reactivation. There is evidence from mouse studies, that the onset of adaptive immune responses against *M.tb* is further delayed in DM cases [50].

1.1.9 Tuberculosis and vaccine development

Overview

Currently, the only approved vaccine against TB is BCG. It was empirically developed and lost its pathogenicity in humans via serial passages in vitro of *Mycobacterium bovis*. Since 1974, BCG vaccination has been part of the Expanded Programme on Immunization, therefore reaching more than 80% coverage in infants. It is used in countries with endemic TB, since it protects children against severe forms of disease, like TB meningitis or disseminated infection. With the emergence of the HIV epidemic, recommendations for the use of BCG in neonates born to HIV-infected mothers has been changed [51]. WHO recommends that BCG should not be given to HIV-exposed infants at birth, only if the infant is confirmed to be HIV-negative. Reasons being that severely compromised infants are at high

risk of developing BCG disease, both in the presence and absence of anti-retroviral treatment [52, 53].

BCG fails to protect against the most prevalent disease form of today, adult pulmonary TB. Furthermore, variable efficacy of BCG vaccination has been reported. Underlying reasons could be that different strains of BCG are used for clinical trials, there are variations among clinical *M. tuberculosis* strains and differences in human populations. Fundamental knowledge about the BCG vaccine like the nature of BCG attenuation is lacking [54]. Vaccination with BCG could cause a false-positive reaction to the diagnostic tuberculin skin test [55].

Hence, new vaccination strategies against TB require induction of a more efficient immunity than that achieved by BCG. New vaccines should ideally feature a low variance concerning the vaccine and its efficacy and should be safe in all populations. Mathematical modeling has revealed that a combination of novel vaccines, drug regimen and diagnostics could reduce the TB incidence by 71% [56].

An overview of vaccine candidate pipeline is given in Figure 1.4 [57]. These different aims are pursued by TB vaccines under development: prevent infection, prevent primary disease, prevent progression to latent infection or prevent reactivation of latent infection or to shorten the course and improve the response to chemotherapy. All currently pursued vaccination strategies for TB involve vaccination with a live vaccine, either as replacement for BCG or as prime for a subunit boost. The 'prime-boost' strategy could include administration of BCG or a new recombinant live replacement vaccine as the 'prime', followed by a 'booster' inoculation with a different vaccine [58].

Protection from most vaccine preventable infectious diseases is conveyed through attaining sterilizing immunity either from natural exposure to the pathogen or by vaccine induced neutralizing antibody production. Sterilizing immunity is not reached upon exposure to *M.tb* and there is a lack of a validated correlate of pro-

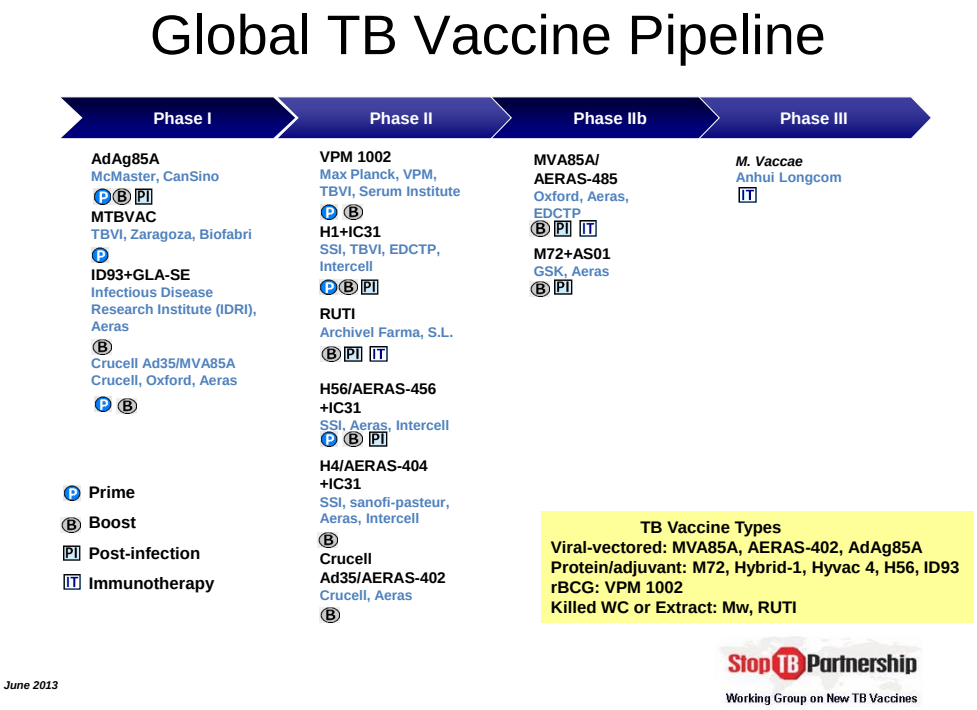

Figure 1.4: Global TB Vaccine Pipeline updated in June 2013 [57].

tection of a TB vaccine. This complicates selection of TB vaccine candidates for progression to phase IIb/III efficacy trials [58]. The most clinically advanced candidate is MVA85A, which consists of a recombinant strain of modified vaccinia virus Ankara expressing the conserved *M.tb* antigen 85A. It is designed as a heterologous boost to BCG vaccination. Human phase I/IIa revealed that the vaccine was safe and immunogenic in adults and induced vaccine-specific Th1 and Th17 responses [59, 60]. The large scale phase IIb trial included 2795 BCG vaccinated infants and follow-up was concluded after 3 years. No detectable improvement of protection against TB was observed, although infants boosted with MVA85A exhibited 1-2 logs greater *M.tb*-specific Th1 and Th17 cells in their blood than those immunized with BCG alone [61].

Summarizing, finding an efficacious TB vaccine that is protective in all populations is challenging. Profound information about (innate) immune mechanisms leading

to improved vaccine immunogenicity and efficacy are of great value.

The Hybrid-1 /IC31® subunit vaccine

The H1 subunit vaccine is composed of the fusion of Ag85B and ESAT-6 called Hybrid-1 (H1) combined with the IC31® adjuvant. Ag85B and ESAT-6 are both secreted, immuno-dominant proteins isolated from *M.tb* culture supernatants. IC31® is a two-component adjuvant system developed by Intercell AG. It is composed of the cationic polyaminoacid KLK and the oligo-deoxynucleotide ODN1a in specific molar ratios of 25:1 KLK to ODN1a. KLK is a cationic peptide composed of the amino acids Lysine (K) and Leucine (L). It exerts the potent role of enabling simultaneous uptake of H1 and ODN1a in antigen presenting cells. Furthermore it provides a platform for hyper-efficient toll-like receptor (TLR) -9 ligand recognition of ODN1a. ODN1a is a single-stranded oligo-deoxynucleotide based on alternating sequences of the nucleic acids inosine and cytidine [62, 63].
The IC31® adjuvant as well as the final vaccine are manufactured by the Statens Serum Institute, Denmark.

Clinical experience with H1/IC31® subunit vaccine

THYB-01 was the first phase I trial conducted at Leiden University Medical Centre (LUMC). 36 mycobacteria-naïve male volunteers were recruited, who received at day 0 and 56 the following dosage: group 1: 50μg Ag, group 2: 50μg Ag + 100nmol KLK + 4nmol ODN1a and group 3: 50μg Ag + 500nmol KLK + 20nmol ODN1a). No local or systemic adverse effects besides transient soreness at the injection site were reported, but strong antigen-specific T-cell responses against H1 and both the Ag85B and the ESAT-6 components was measured. These strong responses were maintained during the 2.5 years of follow-up, indicating the induction of a

substantial memory response in the vaccine recipients [64].

The following THYB-02 study used the same protocol in 20 tuberculin test positive volunteers at LUMC (half BCG vaccinated, half with prior *M.tb* infection). Again the vaccine was safe with only one possible transient vaccine related adverse event recorded (mild fever lasting one day) [65].

THYB-03 was conducted in Ethiopia and was carried out with the Armauer Hansen Research Institute (AHRI) as a single-center, open, phase 1 trial including 4 groups of 12 volunteers: 2 groups of 12 tuberculin skin test-negative volunteers, one group with 12 BCG vaccinated volunteers and one group with 12 volunteers who have (had) latent TB infection at least 2 years previously, using the same schedule followed in THYB-02. Again, the vaccine appeared to be safe and well tolerated (data unpublished).

1.1.10 From H1/IC31®-vaccine induced innate immune responses to immunological memory

Due to low inherent immunogenicity, subunit vaccines rely on adjuvants to induce immunity [66]. The adjuvant's role is to enhance the magnitude and modulate the quality, breadth [67], [68] and persistence of the initiated immune response [69].

One of the most successful vaccines ever developed is the yellow fever vaccine YF-17D [70]. The basis of its immunogenicity is activation of DCs via TLR-2,-7,-8,-9 to stimulate proinflammatory cytokines [71], which in turn induces genes that regulate virus innate sensing and type I IFN production [72]. Therefore, TLR ligands have great potential as vaccine adjuvants [66]. The ODN1a component of the IC31® adjuvant has the ability to stimulate endosomal TLR-9 on conventional dendritic cells (cDC) and monocytes inducing a MyD88-NF-κB dependent signaling cascade [73]. This leads to secretion of pro-inflammatory cytokines including

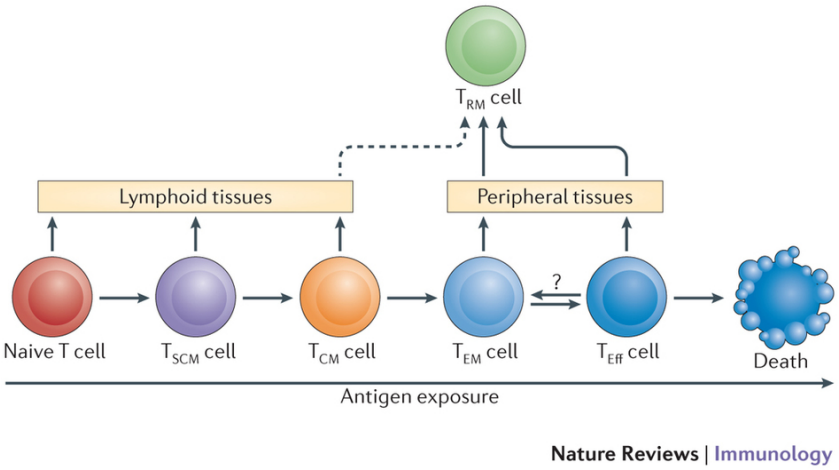

Figure 1.5: A model for the differentiation hierarchy of human memory T cells [77]. The progressive differentiation of circulating T_{SCM}, T_{CM} and T_{EM} starting from naive T cells is shown relative to the extent of antigen exposure. T_{EFF} are terminally differentiated cells, that die upon increased antigen exposure. T_{RM} reside in peripheral tissues and may rise from T_{EFF} or T_{EM}. Rise from T_{CM} could also be possible. Stem cell memory T cells = T_{SCM}, central memory T cells = T_{CM}, effector memory T cells = T_{EM}, effector T cells = T_{EFF}, resident memory T cells = T_{RM}

IL-12. Additionally to the MyD88-NF-κB dependent signaling, plasmacytoid dendritic cells (pDC) have the unique ability to couple TLR-7 and TLR-9 signaling in a MyD88-IRF7 dependent way. This yields in production of abundant quantities of type I IFN [74, 75]. Activated DCs mature and home to draining lymph nodes, where they present the loaded antigen (H1) to naive $CD4^+$ T cells. This together with co-stimulatory and cytokine signals gives rise to effector T cells. Effector T cells proliferate and polarize into distinct helper T cell subsets, a process depending on the cytokine milieu and thus which TLR pathway was initially activated. TLR-9 signaling induces DC to secrete type I IFN and IL-12, both known as Th1 polarizing cytokines [76].

Mouse studies suggest that the proliferative expansion of effector T cells gives rise to a progeny with effector and memory fates, a process ensuring immediate together with long-term protection [78]. The exact mechanisms of induction and

maintenance of memory $CD4^+$ T cell responses in humans is still unresolved [77]. It is known, that the memory T cells are heterogeneous and comprise several subsets with different functional capacities. The first identified memory subsets in humans were the central memory (T_{CM}) and the effector memory T cells (T_{EM}). They are distinguished by expression of the lymph node homing CC chemokine-receptor7 (CCR7), which is also present on naïve T cells, and expression of CD45-RA, which is present on naïve but not memory T cells. T_{CM} are $CCR7^+$ and $CD45\text{-}RA^-$ and therefore traffick to secondary lymphoid tissues. T_{EM} are $CCR7^-$ and $CD45\text{-}RA^-$ and migrate to multiple peripheral tissue sites [79]. The stem cell memory T cells (T_{SCM}) were later identified as another circulationg memory subset with a high proliferative capacity. T_{SCM} are selfrenewing and 'multipotent', since they can further differentiate into other T cell subsets, including T_{CM} and T_{EM} (thus stem cell like). They resemble naïve T cells, in that they express both CD45-RA and CCR7 [80]. The functional capacities of these three subsets differ as follows: T_{CM} are more proliferative than T_{EM}. T_{EM} have the highest proportion of IFN-γ and TNF-α and the lowest proportion of IL-2 producing cells. T_{CM} and T_{SCM} have the highest proportion of IL-2 expressing cells, while IFN-γ and TNF-α expression by T_{CM} is between T_{SCM} (lowest) and T_{EM} (highest) [77]. The tissue resident memory T cells (T_{RM}) comprise a further non-circulating subset, whose hallmark is rapid *in situ* protective responses [81]. They exert different functions depending on their location. T_{RM} from bone marrow, lungs or intestines are polyfunctional and produce pro-inflammatory cytokines [81–83]. Expression of IL-17 for instance is produced by a subset of T_{RM} on mucosal sites [83]. A clear differentiation hierarchy of which subset is the precursor of another based on signal strength and/or extent of activation (antigen exposure) does not exist, as different studies report contradicting models. One of these models is represented in figure 1.5 [77].

In summary, due to the lack of knowledge on the induction and maintenance of

memory T cells, information about immune mechanisms that correlate with vaccine induced memory T cell responses are highly warranted.

1.1.11 HIV infection and vaccination outcome

Administration of vaccines to HIV infected individuals is challenging. Vaccination has proved pivotal for survival [84], but vaccine immunogenicity and memory maintenance are problematic, since they are negatively affected upon manifestation of progressed HIV disease [85]. Vaccination could worsen the course of the HIV infection, since activation of $CD4^+$ T cells could result in reactivation and replication of the HI-virus [86].

The most obvious reason for reduced vaccine immunogenicity in the HIV infected is the reduced number of $CD4^+$ T cells [87].

The innate immune system senses the HI-virus by recognition of viral nucleic acids and the following PRRs are known to bind single stranded viral RNA: Endosomal TLR-7 and -8 and cytosolic RIG-1 like receptor. Signaling through these PRR results in secretion of pro-inflammatory cytokines and type I IFNs [88]. HIV progressors display a type I IFN chronic exposure signature that is absent in elite controllers of HIV infection [89,90]. HIV induces a semi-mature phenotype on pDC, that might be related to prolonged type I IFN secretion upon chronic manifestation of the infection [91]. The secretion of type I IFNs is delayed and sustained up to 48h by the HI-virus when compared to other TLR-7 agonists such as imiquimod [91]. Moreover, pDCs from viraemic HIV patients are exhausted due to hyperreaction and they are refractory to in vitro stimulation with TLR-7 or TLR-9 agonists [92]. Taken together, another reason for poor vaccine immunogenicity in HIV infected individuals could be, that a chronically activated innate immune system poorly responds to activation by vaccination. Stelekati *et al.* demonstrated in a mouse model,

that chronic bystander immune activation by lymphocytic choriomeningitis virus infection impaired the effector to memory differentiation of $CD8^+$ T cells specific to *Listeria monocytogenes*-OVA. Chronic administration polyIC, a TLR-3 agonist and potent inducer of type I IFN, resulted in the same impairment of transitioning to memory T cells [93]. Since vaccination with H1/IC31® potentially results in a Th1 response induced by pro-inflammatory cytokines such as type I IFN, vaccine immunogenicity could be problematic in HIV infected volunteers. Adding to the complication, the ODN1a component of the vaccine and HIV signal through the same pathway downstream of TLR-7 and -9.

1.2 Interactions of Malaria, helminths and the microbiome

1.2.1 Malaria tropica

Malaria epidemiology

At present, malaria is considered endemic in a total of 104 countries and territories with an estimated 3.4 billion individuals at risk of malaria. In 2012, WHO estimates that approximately 207 million cases of malaria occurred globally with about 627'000 deaths. Africa accounted for most cases (80%) and deaths (70%), which mainly affected children under 5 years of age (77% of all deaths). Due to effective control strategies between 2000 and 2012, the malaria mortality rates reduced by ∼42% in all age groups and by ∼48% in children under 5 years of age.
Five species belonging to the genus *Plasmodium* cause malaria in humans: *Plasmodium falciparum* (*P. falciparum*), *P. vivax*, *P. ovale*, *P. malariae* and *P. knowlesi*. Of these, *P. falciparum* causes the most deadly manifestation of disease called Malaria tropica, which predominates in Africa [94].

Malaria life cycle and clinical manifestations

Malaria is a vector borne disease. During the life cycle (Figure 1.6), *Plasmodia* get transmitted through infected female anopheline mosquitoes. By biting a human for blood meal, the parasites get injected into the subcutaneous tissue in the form of sporozoites, that invade the blood and migrate to the liver infecting hepatocytes. The sporozoites develop further into tens of thousands of merozoites, that are each capable of infecting red blood cells (RBC). This coincides with the beginning of the asexual intraerythrocytic developmental cycle (IDC) and the beginning of clin-

ical disease [95]. The IDC can be divided into four major stages: merozoite, ring, trophozoite and schizont. The merozoite is also referred to as the invasive stage of the parasite. By leaving one RBC and entering the next, it is briefly exposed to antibodies of the host. After invasion, the parasite flattens into the ring shaped form and starts feeding on haemoglobin converting it into hemozoin crystal accumulations. The trophozoite stage is generally characterised by rearranging the host cell. It exports various parasite proteins into the RBC cytoplasm and surface. The next stage, the schizont, is characterised by repetitive nuclear divisions. Each schizont produces about 16 to 20 nuclei. When the schizonts reach the 16 to 20 nuclei stage they burst and release fresh merozoites to find and exploit new RBCs [96]. Uniquely to *P. falciparum*, only ring forms are found in peripheral blood. The RBCs infected with later stages express knob-like structures on their surface, that adhere to the endothelium and placenta. Because of this sequestration, the parasites avoid rapid clearance in the spleen [95]. Alternately to the IDC, a small proportion of the parasites undergo sexual differentiation. The resulting gametocytes are essential for transmission to the *Anopheles* vector [97].

The burst of the schizonts coincides with the release of 'malaria toxins', which are thought to be responsible for many of the symptoms and signs of the disease [98]. A deleterious activation of innate immune cells with *Plasmodium*-derived components (discussed in detail in section 1.2.1) causes the development of flu-like symptoms and fever in non-immune individuals. If left untreated, a systemic inflammation develops that leads to severe forms of the disease, which could become lethal in a proportion of people. The release of pro-inflammatory cytokines, sequestration of infected RBC to capillaries and venules and the rupture and removal of parasitized RBCs are associated with pathological events during infection. Systemic inflammation, anaemia, metabolic acidosis and cerebral and placental malaria are the consequences [99–101].

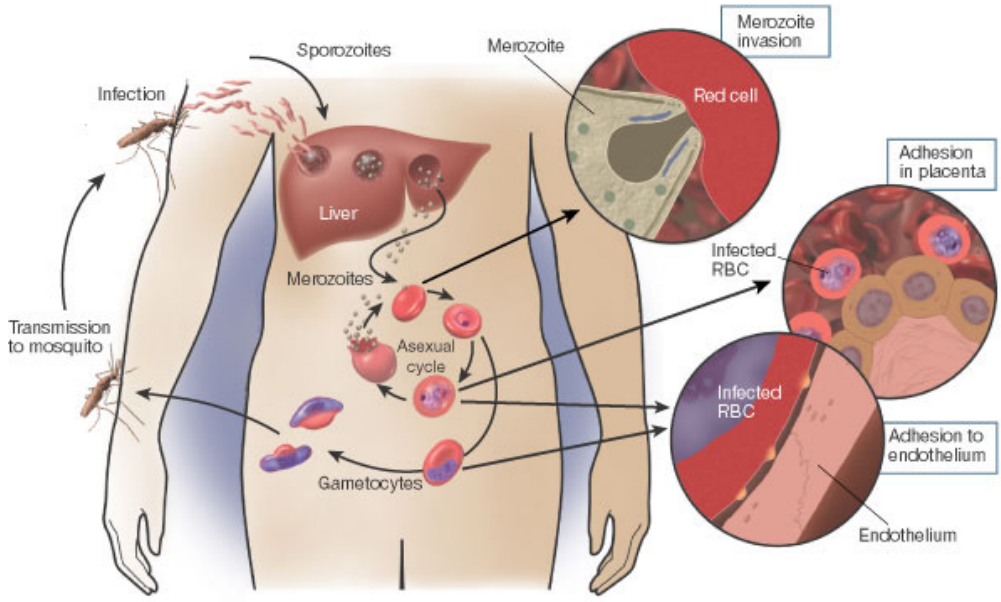

Figure 1.6: The life cycle of *Plasmodium falciparum* in the intermediate human host [95].

Malaria diagnosis, treatment and control strategies

WHO-recommended diagnostic tools for malaria detection are microscopic examination of peripheral blood or the use rapid diagnostic tests (RDTs) in patients with suspected malaria prior to treatment [94]. Malaria RDTs detect *Plasmodium*-specific antigens (*P. falciparum*-specific histidine-rich protein 2, aldolase or lactate dehydrogenase) in peripheral blood [94]. The two tools have limited sensitivity due to several factors: i) due to synchronized sequestration, the examined blood droplet might not contain parasites at the time of examination ii) adults or older children, that have a certain immunity to the parasite due to repeated exposure, might have sub-microscopic parasite densities. Most importantly, the latter individuals still transmit parasites to the vector. In these cases, PCR based technologies to detect malaria parasites prove more sensitive [102].

Currently, the standard care for uncomplicated malaria tropica consists of artemisin based combination therapy. Artemisinin monotherapy is no longer recommended by WHO, as these cause emergence and spread of resistance. Intravenous arte-

sunate or quinine are used for severe malaria cases [94, 103].

The following three control strategies are implemented to reduce malaria morbidity and mortality. i) Exposure prophylaxis with usage of insecticide treated bed nets or indoor residual spraying ii) preventive chemotherapy in infants and pregnant women (IPTp and IPTi) and iii) treatment with artemisin based combination chemotherapy. Two main obstacles regarding malaria control are the emergence of drug resistance to anti-malarials and insecticides and the lack of an effective vaccine. The most advanced malaria vaccine RTS,S/AS01 showed 50.4% efficacy in children aged 5 to 17 months [104], and 30.1% efficacy in infants aged 6 to 12 weeks [105]. A new promising vaccine candidate consisting of attenuated, aseptic, purified, cryopreserved *P. falciparum* sporozoites (PfSPZs) showed excellent dose-dependent protection from controlled human malaria infection in malaria naïve volunteers [106].

The immune response against *P. falciparum*

Figure 1.7 summarizes innate and adaptive (acquired) immune mechanisms during an infection with *P. falciparum*. As mentioned above, the innate immune system recognizes pathogens by sensing conserved PAMPs via PRRs. PRRs important during malaria infections consist of TLR located at the cell surface or at the membrane of endosomes [107] and the cytosolic RIG-I-like receptors (RLRs) [108] and NOD-like receptors (NLRs) [109]. Triggering of PRRs results in activation of multiple downstream pathways and finally parasite clearance, whereas excessive activation can lead to deleterious systemic inflammation and disease. Following PAMPs of *P. falciparum* have been identified: plasmodial RNA [110], haemozoin, plasmodial DNA [111] and glycosylphosphatidylinositol anchors (GPIs) [112].

Sporozoite RNA is sensed by the RIG-I like receptor MDA5 (Melanoma Differ-

entiation Associated protein 5), which leads to expression of type I IFNs in hepatocytes [110]. Blood-stage plasmodial RNA is also sensed by TLR-7, a process mediating rapid response to early infection by induction of pro-inflammatory type I IFN, IFN-γ and IL-12 [113].

Hemozoin is strongly adsorptive and can be bound to proteins, lipids and nucleic acids of host or pathogen origin [111, 114]. Hemozoin bound to plasmodial DNA can activate endosomal TLR-9, which yields in production of pro-inflammatory cytokines by monocytes and DCs [111]. Sensing of the DNA-hemozoin complex by NLRP-3 and -12 and AIM2 (Absent In Melanoma) causes assembly of inflammasomes and thus secretion of pro-inflammatory IL-1β.

GPIs anchor most surface proteins to the plasmodial plasma membrane. They bind to TLR-1 and -2 heterodimers, TLR-2 and -6 heterodimers and TLR-4 homodimer. This signaling induces monocytes and DC to release pro-inflammatory mediators (TNF-α and nitric oxide) and increases the expression of adhesion molecules on endothelial cells [112, 115].

DCs form the bridge between innate and adaptive immune responses. After multiple episodes of treated symptomatic malaria, most individuals living in hyperendemic areas develop natural acquired immunity, which protects them from clinical disease. The exact mechanism underlying the induction of natural immunity is unresolved [117]. It is believed that a delicate balance between pro- and anti-inflammatory processes is necessary to develop an asymptomatic infection. Proinflammatory responses inhibit parasite proliferation, while anti-inflammatory mechanisms are required to avoid immunopathogenesis due to the deleterious cytokine storm [118]. A central immune mechanism in controlling parasite proliferation during the blood stage is production of IL-12 by DCs and subsequent release of IFN-γ by natural killer (NK cells) [119]. After activation of $CD4^+$ T cells by DC, the presence of IFN-γ leads to a Th1 polarization. Th1 cells release more IFN-γ that

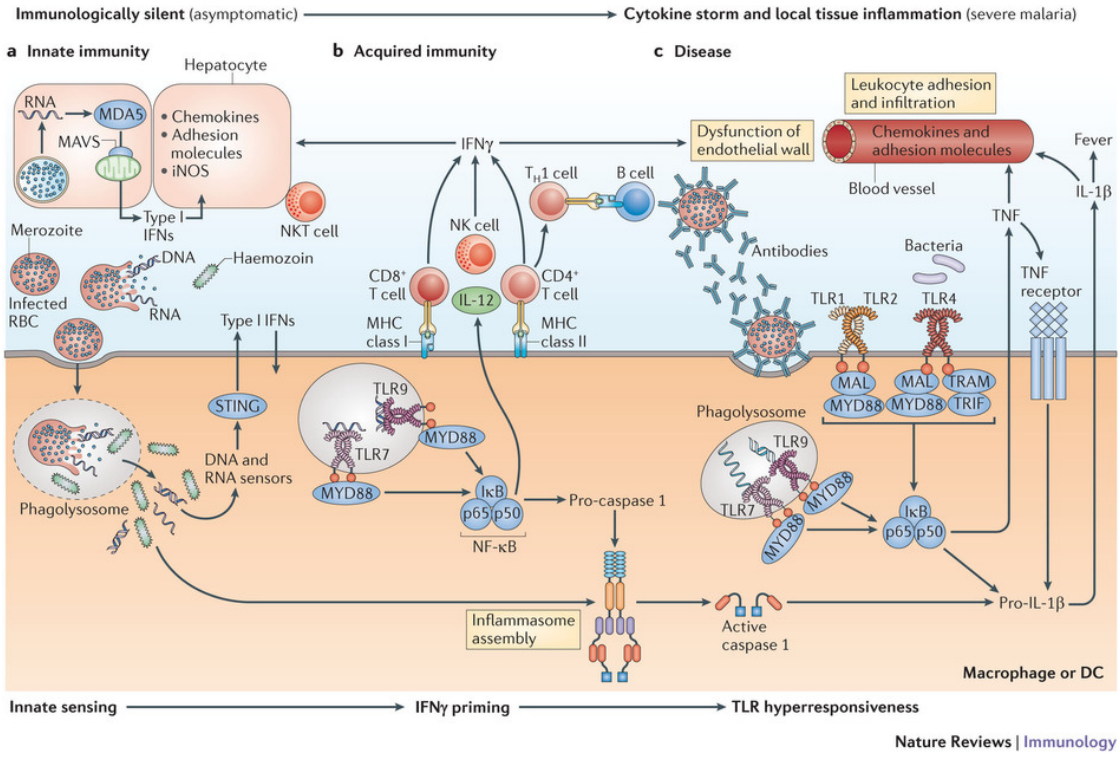

Figure 1.7: Innate and adaptive immune responses during malaria infection and associated pathogenesis [116].

enhances the activation of monocytes to produce nitric oxide and to phagocytose parasites [120]. Th1 lymphocytes activate B cells to secrete antibodies, that exhibit protective effects on several levels. Binding to free merozoites avoids invasion of new RBCs, coating parasitized RBC induces opsonization followed by inhibition of parasite growth or phagocytosis by activated monocytes. This process also avoids sequestration [121,122]. Antibodies can further neutralize 'malaria toxins'. By binding to plasmodial PAMPs such as GPIs, the antibodies prevent PRR triggering that would add to the deleterious cytokine storm [123]. The anti-inflammatory cytokines IL-10 and transforming growth factor-β (TGF-β) are associated with control of immunopathogenic processes [124, 125]. IL-10 and TGF-β can be produced by both, innate and adaptive immune cells [120]. IL-10 release in monocytes and DC is triggered by PRR signalling, especially by TLR-2 ligation [126].

1.2.2 Soil-transmitted helminths

Soil-transmitted helminths: Epidemiology, transmission and clinical manifestations

Soil-transmitted helminths are part of the neglected tropical diseases [127]. Following soil-transmitted helminth species are most common: Hookworm (*Ancylostoma duodenale*, *Necator americanus*), roundworm (*Ascaris lumbricoides*) and whipworm (*Trichuris trichiura*). Transmission occurs via ingestion of the parasites' eggs with for example contaminated food, whereas larvae originating from hookworm infections penetrate bare skin [128, 129]. After contact with infective larvae or eggs, adult worms develop and live in the intestines of the human host. Eggs or larvae are excreted with faeces into the soil and under favorable conditions they mature to reach the infectious stage. Infections are most prevalent in areas with poor hygiene and sanitation and where the environment favors rapid transmission. In 2010, 1.45 billion individuals were estimated to be infected with at least one intestinal helminth species [130]. Very common in children is infection with all three helminth species. Consequences are stunting, malnutrition, intellectual retardation and cognitive and educational deficits. Hookworm disease accounts for the biggest part of the burden estimates. During hookworm infection anaemia and iron deficiency can develop due to considerable blood loss at the site of intestinal attachment of the adult worms [129].

Additionally to the aforementioned helminth species there are two intestinal nematodes infecting humans, that are most neglected: the pinworm *Enterobius vermicularis* (*E. vermicularis*) and the threadworm *Strongyloides stercoralis* (*S. stercoralis*). Due to laborious diagnosis and difficulties to assess associated morbidity, these two species are mostly neglected in prevalence reports and estimates of global disease burden [127, 128, 131, 132].

The life cycle of *S. stercoralis* is more complex than the one of most other nematodes. It alternates between free living and parasitic cycles and has the ability to autoinfect the host. This can lead to maintenance of the lifecycle for decades [128,133]. Infections in healthy individuals mostly remain asymptomatic, otherwise skin lesions, pulmonary and gastro-intestinal symptoms and blood eosinophila are associated [134–136]. Immunocompromised patients are at high risk of developing a disseminated and lethal infection due to the ability of the parasite to reproduce within the host [137]. Adequate information about the burden of *S. stercoralis* is lacking, but it is estimated that between 10% and 40% of the population in tropical and sub-tropical regions might be affected [138].

Transmission of *E. vermicularis* occurs via ingestion of eggs in water, dust, food or sticking to hands. Female adults live in the intestines and move to the perianal region of the host during the night and lay their eggs on the perianal skin [128]. Eggs become infective within hours, hence autoinfection is common. Symptoms include intense pruritus in the perianal region, appendicitis and genitourinary tract complications. Infrequent ectopic infections of liver, lung, kidneys and other organs occur [139]. According to Fry et al. [140], Enterobiasis is one of the most common helminth infections worldwide, but recent prevalence and burden estimates are missing. Enterobiasis is estimated to affect 4-28% of children globally [129].

Soil-transmitted helminths: Diagnosis, treatment and control strategies

One of the most commonly used diagnostic tools for detection of soil-transmitted helminths is the Kato Katz technique (microscopic analysis of filtered stool samples). Another technique that relies on microscopic analysis of stool samples is the recently developed FOTAC. It proves more sensitive than the Kato Katz method, but requires more sophisticated laboratory equipment. Real time PCR (RT-PCR)

detects helminth DNA or ribosomal RNA from stool samples. Diagnosis of light intensity Hookworm infection with RT-PCR is as sensitive as the Kato Katz technique. In case of *S. stercoralis* infection, RT-PCR was reported to have poor sensitivity when compared to the Baermann method, which includes an enrichment step of living larvae. Combination of the Baermann method and stool culture techniques, such as the Koga agar plate, reveal the highest sensitivity for detection of *S. stercoralis* [132]. Presence of *E. vermicularis* is microscopically verified using an adhesive tape, that was applied to the anus in the morning or during the night [141].

Soil-transmitted helminths are treated with benzimidazoles (albendazole or mebendazole) alone or preferably in combination with ivermectin, due to emerging resistances to benzimidazoles [129, 139]. *S. stercoralis* is treated with ivermectin [137]. The strategy for control of soil-transmitted helminths is to prevent morbidity by periodic deworming of the population at risk, including preschool aged and school aged children and pregnant or breastfeeding women and women of childbearing age. Education on health and hygiene and if possible provision of adequate sanitation is used to prevent transmission [142, 143].

The immune response against Helminth infections

The danger of rapid expansion is absent during an infection with helminths. Unlike infections with *M.tb.* or *P. falciparum*, protective immune mechanisms against helminths are similar to tissue healing processes [144]. It is unclear how large multicellular pathogens are recognized by the innate immune system, but most likely helminth excretory secretory proteins are the mediators [145]. They are able to bind to host PRRs such as TLRs and mannose receptors [146, 147]. Physical tissue damage evoked by the helminth can also initiate inflammation. Danger associated

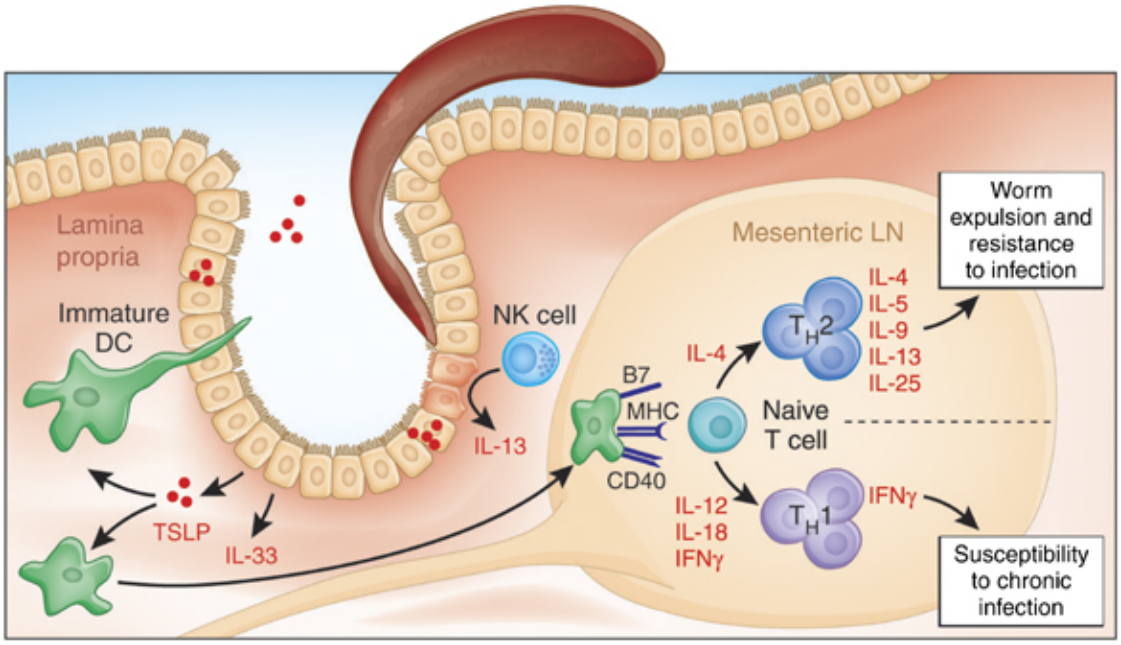

Figure 1.8: Protective and pathologic immune mechanism during intestinal helminth infections [151].

molecular patterns (DAMPs), have been demonstrated to play an important role in initiating protective immune mechanisms against nematodes [148]. Epithelium derived alarmins such as thymic stromal lymphopoietin (TSLP) or the cytokine alarmin IL-33 activate DCs, which initiates a type 2 immune response typical for tissue healing (Figure 1.8) [149, 150]. Cell types related to a type 2 response are Th2 cells, Tregs, alternatively activated macrophages (M2), eosinophils and B cells. Upon activation by DCs, Th2 cells release IL-4, -5, -10 and IL-13. This furthermore activates and recruits eosinophils and promotes the differentiation to M2. Eosinophils and M2 are able to secrete proteins that are necessary for each stage of wound healing (various growth factors including TGF-β and matrix metalloproteinases) [144]. The production of IgG and IgE by B cells can increase resistance to many helminths [152]. The antibodies neutralize helminth excretory secretory proteins, therefore avoiding additional activation of immune cells [153]. Binding of IgE to Fcϵ receptor on mast cells results in mast cell degranulation and release of

mediators that in some cases lead to helminth expulsion [154]. There is also increasing evidence that the helminths may indirectly affect inflammation by influencing the composition of the microbiota [155].

1.2.3 The human gastrointestinal microbiome

The human gastrointestinal (GI) tract is populated by a vast number of bacteria, archaea, viruses, fungi and protozoa [156]. The total amount of microbial cells is estimated to exceed the mammalian counterparts by 3-fold [157]. The term microbiome has been defined as "the ecological community of commensal, symbiotic and pathogenic microorganisms that share our body space" [158]. It influences many of the functions required for host physiology and survival, therefore also named "the forgotten organ" [159]. It is formed directly at birth and depends on the mode of delivery. The newborns acquire either a microbiome similar to the mothers vaginal or in case of a cesarean the skin microbiome [160]. Especially during the first year of life, the microbiome varies greatly comparing baby to baby and also within the same individual [161]. At 3 years of life the child's microbiome resembles that of an adult, which remains almost stable but highly heterogeneous during lifetime [162]. Dietary changes [163], the use of antibiotics [164], age [165], hormonal cycles [166], travel [167] and illness [164] including helminthiasis [168] are associated with fluctuations in the microbiome.

The human GI microbiome is estimated to account for over 5 million genes and is composed of more than 1000 different species [169, 170]. The number of phyla is comparatively small with *Firmicutes*, *Bacteroidetes* and *Actinobacteria* being the most abundant [171]. A 'healthy' microbiome has yet to be defined, but is considered to have a high bacterial diversity as stated in the "Disappearing Microbiota Hypothesis". This hypothesis links the western lifestyle (high fat/high sugar

diet, overuse of antibiotics, clean water) to a lower diversity of the microbiota and increasing cases of allergies and metabolic diseases [172].

Main functions of the human GI microbiome

The metabolome produced by the GI microbiota yield both, beneficial and hazardous compounds and have a systemic effect on human health [173]. Resistant carbohydrates, that cannot be digested by human enzymes, reach distal parts of the GI tract, where they are available for microbial conversion. Host derived mucus glycoproteins are additionally available for microbial fermentation. Fermentation of resistant carbohydrates is generally considered beneficial [174]. The end product of this process are gas and short chain fatty acids (SCFAs - acetic, propionic and butyric acids) [175]. Butyrate is used as an energy source by the gut epithelial cells and it has anti-carcinogenic and anti-inflammatory properties [174,175]. Propionate is also anti-inflammatory, has been demonstrated to increase insulin sensitivity and suppress proliferation of cancer cells [176]. Acetate is directly used as energy source or precursor for sysnthesis of complex molecules in peripheral tissues [174]. Protein degradation in the colon can yield beneficial SCFAs, but also toxic metabolites like ammonia, amines, N-nitroso compounds, phenolic compounds and sulphides [177]. A balanced diet that includes high protein and complex carbohydrate intake has been associated with health-promoting effects rather than accumulation of toxins [178]. There is no evidence that the third major part of the human diet, lipids, are degraded by the GI microbiota. However, ingestion of lipids is associated with secretion of bile acids, which partially reach the terminal ileum and colon. There they undergo microbe-mediated enzymatic deconjugation, which is required for microbial survival and protection of the colon [179]. A small proportion of deconjugated bile acids undergo further enzymatic digestion yielding secondary bile

acids. Microbial transformation of bile salts have a huge impact on host physiology, as bile salts have important roles in signaling their biosynthesis, lipid absorption, cholesterol homoeostasis, and immune response [180]. Inefficient transformation of bile acids in the colon are associated with inflammatory bowel disease, loss of anti-inflammatory activity and therefore pathogenesis [181]. The human GI microbiome has been further implicated in beneficial production of vitamins of the group K and B and maintenance of the normal barrier function [182, 183]. Commensal microbes do this partly by competing for space and nutrition and furthermore by inhibition of pro-inflammatory signaling pathways that pathogens require for invasion [184].

The immune response against the GI microbiome

The close proximity of microorganisms and host cells in the GI tract requires a delicate balance of immune tolerance but also vigilance to guard against infectious agents and opportunistic pathogens. The resulting cross-talk between host cells and microbes is extensive and includes innate and adaptive immune mechanisms. Commensals lack virulence factors required for penetration of the epithelium. Triggering of PRRs via PAMPs present in the GI tract (such as LPS, peptidoglycan and flagellin) on the apical surface of the endothelium induces tolerance and homeostasis, whereas ligand engagement on the baso-lateral surface leads to strong pro-inflammatory responses [186].

The only route of entry into the body for commensals is through capture by M cells in Peyer's patches, since epithelial cells are protected by a layer of mucus. The M cells transfer them to local DCs that migrate to a mesenteric lymph node. DCs loaded with commensals directly activate naïve B cells to become IgA- expressing B lymphocytes, which will migrate to the lamina propria as plasma cells. Following transcytosis, IgA inhibits adherence and penetration of the epithelium

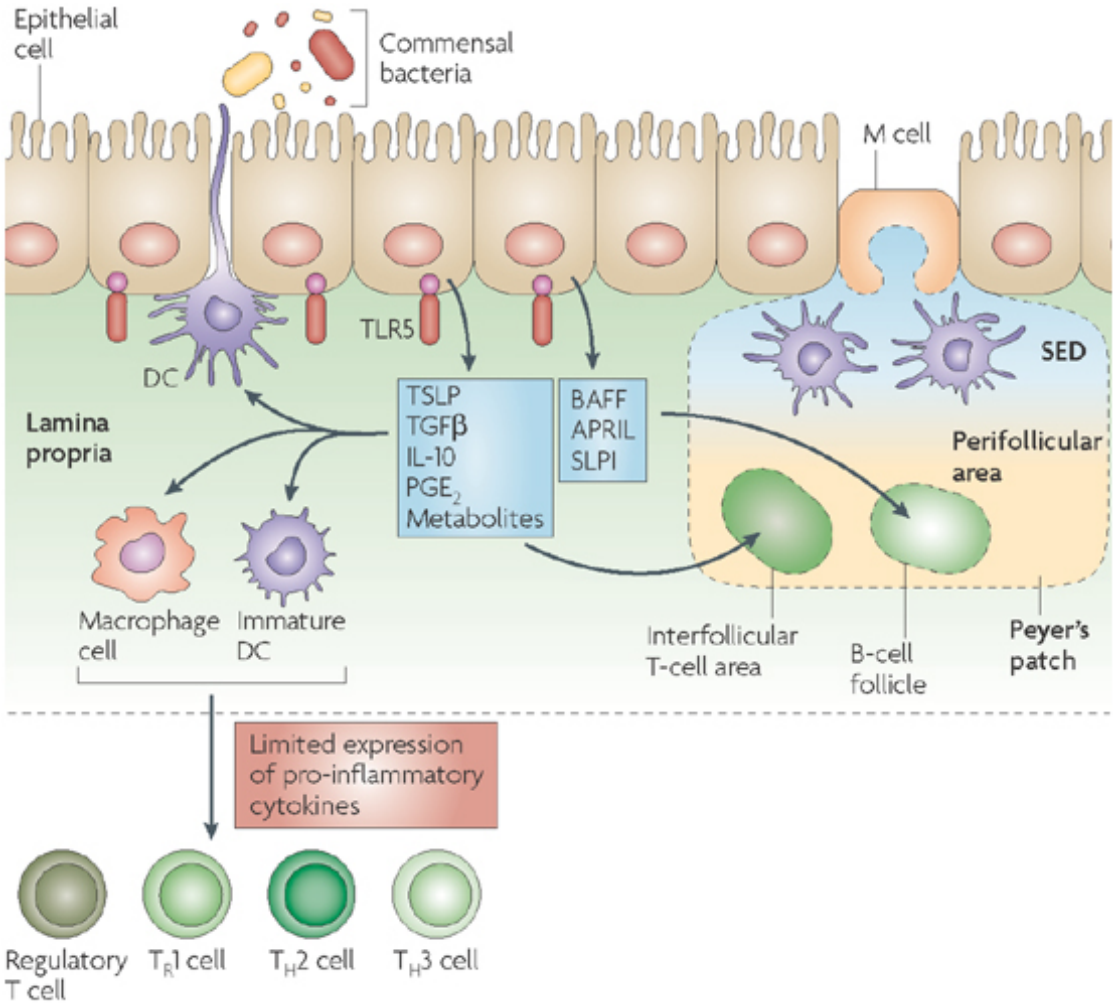

Figure 1.9: Immune response against the GI microbiome during homeostasis [185].

by commensals [187]. In case of homeostasis, there is constitutive production of anti-inflammatory TGF-β, TSLP and prostaglandin E_2 (PGE_2) by epithelial and mesenchymal cells. This keeps immature DCs in a quiescent state with low expression of co-stimulatory molecules. When these DCs stimulate naïve T cells in the mesenteric lymph nodes, T cells polarize into anti-inflammatory and regulatory T cells (Figure 1.9) [185]. The protective role of the commensal flora is dramatically illustrated when using broad spectrum antibiotics. These antibiotics kill large numbers of commensal bacteria creating a niche for bacteria that normally are not able to compete with the normal microbiota. They cause serious disease as for example in case of an infection with *Clostridium difficile* [188].

Immunomodulation by GI microbiota derived products

Microbial derived products have a critical role in development, homeostasis and function of innate and adaptive immune cells. They can either be diet dependent, such as SCFA, bile acids and vitamins, or diet independent, such as LPS and peptidoglycan [189]. Bile acids derived from commensal bacteria are sensed by the G protein-coupled bile acid receptor1 (GPBAR1) and the nuclear receptor subfamily 1, group H, member 4 (NR1H4). Highest expression of GPBAR1 and NR1H4 is found on monocytes and macrophages [190, 191]. Signaling of these receptors is associated with an anti-inflammatory response and inhibition of NF-κB activity and repression of NF-κB dependent transcription [192, 193]. This results in attenuated induction of the pro-inflammatory cytokines TNF-α, IL-6 and IL-1β in response to LPS [194]. SCFAs modulate the immune response by activating GPR43 (free fatty acid receptor 2, FFA2) [195], inhibition of histone deacetylases [196] and the regulation of autophagy [197]. GPT43 recognises acetate, propionate and butyrate and is expressed on many immune cells, such as neutrophils, macrophages, monocytes,

dendritic cells, T cells and intestinal epithelial cells. SCFA promote neutrophil chemotaxis. Treatment of human peripheral blood mononuclear cells (PBMCs) with SCFAs results in diminished expression of monocyte chemotactic protein-1 (MCP1), TNF-α, IFN-γ and IL-10 in response to LPS [198]. Treatment of DCs with butyrate is associated with decreased expression of pro-inflammatory IL-12 and IFN-γ and increased expression of IL-10 and IL-23 and downregulation of the antigen presentation machinery [199, 200]. There is evidence that butyrate has an influence on colonic epithelial cells, as Caco-2 cells treated with butyrate and IL-1β produce less IL-8 than those treated with IL-1β alone [201]. Butyrate has a role in maintenance of intestinal barrier integrity by accelerating the assembly of tight junctions in Caco-2 cells [202]. The synthesis of essential vitamins of the group B and K by commensal bacteria are an important source for the human body. These vitamins have immunomodulatory roles and influence the susceptibility to and the course of infectious diseases [203]. A direct influence of vitamin synthesis by the microbiota was shown for the the monomorphic major histocompatibility complex class I-related protein (or MR1) presenting vitamin from the biosynthetic pathway of vitamin B_2 to mucosa associated invariant T cells [204]. This is a population of T cells producing IL-17 and IFN-γ in response to microbe-derived products of the riboflavin biosynthetic pathway [205, 206]. This indicates that not only the end-product, but also metabolites from the biosynthetic pathways play an important role [189].

The immune response in the GI tract to diet-independent microbiota products was discussed in section 1.2.3. Microbial derived PAMPs like LPS and peptidoglycan have a special role during gut barrier dysfunction, also called “leaky gut”, which can be a result of dysbiosis and inflammation [207]. Commensal bacteria can breach the gut, leading to bacterial infection and endotoxemia as a result of increased immune activation by bacterial PAMPs [208]. Interestingly, SCFAs have been shown

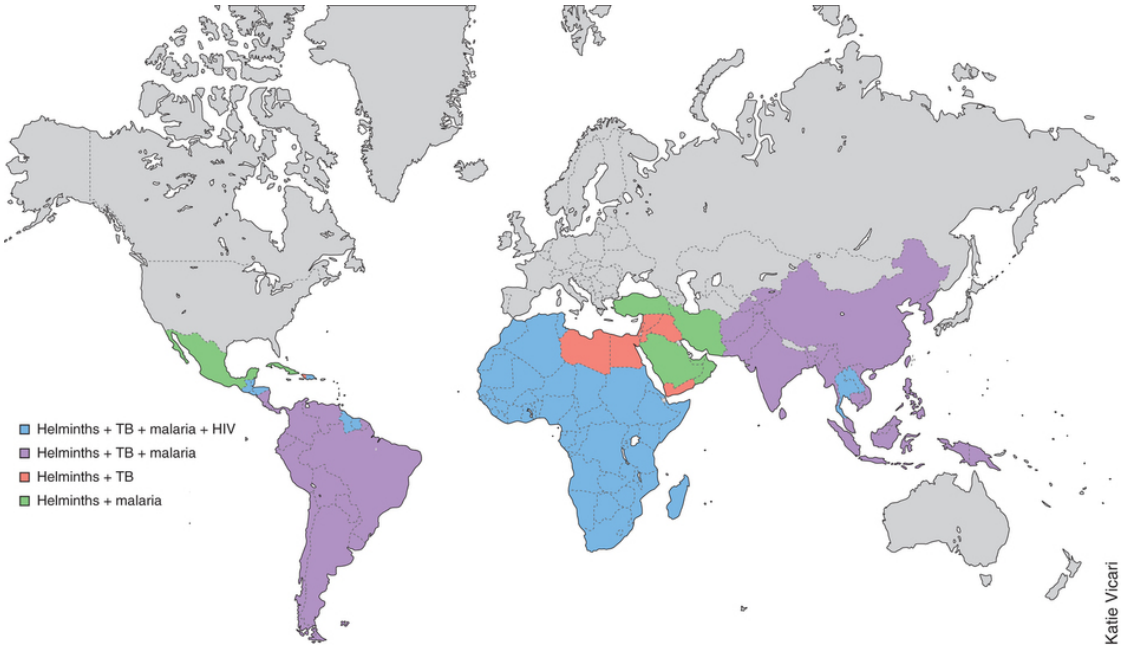

Figure 1.10: Geographic overlap of helminths and the big three infectious diseases, HIV, malaria and TB [212]

to decrease gut barrier permeability [209].

1.2.4 Interactions of *P. falciparum*, Helminths and GI microbiome

P. falciparum - Helminths

There is substantial geographic overlap between neglected tropical diseases and the big three infectious diseases (HIV, TB and malaria) (Figure 1.10) [210]. Occurrence of co-infections of malaria and helminths are common in Sub-Saharan Africa, South East Asia and South America mainly affecting school-aged children and pregnant women [211]. Helminth infections are considered highly immuno-modulatory to the extent that they can affect concomitant infections taking place at distant sites in the human body [46]. In the presence of rapidly replicating pathogens that induce a type 1 response, they are able to skew the response towards type 2 and tissue

healing processes [213]. In case of a co-infection with *P. falciparum*, this could be beneficial, since anti-inflammatory processes during malaria avoid pathogenesis induced by the deleterious cytokine storm. On the other hand, anti-inflammatory processes could dampen pro-inflammatory processes that are required to control parasite proliferation.

Although helminths could protect against clinical malaria, a co-infection could affect the establishment of naturally acquired immunity to malaria. It was demonstrated in a mouse model, that the cytokine milieu induced by an intestinal nematode infection (*Heligmosomoides polygyrus*; *H. polygyrus*) promoted an isotype switch that reduced the protection of antibodies targeted against malaria epitopes [214]. Helminth treatment could therefore lead to a higher susceptibility to clinical malaria by impairing protective immune responses [215].

Co-morbidity studies of helminths and malaria reveal contradictory findings, possibly due to heterogenuous study designs. Differences in investigated age group, the included malaria/helminth species, the intensity of helminth infection, the classification of clinical malaria and integration of common risk factors are observed [211, 216]. Therefore, drawing a general conclusion is challenging. Within the scope of this thesis, three soil-transmitted helminth species are included, Hookworm, *S. stercoralis* and *E. vermicularis*.

Righetti *et al.* found a significant positive association of light-intensity Hookworm and malaria in 6-8 year old children in the Ivory Coast [217]. Additionally, these co-infected children were at lower odds of developing anemia and iron deficiency [217]. A similar study in Uganda also found a positive association of hookworm and malaria in pre-school aged children [218]. Nkuo-Akenji *et al.* associated the development of anemia in co-infected children with increasing intensity of Hookworm infection [219]. No association was found in Tanzania in school aged children [220]. A study investigating the immunological outcome of Hookworm and malaria co-

infection conducted in adult volunteers documented no influence [221].The only study assessing infections with *S. stercoralis* and *P. falciparum* was in pregnant women from Uganda, and revealed no association [222]. To my knowledge no study investigating the co-infection with *E. vermicularis* was performed.

Helminth - Microbiome

GI helminths and the microbiota co-evolved in the same niche in the human host and thus closely relate [223]. Symbiotic interactions between *H. polygyrus bakeri* and *Lactobacillus* bacteria have been reported in mice studies. Infection with *H. polygyrus bakeri* increased the abundance of *Lactobacillus* bacteria and this positively correlated with Tregs and Th17 responses. This effect was also observed vice versa, since enrichment of the microbiota with *Lactobacillus taiwanensis* prior to helminth infection raised Treg frequencies and resulted in greater helminth establishment [224]. An experimental infection model of mice infected with *T. muris* demonstrated, that the helminths utilise the cecal microbiota to enable hatching and the exit of the larvae [225]. Infection of pigs with *Trichuris suis* (*T. suis*) did not reveal any change in overall microbiota diversity, but there was a statistically significant change in metabolic potential. The microbiome of pigs infected with *T. suis* presented a decrease in genes related to carbohydrate metabolism and the biosynthesis of the amino acids lysine, cysteine and methionine [226].

There are only few publications assessing the impact of helminth infection on the microbiome in humans. No statistically significant difference in fecal microbiota composition was found in Ecuadorian school children infected with *T. trichiura* alone or co-infected with *Ascaris lumbricoides* [227]. A study conducted in Malaysia found an association with increased diversity of the fecal microbiota in individuals infected with helminths. The cohort consisted of volunteers aged 0.4-48 years

and infection with *Trichuris trichiura* predominated over *Ascaris lumbricoides* and Hookworm. Higher abundance of *Paraprevotellacea* was observed in individuals infected with *T. trichiura*. This study also assessed alterations of microbial function during helminth infection and observed a decrease in carbohydrate metabolism in individuals infected with *A. lumbricoides* and an enrichment of nucleotide metabolism and pathways for cell growth and death in *T. trichiura* infected [228]. Experimental hookworm infection of 8 healthy volunteers did not reveal any significant change in fecal microbiota composition comparing before and after infection [229].

As discussed in section 1.2.3, helminths can directly modulate the immune system. It is possible, that the helminths do this in addition indirectly by interacting with the microbiome, since the microbiome has immunomodulatory capacities as well (discussed in section 1.2.3). Nonetheless, scientific proof is lacking so far [155].

Taken together, there is evidence of an extensive cross-talk between GI helminths and the microbiota and GI helminths not only influence the bacterial diversity but also the functional capacity of the microbiota. Conflicting results of studies in humans indicate, that the influence of GI helminths on the microbiome depends on the helminth species and the host's background. Importantly, as demonstrated by Broadhurst et al. and Wu et al. in experimental helminth infections of macaques and pigs, history of helminth infection (even in animals that have cleared infection) and helminth infection intensity can affect the gut microbiome ecology [230, 231].

P. falciparum - Microbiome

There exists very limited information about interactions of *Plasmodium spp.* and the microbiome. Yilmaz et al. report a protective effect of IgM binding to anti-Galα1-3Galβ1-4GlcNAc-R(α-gal) glycan located on sporozoites of *Plasmodium*

spp. by inhibiting invasion of hepatocytes. They showed in a mouse model, that enteric *Escherichia coli* O87:B7 expressing high levels of α-gal could induce the production of anti-α-gal IgM in the circulation and that these antibodies conferred protection from *Plasmodium berghei* ANKA transmission by *Anopheles* mosquitoes [232].

During *P. falciparum* infection, parasitized RBC sequester also to the endothelium of micro vessels present in the intestine [233]. Molyneux et al. and Wilairatana et al. report an increased GI permeability in patients with severe malaria [234, 235]. This might lead to a gut-barrier dysfunction and influx of enteric gram-negative organism, the underlying cause of the commonly observed endotoxemia in children with malaria disease [236].

1.3 Aims of the thesis

A safer and more immunogenic vaccine than BCG represents one major aim to meet the Stop TB Partnership targets of WHO. As mentioned above, finding a TB vaccine that is protective in all populations is challenging. Main reasons are a lack of understanding natural protective mechanisms against TB and as a result a lack of a vaccine induced cellular correlate of protection. Furthermore, the exact mechanisms of induction and maintenance of immunological memory are only partially known and the characteristics of a vaccine, that is safe and immunogenic in HIV infected individuals, has to be tested in this target group separately.

The aim of the first part of this thesis was to investigate the safety and immunogenicity of the TB vaccine H1/IC31® in HIV infected adults. The safety was determined by observing $CD4^+$ lymphocyte counts, viral load and adverse events. Immunogenicity was defined via ex vivo stimulation of whole blood with vaccine components and subsequent measurement of the release of IFN-γ, IL-2, TNF-α

and IL-17 by $CD4^+$ and $CD8^+$ T cells.

The aim of the second part of this thesis was to identify innate immune mechanisms that resulted in improved induction and maintenance of the H1/IC31®-induced memory $CD4^+$ T cell response in HIV positive individuals not undergoing anti-retroviral treatment. Ex vivo stimulation of whole blood with H1 was performed and the release of IFN-γ, IL-2 and TNF-α by distinct memory $CD4^+$ T cell subsets was measured. Analysis of peripheral whole blood transcriptome by the novel method based on selective amplification of 1300 genes followed by next generation sequencing (AmpliSEQ) was used to identify innate immune mechanisms that lead to improved memory maintenance.

The establishment of an asymptomatic *P. falciparum* infection relies on a delicate balance of pro- and anti-inflammatory immune responses with the exact mechanism being unknown. Helminths and the gut microbiota share the same niche in the human host and both impact on local and systemic immunity. We hypothesized that the co-infection of *P. falciparum* with helminths and the interplay with associated microbiota could either lead to a balance of pro- and anti-inflammatory immune responses and asymptomatic malaria or imbalance and malaria disease.

The aim of the third part of this thesis was to assess the impact of helminth infection on malaria disease outcome in children aged between 2 months and 9 years from the Bagamoyo District, United Republic of Tanzania. Prevalence of the following three helminth species was highest in the study area: Hookworm, *S. stercoralis* and *E. vermicularis*. We have observed that children infected with *E. vermicularis* tend to develop less clinical malaria episodes during a cross-sectional study. In order to understand this relationship a systems biology approach was developed. From a subset of these children the fecal microbiome and the innate immune response was measured to gain more insight into possible mechanisms

yielding protection from malaria disease. Sequencing of the variable 3 region of the 16S ribosomal RNA of fecal microbiota was used to assess bacterial diversity and metagenomic analysis was performed to gain insight into the metabolic function. In vitro stimulation of PRRs of whole blood by common TLR agonists was used to measure cytokine expression of major antigen presenting cells by flow cytometry. Gene expression analysis of whole blood was performed using dual-color reverse transcriptase multiplex ligation-dependent probe amplification (dcRT-MLPA).

Chapter 2

Safety and Immunogenicity of H1/IC31® in HIV infected adults

This chapter is an adapted version of the following publication:
Reither K, Katsoulis L, Beattie T, Gardiner N, **Lenz N**, Said K, Mfinanga E, Pohl C, Fielding KL, Jeffrey H, Kagina BM, Hughes EJ, Scriba TJ, Hanekom WA, Hoff ST, Bang P, Kromann I, Daubenberger C, Andersen P and Churchyard GJ. Safety and Immunogenicity of H1/IC31®, an adjuvanted TB Subunit Vaccine, in HIV-Infected Adults with $CD4^+$ Lymphocyte Counts Greater than 350 cells/mm^3: a Phase II, Multi-centre, Double-Blind, Randomized, Placebo-Controlled Trial. PLoS ONE 9(12): e114602. doi:10.1371/journal.pone.0114602, 2014

2.1 Abstract

Background: Novel tuberculosis vaccines should be safe, immunogenic and effective in various population groups, including HIV-infected individuals. In this phase II multi-centre, double-blind, placebo-controlled trial, the safety and immunogenicity of the novel H1/IC31® vaccine, a fusion protein of Ag85B-ESAT-6 (H1) formulated with the adjuvant IC31®, was evaluated in HIV-infected adults.

Methods: HIV-infected adults with $CD4^+$ T cell counts $>350/mm^3$ and without evidence of active tuberculosis were enrolled and followed until day 182. H1/IC31® vaccine or placebo was randomly allocated in a 5:1 ratio. The vaccine was administered intramuscularly at day 0 and 56. Safety assessment was based on medical history, clinical examinations, and blood and urine testing. Immunogenicity was determined by a short-term whole blood intracellular cytokine staining assay.

Results: 47 of the 48 randomised participants completed both vaccinations. In total, 459 mild or moderate and 2 severe adverse events were reported. There were three serious adverse events in two vaccinees classified as not related to the investigational product. Local injection site reactions were more common in H1/IC31® versus placebo recipients (65.0% vs. 12.5%, p=0.015). Solicited systemic and unsolicited adverse events were similar by study arm. The baseline $CD4^+$ T cell count and HIV viral load were similar by study arm and remained constant over time. The H1/IC31® vaccine induced a persistent Th1-immune response with predominately TNF-α and IL-2 co-expressing $CD4^+$ T cells, as well as polyfunctional IFN-γ, TNF-α and IL-2 expressing $CD4^+$ T cells.

Conclusion: H1/IC31® was well tolerated and safe in HIV-infected adults with a $CD4^+$ Lymphocyte count greater than 350 cells/mm^3. The vaccine did not have an effect on $CD4^+$ T cell count or HIV-1 viral load. H1/IC31® induced a specific and durable Th1 immune response.

Trial registration: Pan African Clinical Trials Registry (PACTR) Identifier: PACTR201105000289276

2.2 Introduction

Tuberculosis (TB) remains a global public health problem. One third of humankind is infected with *Mycobacterium tuberculosis* (*M.tb*), which according to the World Health Organization (WHO) led to almost 8.6 million new active TB cases and 1.3 million TB deaths in 2012 [237]. Mycobacterium bovis Bacille Calmette-Guérin (BCG), the only currently licensed TB vaccine, is effective in preventing severe progressive disease in children but has limited impact on adult pulmonary TB, the driving force of the TB global pandemic [238,239]. Consequently, there is an urgent need to develop safe and effective TB vaccines to accelerate progress towards TB elimination.

Vaccination campaigns may administer TB vaccines to persons without knowing their HIV status. It is therefore essential to evaluate the safety and immunogenicity of TB vaccines in HIV-infected persons. Furthermore, HIV-infected individuals have an increased risk of developing active TB, which may be decreased by an effective TB vaccine that reduces the risk of reactivation of latent TB infection (LTBI) or prevents TB infection or reinfection.

The Statens Serum Institut Hybrid (H1) recombinant fusion protein (antigen (Ag) 85B- Early Secretory Antigenic Target (ESAT)-6) TB vaccine, adjuvanted with IC31®, has been shown to be safe and immunogenic in BCG unvaccinated, TB uninfected participants and in BCG vaccinated and latently TB infected participants [64,65]. In this phase II trial we evaluated the safety and immunogenicity of H1/IC31® administered to HIV-infected adults with $CD4^+$ lymphocyte counts greater than 350 cells/mm^3 and without evidence of active TB disease (PACTR

Identifier: PACTR201105000289276).

2.3 Methods

2.3.1 Regulatory approval

The study was conducted in accordance with the Helsinki Declaration and Good Clinical Practice (GCP) and approved by the following local and national ethics committees and regulatory authorities: Medical Research Coordinating Committee of Tanzania, Institutional Review Board of the Ifakara Health Institute, Tanzanian Food and Drug Authority, South African Medicines Control Council and the Human Research Ethics Committee, University of Witwatersrand.

2.3.2 Study design and sites

This was a phase II, multicentre, double-blind, randomized, placebo-controlled trial. Participants were eligible if they were between 18 and 55 years of age, HIV infected with $CD4^+$ lymphocyte counts greater than $350/mm^3$, antiretroviral therapy naïve, generally healthy, had no evidence of active TB, had no history of receiving immunosuppressive medication, immunoglobulins, blood products or known hypersensitivity to any of the vaccine components. Women of child bearing potential were eligible if pregnancy was excluded and they agreed to use at least two forms of acceptable contraception from 21 days prior to administration of the study vaccine through to the end of the study.

The trial took place at two African research facilities, the rural Bagamoyo Site of the Ifakara Health Institute in Tanzania and the urban Tembisa Site of the Aurum Institute in South Africa. It was carried out between 19th of December 2011 (first participant first visit) and 10th of September 2012 (last participant last visit); the

first participant last visit was on the 2nd of July 2012. Written informed consent was obtained from all literate patients. In case of illiteracy, informed oral consent was attested by an impartial witness and documented with the patient's fingerprint according to ICH GCP guidelines (E6 (R1); 4.8.9), as approved by the above mentioned ethics committees and regulatory authorities. The protocol for this trial and CONSORT checklist are available as supporting information; see Protocol S1 and Checklist S1 2.6.

2.3.3 Randomisation and blinding

Participants were randomly allocated in a 5:1 ratio to receive either H1/IC31® vaccine or placebo according to a computer-generated randomisation list. The pharmacist prepared the vaccination according the pre-prepared study randomisation list. The unequal randomisation was employed to maximise exposure to the H1/IC31® vaccine thereby increasing the chance of detecting a serious adverse event to the vaccine. The study monitors, investigators, and participants were blinded to study product. The study pharmacists prepared the investigational product. Syringes were masked with red tape in order to conceal a slight difference in the appearance of the H1/IC31® and placebo.

2.3.4 Investigational product and vaccination

The Hybrid 1 (H1) vaccine is a recombinant fusion protein of the antigens Ag85B and ESAT-6 (Ag85B-ESAT-6), developed and manufactured by the Statens Serum Institut (Denmark). The adjuvant IC31® was developed by Intercell AG (Austria) and consists the cationic polyaminoacid KLK, which is composed of the amino acids lysine (K) and leucine (L), and ODN1a, a single stranded oligodeoxynucleotide with alternating sequences of the nucleic acids inosine and cytidine. A volume of 0.5 mL

was administered providing a dose of 50 μg Ag85B-ESAT6 (antigen) and 500 nmol KLK + 20 nmol ODN1a (adjuvant) or 0.5 mL Tris buffer (placebo).
The H1/IC31® vaccine or placebo was administered intramuscularly with a 22 to 25-gauge needle at study day 0 and 56, after confirming eligibility criteria. The first injection was given into the right and the second into the left deltoid muscle.

2.3.5 Safety

All solicited local (pain, tenderness, erythema, induration, nodules) and systemic adverse events (AEs) (malaise, myalgia, headache, nausea, vomiting, athralgia, fatigue, chills, fever) and unsolicited AEs were coded by the Aurum Institute according to the MedDRA Dictionary Version 15.1. AEs and laboratory measures of safety were graded using the Division of AIDS Table for Grading the Severity of Adult and Pediatric Adverse Events (version 1.0, 2004) as mild, moderate, severe or potentially life-threatening and assessed for their relationship to study product. $CD4^+$ T cell count and HIV-1 viral load were measured pre and 14 days post vaccination and at the study end.

2.3.6 IFN-γ release assay

QuantiFERON-TB Gold In-Tube assay (QFT) (Celestis) was performed at screening and at day 182 to identify whether H1/IC31® induced a false positive result. The assay was carried out according to manufacturer's instructions with a cut-off value of 0.35 IU IFN-γ/mL to either antigen (ESAT-6/CFP-10).

2.3.7 Immunological assays

All immunological assays described below were performed by the South African TB Vaccine Initiative (SATVI) laboratory in Cape Town, South Africa.

The whole blood intracellular cytokine staining assay was used to quantify antigen specific $CD4^+$ and $CD8^+$ T cell responses (interferon-gamma (IFN-γ), tumour necrosis factor-alpha (TNF-α), interleukin (IL)-2 and IL-17) after stimulation with peptide pools of Ag85B and ESAT-6 peptides (each consisting of 15-mer peptides, overlapping by 10 amino acids, final concentration of 2μg/mL, GenScript) and recombinant H1 fusion protein (final concentration of 5μg/mL, Statens Serum Institute). $CD4^+$ and $CD8^+$ T cell expression of IFN-γ, TNF-α and IL-2 was measured to assess the polyfunctional characteristics of H1/IC31® induced T cells. The primary immunogenicity endpoint was assessed at day 70 (14 days post 2nd vaccination).

Processing of whole blood started within 75 minutes after phlebotomy. One ml whole blood from each study participant and time point were either left unstimulated (negative control) or stimulated with peptide pools of Ag85B, ESAT-6, the H1 fusion protein and phytohemagglutinin (PHA) (positive controls). The costimulatory antibodies anti-CD28 and anti-CD49d (BD Biosciences, at 0.5μg/mL each) were included in all assay conditions. The whole blood was incubated at 37°C for 7 hours and Brefeldin-A (Sigma-Aldrich, 10μg/mL) was added thereafter. The blood sample was transferred to a waterbath at 37°C and incubated for a further 5 hours. Thereafter the waterbath was switched off and allowed to reach room temperature. Within the following 10 hours the blood was harvested with EDTA (Sigma-Aldrich, at 1.8mM), red blood cells were lysed and white cells fixed with 9ml of FACS lysing solution (BD Biosciences). Thereafter, white cells were pelleted and cryopreserved in cryosolution containing 50% RPMI (Lonza), 40% fetal calf

serum (BioWest) and 10% DMSO (Sigma-Aldrich). The specimens were shipped to SATVI ensuring that the cold chain was maintained.

The subsequent intracellular cytokine staining (ICS) procedure was performed as follows: the stimulated, fixed and frozen white cells from whole blood were thawed in a water bath at 37°C. The thawed cells were transferred to labelled tubes containing phosphate buffered saline (PBS, BioWhittaker) and washed. Next, the cells were permeabilised using Perm/Wash solution (BD Biosciences). Cells were then stained with the following anti-human antibodies: CD3 BV421 (BD Biosciences, MOPC-21), CD4-QDot605 (Invitrogen, S3.5), CD8-Cy5.5PerCP (BD Biosciences, SK1), CCR7-PE (eBioscience, 150503), IFN-γ-Alexa 700 (BD Biosciences, B27), TNF-α-Cy7PE (eBioscience, Mb11), IL-2-FITC (BD Biosciences, 5344.111), IL-17-Alexa 647 (eBioscience, SCPL1362) and CD45RA BV 570 (eBioscience, H1100). Results of CCR7 and CD45RA staining are not presented here. Samples were stained, acquired and analysed in batches. For every ICS assay experiment, compensation controls (single stained positive and negative mouse kappa compensation beads) were included. These controls were processed in parallel with the study samples during the staining and acquisition process to allow post acquisition flow cytometry data compensation. After the samples were acquired on the BD LSRII cytometer (BD Biosciences, San Jose, CA), flow analysis was performed using FlowJo software (TreeStar version 9.6.2).

Anti-Ag85B-ESAT-6 specific IgG antibody assay was used to measure antibodies specific to antigens of H1/IC31® as an indicator of humoral reactivity. Plasma was collected and frozen from ex vivo whole blood.

2.3.8 IFN-γ EliSpot assay

Prior to the start of the study both sites laboratories were trained on specimen processing and storage. Both sites passed their proficiency tests for PBMCs cell viability and number and were IATA certified for shipping specimens. IFN-γ EliSpot assay was not possible to conduct on PBMCs collected from the Tembisa site because the cell recovery upon thaw was too low (less than 100'000 cells). The cell recovery and yield was excellent for PBMCs from Bagamoyo. However, on Elispot assay, these PBMCs showed high level of spot forming units in the negative control wells that was indistinguishable from the response detected with the assay's positive control (stimulation with PHA). Therefore, we could not reliably report the IFN-γ EliSpot assay results.

2.3.9 Statistical considerations

A sample size of 40 vaccine and 8 placebo recipients was adequate to assess the safety and immunogenicity of the vaccine. Assuming an incidence of adverse events in the vaccine and placebo arm of 10 and 15 per 100 person years, the probability of observing at least one adverse event was 0.87 and 0.95, respectively. The sample size for immunogenicity response rates were based on the phase I study results where 100% responded by the 2nd vaccination. The sample size was adequate to show an immune response in 70-90% of vaccine recipients and an absolute difference of 66% in the proportion of vaccine and placebo recipients with an immune response with 90% power.

Laboratory and immunogenicity parameters were summarised by study arm and visit. The baseline is defined as the measurement at day 0. Comparing cytokine responses (magnitude of response using all participants) between study arms was conducted using the Wilcoxon rank-sum test and between time points using the

Wilcoxon signed-ranks test. The CD4 and log10 (HIV-1 viral load) change over follow-up was estimated for each individual using linear regression and the estimated slopes compared by study arm using the Wilcoxon rank-sum test. All AEs were summarised by system organ class and preferred term by treatment group and visit. The statistical analysis was performed using software STATA version 13.0.

The study protocol and the CONSORT checklist are available as supporting information 2.6.

2.4 Results

2.4.1 Study population

In total, 167 adults were screened and 48 volunteers were enrolled (24 in Tanzania and South Africa respectively); 47 participants completed both vaccinations. The CONSORT diagram is shown in Figure 2.1. Participants in the H1/IC31®, versus placebo, arm were older (median age 35 vs 29.5 years, respectively) and less likely to be female (52.5% vs 75%, respectively) (Table 2.1). The overall proportion of self-reported BCG vaccination was 81.3%, similar by study arm. The median $CD4^+$ T cell count, viral load and other baseline characteristics were similar by study arm (Table 2.1).

2.4.2 Safety and reactogenicity

The safety analysis included data from both study sites. In total 461 AEs were reported (Table 2.2).

H1/IC31® versus placebo recipients were more likely to have one or more local injection site AE (H1/IC31®: 26/40 (65.0%), placebo: 1/8 (12.5%), p=0.015). The

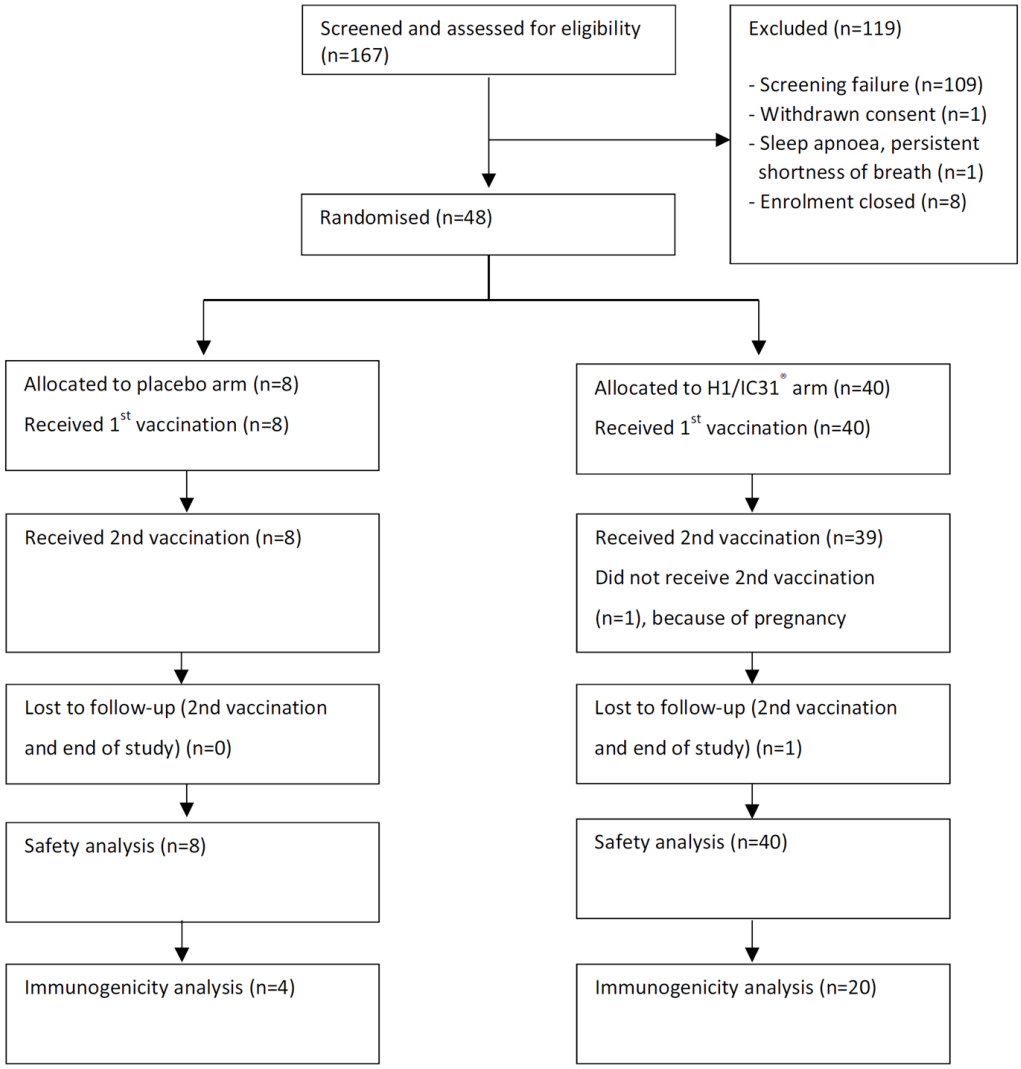

Figure 2.1: CONSORT diagram of subjects for screening, exclusions, randomisation, vaccination and follow-up in the vaccine trial.

Table 2.1: Demographic and baseline characteristics of the study participants by vaccination group.

Variable		**Placebo (n=8)**	**H1/IC31® (n=40)**
Age	Median (IQR)	29.5 (28-41)	35 (30.5-41.5)
Gender	Female n (%)	6 (75.9)	21 (52.5)
Ethnic group*	Black n (%)	8 (100)	40 (100)
Body Mass Index	Median (IQR)	23.1 (20.2-27.0)	23.8 (20.3-30.8)
BCG vaccination (self report)	Yes n (%)	6 (75.0)	33 (82.5)
CD4† (cells(μl)	Median (IQR)	556.5 (464-708)	620.5 (475-725)
Viral load‡ (cp/ml)	Median (IQR)	17887 (544, 43297)	16968 (2228,42547)

* other groups included Indian, White, Asian or mixed heritage
† based on arithmetic mean of participant data from the two screening visits and day 0
‡ based on arithmetic mean of participant data from the first screening visit and day 0
IQR interquartile range

Table 2.2: Adverse events (AEs) during trial period (day 0-182) by vaccination group.

	Placebo n=8		**H1/IC31® n=40**	
	All grades	**Grade ≥3**	**All grades**	**Grade ≥3**
Solicited local AEs				
Any	**1**	**0**	**62**	**0**
Pain	0	0	21	0
Tenderness	0	0	10	0
Erythema	0	0	9	0
Induration	1	0	20	0
Nodules	0	0	2	0
Solicited systemic AEs				
Any	**17**	**0**	**84**	**0**
Malaise	0	0	2	0
Myalgia	4	0	15	0
Headache	4	0	23	0
Nausea	2	0	0	0
Vomiting	0	0	1	0
Arthralgia	1	0	15	0
Fatigue	3	0	22	0
Chills	2	0	2	0
Fever	1	0	4	0
Unsolicited AEs				
Any	**46**	**0**	**251**	**2***
Blood / lymphatic disorders	12	0	48	0
Infections and infestations	10	0	44	0
Renal / unrinary disorders	2	0	28	0
Other AEs	22	0	131	2*
TOTAL	**64**	**0**	**397**	**2***

*reported as possibly related

local AEs in the H1/IC31® arm were graded as mild (55/62, 88.7%) or moderate (7/62, 11.3%) and were either not related (1/62, 1.6%), possibly (23/62, 37.1%), probably (37/62, 59.7%) or (1/62, 1.6%) definitely related. In the H1/IC31® arm, the most frequent solicited local AEs were pain (21/62, 33.9%) and induration (20/62, 32.3%). The one local AE in the placebo arm was assessed as mild and probably related.

29/40 (72.5%) of H1/IC31® participants experienced a total of 84 solicited systemic AEs, which were graded as mild (72/84, 85.7%) or moderate (12/84, 14.3%) and 51.2% (43/84) and 22.6% (19/84) were assessed as possibly or probably related respectively. In the placebo arm, 7/8 (87.5%) participants experienced a total of 17 systemic AEs. These were graded as mild (17/17, 100%) and either unrelated (4/17, 23.5%) or possibly related (13/17, 76.5%). In the H1/IC31® and placebo arms, headache (23/84, 27.4%; 4/17, 23.5%) and fatigue (22/84, 26.2%; 3/17, 17.6%) were the most common solicited systemic AEs. The percentage of patients with at least one solicited systemic AE was similar by study arm (H1/IC31® 29/40 [72.5%] vs placebo 7/8 [87.5%]; p=0.4).

All participants reported one or more unsolicited systemic AE (297 in total). The 40 H1/IC31® recipients experienced 251 unsolicited AEs, which were graded as either mild (215/251, 85.7%), moderate (33/251, 13.2%) or severe (2/251, 0.8%), and one AE was ungraded (pregnancy). Of the 251 unsolicited AEs among H1/IC31® recipients, 152 (60.6%) were not related, 96 (38.3%) were possibly related and 3 (1.2%) were probably related. 46 unsolicited AEs were reported in the placebo group, all considered unrelated (34/46, 73.9%) or possibly related (12/46, 26.1%) and graded as either mild (40/46, 87%) or moderate (6/46, 13%). There were three serious individual case safety reports from two H1/IC31® participants, all classified as unrelated to the investigational product. One participant had two separate hospitalizations for malaria and drainage of a perianal abscess. The second partic-

ipant delivered a premature baby that died as a result of respiratory failure. The participant had a history of one miscarriage in the last trimester and one delivery of another child, who died soon after birth. In the H1/IC31® and placebo arms, unsolicited systemic AE were most frequently categorised as blood and lymphatic disorders (48/251, 19.1%; 12/46, 26.1%) or infections and infestations (44/251, 17.5%; 10/46, 21.7%).

The frequencies of one or more local and systemic solicited AE per participant was similar after the first and the second vaccination with H1/IC31® (solicited local: 50% vs 32.5%, p=0.18; solicited systemic: 60% vs 50%, p=0.25), while unsolicited AEs were less frequent after the second H1/IC31® vaccination (97.5% vs 80%, p=0.007).

QFT positive, versus negative, H1/IC31® recipients had more solicited local reactions (82.3% vs 47.8%, p=0.046), but not solicited systemic (82.3% vs 65.2%, p=0.3) or unsolicited AEs (100% vs 100%).

There were no significant differences in haematology, biochemistry or urinalysis test results at any visit by study arm. The median CD4 slope (per day) over the 182 day follow-up period was -0.86 and -0.59 cells per μl in the H1/IC31® and placebo arms, respectively, indicating no difference by study arm (p=0.85). The median log10 (HIV-1 viral load) slope per day (median -2.9x10^{-4} and -0.54x10^{-4} copies/ml in the H1/IC31® arm and placebo arms, respectively) was also similar by study arm (p=0.93).

2.4.3 QuantiFERON status

At baseline, 17/40 (42.5%) of the H1/IC31® and 3/8 (37.5%) of the placebo participants and participants had a positive QFT result. Conversion from QFT negative to QFT positive was observed in 8 of the 23 (34.8%) H1/IC31® recipients, and

Table 2.3: QuantiFERON status at baseline and at day 182.

					QuantiFERON conversion	
Vaccination Group	**Study day**	**n**	**Positive N (%)**	**Negative N (%)**	**Negative to Positive**	**Positive to Negative**
Placebo	Baseline	8	3 (37.5)	5 (62.5)		
	Day 182	7	1 (14.3)	6 (85.7)	0	1
H1/IC31®	Baseline	40	17 (42.5)	23 (57.5)		
	Day 182	31	17 (54.8)	14 (45.2)	8	2

in none of the placebo recipients. Two of the 17 QFT positive H1/IC31® participants (11.8%) converted to QFT negative by day 182. One initially QFT positive placebo recipient (33.3%) was QFT negative after 182 days. 10 QFT results from 9 H1/IC31® and 1 placebo recipient were missing at day 182 (Table 2.3).

2.4.4 Immunogenicity

Only samples from the 24 participants from the Bagamoyo Site were used for the immunogenicity analysis. None of the whole blood intracellular cytokine assay specimens from the Tembisa site were useable, as they thawed as a result of the liquid nitrogen tank in which they were stored running dry. The gating strategy for flow cytometry analysis is shown is shown in Figure 2.2.

Among H1/IC31® recipients, the median magnitude of $CD4^+$ T cells expressing one or more cytokines (IFN-γ and/or IL-2 and/or TNF-α) in response to Ag85B, ESAT-6 and H1 were greatest two weeks after the second vaccination (day 70), and remained elevated compared with baseline up to day 182 (Figure 2.3).

The greatest $CD4^+$ T cell responses were observed after stimulation with H1 (Figure 2.3). A similar kinetics of response was seen for $CD4^+$ T cell expressing either IFN-γ, IL-2 or TNF-α in response to H1, and there were no significant IL-17 re-

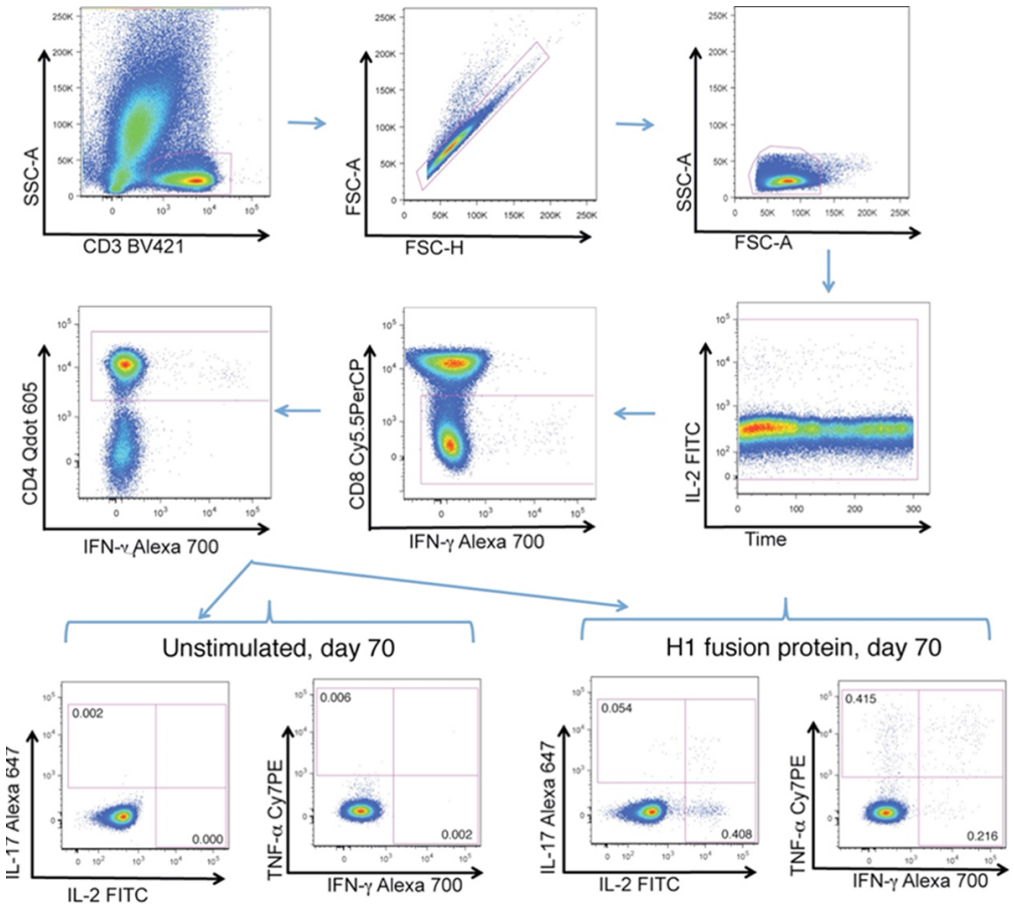

Figure 2.2: Gating strategy used for flow cytometric analysis of H1-induced T cell cytokine expression. The plots show sequentially the gating hierarchy of one representative sample: $CD3^+$ T cells, single cells, lymphocytes, time, $CD8^+$-T cells, which were further gated for $CD4^+$ cells. The plots on the lowest row include the cytokine expression gates for either unstimulated or H1 fusion protein stimulated PBMC at day 70 divided in the co-expression of IL-17 and IL-2 or TNF-α and IFN-γ by $CD4^+$ T cells.

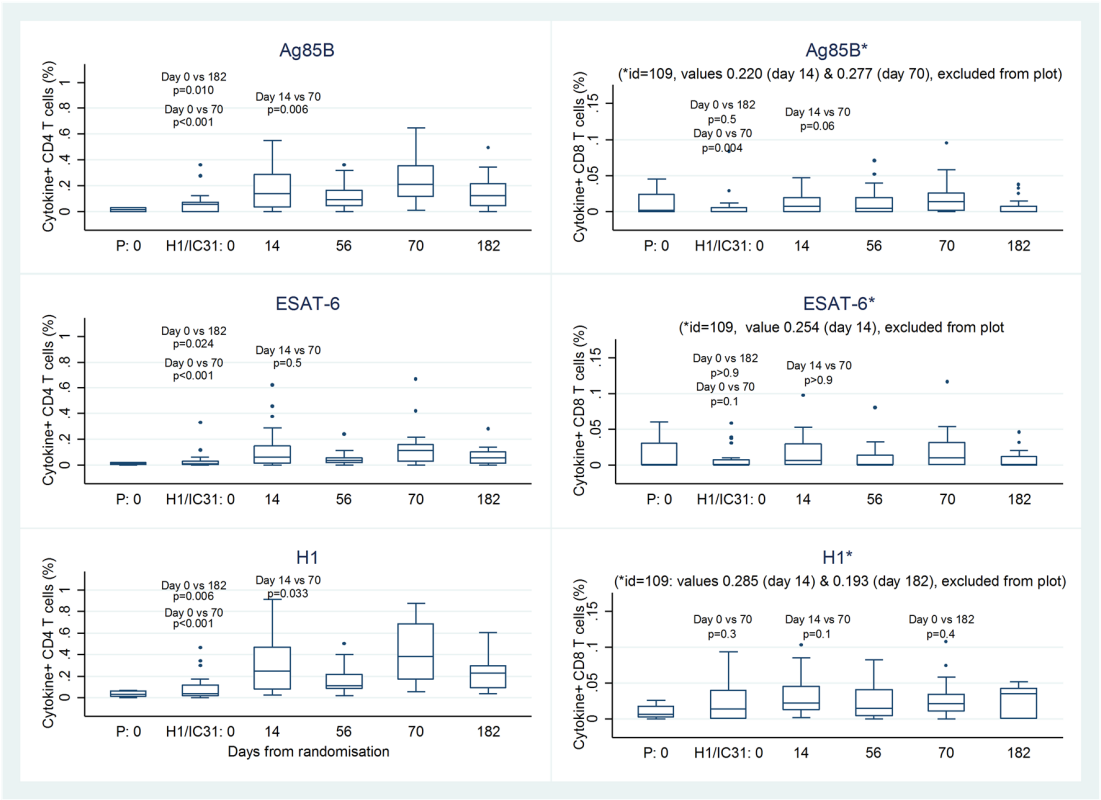

Figure 2.3: Kinetics of Ag85B, ESAT-6 and H1 specific $CD4^+$ and $CD8^+$ T cells expressing IFN-γ, TNF-α or IL-2 for day 0 for the placebo arm (P: day 0) and over a 6-month period (day 0-182) in the vaccine (H1/IC31®) arm detected by a short-term whole blood intracellular cytokine assay.

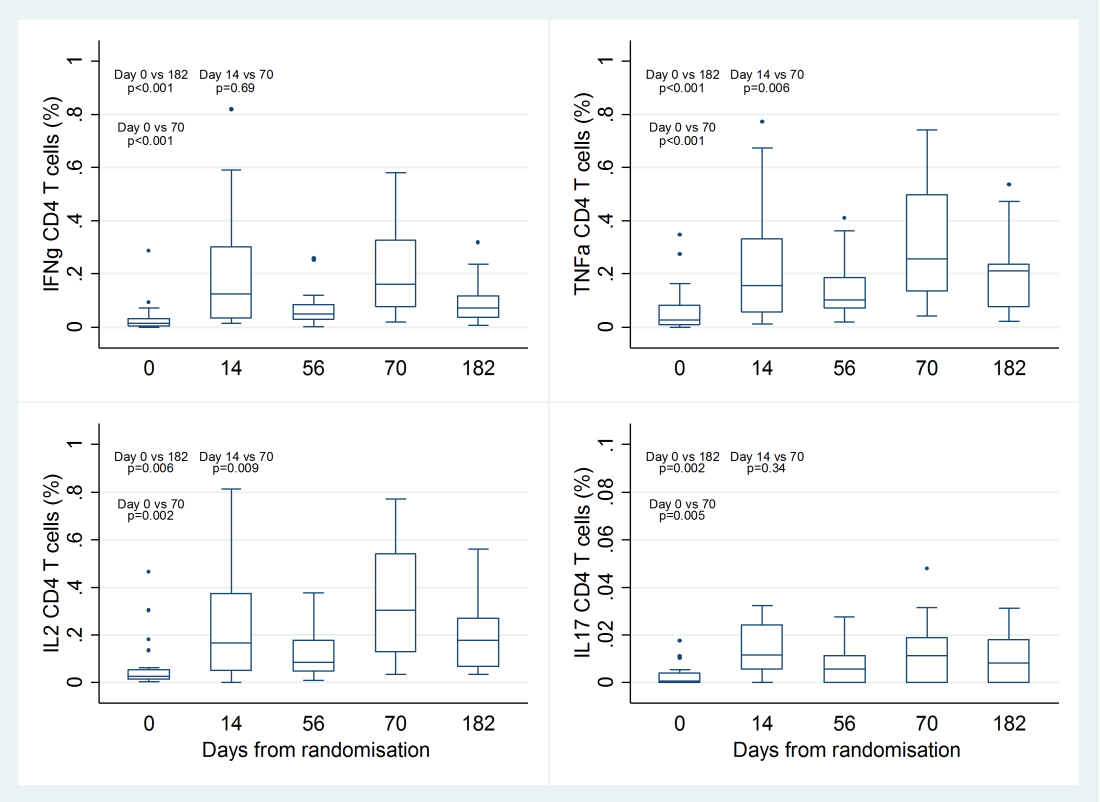

Figure 2.4: Kinetics of IFN-γ, TNF-α, IL-2 and IL-17 expressing $CD4^+$ T cells after stimulation with H1 over a 6-month period (day 0-182) in the H1/IC31® vaccination group detected by a short-term whole blood intracellular cytokine assay. Footnote: sample size for all measurements at days 0, 14 and 56 was n=20 and for day 70 and 182 was n=19.

sponses (Figure 2.4). Among H1/IC31® recipients the magnitude of $CD8^+$ T cells responses to Ag85B, ESAT-6 and H1 did not exceed pre-vaccination levels two weeks after the second vaccination (Figure 2.3).

Among H1/IC31® recipients, the median $CD4^+$ T cell IFN-γ and/or IL-2 and/or TNF-α responses to H1 two weeks post second vaccination (day 70) did not differ by baseline CD4 count (CD4 count<500: 0.34%, 500: 0.38%, p=0.9), or by QFT status (QFT positive: 0.39%, negative 0.38%, p=0.5, Figure 2.5a and 5 2.5b).
The functional capacity of the $CD4^+$ T cells was assessed in the 7 possible cell subsets producing any combination of the IFN-γ, TNF-α or IL-2 in response to H1 stimulation at day 0, 14, 56, 70 and 182 (Figure 2.6). Most reactive $CD4^+$ T cells expressed IFN-γ, TNF-α and IL-2 or TNF-α and IL-2 in response to H1 with a minimum at day 0, a maximum at day 70 and elevated levels at day 182. Single cytokine producing $CD4^+$ T cells most commonly produced IL-2 in response to H1.

2.4.5 Humoral response determined by Anti-Ag85B-ESAT-6 specific IgG antibody assay

There was no difference in IgG levels by study arms two week post second vaccination (day 70) and 182 (data not shown).

2.5 Discussion

This is the first report on safety and immunogenicity of the H1/IC31® subunit TB vaccine administered to HIV-infected adults with $CD4^+$ lymphocyte counts > 350 cells/mm^3. Key findings are: (i) H1/IC31® was safe and well tolerated; (ii)

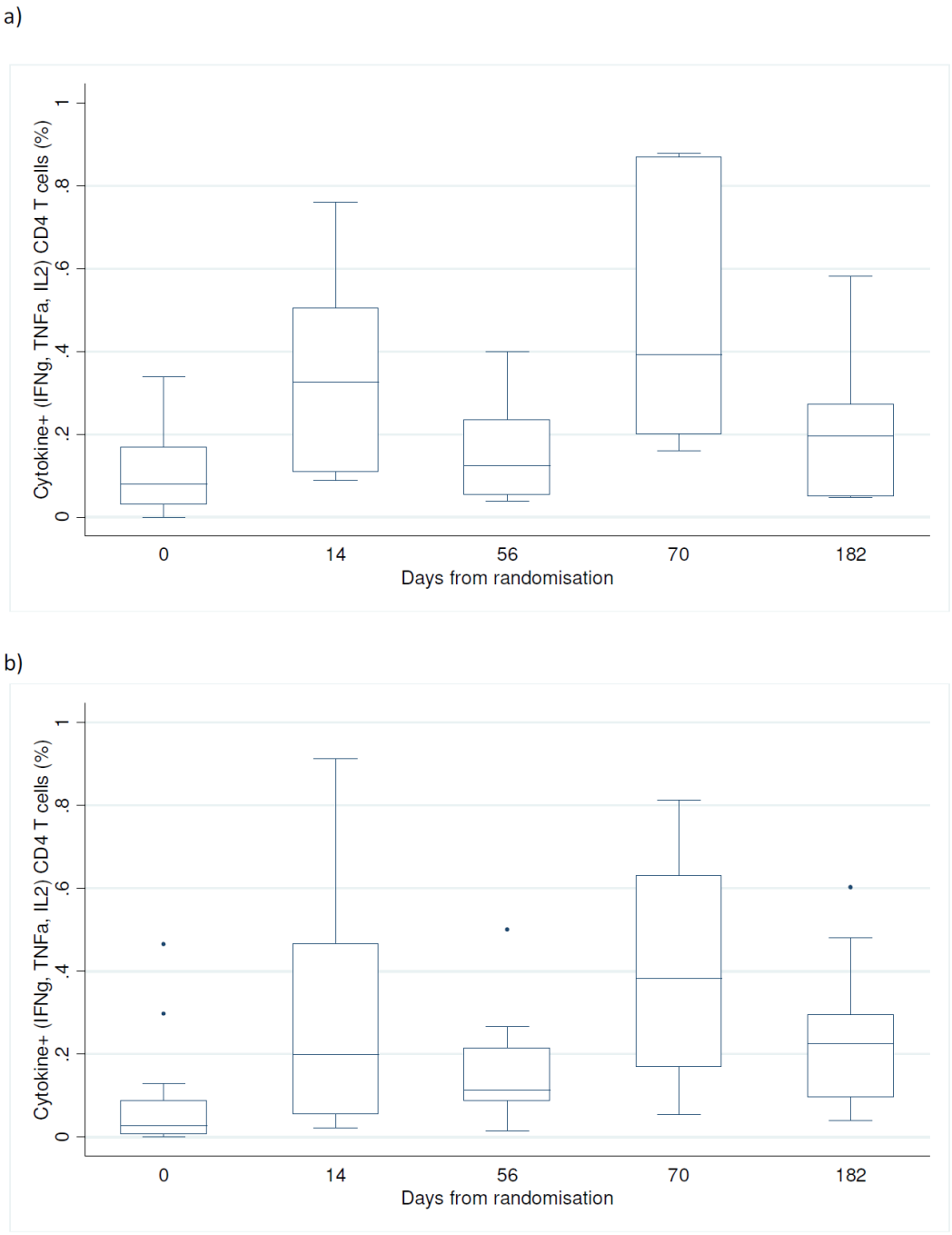

Figure 2.5: Frequencies of H1 specific $CD4^+$ T cells expressing IFN-γ, TNF-α or IL-2 at day 0, 14, 56, 70 and 182, for vaccination group H1/IC31® group [unstimulated frequencies have been subtracted] for a) QFT positive n=6 and b) QFT negative n=14.
Footnote: comparison of $CD4^+$ T cell IFN-γ and/or IL-2 and/or TNF-α responses to H1 at day 70 by those QFT positive or negative, p=0.5.

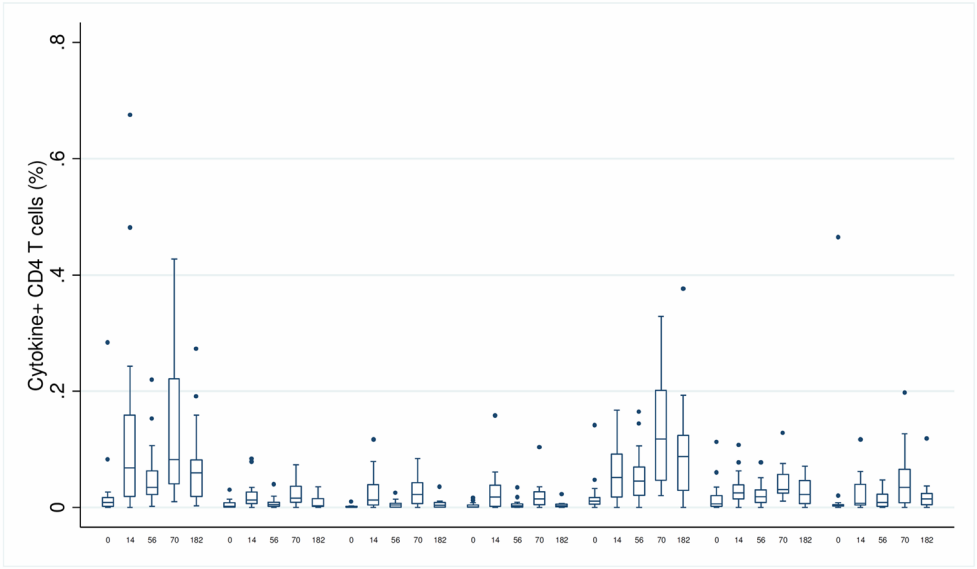

IFN-γ	•	•	•	•			IFN-γ
TNF-α	•	•			•	•	TNF-α
IL-2	•		•		•		• IL-2

P-values from the Wilcoxon signed-ranks test:

Day 0 vs 70	<0.001	<0.001	<0.001	<0.001	<0.001	0.005	0.006
Day 0 vs 182	<0.001	0.03	0.01	0.2	<0.001	0.06	0.06
Day 14 vs 70	0.7	0.8	0.9	0.5	<0.001	0.3	0.03

Figure 2.6: Frequencies of H1 specific $CD4^+$ T cells expressing any combination of IFN-γ, TNF-α and IL-2 at day 0, 14, 56, 70 and 182 in the vaccination group [unstimulated frequencies have been subtracted].

H1/IC31® did not have a negative impact on $CD4^+$ T cell count or on HIV-1 viral load. (iii) H1/IC31® induced a strong, specific and long lasting, $CD4^+$ T cell response; (iv) H1/IC31® vaccination induced primarily triple (IFN-γ, TNF-α and IL-2) or double (TNF-α and IL-2) positive $CD4^+$ T cells.

There is a concern that in HIV-infected individuals, TB vaccines may promote immune activation leading to increased adverse events and progression of HIV. Vaccination with Modified Vaccinia Ankara virus expressing antigen 85A (MVA85A) [240–242] and inactivated *M. vaccae* [243,244] in HIV-infected persons had favourable safety profiles. RUTI vaccination (heat killed *M.tb*, fragmented) of HIV-infected adults was associated with an increased risk of local reactions, including nodules and sterile abscesses [245]. In our study, H1/IC31® vaccination in HIV-infected individuals was tolerable and had a safety profile similar to that seen among H1/IC31® vaccinated, HIV-uninfected, mycobacterially-naive, BCG vaccinated and latently TB-infected individuals in Europe [64,65]. In the present study, there was no major change in $CD4^+$ T cell count and HIV-1 viral load trends, similar to reports on vaccination with MVA85A [240, 241] and Aeras 402 [246].

TB vaccines in HIV-infected individuals potentially may be less immunogenic due to HIV-associated immunosuppression. H1/IC31® vaccination of HIV-infected participants with a high CD4 count (>350 cells/mm^3) induced a specific Th1-type response to the H1 antigen, and its Ag85B and ESAT-6 subunits. We observed some $CD4^+$ T cell IFN-γ responses to the vaccine antigen H1 at enrolment - prior to vaccination. The responses were most prominent in the QFT positive individuals, and probably due to latent TB infections or possibly cross reacting environmental mycobacterial infections. Despite these baseline responses, H1/IC31® vaccination induced significantly higher $CD4^+$ T cell responses that were durable. These results are encouraging and suggest that latent TB infection will not mask an H1/IC31® specific immune response. The magnitude and durability of the Th1 responses in

HIV-infected participants, and the lack of humoral response, has similarly been observed in HIV-uninfected participants [64, 65].

In our study, H1/IC31® induced predominately TNF-α/IL-2 and IFN-γ/TNF-α/IL-2 co-expressing CD4$^+$ T cells with a peak two weeks after the second vaccination which remained elevated for up to 6 months. Both cell subsets, in particular the TNF-α/IL-2 double positive subset, have been found to include a high proportion of central memory T cells [247] [248] and to be less differentiated [249], more long lived [249, 250] and functionally superior [251] to IFN-γ single cytokine expressing T cells. The protective role of polyfunctional CD4$^+$ T cells against tuberculosis infection is still debated. However, several studies have observed a positive correlation between protection against disease and induced T cell polyfunctionality, particularly those expressing IL-2, which is associated with long-term persistence of primed CD4$^+$ T cells in vivo [252–255]. The TNF-α/IL-2 central memory T cell population may be of particular relevance for the activity of these vaccines. In a recent murine study TNF-α/IL-2 central memory T cells were implicated in the long-term control of chronic TB infection [37]. This predominance of the TNF-α/IL-2 subset seems to be characteristic for the IC31® and CAF01 adjuvant. In comparison, the MVA85A, M72/AS01 and M72/AS02 vaccines primarily induced polyfunctional IFN-γ/TNF-α/IL-2 CD4$^+$ T cells [256, 257], while Aeras 402 induced both polyfunctional CD4$^+$ and CD8$^+$ T cells [258].

The role of Th17 cells producing IL-17 is the subject of ongoing debate. Reports suggest that IL-17 producing T cells support a balanced immune response improving the protective efficacy of novel vaccines [257, 259]. In our study, H1/IC31® induced IL-17 mono- or co-expressing CD4$^+$ T cells that were barely detectable post vaccination and contrasts with MVA85A which induced IL-17 producing T cells [257].

H1/IC31® vaccine induced poor CD8$^+$ T cell responses, which has likewise been

described for other vaccine candidates [240, 256]. These findings may be explained by methodological issues of the ex vivo assay system, such as the possible suboptimal length of the peptides used in the assay (15 amino acids) or an inadequate limit of detection [240, 256].

As formerly reported, H1/IC31® vaccination can lead to conversion of the QFT result because of its ESAT-6 component [64, 65]. In our study, this phenomenon occurred in one third of initially QFT negative participants. However, reversions suggest that some of the observation might also be attributed to within-subject variability of the QFT assay [260]. The concern that H1/IC31® can interfere with IFN-γ release assays (IGRA) such as QFT for detection of LTBI has becomes less important since the WHO does not recommend IGRA to replace tuberculin skin tests in resource-constrained settings [261], where the vaccine would be broadly used. Furthermore, new tests using diagnostic markers other than ESAT-6 for disease screening are under development and have the potential to eliminate the issue of interference with the vaccine for low- and high-burden countries [262].

New subunit TB vaccines should boost the efficacy of BCG and prevent TB infection and prevent latent TB infection from progressing to active disease. Both mechanisms are essential for the control of the TB epidemic. In order to achieve a better post-exposure protection, the Statens Serum Institute has added a latency-associated antigen (Rv2660c) to the H1/IC31® backbone, to create a multistage vaccine, H56 (Ag85B-ESAT-6-Rv2660c) [263]. Our trial of H1/IC31® provides valuable information to support the clinical development of the novel multistage vaccine H56. Particularly important is that H1/IC31® induces multifunctional T cells expressing TNF-α and IL-2, markers of central memory T cells, which are required for long-term protection against both reactivation and infection [37]. This is critical for the vaccination of vulnerable populations such as HIV-infected individuals who often have a high level of exposure to TB and a relatively high

prevalence of latent TB infection. Inevitably, the multistage H56 vaccine should also be evaluated in HIV-infected individuals to ensure that it confers durable immune protection in this target group.

The present study had a number of limitations. The study was not powered to show difference between subgroups, particularly by baseline QFT status. The whole blood intracellular cytokine staining data from one site and IFN-γ EliSpot assay data from both sites did not meet the internal quality control standards, which limits comparability to other TB vaccine trials. The restriction to HIV-infected individuals with $CD4^+$ lymphocyte counts greater than 350 cells/mm^3 was necessary because of safety concerns, but limits the generalizability of the results.

In conclusion, the intramuscular injection of the adjuvanted TB subunit vaccine H1/IC31® was safe and immunogenic in HIV-infected adults, with $CD4^+$ lymphocyte counts greater than 350 cells/mm^3, from TB endemic areas.

2.6 Supporting Information

S1 Protocol. Study protocol of the study 'Phase II Double-Blind, Randomized, Placebo-Controlled Study to Evaluate the Safety and Immunogenicity of H1/IC31®, an adjuvanted TB Subunit Vaccine, in HIV-Infected Adults with $CD4^+$ Lymphocyte Counts Greater than 350 cells/mm^3.'

`http://www.plosone.org/article/fetchSingleRepresentation.action?uri=info:doi/10.1371/journal.pone.0114602.s001` (PDF)

S1 Checklist. Consolidated Standards of Reporting Trials (CONSORT) checklist.

`http://www.plosone.org/article/fetchSingleRepresentation.action?uri=info:doi/10.1371/journal.pone.0114602.s002` (DOC)

2.7 Acknowledgments

We want to thank all participants in this trial. The authors are grateful to the sponsor, the Statens Serum Institut, and the members of the Data Safety Monitoring Board: Dr. Anthony Hawkridge, Prof. Jaap van Dissel, Prof. Clive Gray, Prof. Eyasu Makonnen, and Prof. Gibson Kibiki.

Chapter 3

Antiviral innate immune activation in HIV infected adults negatively affects H1/IC31® induced vaccine-specific memory $CD4^+$ T cells

---

This chapter is an adapted version of the following publication:
Lenz N, Schindler T, Kagina BM, Zhang JD, Lukindo T, Mpina M, Bang P, Kromann I, Hoff ST, Andersen P, Reither K, Churchyard GJ, Certa U, Daubenberger CA. Antiviral innate immune activation in HIV infected adults negatively affects H1/IC31® induced vaccine-specific memory $CD4^+$ T cells. Clin Vaccine Immunol., pii:CVI00092-15, 2015

3.1 Abstract

Tuberculosis (TB) remains a global health problem, with vaccination being a necessary strategy for disease containment and elimination. A TB vaccine should be safe and immunogenic as well as efficacious in all affected populations, including HIV infected individuals. We investigated the induction and maintenance of vaccine-induced memory $CD4^+$ T cells following vaccination with the subunit vaccine H1/IC31®. H1/IC31® was inoculated twice on study days 0 and 56 among HIV infected adults with $CD4^+$ lymphocyte counts greater than 350 cells/mm^3. Whole venous blood stimulation was conducted with the H1 protein and memory $CD4^+$ T cells were analysed using intracellular cytokine staining and polychromatic flow cytometry. We identified high, intermediate and non-responders based on detection of IL-2, TNF-α and IFN-γ expressing central and effector memory $CD4^+$ T cells (T_{CM} and T_{EM}) 182 days after first immunization. Amplicon based transcript quantification using next generation sequencing was performed to identify differentially expressed genes that correlate with vaccine-induced immune responses. Genes implicated in resolution of inflammation discriminated responders from non-responders three days after the first inoculation. Volunteers with higher expression levels of genes involved in anti-viral innate immunity at baseline showed impaired H1-specific T_{CM} and T_{EM} maintenance 6 months after vaccination. Our study showed that in HIV infected volunteers expression levels of genes involved in anti-viral innate immune response affected long-term maintenance of H1/IC31® vaccine induced cellular immunity.

3.2 Introduction

Vaccination represents one of the most successful health interventions for disease containment, elimination and eventual eradication [264]. Despite more than fifty years of wide-spread vaccination with Bacille Calmette-Guérin (BCG), tuberculosis (TB) remains one of the world's most serious infectious diseases. In 2012, the World Health Organization (WHO) estimated there were 9 million new clinical TB cases and 1 million people died from TB [1]. Infection with the human immunodeficiency virus (HIV) impairs host resistance leading to a faster and higher rate of progression from latent to clinical TB [265]. Consequently, there is an urgent need for developing improved TB vaccines, which are more efficacious, safer and more immunogenic than BCG in all populations, including HIV infected individuals. H1/ IC31® is a protein subunit vaccine against *Mycobacterium tuberculosis* (*M.tb*), consisting of a fusion protein of the mycobacterial antigen-85B and early secretory antigenic target-6 called Hybrid 1 (H1) in combination with the adjuvant IC31®. IC31® is composed of the cationic polyaminoacid KLK and a single stranded oligodeoxynucleotide with alternating sequences of the nucleic acids inosine and cytidine (ODN1a) [266]. KLK enables simultaneous uptake of H1 and ODN1a in antigen presenting cells and provides a platform for hyper-efficient toll like receptor (TLR)-9 ligand recognition of ODN1a. Upon triggering of TLR-9, conventional dendritic cells and monocytes activate the MyD88-NF-κB dependent signalling cascade [73]. This leads to secretion of pro-inflammatory cytokines and finally induction of adaptive immune responses. Additionally to the MyD88-NF-κB dependent pathway, plasmacytoid dendritic cells (pDC) have the unique ability to signal in a MyD88-IRF7 dependent way. This yields in production of abundant quantities of type I interferon (IFN) [74, 75].

In HIV infected individuals, vaccine take and durability of the immunity are neg-

atively affected upon manifestation of progressed HIV disease [85]. The HI-virus is detected by the innate immune system primarily by recognition of viral nucleic acids. Endosomal TLR-7 and -8 and cytosolic RIG-1 like receptors sense single stranded viral RNA (ssRNA), which leads to secretion of pro-inflammatory cytokines and type I IFNs [88]. Using a TLR-9 agonist as adjuvant could needs to be tested and analysed carefully in HIV infected individuals, since the downstream signalling cascades of TLR-7, TLR-8 and TLR-9 are shared [74, 75].

We conducted a phase II, double blind, randomized and placebo controlled trial to evaluate the safety and immunogenicity of H1/ IC31® in BCG vaccinated, HIV infected adults with a $CD4^+$ lymphocyte count greater than 350 cells/mm^3 [267]. Principal findings were that the vaccine was safe and immunogenic. $CD4^+$ lymphocyte counts and viral loads remained stable during the entire study period. The aim of this study was to analyse mRNA expression levels before and shortly after H1/ IC31® vaccination and correlate these with vaccine specific central and effector memory $CD4^+$ T cell (T_{CM} and T_{EM}) responses. Whole venous blood stimulation assay [267] was used to monitor the vaccine induced cellular immune response over a follow up period of 182 days. Using AmpliSeq and next generation sequencing the expression changes of 1388 genes in peripheral blood was determined [268]. We describe for the first time that a higher expression level of genes involved in anti-viral innate immunity at baseline reduces long-term maintenance of vaccine responses in HIV infected volunteers.

3.3 Methods

3.3.1 Ethics statement

This study was conducted according to Good Clinical Practice Guidelines and the declaration of Helsinki. Informed consent was obtained from all participants. Detailed description of ethical approvals can be obtained from Reither et al. [267]. The clinical trial is registered in the Pan African Clinical Trials Registry (PACTR) with the identifier PACTR201105000289276.

3.3.2 Participant enrolment and blood collection

24 HIV-positive, BCG vaccinated volunteers with $CD4^+$ T cell counts greater than 350 cells/mm^3 from Bagamoyo, United Republic of Tanzania, were enrolled. Participants were randomly allocated in a ratio of 5:1 to receive placebo or H1/IC31® vaccine. One H1/ IC31® vaccine recipient dropped out before booster vaccination due to pregnancy. 0.5ml containing 50μg Ag85B-ESAT-6 and 500nmol KLK +20nmol ODN1a (adjuvant) or 0.5ml Tris buffer (placebo) were administered intramuscularly on study day 0 and 56. For transcriptomics analysis, 2.5ml of peripheral blood was collected via sterile venipuncture in RNA PaxGene vacutainers (PreAnalytiX) on day 0, 3 and 59. 9ml of peripheral blood was collected in sodium heparin tubes and directly processed in whole blood stimulation assays on day 0, 14, 56, 70 and 182. An extended description of the study design can be obtained from Reither et al. [267].

3.3.3 Intracellular cytokine staining (ICS) and analysis by flow cytometry

The ICS and flow cytometry analysis have already been described in [267]. Present project focused on the analysis of cytokine producing memory $CD4^+$ T cell subsets. Briefly, ex vivo whole blood was directly stimulated with either the H1 fusion protein (Statens Serum Institute (SSI), at 5μg/ml) or with phytohaemagglutintin (Bioweb at 5μg/ml) or left unstimulated. The co-stimulatory antibodies anti-CD28 and anti-CD49d (Becton Dickinson (BD) Biosciences, at 0.5μg/ml) were included in all assay conditions. Whole blood was incubated for 7 hours at 37°C and 5% CO_2 and then treated with Brefeldin-A (Sigma Aldrich at 10μg/ml). Subsequently, whole blood was transferred to a waterbath at 37°C and incubated for 5 hours. The waterbath was switched off and was allowed to reach room temperature. Within 10 hours the blood was harvested, EDTA (Sigma Aldrich at 1.8mM) was added and red blood cells were lysed in FACSlysing solution (BD Biosciences). Remaining white blood cells were preserved in cryosolution containing 50% RPMI (Lonza), 40% fetal calf serum (BioWest) and 10% DMSO (Sigma Aldrich).

For ICS, samples of each phlebotomy date of one particular participant were thawed simultaneously in a waterbath at 37°C. Cells were transferred to tubes containing PBS (BioWhittaker), washed and permeabilised using Perm/Wash solution (BD Biosciences). The flow cytometry staining was completed with the following anti-human antibody panel: CD3-BV421 (BD Biosciences, MOPC-21), CD4-QDot605 (Invitrogen, S3.5), CD8-Cy5.5PerCP (BD Biosciences, SK1), CCR7-PE (eBioscience, 150503), IFN-γ-Alexa 700 (BD Biosciences, B27), TNF-α-Cy7PE (eBioscience, Mb11), IL-2-FITC (BD Biosciences, 5344.111), IL-17-Alexa 647 (eBioscience, SCPL1362) and CD45RA BV 570 (eBioscience, H1100). For each fluorochrome a single stained mouse κ CompBead (BD Biosciences) control was in-

cluded. The samples were acquired on a LSR II flow cytometer (BD Biosciences, San Jose CA) and data analysis was performed using FlowJo software (version 10.0.7, treestar). The following gating strategy was used (Figure 3.1): CD3 positive cells were gated plotting CD3-BV421 versus side scatter-area (SSC-A). The singlets were selected plotting forward scatter-area (FSC-A) versus forward scatter-height (FSC-H) and the lymphocytes were gated with FSC-A versus SSC-A. Time versus IL-2-FITC was gated to exclude bubbles and varying fluidics pressure. The IFN-γ-Alexa 700 versus CD8-PerCp-Cy5.5 plot was used to gate the CD8 negative cells. The CD4 positive cells were selected plotting IFN-γ-Alexa 700 versus CD4-Qdot 605. The memory subsets were defined using the CD45-RA-BV570 versus CCR7-PE plot. To identify cytokine positive cells from all 4 memory subsets, each cytokine was plotted against CD4-Qdot605. FlowJo version 10.0.7 (Tree Star) was used for the analysis. This project focused on the detection of the cytokines IL-2, IFN-γ and TNF-α. The production of IL-17 by $CD4^+$ T cells was not significantly different after booster vaccination [267].
A detailed description following the MIFlowCyt reporting standard for flow cytometry experiments can be accessed in the appendix 6.1 [269].

3.3.4 Extraction of total RNA

Total RNA was directly extracted from PAXgene Blood RNA tubes using the PAXgene Blood RNA Kit (PreAnalytiX, Hombrechtikon, Switzerland) according to the manufacturer's protocol. The concentration of total RNA and RNA Integrity Number were determined by Agilent RNA 6000 Nano Kit (Agilent Technologies, Waldbronn, Germany). RNA samples were stored at -80°C.

3.3.5 AmpliSeq panels

We used two custom-made AmpliSeq primer panels to quantify gene expression. The Pathway Reporter Panel covered 917 genes providing a general snapshot of the whole human transcriptome. The rationale and design of this panel is described elsewhere (Zhang et al., manuscript submitted). The second AmpliSeq primer panel, the Immune Response Panel, was developed based on a literature-driven collection of 826 genes implicated in innate and adaptive immune responses. Functional enrichment analysis with Biological Process (BP) terms of Gene Ontology suggests that the prioritized genes are highly enriched in innate and adaptive immune response pathways. The selected genes were submitted via web interface for primer design and synthesis using proprietary algorithms (`www.ampliseq.com`).

3.3.6 Amplicon-based transcript quantification by semiconductor sequencing

The amplicon based transcript quantification was performed using an Ion Proton semiconductor sequencer. This methodology was previously described by Zhang et al. [268] and strictly followed. Briefly, AmpliSeq libraries were prepared using 30 ng total RNA according to the protocol supplied with the Ion AmpliSeq RNA Library Kit (Life Technologies, Carlsbad, USA, Catalog number 4482335). The amplified and purified libraries were stored at -20°C. Library size distribution and concentration were measured using an Agilent High Sensitivity DNA Kit (Agilent Technologies, Waldbronn, Germany) according to the manufacturer's recommendation. Following library preparation barcoded samples were pooled and processed together. Total 8 pM of the multiplexed library was linked to Ion Sphere Particles and clonally amplified by emulsion PCR using the Ion PI Template OT2 200 Kit v3 with the Ion OneTouch 2 Instrument according to the manufacturer's proto-

col (Life Technologies, Carlsbad, USA). Sequencing was performed using the Ion PI Sequencing 200 Sequencing Kit v3 and the Ion Proton chip I following manufacturer's instructions on the Ion Proton Sequencer (Life Technologies, Carlsbad, USA). The generated reads were aligned to the Homo sapiens RNA Canonical Transcript reference hg19 and mapped to the genes of the corresponding AmpliSeq panel using the Torrent Mapping Alignment Program. Simultaneously, single nucleotide polymorphisms (SNPs) within the amplicons were identified during this process using the Ion Torrent Variant Caller.

3.3.7 Statistical analysis

Analysis of memory $CD4^+$ T cells: Two-sided Wilcoxon signed rank test was performed to test for significance of polyfunctional memory $CD4^+$ T cells subsets between study days. Participant's responses to the vaccine were calculated using the Mimosa package within R software [270, 271]. After correcting for the T cell response obtained from unstimulated controls, absolute counts of cytokine (IFN-γ and/or IL-2 and/or TNF-α) expressing T_{CM} or T_{EM} and counts of T_{CM} or T_{EM} negative for cytokine expression were compared between day 0 and each follow-up (day 14, day 56, day 70 and day 182) (Table 3.1). Final responder were defined based on comparison of day 0 to day 182 and with a false discovery rate (FDR) >0.0001 for non-responder, FDR $>10^{15}$ for intermediate and a FDR $<10^{15}$ for high-responder.

AmpliSeq Data Analysis: AmpliSeq data were analysed using the Bioconductor edgeR package based on negative binomial distribution [272]. For each vaccine responder group we performed differential expression analysis through the time course comparing the two post-vaccination time points to the pre-vaccination time point. Furthermore, gene expression was compared between the vaccine respon-

der groups in order to identify gene expression which differs at baseline. Standard settings were used and only those genes with higher expression than 5 counts-per-million reads (cpm) in at least 3 samples and a FDR <0.1 were considered as differentially expressed. Annotation of differentially expressed genes was performed using the previously published blood transcription modules (BTMs) [273]. Statistical analysis and plots were made using R version 3.1.0 [271].

3.4 Results

3.4.1 Cytokine producing memory CD4$^+$ T cell subsets

Based on chemokine receptor CCR7 and the surface marker CD45-RA expression, four subsets of CD4$^+$ memory T cells could be identified: stem cell memory T cells (T_{SCM}), T_{CM}, T_{EM} and effector memory T cells re-expressing CD45-RA (T_{EMRA}) (Figure 3.1) [79,80,274]. We measured the development and magnitude of the H1/ IC31® induced memory CD4$^+$ T cell subsets expressing IL-2, IFN-γ and TNF-α following in vitro stimulation with the H1 protein. At day 182, T_{CM} and T_{EM} were significantly elevated compared to placebo controls (Figure S3.1). To measure the quality of the immune response, we discriminated the memory CD4$^+$ T cell subsets according to their polyfunctional cytokine expression profile. Figure 3.2a displays the mean percentages of cytokine expression of all memory subsets according to their polyfunctionality. The T_{SCM} and T_{EMRA} compartments were too low to appear on the graph. In agreement with Reither et al. [267], the H1/ IC31® specific T_{CM} and T_{EM} were predominantly tri-functional or bi-functional expressing IL-2 and TNF-α.

In Figure 3.2b and c T_{CM} and T_{EM} are displayed separately. Comparing day 0 to day 182, a statistically significant increase of bi-functional T_{CM} expressing IL-2

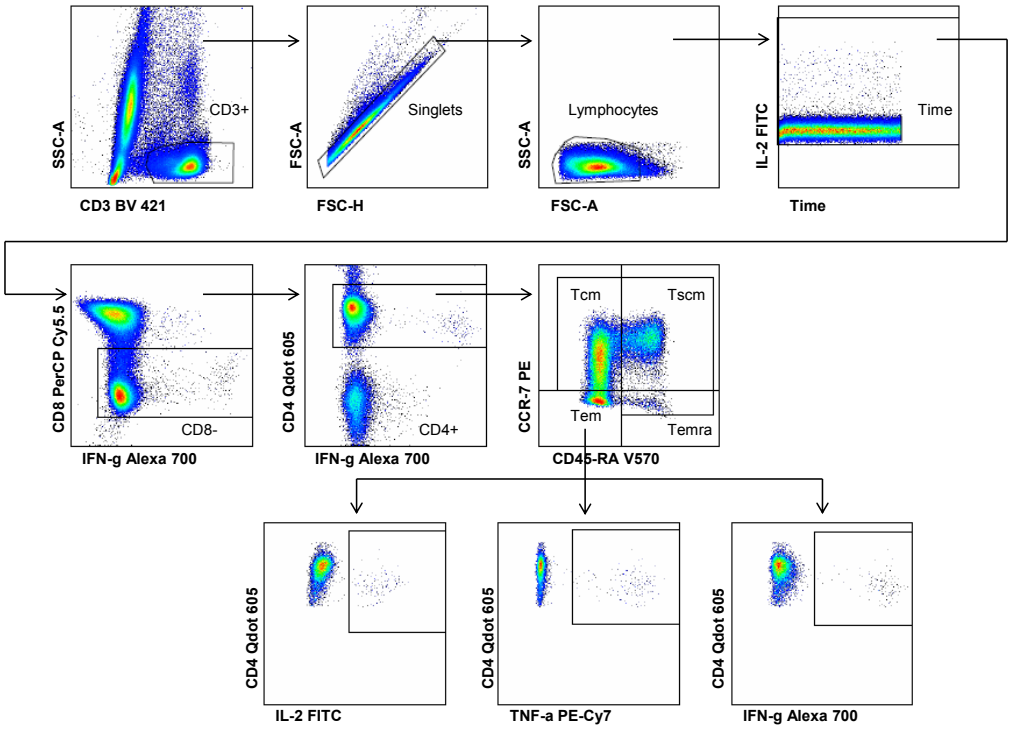

Figure 3.1: Gating strategy used for flow cytometric analysis of H1-induced memory $CD4^+$ T cell cytokine expression. The plots show sequentially the gating hierarchy of one representative sample: $CD3^+$ T cells, single cells, lymphocytes, time, $CD8^+$ T cells, which were further gated for $CD4^+$ cells and split into all memory subset on the basis of CCR7 and CD45-RA surface markers. The lowest row comprises the plots with the cytokine expression gates for H1 fusion protein stimulated T_{EM} at day 182. IL-2, TNF-α and IFN-γ expression was measured. T_{SCM}=stem cell memory T cell, T_{CM}=central memory T cell, T_{EM}=effector memory T cell, T_{EMRA}=effector memory T cell re-expressing CD45-RA, H1=Hybrid 1.

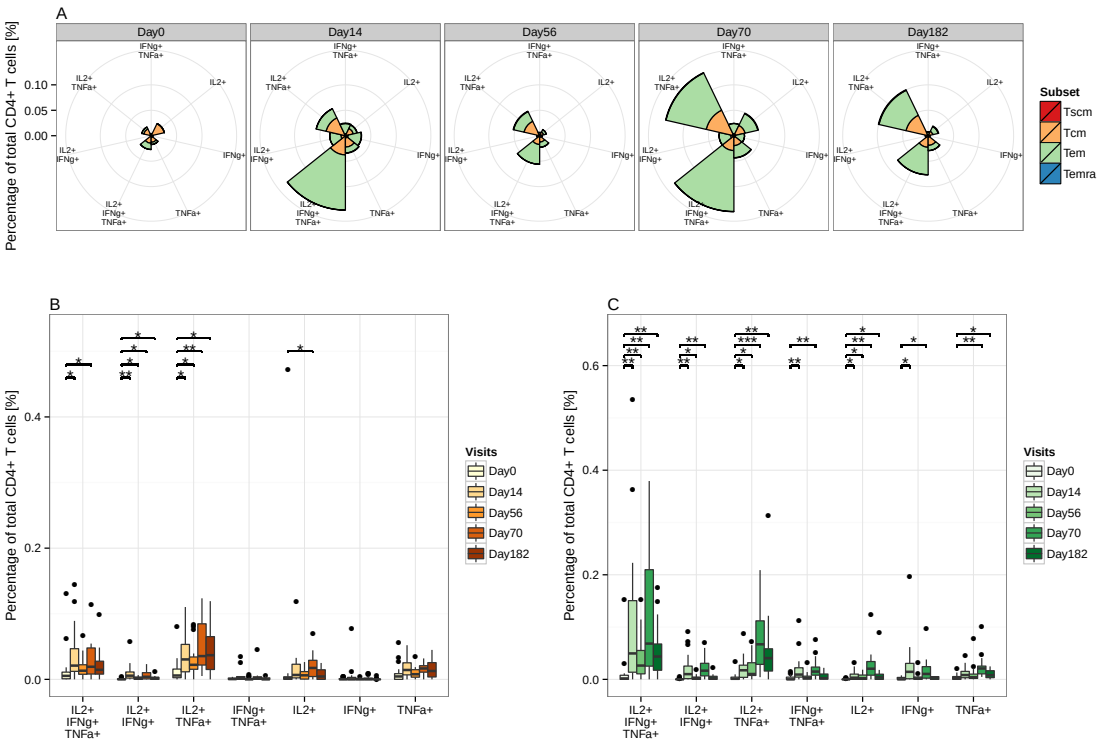

Figure 3.2: Cytokine expression profile of memory CD4$^+$ T cell subsets following H1 fusion protein stimulation. Volunteers receiving H1/IC31® are included A) Mean percentage of all memory CD4$^+$ T cell subsets on the basis of all possible combinations of IL-2, IFN-γ and TNF-α expression. REMARK: Radii and not area of each segment represent percentage of CD4$^+$ T cells. B) T_{CM} and C) T_{EM} expressing all combinations of IL-2, IFN-γ and TNF-α following stimulation with H1. P-values correspond to significance testing comparing each study day to study day 0 ($*$=p-value$<$0.0125, $**$=p-value$<$0.001, $***$=p-value$<$0.0001).
Two-sided Wilcoxon signed rank test with the Bonferroni correction was applied. T_{SCM}=stem cell memory T cell, T_{CM}=central memory T cell, T_{EM}=effector memory T cell, T_{EMRA}=effector memory T cell re-expressing CD45-RA, H1=Hybrid 1.

with TNF-α (p-value<0.05) was observed. This was also observed in bi-functional T_{CM} expressing IL-2 with IFN-γ, although at extremely low percentages.
Tri-functional and bi-functional (IL-2 and TNF-α) T_{EM} were most significantly elevated comparing day 182 to day 0 (p-value<0.01), which is followed by mono-functional (IL-2 or TNF-α) T_{EM} (p-value<0.05).

3.4.2 Definition of vaccine responder groups

To investigate potential innate immune mechanisms that yield differential vaccine immunogenicity in our study participants, we divided the volunteers according to their cytokine responses (IFN-γ, IL-2 and/or TNF-α) comparing H1 specific T_{CM} and T_{EM}.

An overview of potential responder grouping comparing each study day to the baseline at day 0 is given in Table 3.1A. Comparing day 70 to day 182 several volunteers shifted from a responder to non-responder, indicating discriminative memory maintenance.
No significant difference in relation to viral load and $CD4^+$ lymphocyte counts between these groups was observed (Table 3.1B).
Grouping the volunteers based on comparison of day 0 to day 182 allowed us to identify innate immune mechanisms that potentially lead to improved T_{CM} and T_{EM} maintenance.

3.4.3 Gene expression data

On average 4'686'802 reads (95% confidence interval (CI) ± 712'607 reads) per sample were generated and mapped to either the 826 genes of the AmpliSeq Immune Response panel or the 917 genes of the Pathway Reporter Panel. A dynamic range of five orders of magnitude was observed ranging from genes with no de-

Table 3.1: A) Overview of responder groups based on either T_{CM} or T_{EM}, B) demographics including information about HIV infection status of final responder groups based on comparison of day 0 to day 182.

A Number of Participants in each group [non/intermediate/high]

	Day14	Day56	Day70	Day182
T_{CM}	6/6/7	11/3/5	5/6/8	8/5/6
T_{EM}	3/5/11	4/5/10	2/2/15	4/6/9

B Day 182

	Responder	n	Age	Gender [F/M]	Viral Load [Log2]	$CD4^+$ Count [cells/μl]
Placebo		4	38 ±13	3/1	11.5 ±5.3	575 ±250
T_{CM}	High	6	35 ±5	2/4	12.1 ±3.8	823 ±266
T_{CM}	Intermediate	5	46 ±5	2/3	14.0 ±3.1	529 ±64
T_{CM}	Non	8	38 ±6	6/2	14.3 ±2.7	618 ±181
T_{EM}	High	9	38 ±7	4/5	12.3 ±3.4	698 ±284
T_{EM}	Intermediate	6	40 ±9	2/4	14.4 ±3.4	604 ±90
T_{EM}	Non	4	39 ±5	4/0	14.9 ±1.2	644 ±226

n=number of volunteers, F=female, M=male, after ±: standard deviation

tectable expression like IFN-κ and genes expressing more than 160'000 reads like lysozyme and CD74. Both AmpliSeq panels shared 355 genes, whose transcript abundance measurement closely correlated (R^2 =0.9829).

The expression levels of nine endogenous control genes did not differ significantly between the 24 volunteers included here across all time points supporting the robustness of the AmpliSeq based targeted transcriptome measurement approach (Figure 3.3a).

3.4.4 Vaccine-induced differential gene expression

Next we addressed if early changes in the whole blood gene expression levels of the targeted 1388 genes could distinguish the three responder groups of each memory subset. The results are comprised in Figure 3.3b and more detailed in Table S3.1. T_{CM} as well T_{EM} intermediate and high-responders showed an up-regulated gene expression three days post vaccination. For T_{CM} responders 5 genes could be identified as up-regulated, namely COL1A1, ELN, CTGF, SERPINE1 and POSTN. T_{EM} responders had an additional 5 genes with increased expression including COL3A1, COL1A2, FN1, ID1 and DCN.

Most of the 10 differentially expressed genes are either annotated in BTMs involved in integrin interactions, extracellular matrix and cell adhesion (COL1A1, COL1A2, COL3A1, CTGF, FN1, POSTN) or known to be part of extracellular matrix remodelling (ELN or SERPINE1). ID1 is involved in leukocyte differentiation. HSPA1A is the only gene which was up-regulated in T_{EM} non-responder. This gene encodes for a heat shock protein and is involved in stress response. No differential gene expression in the placebo controls was observed.

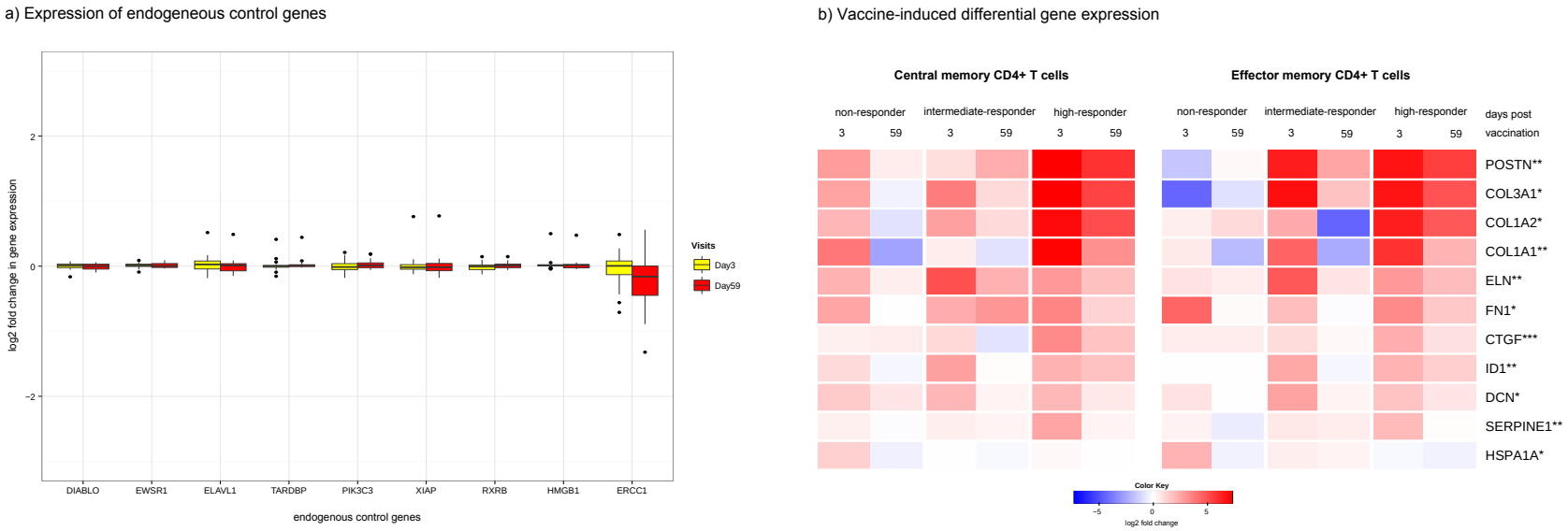

Figure 3.3: A) Gene expression of endogenous control genes. Variation in expression of nine control genes between subjects and over time and log2 fold changes between baseline and the two visits after each vaccination for all 24 volunteers are demonstrated. B) Heat map demonstrating vaccine induced differential gene expression between T_{CM} and T_{EM} responder groups. Log2 fold changes in gene expression 3 or 59 days after vaccination compared to pre-vaccination levels are shown. Differentially expressed genes were identified using edgeR with FDR < 0.1 (**=significant for T_{CM} and T_{EM}, *=significant for T_{EM} only). Only changes in gene expression three days after vaccination were significant.

3.4.5 Differential immune activation at baseline

Next we addressed if gene expression levels at baseline before first vaccination could distinguish the responder groups. Table 3.2 comprises an overview of all genes that differed significantly at baseline between the vaccine responder groups either based on T_{CM} or T_{EM}. Compared to non-responder, higher gene expression was observed for ITGB4, CLEC1C and CXCL6 for T_{CM}-high-responder and PRKDC, CD19, DNAJB5, MARCO and IRS2 for T_{EM}-high-responder. TGM2, **OAS1** and **IFI27** showed the lowest expression among T_{CM}-high-responder, whereas AICDA, NFATC2, **IFI27**, **IFIT3**, **IFIT1** and **CXCL10** were lower expressed in T_{EM}-high-responder. Tissue transglutaminase (TGM) has a role in HIV pathogenesis and enhanced levels of its degradation product, $\epsilon(\gamma$-glutamyl)lysine, is found in the blood in patients with progressed HIV [275]. AICDA and NFATC2 take part in the antiviral immune response with the role of affinity maturation and class switching of antibodies and inhibition of viral replication [276, 277]. According to annotation with BTMs, lower expressed genes in bold are members of the innate antiviral immunity. We analysed the gene expression of all genes available in both AmpliSeq panels that belonged to these BTMs (Figure 3.4a). Clearly, at baseline both non-responder groups showed a higher transcription of members of BTM M150 (innate antiviral response), M165 (enriched in activated dendritic cells), M75 (anti-viral IFN signature), M127 (type I interferon response), M13 (innate activation by cytosolic DNA sensing) and M68 (RIG-1 like receptor signalling).

The expression levels of genes involved in innate immunity to viruses (IRF7, IFI27, IFIT3, EIF2AK2, DHX58, IFIT1, CCL8, OAS1) showed an association with HIV-1 viral loads (Figure 3.4b).

Table 3.2: Table including genes which are differentially expressed between the different vaccine responder groups for T_{CM} and T_{EM}.

	Gene Expression levels at baseline: High responders compared to low responders.	
	Higher expressed genes	Lower expressed genes
T_{CM}	ITGB4	TGM2
	CLEC1A	**OAS1**
	CXCL6	**IFI27**
T_{EM}	PRKDC	AICDA
	CD19	NFATC2
	DNAJB5	**IFI17**
	MARCO	**IFIT3**
	IRS2	**IFIT1**
		CXCL10

Differentially expressed genes were identified using edgeR with FDR <0.1 and grouped in genes higher or lower expressed in the high-responder group compared to non-responder.

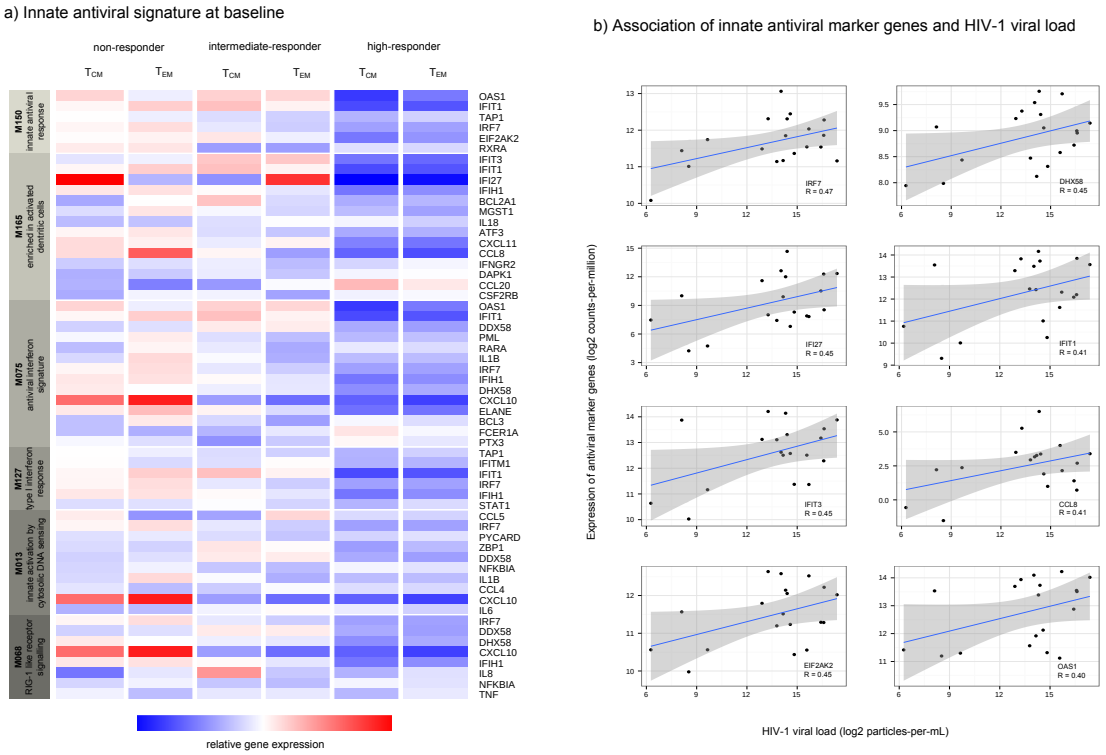

Figure 3.4: Differential gene expression at baseline prior to vaccination. A) Innate antiviral signature at baseline. The expression the five genes involved in innate antiviral immunity with their corresponding members of BTMs are shown for T_{CM} and T_{EM} responder groups. B) Correlation of innate antiviral markers and viral load. Pearson correlation coeficients and 95% CI (confidence intervals) are shown. Only genes with a Pearson correlation coefficients >0.4 were considered. T_{CM}=central memory $CD4^+$ T cells, T_{EM}=effector memory $CD4^+$ T cells.

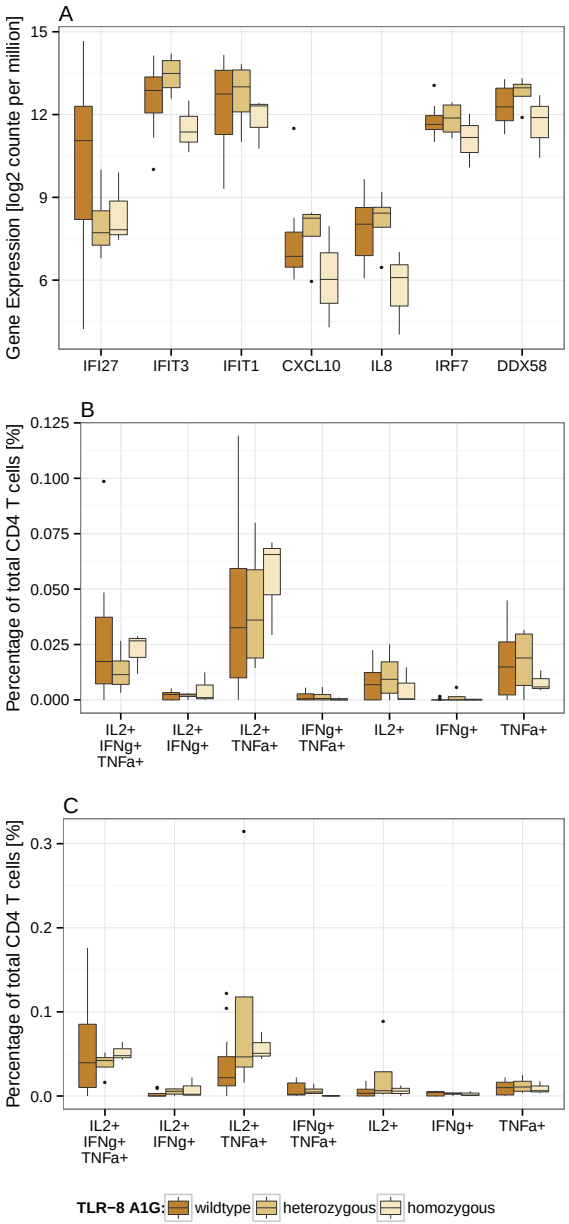

Figure 3.5: A. Baseline expression of genes implicated in innate antiviral immunity comparing volunteers with either wildtype, heterozygous or homozygous TLR-8 A1G. B and C. Cytokine expression profile of T_{CM} and T_{EM} following H1 fusion protein stimulation at day 182. Difference between volunteers with wildtype, heterozygous and homozygous TLR-8 A1G is represented. Due to low numbers of volunteers with homozygous TLR-8 A1G no statistical test was applied.

3.4.6 Toll-like receptor 8 variant

The AmpliSeq approach allows for nucleotide sequencing of the amplified fragments using the IonTorrent approach. We are aware that this study was not designed (e.g. powered) to assess the association of polymorphic genes with vaccine-induced immune responses. One single nucleotide polymorphism (SNP) in TLR-8 (rs3764880) was previously reported to result in a slower disease progression in HIV infected individuals and reduced activation of the NF-κb pathway [278]. The functional variant of TLR-8 showed the A1G polymorphism (rs3764880) that alters the start ATG codon of TLR-8 into a GTG triplet. The resulting truncated TLR-8 (1038 aa) exhibits a shorter signal peptide. Seven volunteers expressed the TLR-8 A1G, of these 3 volunteers harboured the homozygous TLR-8 A1G. Interestingly, none of the volunteers with the TLR-8 A1G belonged to the T_{EM}-non-responder group and all three subjects expressing the homozygous TLR-8 A1G were T_{EM}-high-responders. Importantly, subjects with the homozygous TLR-8 A1G have a reduced expression of antiviral gene signatures at baseline (Figure 3.5a). Independent of the responder grouping, at day 182 volunteers with homozygous TLR-8 A1G have on average highest percentages of tri-functional and bi-functional (IL-2 and TNF-α) T_{CM} and T_{EM} (Figure 3.5b and c).

3.5 Discussion

The study presented here provides first insights into the possible link between chronic immune activation in HIV infection and lack of maintenance of vaccine induced T_{CM} and T_{EM} responses. Data of the impact of chronic, untreated HIV infection on experimental and routine vaccination outcome are scarce [279]. The identification of immune related genes expressed before vaccination or that are

induced shortly after vaccination influencing cellular immune responses in HIV positive volunteers will be of great value [280].

Determinants of induction and long-term maintenance of memory $CD4^+$ T cell responses generally in humans are only partially known [77]. The H1/IC31® vaccine has been tested in several phase I clinical trials including HIV negative and BCG unvaccinated, BCG vaccinated and *M.tb* exposed European volunteers [64,65]. In BCG and *M.tb* naïve European volunteers, IFN-γ producing H1-specific T cells were detectable by ELISpot analysis until 131 weeks after first vaccination. Only limited retraction of IFN-γ production in cell culture supernatants from H1 stimulated PBMC was measured between study week 14 and 131 [64]. In the current study, we observed an expansion of H1-specific T_{CM} and T_{EM} in all volunteers at study day 70 which is two weeks after the booster vaccination. However, when followed up until day 182, a retraction of H1-specific T_{CM} and T_{EM} was observed. Interestingly, this retraction differed greatly between volunteers, which allowed us to group them based on comparing H1/IC31®-induced T_{CM} and T_{EM} responses on day 182 in relation to day 0.

Compared with microarray analyses, the AmpliSeq has a higher sensitivity and dynamic range and it compares exquisitely with RNA-Seq derived whole transcriptome data [268]. Results obtained with both gene panels strongly supported the idea that the AmpliSeq based transcriptome monitoring approach is very robust and results in highly reproducible data sets suitable for high throughput analysis of clinical samples. Here, we have employed to our knowledge for the first time this targeted transcriptome monitoring tool in an experimental vaccine trial.

Higher expression of genes involved in extracellular matrix and integrin interactions and cell adhesion were observed in volunteers that maintained H1-specific T_{CM} and T_{EM} responses until day 182. Searching the literature, cells involved in wound healing like alternatively activated macrophages [281], monocyte-derived

multi-potential cells [282], fibrocytes [283] or endothelial progenitor cells [284], have all been described to express these particular genes.

Muyanja et al. showed that cellular and humoral immune responses to the highly efficacious live yellow fever vaccine YF-17D in East African individuals were substantially lower compared to European volunteers treated identically [285]. Prior to vaccination, the East African volunteers presented an increased activated immune microenvironment with higher frequencies of exhausted and activated natural killer cells, differentiated B and T cells and pro-inflammatory monocytes [285]. We therefore compared the gene expression profiles measured at baseline between our responder groups. Significantly higher expression levels of genes involved in innate antiviral immune responses like type I IFN signalling and viral sensing through cytosolic RIG-1 like receptors was observed in the non-responders. A close correlation between HIV viral load and expression level of this group of genes indicates that the chronic HIV infection is driving the higher expression levels of these antiviral responses. In line with these results, HIV progressors are known to display a type I IFN chronic exposure signature when contrasted to HIV elite controllers [89,90]. We concluded from these observations that the higher activation of components of the innate immunity due to HIV virus stimulation at baseline results in impaired H1-specific T_{CM} and T_{EM} maintenance.

In addition to the expression level, the AmpliSeq approach also provides access to the nucleotide sequence of the respective amplified gene fragment. This enabled us to identify volunteers carrying the previously known TLR-8 A1G single nucleotide sequence variant. Volunteers expressing this TLR-8 A1G gene on both chromosomes had lower gene expression levels of the innate antiviral immune response genes. This was linked to longer maintenance of vaccine-specific T_{EM} responses until day 182 when compared to wild-type TLR-8 carriers.

The inverse relationship between chronic innate anti-viral immune activation by

HIV and sustained H1/IC31®-induced vaccine specific cellular immune responses is of high relevance for future vaccine development and monitoring programs. The presence of the TLR-8 A1G variant in HIV infected individuals might provide an immune-genetic background supporting a more desired vaccination outcome. This observation warrants future studies using larger numbers of HIV infected and non-infected volunteers undergoing experimental or routine vaccination.

3.6 Acknowledgements

This work was supported by the European Developing Countries Clinical Trials Partnership (EDCTP) [grant number IP.2009.32080.002] and the State Secretariat for Education and Research. The AmpliSeq analysis has been funded by the Roche Innovation Center Basel.

The authors are grateful to all study participants. We also thank the sponsor, the Statens Serum Institut, and the members of the Data Safety Monitoring Board: Dr. Anthony Hawkridge, Prof. Jaap van Dissel, Prof. Clive Gray, Prof. Eyasu Makonnen, and Prof. Gibson Kibiki. We appreciate the support of Biolytix AG (`www.biolytix.ch`), who provided their RNA extraction platform.

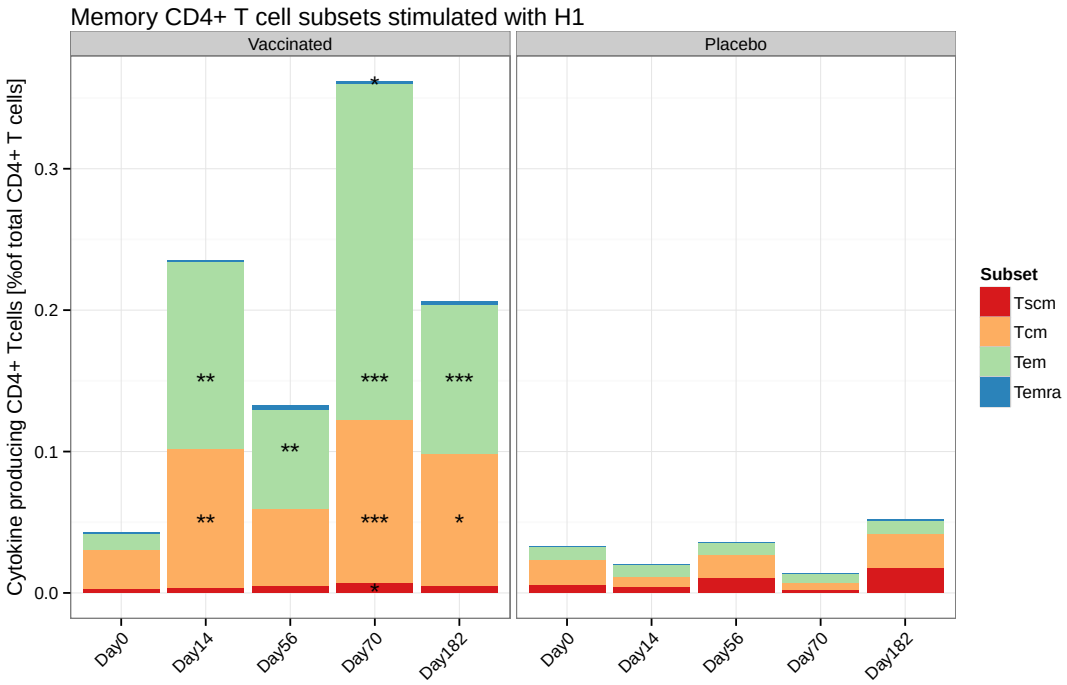

Supplementary Figure 3.1: Cytokine expression of memory $CD4^+$ T cell subsets following H1 fusion protein stimulation. IL-2, IFN-γ and TNF-α were measured. Comparison of percentage of cytokine positive memory $CD4^+$ T cell subsets from H1/IC31® vaccinated and placebo controls is illustrated. Wilcoxon rank sum test was applied for significance testing comparing placebo with vaccinated control group ($*$ = p-value$<$0.05, $**$= pvalue$<$0.01, $***$ = p-value$<$0.001).

Supplementary Table 3.1

			Central memory T-cells			Effector memory T-cells			
		placebo	non	intermediate	high	non	intermediate	high	Annotation
Collagen, type I, alpha 1	COL1A1	- / -	- / -	- / -	7.1 / -	- / -	- / -	5.9 / -	integrin cell surface interactions (M1.0, M1.1) axon guidance (M110) extracellular matrix (M2.0, M2.1) platelet activation (M42) cell adhesion (M51) signal transduction, plasma membrane (M82) platelet activation and degranulation (M85) muscle contraction, SRF targets (M195)
Collagen, type I, alpha 2	COL1A2	- / -	- / -	- / -	- / -	- / -	- / -	6.4 / -	targets of FOSL1/2 (M0) integrin cell surface interactions (M1.0, M1.1) axon guidance (M110) extracellular matrix (M2.0, M2.1, M2.2) collagen, TGFB family et al (M77) signal transduction, plasma membrane (M82) platelet activation and degranulation (M85)
Collagen, type III, alpha 1	COL3A1	- / -	- / -	- / -	- / -	- / -	- / -	6.7 / -	integrin cell surface interactions (M1.0,) extracellular matrix (M2.0, M2.1, M2.2) cell activation, IL15, IL23, TNF (M24) cell adhesion (M51) collagen, TGFB family et al (M77)
Elastin	ELN	- / -	- / -	5 / -	- / -	- / -	4.8 / -	2.9 / -	Lu P et al. Cold Spring Harbor perspectives in biology 2011;3(12):10
Fibronectin 1	FN1	- / -	- / -	- / -	- / -	- / -	- / -	3.2 / -	integrin cell surface interactions (M1.0, M1.1) cell activation, IL15, IL23, TNF (M24) platelet activation (M32.0, M32.1) cell adhesion (M51) collagen, TGFB family et al (M77) signal transduction, plasma membrane (M82) platelet activation and degranulation (M85)
Connective tissue growth factor	CTGF	- / -	- / -	- / -	3.3 / -	- / -	- / -	2.3 / -	extracellular matrix, collagen (M210) regulation of signal transduction (M3) cell movement, Adhesion & Platelet activation (M30) cytoskeletal remodeling (enriched for SRF targets) (M34) immune activation - generic cluster (M37) myeloid, dendritic cell activation via NFkB (M43) lymphocyte generic cluster (M60) T & B cell development, activation (M62) transcriptional targets of glucocorticoid receptor (M74)
Serpin peptidase inhibitor, clade E	SERPINE1	- / -	- / -	- / -	2.5 / -	- / -	- / -	1.9 / -	platelet activation and degranulation (M85), Simone TM et al. Advances in Wound Care 2014;3(3):281-290.
Periostin, osteoblast specific factor	POSTN	- / -	- / -	- / -	- / -	- / -	- / -	6.7 / -	extracellular matrix (M2.1) cell adhesion (M51)
Inhibitor of DNA binding 1	ID1	- / -	- / -	2.7 / -	- / -	- / -	2.5 / -	2.1 / -	leukocyte differentiation (M160)
Heat shock 70kDa protein 1A	HSPA1A	- / -	- / -	- / -	- / -	2.2 / -	- / -	- / -	heat shock protein 1A

Differentially expressed genes following vaccination:

Volunteers are grouped according to their ability to induce either T_{CM} or T_{EM} cellular-mediated vaccine-specific immunity. The log2 fold changes between basline and day 3 or day 59 are indicated (day 3 / day 59). No differential expression is indicated as "-/-". The last column contains the annotations used in this work for each gene.

Chapter 4

Enterobius vermicularis modifies human gut microbiome and suppresses pro-inflammatory immunity

---

This chapter is an adapted version of the following publication:
Lenz N, Schindler T, Salim N, Haks MC, Mpina M, Smolen K, Quinten E, Knopp S, Rothen J, Ottenhof THM, Abdulla S, Tanner M, Certa U, Genton B, Daubenberger CA. *Enterobius vermicularis* modifies human gut microbiome and suppresses pro-inflammatory immunity. Planned to be submitted to *Science*, 2015

4.1 Abstract

Co-infection of *Plasmodium falciparum* (*P. falciparum*) and soil transmitted helminths (STH) affects a significant proportion of the Sub-Saharan African population. Contradictory results have been published on the impact of STH on malaria and there is an ongoing debate on whether general anti-helminthic treatment is desirable. Here, the interplay of co-infection between the Nematode *Enterobius vermicularis* (*E. vermicularis*) and *P. falciparum* in Tanzanian children has been investigated. *E. vermicularis* positive children showed a reduced prevalence of severe or uncomplicated malaria cases while malaria infection prevalence was comparable to either helminth uninfected or hookworm infected children. Production of pro-inflammatory cytokines TNF-α and IL-6 by monocytes and conventional dendritic cells in peripheral blood after toll like receptor agonist stimulation was significantly reduced in *E. vermicularis* and asymptomatic malaria co-infected children. The analysis of the transcription level of selected genes in whole blood demonstrated that *E. vermicularis* single and asymptomatic malaria co-infected children had reduced expression of genes involved in type I and type II IFN activation pathways. *E. vermicularis* modifies the gut microbiome towards increased short chain fatty acids and concurrent reduction of lipopolysaccharide and peptidoglycan production. Further studies are needed to assess the relationship between different STH infection, associated changes in the gut microbiome, functional status of the gut barrier and systemic inflammatory immune responses in malaria.

4.2 Introduction

The pinworm *Enterobius vermicularis* (*E. vermicularis*) is the most common helminth species infecting humans worldwide [286]. The highest prevalence is observed in

young school children between five and ten years of age and estimates - most likely very imprecise due to the limitations of available diagnostic tools - range from 400 million to up to one billion cases [128, 287–289]. Infections with *E. vermicularis* are either clinically silent or characterized by local irritation due to migrating worms and their eggs commonly known as pruritus ani [290, 291]. The life cycle of *E. vermicularis* starts by ingestion of eggs that hatch in the stomach and upper small intestine. The larvae migrate to the ileum, caecum, and appendix and moult twice on their way to become adults. Copulation occurs in the lower ileum and females settle in the caecum, appendix or ascending colon, while forming minute ulcerations at the attachment sites in the gut. Infected individuals can harbor few to several hundred adult worms. When uteri are loaded with eggs, the females migrate towards the anus, where about 11'000 eggs are expulsed that can re-infect the original host or other members of the household [286]. We previously reported a significant geographical overlap between *E. vermicularis* and *P. falciparum* infections in the coastal region of Tanzania [141].

Malaria is caused by mosquito-borne hematoprotozoan parasites of the genus *Plasmodium*. Five *Plasmodium* species are known to infect humans with *Plasmodium falciparum* (*P. falciparum*) being the major causative organism for disease and death. A wide spectrum of presentations including asymptomatic infection, uncomplicated malaria with fever, severe malaria with anemia, impairment of consciousness or acidotic breathing and death are observed [292]. Several studies have shown that high tumor necrosis factor (TNF)-α serum level correlate with disease severity and death [293]. Genome wide association studies demonstrated that genes encoding molecules involved in cell to cell adhesion (intercellular adhesion molecule 1; ICAM1) as well as the pro-inflammatory response (TNF-α, lymphotoxin-α, interleukin (IL)-1α) are likely to be associated with development of severe malaria [293, 294]. Gastro-intestinal symptoms are common in malaria

and histo-pathological changes and evidence for impaired absorption together with parasite sequestration have been provided [233, 235]. Interestingly, severe malaria seems to be accompanied with endotoxaemia most likely linked to damaged gut barrier [236].

STH cause chronic infectious diseases characterized by increased suppression of host immunity through induction of regulatory T cells (Tregs) and priming of T cells producing elevated levels of interleukin (IL)-4, IL-5, IL-10, IL-13 and transforming growth factor beta (TGF)-β [295]. Excretory/secretory products of STH mediating immune-modulatory activities have gained much attention in this context [155, 296]. The interplay between STH and malaria in humans has been reviewed recently. In general, high variations in study outcomes have been published and different STH species seem to have diverse effects on infection and malaria disease [216, 297].

The intestinal microbiome plays a central role in synthesis of metabolites like vitamins, repair of epithelial tissues, production of new blood vessels, protection against pathogens and development and modulation of the gut and systemic immune system [298, 299]. The composition and diversity of the gut microbiome has attracted much attention with the advent of high throughput next generation sequencing technologies [300]. Helminths and the gut microbiome share the same environment and helminths have been associated with changes in the microbiome composition in experimental animal studies [226, 301]. Interestingly, a symbiotic relationship between the microbiota and *Heligmosomoides polygyrus* infection has been described in mice [224]. The gut microbiome of mice and humans differ significantly and studies in humans are just beginning to shed more light on these potential relationships [227, 228].

The aim of this study was to investigate the impact of STH infection on clinical presentation of malaria in Tanzanian children and associated changes in the

innate immune responses. We describe here a protective effect of *E. vermicularis* co-infection on clinical malaria. Diversity and composition of the gut microbiome changed in presence of *E. vermicularis* resulting in a significant increase of short chain fatty acid (SCFA) producing bacteria. In peripheral blood pro-inflammatory responses were reduced in *E. vermicularis* infected children. Increased production of SCFA by the gut microbiome might provide a novel mechanism of interaction between STH, microbiome and inflammatory response during malaria episodes.

4.3 Results

4.3.1 Impact of STH infection on malaria acquisition and progression to disease

The study was conducted between July 2011 and November 2012 in Bagamoyo, located at the coastal region of Tanzania. To investigate the effect of STH infections (*E. vermicularis*, *Strongyloides stercoralis*, and hookworm) on malaria acquisition and progression to clinical malaria, a case-control study designs was utilized. A total of 1'130 children were screened and enrolled in the study. In total, 893 no malaria cases, 94 cases with asymptomatic malaria and 136 cases with clinical malaria (124 uncomplicated and 19 severe) were identified. Two different models were applied to investigate the effect of STH on malaria infection and clinical disease, namely the Malaria Infection Model and the Malaria Disease Model (Fig. S4.1). For the Malaria Infection Model, children with malaria were considered as cases, irrespective of clinical malaria status, and children without malaria as controls. For the Malaria Disease Model, children with malaria disease were regarded as cases and children with asymptomatic malaria as controls. After matching for age, location (village) and education level, 237 cases and 473 controls were included

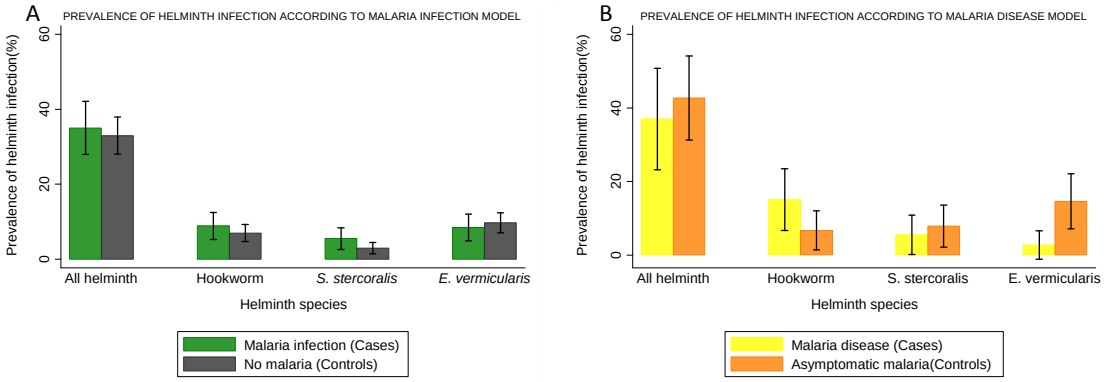

Figure 4.1: Prevalence of helminth infection according to the two models of the case control studies. A. Malaria Infection Model and B. Malaria Disease Model. Malaria Infection Model: Cases were all children with malaria infection (asymptomatic, uncomplicated and severe) and controls were children with no malaria Malaria Disease Model: Cases were all children with malaria disease (uncomplicated and severe) and controls were children with asymptomatic malaria

in the Malaria Infection Model and 73 cases and 89 controls in the Malaria Disease Model (Table S4.1). No effect of STH infection on malaria acquisition was observed neither considering pooled nor separate STH species (Fig. 4.1A, Table S4.1). In a simple conditional logistic regression model, there was a tendency for all STH infections combined to protect against clinical malaria [OR= 0.6, 95% CI of 0.3 - 1.3] (Fig. 4.1B, Table 4.1). When dissected for distinct STH infections, this protection became particularly eminent for *E. vermicularis* infection [OR= 0.2, 95% CI of 0.0 - 0.9] while hookworm infections enhanced the probability of developing uncomplicated and severe malaria [OR= 3.0, 95% CI of 0.9 - 9.5]. In a multiple conditional regression model (with adjustment for gender, nutritional status, bed net and anti-helminthic drug use (albendazole and/or mebendazole), the protective effect of all STH infections combined became marginal [OR= 0.8, 95% CI of 0.3 - 1.9]. For *E. vermicularis* the protective effect became stronger [OR= 0.1, 95% CI of 0.0 - 1.0; p=0.049] while hookworm increased the likelihood of developing clinical malaria [OR= 3.6, 95% CI of 0.9 - 14.3].

Table 4.1: Strength of association between helminth and malaria using Malaria Disease Model

	Cases	Controls	**Simple conitional logistic**		**Multiple conditional logistic**	
Variables	N = 73 n (%)	N = 89 n (%)	OR (95% CI)	p-value	OR (95% CI)	p-value
Helminth[#]						
Helminth (+ve)	19 (27.5)	34 (39.1)	0.6 (0.3-1.3)	0.241	0.8 (0.3-1.9)	0.558
Helminth (-ve)	50 (72.5)	53 (60.9)	NA NA		NA NA	
Single Helminth Species						
Hookworm	11 (15.1)	6 (6.7)	3.0 (0.9-9.5)	0.065	3.6 (0.9-14.3)	0.063
S. stercoralis	2 (5.5)	7 (7.9)	0.6 (0.1-2.5)	0.501	1.0 (0.2-4.9)	0.984
E. vermicularis	2 (2.7)	13 (14.6)	0.2 (0.0-0.9)	0.037	0.1 (0.0-1.0)	0.049

[#]Total number of cases were 69 and controls were 87. 6 groups (7 observations) dropped because of all positive/all negative outcomes. OR= odds ratio, CI= confidence interval.

4.3.2 Monocytes and dendritic cells in children with *E. vermicularis* and asymptomatic *P. falciparum*-malaria infection have reduced IL-6 and TNF-α production

In a subset of children aged 2-9 years enrolled into the case-control study the innate immune responses in peripheral blood at the single cell level were measured. Venous blood was collected and stimulated within 30 minutes with toll-like receptor agonists including the (TLR)-1/2 agonist PAM3CSK (PAM), TLR-4 agonist lipopolysaccharide (LPS) and the TLR-7/8 agonist resiquimod (R848). The children included here were either uninfected from malaria and helminthes (n=6), infected with *E. vermicularis* (n=5), infected with asymptomatic malaria (n=10) and co-infected with *E. vermicularis* and asymptomatic malaria (n=4). A detailed description of the flow cytometry analyses performed following the MyFlowCyt reporting standard [269] can be obtained in the appendix. The intracellular expression of the pro-inflammatory cytokines IFN-α2, IL-12, IL-6 and TNF-α in conventional dendritic cells (cDC), plasmacytoid dendritic cells (pDC) and monocytes was determined (Fig. 4.2). Expression of IFN-α2 and TNF-α in pDC following TLR-7/8 stimulation was detected while IL-12 and IL-6 expressing pDC above the unstimulated controls were not found. Although the cytokine expression in pDC from helminth and malaria uninfected children (controls) is higher compared to the other groups, this difference did not reach statistical significance.

Monocytes responded to stimulation with PAM, LPS and R848 with increased expression of IL-12, IL-6 and TNF-α. IFN-α2 expressing monocytes above the unstimulated control were not detected. The percentages of monocytes expressing IL-12 did not differ between the four groups tested. Clearly, independent of the stimulus, expression of IL-6 and TNF-α was lower in children infected with *E. vermicularis*, malaria only or that are co-infected. Interestingly, the lowest percentage

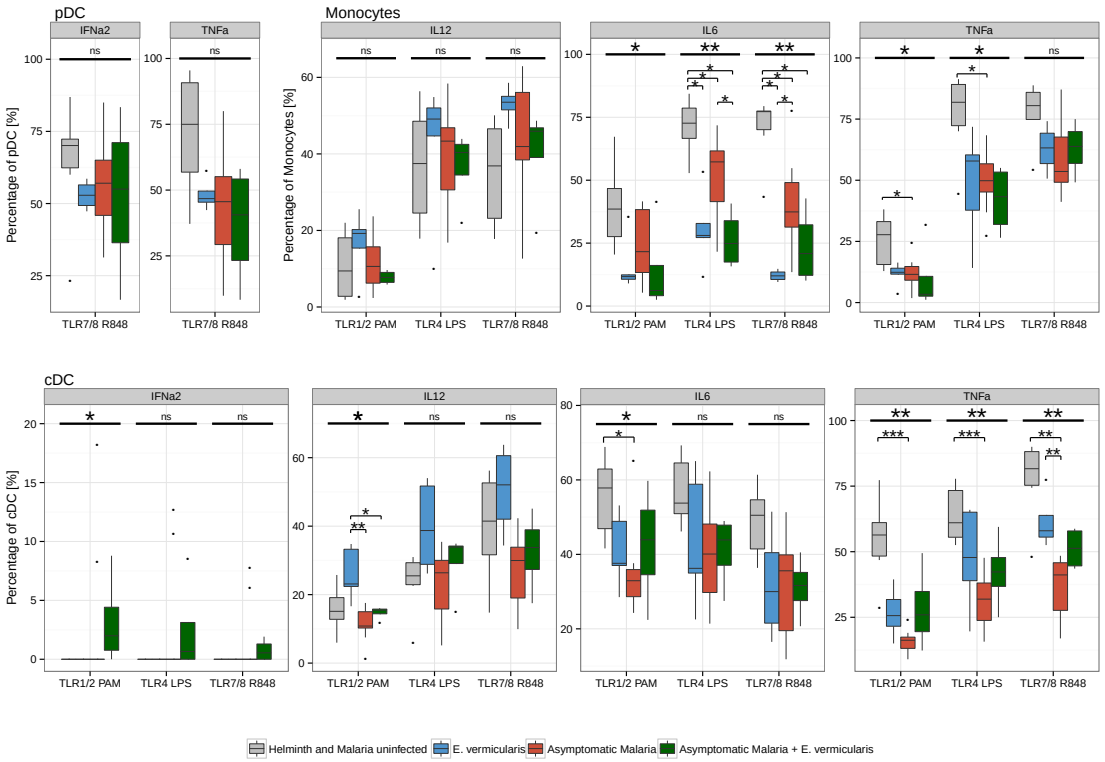

Figure 4.2: Innate immune response of TLR stimulated peripheral whole blood from children infected with *E. vermicularis*, asymptomatic malaria or both. Expression of IFN-α2, IL-12, IL-6 and TNF-α of pDC, monocytes and cDC following stimulation either PAM3CSK (PAM; TLR1/2 agonist), lipopolysaccharide (LPS; TLR4 agonist) or resiquimod (R848, TLR7/8 agonist). Children either uninfected from helminths and malaria or single or co-infected with *E. vermicularis* and asymptomatic *falciparum*-malaria were included. $*$: p-value < 0.05, $**$: p-value < 0.01, $***$: p-value < 0.001, ns = not significant. TLR = toll-like receptor pDC = plasmacytoid dendritic cells, cDC = conventional dendritic cells.

of monocytes expressing IL-6 and TNF-α were extracted from children infected with *E. vermicularis* or co-infected with *E. vermicularis* and malaria.
cDC responded to stimulation with PAM, LPS and R848 with increased expression of IFN-α2, IL-12, IL-6 and TNF-α. Significantly higher percentages of IL-12 expressing cDC were observed in children infected with *E. vermicularis* only. Similar to results obtained with monocytes, IL-6 and TNF-α expression was significantly reduced in all *E. vermicularis* and *P. falciparum* infected children when compared to uninfected children. The lowest expression of IL-6 and TNF-α was observed in children presenting with asymptomatic malaria. IFN-α2 expression was observed in PAM stimulated cDC but compared to the percentages observed in pDC, this population most probably contributed little to the overall IFN-α2 expression. Taken together, monocytes and cDC from children co- or mono-infected with *E. vermicularis* and asymptomatic malaria showed significantly less IL-6 and TNF-α production in comparison to uninfected controls after TLR 1/2, TLR4 and TLR7/8 stimulation.

4.3.3 Genes involved in Th1 and IFN signaling are lower expressed in peripheral whole blood of children that are infected with *E. vermicularis*

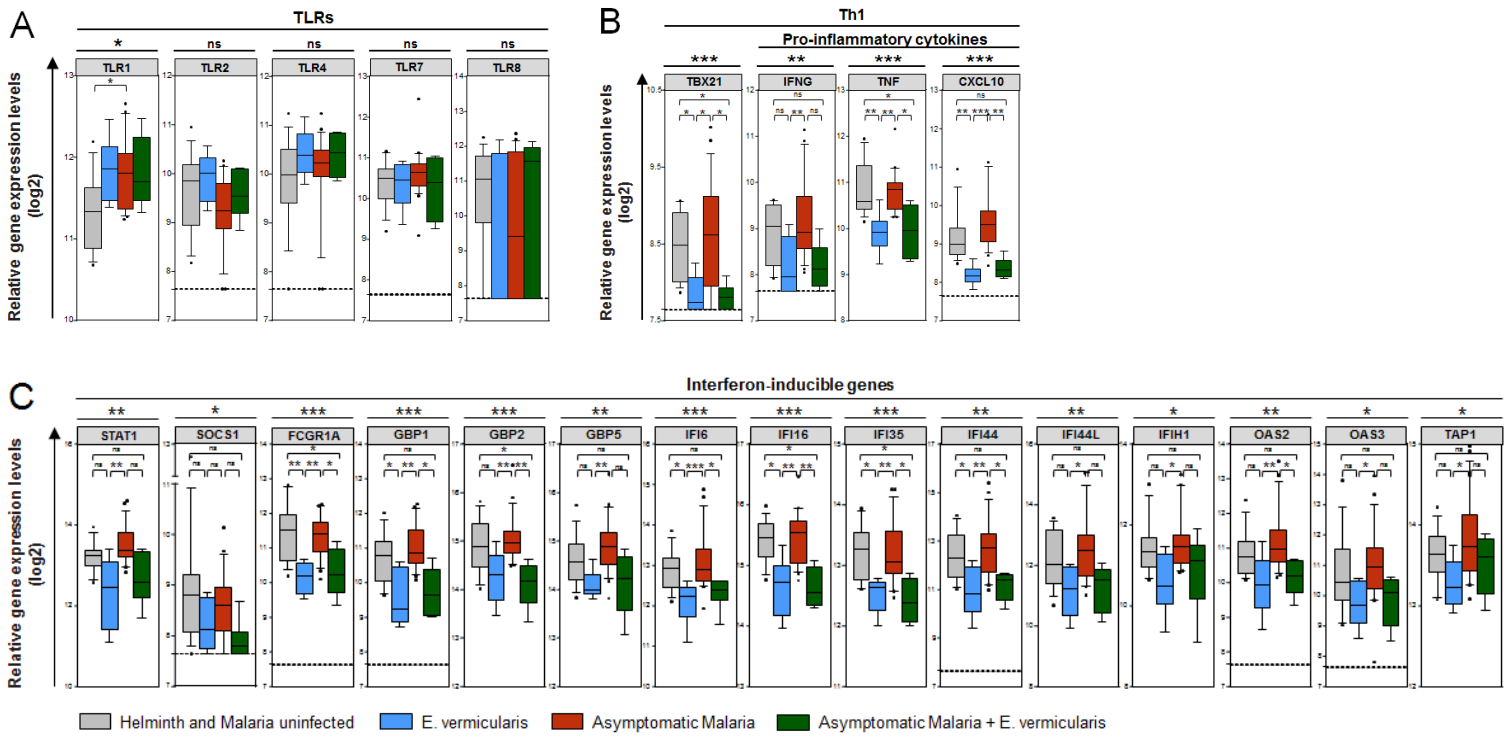

Figure 4.3: Direct ex vivo differential gene expression of immune markers in whole blood. Dual-color RT-MLPA was performed on direct ex vivo RNA isolated from PAXgene tubes derived from children in Tanzania either uninfected or infected with *E. vermicularis*, asymptomatic malaria or both. Median gene expression levels (peak areas normalized to GAPDH and log2 transformed) of (A) toll-like receptors (TLRs) relevant to Fig. 4.2, (B) T cell subset markers including pro-inflammatory and anti-inflammatory cytokines, (C) interferon-inducible genes are shown as box-and-whisker plots (5-95 percentiles; dots indicate outliers; dotted line represents assay cutoff). Significant differences of individual genes between study groups were determined using Kruskal-Wallis H and Dunn's multiple comparison tests. ns = not significant, $*$ = $0.01<P<0.05$, $**$ = $0.001<P<0.01$ and $***$ = $P<0.001$.

To characterize further the human immune response to infection with *E. vermicularis*, asymptomatic malaria, or both, direct ex vivo whole-blood gene expression profiles were determined using dual-color RT-MLPA. Genes incorporated in the assay (Table S4.3) were selected to assess different compartments of the innate and adaptive immune response including immune cell subset markers of B/T/NK cells and monocytes, Th1/2/9/17/22 responses, Treg responses, T cell cytotoxicity, myeloid associated markers and scavenger receptors, pattern recognition receptors, inflammasome components and inflammatory and IFN signaling genes. Gene expression profiles of 14 helminth and malaria uninfected children, 8 *E. vermicularis* infected children, 22 children with asymptomatic malaria, and 6 children co-infected with *E. vermicularis* and asymptomatic malaria were analyzed and individual genes that were differentially expressed between the study groups were identified (Fig. 4.3, Fig. S4.2, Table S4.2). Expression of TLR genes relevant to the single cell flow cytometry analysis remained unchanged with the exception of TLR-1 (Fig. 4.3A), whereas infection with *E. vermicularis* markedly down-regulated genes associated with Th1 responses (Fig. 4.3B), and IFN-inducible genes (Fig. 4.3C). Strikingly, these observations were independent of malaria co-infection. The finding that *E. vermicularis* infection suppresses the expression levels of genes implicated in Th1 and pro-inflammatory responses nicely correlates with reduced expression of IL-6 and TNF-α in antigen presenting cells following TLR stimulation (Fig. 4.2). Taken together, *E. vermicularis* infection modifies Th1, pro-inflammatory and IFN inducible responses, while reduced expression remained in the presence of asymptomatic malaria co-infection.

4.3.4 The gut microbiome diversity and function changes in *E. vermicularis* infected volunteers

The relative abundance and diversity of the intestinal microbiome in 34 Tanzanian subjects were analysed. We sequenced the V3 region of 16S rRNA genes from fecal samples of individuals with no *E. vermicularis* and malaria (n=8), *E. vermicularis* only (n=10), asymptomatic malaria only (n= 10) and *E. vermicularis* and malaria co-infections (n=6). A total of 10'476'914 quality-filtered sequences were obtained from these 34 samples with an average of 308'145 ±76'712 sequences per sample. The reads were clustered into 5643 unique operational taxonomic unit (OTU) with an average of 1748 OTUs per subject.

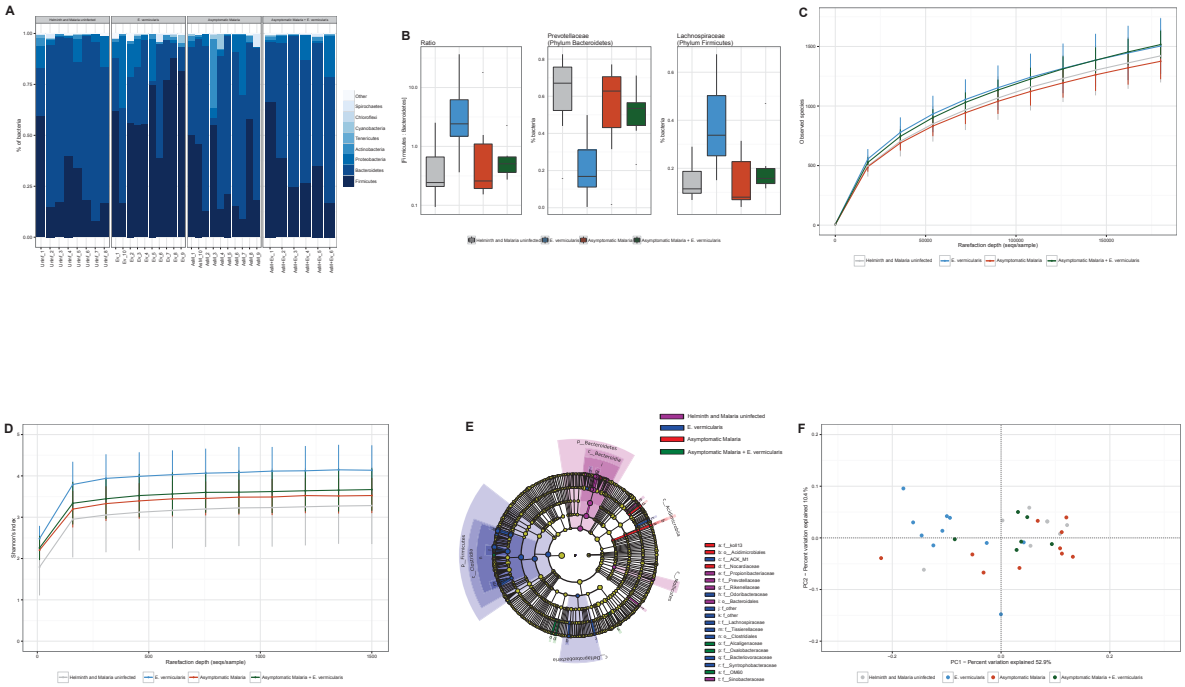

Figure 4.4: A) Relative abundance of the top phyla represented across the 34 subjects grouped by infection status. The abundance patterns showed an increased abundance of *Firmicutes* in the *E. vermicularis* infected children. B) The ratio between the two main phyla, *Firmicutes* and *Bacteroidetes*, as well as the relative abundances of the main family for each of the two phyla. The *E. vermicularis* infected children show an increased ratio, which is driven by high abundances of species within *Lachnospiraceae* and low abundances of species within *Prevotellaceae*. Rarefaction curves calculated for observed species (C) and Shannon's index (D) demonstrating the higher microbial diversity found among *E. vermicularis* positive children. E) Microbial biomarker discovery and visualization. Differentially abundant microbial clades between all study groups were analysed and visualized with LEfSe. F) PCoA using weighted UniFrac distances of gut microbial communities obtained from stool samples. All beta-diversity measures were performed on OTU tables rarefied to 180'000 sequences/sample. Uninf = Helminth and Malaria uninfected, Ev = *E. vermicularis*, AsM = Asymptomatic Malaria, AsM+Ev = Asymptomatic Malaria + *E. vermicularis*, LDA = linear discriminant analysis, OUT = operational taxonomic units, PCoA=Principal coordinates analysis

In Figure 4.4A, the relative abundances and diversity of the phyla in the intestinal microbiome stratified according to their infection status is given. The most dominating phyla are *Firmicutes*, *Bacteroidetes* and *Proteobacteriae*. In *E. vermicularis* only positive children, the relative abundance of *Firmicutes* is greatly augmented resulting in a significantly increased *Firmicutes* to *Bacterioidetes* ratio (Fig. 4.4B). This change is mainly driven by an increase in the species within the *Lachnospiraceae* and a reduction of species within the *Prevotellaceae* (Fig. 4.4B). Rarefaction curves calculated for observed species and the Shannon index showed that *E. vermicularis* positive children in presence or absence of malaria co-infection showed greater species diversity compared to control and only malaria infected children (Fig. 4.4C-D). A supervised comparison of the microbiota of these four volunteer groups by utilizing the LEfSe algorithm at a LDA threshold of 2.0 to identify taxonomic differences associated with helminth and malaria infection status was performed. *E. vermicularis* positive children without malaria showed an increased abundance of species belonging to the classes *Clostridia* and *Deltaproteobacteria* while in contrast the uninfected children displayed a higher prominence of members of the classes *Bacteroidia* and *Mollicutes* (Fig. 4.4E). Fig. 4.4F represents principle coordinate analysis of weighted UniFrac distances of gut microbial communities obtained from stool samples. Clearly, *E. vermicularis* only infected children clustered distinctively and rather homogenously in the left upper quadrant when compared to the other children analyzed here. We next utilized inferred metagenomics data calculated with PICRUSt to investigate the relative abundances of KEGG pathways in the microbiota of these 34 individuals grouped according to helminth and malaria infection status. These microbiomes are dominated by the KEGG pathways metabolism followed by genetic information processing and environmental information processing (Fig. 4.5A). We found a significantly increased abundance of pathways associated with short chain fatty acid synthesis (SCFA) including Butanoate

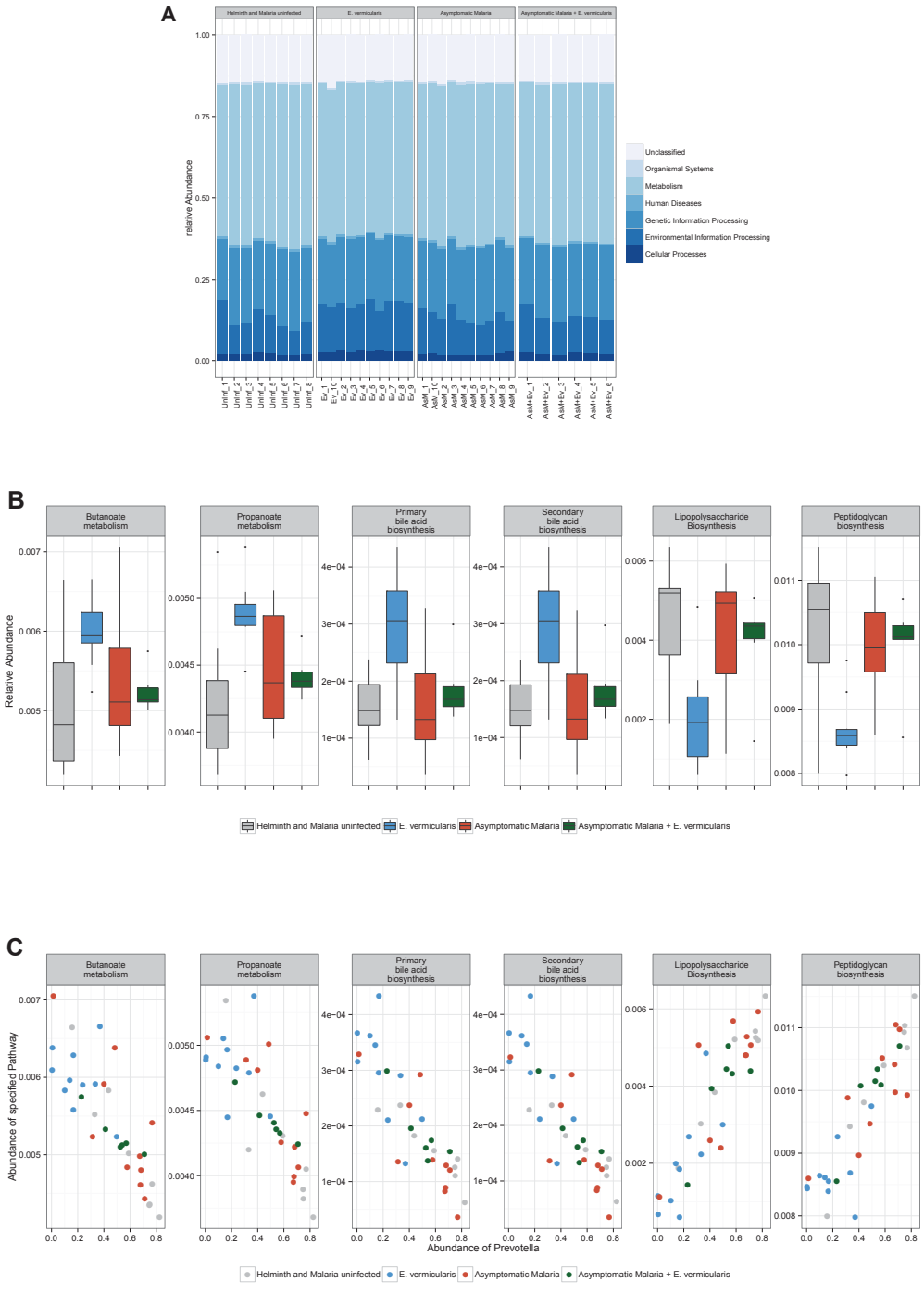

Figure 4.5: A) Relative abundances of KEGG pathways encoded in the gut microbiota. B) Selection of differentially abundant KEGG pathways. C) Correlation of these pathways with abundance of *Prevotella*.

and Propanoate metabolism and primary and secondary bile acid biosynthesis in *E. vermicularis* only infected children. In contrast, the LPS and peptidoglycan biosynthesis was markedly reduced in these children (Fig. 4.5B). Interestingly, in the presence of asymptomatic malaria, these differences in the pathway expressions were lost. After having identified these significant differences in metabolic pathways, we tried to find the potential genus that is present in diverse abundance and could therefore be accountable. A reverse relationship between the relative abundance of members of the genus *Prevotella* to the metabolic pathways analyzed here could be detected.

4.4 Discussion

The fact that intestinal helminths and gut microbiota share their habitats calls for studies describing their interactions and the consequences for the human host [223]. Very little attention has been paid to the effects of *E. vermicularis* infection in African children [132, 141]. In addition, no evidence has been to our knowledge provided that *E. vermicularis* has modulatory effects on the human immune system. We provide here first time evidence that the microbiome in *E. vermicularis* infected children living in East Africa differs from uninfected age matched controls. *E. vermicularis* lives within the lumen of the intestine and rarely - if ever - invades its lining. This may limit its direct interaction with the immune system although there is evidence from rodent pinworm infection models that it influences peripheral immune responses [302]. *E. vermicularis* was most likely inherited from its human ancestors since it is shared with its closest relatives [303]. Based on 16S rRNA-targeted molecular analyses, we provide evidence that *E. vermicularis* infection results in a microbiome that is characterized by a significantly increased ratio of *Firmicutes*/*Bacteroidetes* and alpha-diversity. The majority of bacteria detected

in fecal samples from healthy human volunteers belong to two phyla, *Bacteroidetes* and *Firmicutes* [304] and the ratio between these phyla has been shown to be associated with systemic diseases like obesity and diabetes mellitus [156,305]. Similar to our results, Lee et al. found that helminth colonization is associated with increased alpha-diversity in gut microbiota [228]. The dominating helminth species infecting this Malaysian indigenous population highly exposed to helminth infections were *Trichuris* spp. and *Ascaris* spp. In contrast, a study in school children in Ecuador did not observe significant effects on the gut microbiome by *Trichuris trichiura* [227].

One of the best-characterized microbial pathway influencing human health involve the production of SCFAs like propionate, butyrate, and acetate. SCFAs are 1 - 6 carbons in length and mostly the end product of microbial fermentation of complex non-digestible polysaccharide in the colon [189,306]. SCFA have been described to protect from infection and inflammation [307,308], recruitment and maturation of various subsets of immune cells [309,310] and metabolism [311]. When we analyzed the metagenome of *E. vermicularis* single positive children, we found a significant increase of metabolic pathways involved in SCFA and bile acid biosynthesis and a decrease of pathways resulting in LPS and peptidoglycan production. In summary, these data strongly suggest the gut metabolome in presence of *E. vermicularis* is characterized by anti-inflammatory metabolites that can potentially diffuse across the gut barrier to have effects in the systemic immune system.

We next analysed ex vivo the pro-inflammatory cytokine production at the single cell level in whole blood in these children. When compared to uninfected controls, significantly reduced production of IL-6 and TNF-α was detected in cDC and monocytes after TLR1/2, TLR4 and TLR7/8 stimulation in *E. vermicularis* positive children suggesting that infection with *E. vermicularis* might result in reduced pro-inflammatory cytokine production in peripheral blood. The expression

of IL-6 and TNF-α from cDC and monocytes from children co-infected with *E. vermicularis* and malaria were similar to children infected only with *E. vermicularis*. IL-6 and TNF-α are both involved in induction of fever and the acute phase response [312,313]. Both cytokines induce expression of adhesion molecules on endothelial cells, which favors sequestration of parasitized RBCs [314,315]. At the same time, TNF-α is associated with protective mechanisms leading to parasite clearance, such as increasing monocyte phagocytosis and expression of Fc receptors [316]. However, high plasma levels of TNF-α correlate with clinical episodes and severity of disease indicating a dual role for TNF-α during malaria infection [317,318]. IL-6 has a major role in T cell activation and induction of pro-inflammatory Th17 responses, allowing effector T cells to overcome suppression by Tregs [319,320]. Summarizing, we found a reduced expression of TNF-α and IL-6 in monocytes and cDC in *E. vermicularis* and asymptomatic malaria infected children which could have relevance to clinical malaria [124].

Using the dual color RT-MLPA assay, we identified - apart from TLR1 - no difference in the TLR2, TLR4 and TLR8 expression levels which were interrogated functionally by the ex vivo flow cytometry analyses. This indicates that the measured lowered expression of IL-6 and TNF-α in monocytes and cDC ex vivo is not due to reduced expression of the TLR. A number of genes were significantly lower expressed in *E. vermicularis* single and malaria co-infections when compared to the other groups. These included genes involved in Th1 and pro-inflammatory responses and a range of IFN inducible genes. IFN inducible genes are activated by type I and II IFN and they have a role in inflammasome assembly [321,322], DNA sensing within the inflammasome [323], PRR RIG-1 down-regulation [324], delay of apoptosis [325], cell cycle arrest [326], signal transduction [327], T cell receptor signalling [328], peptide loading to major histocompatibility complex 1 [329], expression of type I IFN [330] or are markers for sepsis [331] and thus central to immune

responses against viruses and bacteria . Plasmodial DNA bound to hemozoin has been shown to signal through TLR-9 leading to high levels of the pro-inflammatory cytokine IL-1β and induction of systemic inflammation [332]. Elevated expression of inflammasome related genes and caspase-1 activation by malaria infection was correlated to hypersensitivity to secondary bacterial infection and lethality due to septic shock in rodents [333]. Similar to TNF-α, a dual role for type I IFN during malaria infection has been described. Induction of type I IFN during liver stage infection is considered protective as it lowers parasite burden [334]. In contrast, during asexual blood stage, elevated levels of type I IFN are associated with development of experimental cerebral malaria [335]. STAT-1 is a transcription factor that has a crucial role in IFN signalling [336]. Lower transcript abundance of type II IFN and STAT-1 in *E. vermicularis* infected children is potentially the reason for the lower expression of the IFN inducible genes, especially since SOCS-1 did not differ. Butyrate is known to inhibit histone deacetylases, which are required for STAT-1 signalling [336]. Butyrate and also bile acids have been implicated in antagonizing nuclear factor-κB and thus with anti-inflammatory activity [192, 337, 338]. Taken together, the lowered expression levels of pro-inflammatory genes and those involved in IFN signaling pathways in *E. vermicularis* positive children could be linked to the increased SCFA and bile acid production in the gut microbiome.

The human intestine as the organ of nutrient digestion and absorption has an estimated surface of 32m^2 [339] and is supported with large numbers of capillary blood vessels. Numerous studies have shown that in patients suffering from severe malaria, parasitized red blood cells sequester to the intestine and gut barrier malfunction becomes evident [233–235]. Olupot-Olupot et al. reported that in about 30% of Kenyan and Ugandan children requiring hospitalization from clinical malaria endotoxaemia is present [236]. The authors hypothesize that these endotoxins, including LPS, originate from the intestine and could drive malaria disease progression

from uncomplicated to severe malaria. What factors exactly trigger progression from malaria infection to severe disease is still not completely resolved [292]. In many studies elevated serum levels of pro-inflammatory cytokines such as IL-6 and TNF-α were associated with severe malaria pathogenesis [293,294,340,341]. In our cohort, the number of severe and uncomplicated malaria cases is smaller in presence of *E. vermicularis* infection when compared to other helminth co-infections even though the prevalence of malaria infection (symptomatic and asymptomatic) did not differ. Although the number of children on which this observation is based is so far small, we think that in combination with our results obtained from the gut microbiome studies, the whole blood transcriptome and ex vivo innate immune response analyses, it provides first time insight into the potential interaction between the highly neglected *E. vermicularis*, the associated gut microbiome and malaria co-infection. Importantly, the discrepancies observed between different studies analyzing the impact of helminth infection on malaria disease outcome might be confounded by the neglect of diagnosing *E. vermicularis* in these protocols.

In summary, using targeted 16S rRNA amplification and next generation sequencing of stool samples we demonstrate that *E. vermicularis* impacts very distinctively on the human gut microbiome. An increase in the relative abundance of pathways resulting in SCFA production and reduction of LPS and peptidoglycan is observed. In peripheral blood, the TLR agonist stimulated production of IL-6 and TNF-α in these children is significantly reduced and genes involved in pro-inflammatory responses and IFN signaling are expressed at lower levels. The hypothesis that *E. vermicularis* might provide one of the links in the "hygiene hypothesis" by modifying the gut microbiome towards anti-inflammation deserves further studies in different human populations.

4.5 Funding

All authors are grateful for the grant provided by the European Commission under the Health Cooperation Work Program of the 7th Framework Program to conduct part of the IDEA project "Dissecting the Immunological Interplay between Poverty Related Diseases and Helminth infections: An African-European Research Initiative" (`http://ec.europa.eu/research/health/infectious-diseases/neglected-diseases/projects/014_en.html`) (Grant agreement nr 241642). The funders played no role in the design, collection, analysis, and interpretation of data; in writing of the manuscript; and in decision to submit the manuscript for publication.

4.6 Competing interest

The authors declare that they have no competing interests.

4.7 Materials and Methods

4.7.1 Ethics statement

The study was conducted under the IDEA project protocol which was approved by the institutional review boards of the Swiss Tropical and Public Health Institute (Swiss TPH; Basel, Switzerland) and the Ifakara Health Institute (IHI; Dar es Salaam, United Republic of Tanzania). The ethical approval for the conduct of the study was granted by the Ethikkomission beider Basel (EKBB; Basel, Switzerland; reference number: 257/08) and the National Institute for Medical Research of Tanzania (NIMR; Dar es Salaam, United Republic of Tanzania; reference number: NIMR/HQ/R.8a/Vol. IX/1098). Sensitization meetings were conducted with the local district, community, school teachers and health authorities to inform about

the purpose, procedures, risk and benefits associated with the study. Study related procedures were implemented once the appropriate and adequate informed consent process has taken place and the informed consent form has been signed off by the parents or his/her legally authorized representative as explained previously [132, 141]. Field procedures were conducted as described previously [141]. Participants infected with helminth and/or malaria or other medical conditions received appropriate treatment/referral according to the National treatment guidelines of Tanzania. Children with STH were treated with albendazole (400mg single oral dose) and those with asymptomatic and uncomplicated malaria received artemether-lumefantrine (ALU). Children with severe malaria received quinine injections until clinically stable and able to take ALU. In order to investigate the impact of STH on treatment outcome (data not reported here), children diagnosed with STH received a delayed antihelminth treatment at the end of study follow up (day 42). To prevent unnecessary complications, children were closely followed up for safety and those with heavy helminth load and severe disease received treatment prior to day 42.

4.7.2 Study Design

The study was conducted in the western rural area of Bagamoyo district, coastal region of Tanzania about 20 to 60 kilometres from Bagamoyo town as described previously [141]. The study was part of the IDEA project, an African-European Research initiative, funded by European community, with the aim of dissecting the immunological interplay between poverty related diseases (malaria, tuberculosis (TB) and Human Immunodeficiency Virus (HIV)) and helminth infections [342]. To investigate the effect of helminth infection on malaria acquisition and clinical malaria status, we used two different models as detailed in the statistical analysis

section.

4.7.3 Participant recruitment and follow-up visits

Inclusion criteria were age 2months to < 10 years, written informed consent as obtained from the parents/legally accepted representative, resident and willing to stay within the study area for at least two months of the study follow up. A case of severe malaria was defined according to WHO malaria case definitions. A case of uncomplicated malaria was defined as temperature 37.5 associated with positive blood slide for *Plasmodium* or positive malaria rapid diagnostic test (mRDT) and no criteria for severe malaria. Asymptomatic malaria was defined as no symptoms of malaria from day 0 to 7 (assessed by history and physical examination on day 0 and 7) and associated with positive blood slide for Plasmodium (or positive mRDT) at day 0 and 7. A community cross sectional study including 1000 children was performed in order to recruit about 100 asymptomatic malaria children (controls) (the prevalence of *Plasmodium* parasitemia being around 10% within the study area) [141]. Recruitment of uncomplicated malaria cases were conducted from the dispensaries, west of the study area. Suspected severe malaria cases were recruited from the Bagamoyo district hospital and received additional investigation in the ward to exclude other medical conditions mimicking malaria syndrome.

4.7.4 Sample collection, diagnosis of Plasmodium and helminth infection

Sample collection and diagnostic procedures have been explained previously [132, 141]. Briefly stool, urine and blood samples were collected and examined using a broad set of quality controlled diagnostic methods for common STH (*Ascaris lumbricoides*, hookworm, *Strongyloides stercoralis*, *Enterobius vermicularis*, *Trichuris*

trichiura), *schistosoma* species and *Wuchereria bancrofti*. Blood slides and malaria rapid tests (mRDTs) were utilized for *Plasmodium* diagnosis.

4.7.5 Clinical data management and statistical analysis

Since age, location (village) and education level (not schooling) were found to be significant predictors of *Plasmodium* and helminth co-infection (Salim et al, Plos neglected tropical disease journal, manuscript accepted), we matched cases and controls for these three variables. Age was categorized as follows: children less than 3 years, preschool children aged 3-5 years and school-aged children from 6-9 years inclusively. A matching program was developed with support from the STATA conference and users group. (`http://www.stata.com/meeting/`). The program reduces to the following syntax, whose arguments are explained below: radmatch varlist [id( ) mpair( ) case( ) k( ) rad( ) seed( ). Briefly the program works as follows: i) first it creates a dataset of controls and cases separately from the variable that defines them (varlist) ii) then it randomly orders the cases using the unique identification id (varname) iii) a variable is then defined that linked a given control to its matched case, mpair( ) iv) using a loop over the observations in case and control datasets, matches are established wherever the cases and controls shares the same values, hence ending up with a dataset with all possible matches called (match) v) for each pair labelled 0 for a control and 1 for a case) vi) k( ) defines the k in the 1: k matching, the default is k = = 1 vii) rad( ) these are the respective radius corresponding to the variables specified in the varlist, viii) seed( ) this is the seed to replicate results. The program has been validated for its function using two different data sets before used in the current analysis. Simple and multiple conditional logistic regression models were used to investigate the strength of association between STH infection and, malaria infection and

malaria disease. Two models were utilized, malaria infection model and malaria disease model. A model of malaria infection, cases being all children infected with malaria (Asymptomatic, uncomplicated and severe) and controls were those with no malaria. A model of malaria disease, cases being children with uncomplicated and severe malaria and controls were children with asymptomatic malaria. Most of the collected explanatory variables (gender, nutritional status and interventions used) were not significant in the simple regression analysis but were still included in the multiple conditional regression as all of them are expected to have an effect on the outcome. No interaction effect was observed with the matched variables used.

4.7.6 Blood collection for immunology assays

2.5ml of peripheral blood was drawn via sterile venepuncture into lithium-heparin vacuettes (Greiner Bio One, catalog no.454082) and into RNA PaxGene vacutainers (PreAnalytiX,catalog no.762165). The lithium-heparin tube was kept at room temperature until further processing and the PaxGene tube was kept at room temperature for 2 hours and was subsequently frozen at -20°C.

4.7.7 Toll-like receptor stimulation and whole blood culture

TLR stimulation and whole blood culture was performed as described in the protocol of [343] and [344]. Whole blood was strictly incubated within 30min from phlebotomy [345]. For this study the following TLR ligands were used at specified concentrations: PAM3CSK4 (PAM; TLR2/1; EMC Microcollections) at 1μg/ml, Lipopolysaccharide (LPS; TLR4; InvivoGen) at 100ng/ml, resiquimod (R848; TLR7/8, InvivoGen) at 100μM and phytohemagglutinin (PHA, positive control, Oxoid) at 10μg/ml. Briey, whole blood was diluted 1:1 in sterile, pre-

warmed RPMI 1640 (Gibco) and was incubated with the TLR ligands for either 6h (with Brefeldin-A at 10μg/ml, Sigma-Aldrich) at 37°C and 5% CO2. The cells were detached by adding ethylenediaminetetraacetic acid at a concentration of 2mM and the cells were incubated for 10min. The cells were lysed in 1.4ml of FACS lysing solution (Becton Dickinson Bioscience, BD) and stored at -80°C.

4.7.8 Intracellular cytokine staining

Cells were thawed in a waterbath at 37°C and spun down. They were washed twice in PBSAN (PBS (Gibco) with 0.1% sodium azide (Sigma-Aldrich) and 1% bovine serum albumin). The cells were permeabilized with FACSPerm (BD) and incubated for 10min. They were subsequently washed three times and re-suspended in this antibody mix: CD11c-APC (BD), TNFa-Alexa 700 (BD), IL-6-FITC (BD), IL-12-eF450 (eBioscience), CD14-V500 (BD), HLA-DR-eF605 (eBiosciences), IFN-α-PE (BD), CD123-PE-Cy7 (eBiosciences) in PBSAN. The cells were incubated at room temperature for 45min. The cells were washed three times in PBSAN and transferred to FACS round bottom tubes (BD). The acquisition was performed using the LSR Fortessa with the FACSDiva 6.0 software (BD). The flow cytometer was calibrated using cytometer setup and tracking beads (BD) and adjusted using the application settings feature of the FACSDiva software according to the manufacturer's recommendation. For quality assurance a biological standard was stained and acquired at the same time. Compensation beads (BD) were used as single stain controls for later compensation. 20μl of anti-mouse Ig and 20μl of anti-rat Ig compensation beads were used with 1μl of either antibody at the same time as cells were stained. Compensation and gates were set in FlowJo V10.0.7 (TreeStar, OR) and results were exported to Excel (Microsoft). The MiFlowCyt reporting standard was implemented in a detailed description of the flow cytometry analysis

and can be accessed in the Appendix [269].

4.7.9 Data analysis of Flow Cytometry

For the analysis of the flow cytometry data unstimulated concentrations have been subtracted and positive values within the 75th percentile of the negative values were set to zero. Kruskall wallis test was applied to test for overall significance. In case of significance (p-value < 0.05), two-sided Wilcoxon rank sum test was used to determine which of the groups of children contributed to the significant differences. P-values were adjusted according to Bonferroni and significance was reached with an unadjusted p-value $< 0.05/3$. Statistical analysis and plots were made using R version 3.1.0 [271].

4.7.10 DcRT-MLPA assay

A dual-colour reverse transcriptase multiplex ligation-dependent probe amplification (dcRT-MLPA) assay was performed as described previously [346]. Briey, for each target-specific sequence, a specific RT primer was designed located immediately downstream of the left and right hand half-probe target sequence. Following reverse transcription of 125ng RNA using MMLV reverse transcriptase (Promega, Leiden, The Netherlands), left and right hand half-probes were hybridized to the cDNA at 60°C overnight. Annealed half probes were ligated and subsequently amplified by PCR (33 cycles of 30 s at 95°C, 30 s at 58°C and 60 s at 72°C, followed by 1 cycle of 20 min at 72°C). Primers and probes were obtained from Sigma-Aldrich Chemie (Zwijndrecht, The Netherlands) and MLPA reagents were purchased from MRC-Holland (Amsterdam, The Netherlands). PCR amplification products were 1:10 diluted in HiDi formamide-containing 400HD ROX size standard and analysed on an Applied Biosystems 3730 capillary sequencer in GeneScan mode (BaseClear,

Leiden, The Netherlands). Trace data were analysed using the GeneMapper software package (Applied Biosystems). The areas of each assigned peak (in arbitrary units) were exported for further analysis in Microsoft Excel spreadsheet software. Signals below the threshold value for noise cutoff in GeneMapper (log2 transformed peak area 7.64) were assigned the threshold value for noise cutoff. Following normalization of the data to the average signal of housekeeping gene GAPDH, signals below the threshold value for noise cutoff (peak area 7.64) were again assigned the threshold value for noise cutoff.

4.7.11 Data analysis of dcRT-MLPA

To test for significant differences of single genes between study groups, Kruskal-Wallis H and Dunn's multiple comparison tests were applied using GraphPad 6.0 software.

4.7.12 Standardization

As demonstrated by [343], technical artifacts can quickly affect the assessment of the innate immune response. Therefore we put an effort on quality assurance to keep occurrence of technical errors at a minimum. The same lot numbers of each reagent was used throughout the study (with the exception of the APC-CD11c antibody). Adequate quantities of master mixes of each reagent were prepared and frozen for later use. All reagents were stored according to the manufacturer's recommendation. PaxGene tubes were shipped on dry ice with a temperature monitor that stayed at -80°C.

4.7.13 Amplification and sequencing of variable 3 (V3) region of 16S ribosomal RNA

(rRNA) genes. The V3 hypervariable region of the 16S rRNA gene was amplified using the Ion Torrent compatible primer sequences designed by Milani et al. [347]. A set of 12 different barcoded forward primers were used to multiplex samples for sequencing. The V3 region of the 16S rRNA gene was amplified by PCR as previously described [348]. Briefly, 20ng template DNA was amplified using the Platinum PCR Super-Mix High Fidelity (Life Technologies) and a primer concentration of 0.2μM in 50μL final reaction volume. The following thermal cycling conditions were used on a TProfessional TRIO thermocycler (Biometra GmbH): 5 min initial denaturation at 95°C; 95°C 30 s, 55°C 30 s, 72°C 90 s for 28 cycles; and a final elongation at 72°C for 10 min. PCR products were analyzed by electrophoresis on a 2% E-Gel EX agarose gel (Invitrogen) and amplicon library products were extracted from gel and purified with the QIAquick Gel Extraction Kit (Qiagen) according to the manufacturers guide. A second round of purification was applied using a column-based size selection in order to remove residual primer dimers (Lexogen). Concentration, size range and purity of the amplicon libraries were measured using the the Agilent High Sensitivity DNA Kit on the Bioanalyzer 2100 instrument (Agilent Technologies).

4.7.14 Ion Torrent PGM

Sequencing of 16S amplicons. Emulsion PCR was performed with 11 pM of the multiplexed library using the PGM^{TM} Template OT2 200 Kit (Life Technologies) according to the manufacturer's instructions. Sequencing of the amplicons was carried out on an Ion 318 chip using the Ion Torrent PGM system and employing the Ion PGM Hi-Q Sequencing Kit (Life Technologies) according to the supplier's instruc-

tions. The PGM quality approved and non-demultiplexed fastq files were exported for data analysis. Microbiome data analysis. The fastq files were processed following the 16S profiling analysis pipeline for Ion Torrent [349] using UPARSE [350] and QIIME 1.8.0 [351]. 16S rRNA Operational Taxonomic Units (OTUs) were defined at 97% sequence homology. All reads were classified to the lowest possible taxonomic rank using the Greengenes reference dataset (gg 13 5 release) [352]. To identify taxa with different abundance, the LDA Effect Size (LEfSe) algorithm [353] was used. Microbial community metagenome prediction was done with PICRUSt [354]. The online interface Galaxy (`http://huttenhower.sph.harvard.edu/galaxy/root`) was used for LEfSe and PICRUSt analysis.

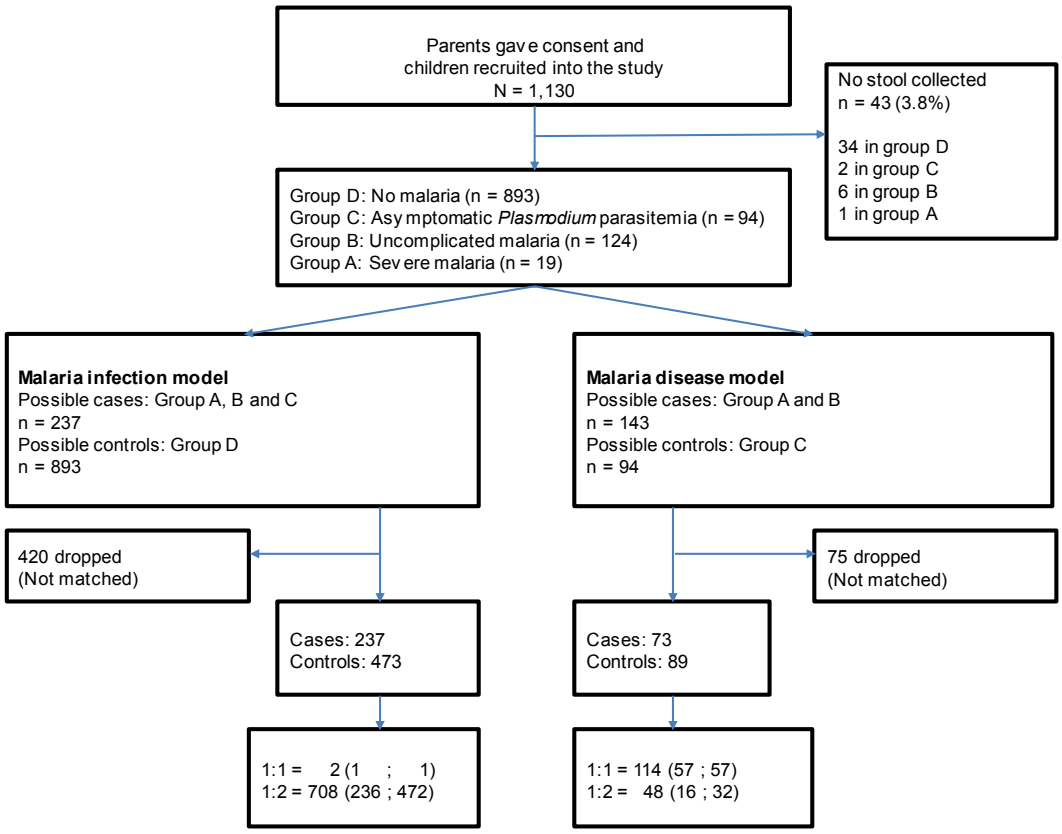

Fig. S4.1: Flow diagram of the participants and matching procedures.

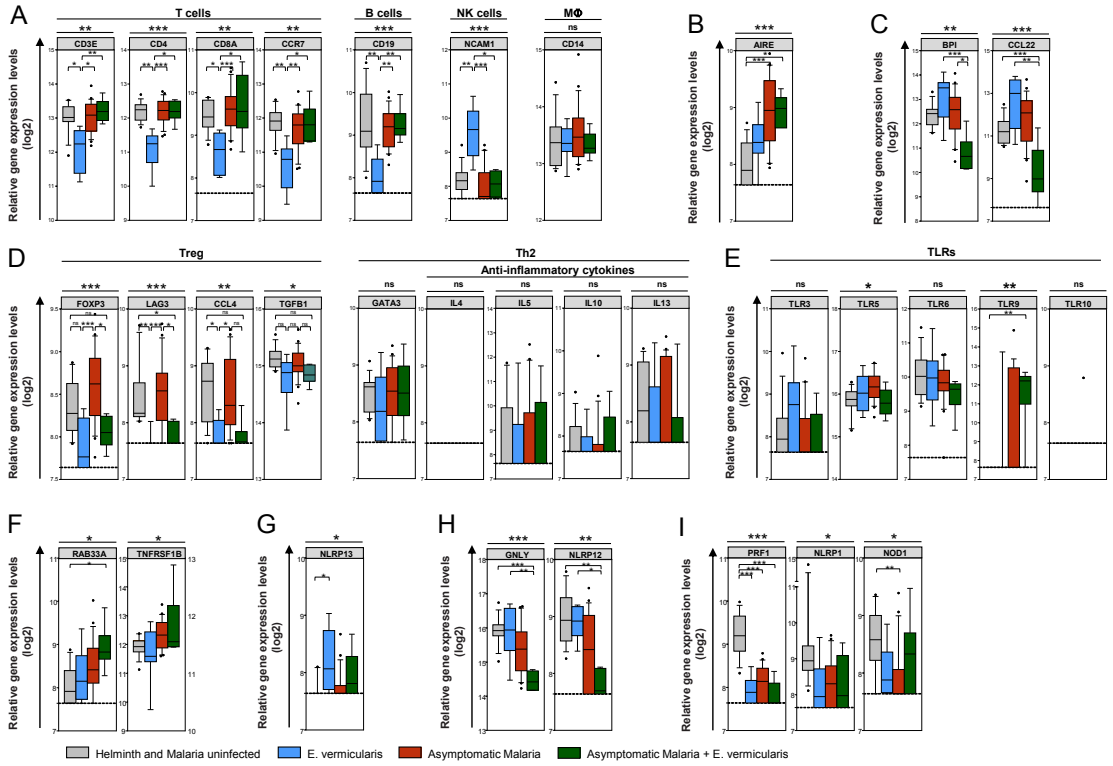

Fig. S4.2: Additional differentially expressed genes obtained from the analysis with dual-color RT-MLPA. Panels A-I represent similar expression patterns observed between the strata and/or similar function.

Table S4.1: Baseline characteristics of cases and controls of Malaria Disease Model

	Malaria disease status	
	Cases (clinical)	Controls (asymptomatic)
	N = 73	N = 89
Characteristics	n (%)	n(%)
Matching variables		
Age group		
< 3 years	15 (20.6)	15 (16.9)
3-5 years	13 (17.8)	14 (15.7)
> 5 years	45 (61.6)	60 (67.4)
Location		
Kiwangwa	71 (97.2)	86 (96.6)
Msata	1 (1.4)	1 (1.1)
Magomeni	1 (1.4)	2 (2.3)
Education level		
Too young	15 (20.6)	15 (16.8)
Not schooling	38 (52.0)	45 (50.6)
Preprimary	11 (15.1)	11 (12.4)
Primary	9 (12.3)	18 (20.2)
Other demographics		
Gender		
Male	39 (53.4)	45 (50.6)
Female	34 (46.6)	44 (49.9)
Nutritional status		
Normal	62 (84.9)	73 (82.0)
Underweight	11 (15.1)	16 (18.0)
Normal	56 (76.7)	63 (70.8)
Stunted	17 (23.3)	26 (29.2)
Normal	73 (100)	86 (96.6)
Wasted	0 (0.0)	3 (3.4)
Intervention coverage		
Bednets		
Slept under a bednet last night	61 (88.4)	74 (88.1)
Antihelminthic		
Used Albendazole	25 (39.1)	40 (44.9)
Used Mebendazole	15 (23.4)	16 (18.0)

Table S4.2: Strength of association between helminth and malaria using Malaria Infection Model.

	Cases	Controls	**Simple conitional logistic**		**Multiple conditional logistic**	
Variables	N = 237 n (%)	N = 473 n (%)	OR (95% CI)	p-value	OR (95% CI)	p-value
Helminth##						
Helminth (+ve)	65 (28.5)	118 (26.0)	1.1 (0.8-1.6)	0.503	1.2 (0.8-1.7)	0.419
Helminth (-ve)	163 (71.5)	336 (74.9)	NA NA		NA NA	
Single Helminth Species						
Hookworm	21 (8.9)	33 (7.0)	1.3 (0.7-2.3)	0.374	1.2 (0.7-2.2)	0.569
S. stercoralis	13 (5.5)	14 (3.0)	1.9 (0.9-4.1)	0.102	1.5 (0.7-3.4)	0.276
E. vermicularis	20 (8.4)	46 (9.7)	0.9 (0.5-1.5)	0.584	1.0 (0.5-1.7)	0.887

##Total number of cases were 228 and controls were 454. 9 groups (17 observations) dropped because of all positive/all negative outcomes. OR= odds ratio, CI= confidence interval

Table S4.3: Direct ex vivo differential gene expression of immune markers in whole blood. Direct ex vivo RNA expression profiling using dcRT-MLPA was performed in whole blood from children either uninfected or infected with *E. vermicularis*, asymptomatic malaria or both. Kruskall wallis test was applied to test for overall significance. ND = Not detected.

Gene Symbol	P-value
Immune cell subset markers	
CD19	0.0010
NCAM1	0.0004
T cell subsets	
CD3E	0.0034
CD4	0.0003
CD8A	0.0015
CCR7	0.0017
IL-7R	0.8459
PTPRCv1	0.2625
PTPRCv2	0.4192
AIRE	0.0001
Th1/Proinflammation associated genes	
CXCL10	<0.0001
IFN-γ	0.0060
IL-1β	0.5168
IL-2	0.2286
IL-15	0.0129
TBX21	0.0009
TNF	0.0001
Th2 asociated genes	
GATA3	0.6454
IL-4	ND
IL-4δ2	0.2488
IL-5	0.1409
IL-6	0.5186
IL-10	0.9248
IL-13	0.6798
Th9 associated genes	
IL-9	0.0161
Th17 associated genes	
IL-17A	0.4625
RORC	0.4954
IL-22RA1	0.7614
Treg associated genes	
CCL4	0.0011
CTLA4	0.9425
FOXP3	0.0004
IL-2RA	ND
LAG3	<0.0001
TGFB1	0.0204
TNFRSF18	0.9320
Cytotoxicity markers	
GNLY	0.0006
GZMA	0.7071
GZMB	0.5552
PRF1	<0.0001
Apoptosis/Survival	
CASP8	0.9973
BCL2	0.4349
FASLG	0.4252
FLCN	0.1058
TNFRSF1A	0.8796

Gene Symbol	P-value
Inflammasome components	
NLRC4	0.2999
NLRP1	0.0190
NLRP2	0.4183
NLRP3	0.6603
NLRP4	0.0911
NLRP6	0.4579
NLRP7	ND
NLRP10	ND
NLRP11	ND
NLRP12	0.0015
NLRP13	0.0140
IFN signaling genes	
CD274	0.7513
GCGR1A	0.0002
GBP1	0.0002
GBP2	0.0002
GBP5	0.0019
IFI6	0.0002
IFI16	0.0002
IFI35	0.0002
IFI44	0.0012
IFI44L	0.0053
IFIH1	0.0152
IFIT2	0.2809
IFIT3	0.2355
IFIT5	0.4625
IFITM1/3	0.3595
INDO	0.7559
IRF7	0.2328
OAS1	0.2340
OAS2	0.0016
OAS3	0.0109
SOCS1	0.1607
STAT1	0.0017
STAT2	0.3758
TAP1	0.0237
TAP2	0.5146
Inflammation	
DSE	0.7021
MMP9	0.4565
SPP1	0.7288
TIMP2	0.6994
TNIP1	0.1803
Cell growth/proliferation	
BMP6	0.2339
TGFBR2	0.6275
AREG	ND
EGF	0.8070
VEGF	0.6502
Cell activation	
HCK	0.0103
LYN	0.9925

Table S4.3 continued: Direct ex vivo differential gene expression of immune markers in whole blood. Direct ex vivo RNA expression profiling using dcRT-MLPA was performed in whole blood from children either uninfected or infected with *E. vermicularis*, asymptomatic malaria or both. Kruskall wallis test was applied to test for overall significance. ND = Not detected.

Gene Symbol	P-value
Apoptosis/Survival	
TNFRSF1B	0.0400
Myeloid associated genes	
CD14	0.8152
CD163	0.2151
CCL2	0.3387
CCL5	0.2306
CCL22	0.0008
CXCL13	0.0521
IL12A	0.2185
IL12B	0.5807
IL23A	0.3982
FPR1	0.8104
Chemokines	
CCL11	0.9767
CCL13	0.0620
CCL19	0.7749
CXCL9	0.8315
CX3CL1	0.2165
Pattern recognition receptors	
CD209	0.2344
CLEC7A	0.4005
MRC1	ND
MRC2	0.1576
NOD1	0.0157
NOD2	0.0813
TLR1	0.0257
TLR2	0.0809
TLR3	0.3952
TLR4	0.3945
TLR5	0.1797
TLR6	0.1797
TLR7	0.5962
TLR8	0.7360
TLR9	0.0065
TLR10	0.7356

Gene Symbol	P-value
Cell activation	
SLAMF7	0.2266
Small GTPases/(Rho)GTPase activating proteins	
ASAP1	0.5395
RAB13	0.5835
RAB24	0.1219
TAGAP	0.3438
TBC1D7	0.4477
Anti-microbial activity	
BPI	0.0015
LTF	0.2381
E3 ubiquitinin protein ligases	
NEDD4L	0.6049
Scavenger receptors	
MARCO	0.2627
Transcriptional regulators/activators	
CAMTA1	ND
TWIST1	0.0620
ZNF331	0.1789
ZNF532	0.4851
Intracellular transport	
SEC14L1	0.8595
KIF1B	0.3310
Mitochondrial Stress/Proteasome	
HPRT	0.1980
G protein-coupled receptors	
BLR1	0.3228

Chapter 5

Conclusion and Outlook

5.1 Conclusion

We conducted a phase II, multi-centre, double-blind, randomized, placebo-controlled trial with the TB vaccine H1/IC31® in HIV infected adults with a lymphocyte count greater than 350/mm^3 (chapter 2). The safety of the vaccine was assessed, CD4$^+$ lymphocyte counts and viral loads were documented and the immunogenicity of H1/IC31® was measured.

Solicited systemic and unsolicited adverse events were similar comparing H1/IC31® vaccinated to placebo controls. CD4$^+$ lymphocytes counts and viral loads remained stable. H1/IC31® induced vaccine specific polyfunctional CD4$^+$ T cells expressing TNF-α and IL-2 or TNF-α, IL-2 and IFN-γ. The vaccine induced poor CD8$^+$ and Th17 responses and there was a lack of humoral response.

Similar solicited and unsolicited adverse events by study arm implies that the vaccine was safe and well tolerated. As discussed in the introduction, vaccination of HIV infected individuals is problematic. HIV infection can yield poor vaccine immunogenicity and maintenance of memory responses. Vaccination can also lead to progression of the HIV infection. We documented no major change in CD4$^+$

lymphocyte count and viral load and conclude that the vaccine did not negatively impact on the HIV infection. The detection of vaccine-specific polyfunctional Th1 responses up to 6 months after initial immunization implies, that H1/IC31® was immunogenic and durable in HIV infected individuals. Polyfunctional and bifunctional $CD4^+$ T cells expressing IL-2 and TNF-α were suggested to be of central memory phenotype and thus less differentiated, more long lived and functionally superior to IFN-γ expressing $CD4^+$ T cells. Baseline QFT status indicated, that some participants were latently infected with *M.tb*. Overall number of participants was low and no stratification according to latency status could be done.

Since direct comparison of HIV infected to HIV negative individuals is missing, no definite conclusion can be made about how much vaccine specific cellular responses were impaired by the HIV infection. What immune responses are protective against *M.tb* infection are still debated and whether a mixture of Th1, Th17, cytotoxic and humoral responses are necessary to clear infection or whether a Th1 response is sufficient is unknown. The lack of detection of $CD8^+$ responses in this study could be due to suboptimal experimental settings and therefore a definite assessment of H1/IC31® induced $CD8^+$ responses cannot be made. Recent evidence suggest a protective role for less differentiated and more proliferative $CD4^+$ T cells that express less IFN-γ as terminally differentiated Th1 cells. These criteria are met by central memory T cells expressing IL-2 and TNF-α. However, whether H1/IC31® induced cellular immune responses confer a protective effect against *M.tb* infection or active disease remains elusive. Vaccination of latently infected individuals with H1/IC31® would possibly boost a pre-existing *M.tb* specific immune response. Since the study population consisted of a mixture of *M.tb* naïve and latently infected individuals, the observed average cellular immune responses are probably higher than expected from a population exclusively consisting of *M.tb* naïve individuals.

Concluding, vaccination with H1/IC31® was safe and well tolerated in HIV infected individuals. Whether the vaccine was more immunogenic and efficacious than BCG could not be elaborated.

In chapter 3 we conducted an ancillary study investigating mechanisms leading to improved induction and maintenance of vaccine specific $CD4^+$ T cells in HIV infected individuals. The memory $CD4^+$ T cell response induced by vaccination was measured by whole blood stimulation assay, intracellular cytokine staining and flow cytometry. Amplicon based transcript quantification of peripheral whole blood using next generation sequencing (AmpliSEQ) was performed to identify differentially expressed genes either induced three days post first vaccination or present at baseline.

Predominantly tri-functional T_{CM} and T_{EM} expressing IL-2, TNF-α and IFN-γ or bi-functional expressing IL-2 and TNF-α were detected with an expansion two weeks after the booster inoculation and a retraction until 6 months after the beginning of the study. This retraction was highly heterogeneous among the volunteers and we divided them into high-, intermediate and non-responder based on either vaccine specific T_{CM} or T_{EM}. $CD4^+$ lymphocyte count and viral load were not statistically significant among these groups. AmpliSEQ analysis revealed higher expression of genes implicated in extracellular matrix, integrin interactions and cell adhesion three days post each inoculation and these were mainly observed in high- and partially in intermediate responder. At baseline, high expression of genes implicated in innate antiviral immunity was observed in non-responder and there was a close correlation of HIV viral load and expression level of these genes. A previously known variant of TLR-8 was detected and the homozygous expression was exclusively found in T_{EM} high-responder. A lower expression of genes implicated in innate antiviral immunity and a longer maintenance of vaccine specific T_{CM} and

T_{EM} was found in volunteers harboring the TLR-8 variant.

In chapter 2 we assumed, that the vaccine specific $CD4^+$ T cells were mainly of central memory phenotype. With the help of this study we could determine that they were of central and effector memory phenotype. One reason for a reduced vaccine immunogenicity in HIV infected individuals is lower $CD4^+$ lymphocyte count. $CD4^+$ lymphocyte counts and viral load did not vary among the responder groups, which implies that impaired memory maintenance is not explained by lower $CD4^+$ lymphocyte counts in this case. Vaccine induced resolution of inflammation was mainly observed in high-responder, which indicates that vaccination induced low inflammation and tissue damage in non-responder. As discussed in the introduction, chronic bystander immune activation by virus infection yields impaired effector to memory differentiation following vaccination. This effect was reproduced by chronic stimulation of TLR-3 by polyIC, a potent inducer of type I IFN. When compared to elite controllers, HIV progressors display a type I IFN chronic exposure signature. This implies, that the high activation of innate antiviral immunity observed in non-responder, which includes higher expression of genes of the type I IFN response, impaired the maintenance of vaccine specific immune responses. This conclusion was confirmed with the close correlation of the HIV viral load and expression levels of genes implicated in innate antiviral immunity. The TLR-8 variant observed in T_{EM} high responder was previously described to result in slower disease progression in HIV infected individuals and thus reconfirms the conclusion.

Since direct comparison to HIV uninfected individuals is missing, no conclusion can be made as to whether the memory maintenance of high responder resembles the one of healthy individuals. One inclusion criterium of the clinical trial was a $CD4^+$ lymphocyte count $>350/mm^3$. Thus, it is unknown whether lower counts would not impair memory maintenance and a definite conclusion about the role of abso-

lute $CD4^+$ numbers cannot be made. There is indication, that higher levels type I IFN impair vaccine specific memory maintenance. However, since measurements of type I IFN in serum samples from participants are missing, the role of circulating levels of type I IFN remains unknown. Peripheral whole blood for analysis by AmpliSEQ was withdrawn at baseline and three days post each immunization. A higher expression of genes implicated in resolution of inflammation was detected comparing baseline with three days post each vaccination. This gives not any direct information on the initial inflammation caused by H1/IC31®. Generally, participant numbers in each responder group were low.

Summarizing, this study demonstrates that high activation of innate antiviral immunity by the HI-virus can render the innate immune system hyporesponsive to the vaccine H1/IC31®. This study warrants further investigations on the role of type I IFN and early innate immune responses on induction and maintenance of vaccine specific memory.

In chapter 4 we conducted an epidemiological survey assessing the influence of STH on malaria acquisition and progression to clinical symptoms (clinical malaria) in children aged 2 months to 9 years from Bagamoyo, coastal region of Tanzania. From a subset of these children aged 2 to 9 years further analysis of the immunological interplay between the highly neglected STH *E. vermicularis* and asymptomatic *falciparum*-malaria was performed. Peripheral whole blood was stimulated with known TLR-1/2, TLR-4 and TLR-7/8 agonists, which was followed by measuring the cytokine profiles of major antigen presenting cells in peripheral blood. Transcript abundance of a distinct gene panel was evaluated in periperal whole blood by dual-color RT-MLPA to further characterise the impact of *E. vermicularis* and asymptomatic *falciparum*-malaria on the immune system. Finally, in order to gain more insight into possible mechanisms by which the strictly enteric STH *E. ver-*

micularis shapes the systemic immune response, we analysed the composition and function of the fecal microbiome.

In the epidemiological study we found highest prevalence of the following STH species: Hookworm, *S. stercoralis* and *E. vermicularis*. No influence of STH infection on *falciparum*-malaria acquisition was observed, neither with pooled nor with separated helminth species. Reduced cases of clinical malaria were found in STH co-infections in comparison to asymptomatic malaria cases. Separate analysis of each STH species revealed a higher risk of clinical malaria in hookworm co-infected and a reduced risk in *E. vermicularis* co-infected children. We observed no impact of *S. stercoralis* co-infection on clinical malaria presentation.

Stimulation of whole blood with known TLR agonists revealed lower expression of IL-6 and TNF-α in monocytes and cDC from children infected with *E. vermicularis*, asypmtomatic *falciparum*-malaria or both. No statistically significant difference was observed in pDC and in expression of INF-α2 and IL-12, apart from elevated expression of IL-12 by PAM stimulated cDC from children exclusively infected with *E. vermicularis*. Decreased expression of IL-6 in monocytes from *E. vermicularis* cases irrespective of malaria infection was especially evident.

Apart from TLR-1, we found no differential expression of TLR-2,-4,-7 and -8 in the dual-color RT-MLPA. Furthermore, reduced expression of genes implicated in the Th1 and pro-inflammatory response and IFN inducible genes was detected in children with *E. vermicularis* irrespective of malaria infection.

E. vermicularis was found to have a significant impact on the composition of the fecal microbiome with a higher abundance of the phylum *Firmicutes* and reduced abundance of *Bacteroidetes* (observed in children exclusively infected with *E. vermicularis*). Enrichment of bacteria of the class *Clostridia* and *Deltaproteobacteria* was detected. Inferred metagenomic analysis revealed a close correlation of metabolism of the microbiome to the results obtained in the immunology assess-

ment. Interestingly, exclusive infection with *E. vermicularis* was associated with higher butanoate and propanoate metabolism, increased biosynthesis of primary and secondary bile acids and decreased biosynthesis of LPS and peptidoglycan. No major change in composition of the fecal microbiome was observed in asymptomatic malaria and co-infected cases.

Because of the reduced cases of clinical malaria in children co-infected with *E. vermicularis*, we can conclude that *E. vermicularis* reduces the risk of progression to clinical symptoms during malaria infection, whereas hookworm increases the risk. The lower expression of IL-6 and TNF-α in major antigen presenting cells in peripheral whole blood of children infected with *E. vermicularis*, asymptomatic malaria or both, implies that i) the strictly enteric STH *E. vermicularis* influences distant sites in the human body and has an immunosuppressive effect on IL-6 and TNF-α expression following stimulation with TLR agonists ii) establishment of asymptomatic malaria requires suppression of IL-6 and TNF-α responses during the immune response, since increased levels of these cytokines are associated with fever and elevated expression of adhesion molecules on endothelial cells leading to sequestration of parasitized RBC, and iii) most probably co-infection with *E. vermicularis* reinforces this effect and thus less clinical malaria cases are observed in *E. vermicularis* co-infected children. The fact that transcript abundance of TLR-2,-4,-7 and -8 was similar in all strata implies that the lower expression of IL-6 and TNF-α was not due to lower TLR expression, apart from PAM stimulation of TLR-1. Lower expression of genes implicated in Th1 and pro-inflammatory responses fit exquisitely to the observations made in the flow cytometric analysis of TLR stimulated whole blood and implies that suppression of specific pro-inflammatory responses leads to establishment of asymptomatic malaria infection. Expression of STAT-1 was significantly decreased in *E. vermicularis* cases. STAT-1 is important in the signaling cascade leading to transcription of IFN inducible genes and thus

lower expression of STAT-1 was associated with lower transcript abundance of IFN inducible genes. The fact that SOCS-1 was not differentially expressed leads to the conclusion that this effect was not dependent on the function of SOCS-1. The higher ratio of *Firmicutes* to *Bacteroidetes* in the fecal microbiome implies that infection with *E. vermicularis* induces an anti-inflammatory enterotype. Close correlation of the outcome of the immunological assays and the metabolome of the fecal microbiome indicates that the gut microflora and its metabolites greatly influence the systemic immunity. Higher biosynthesis of the SCFAs butyrate and propionate and primary and secondary bile acids was observed in children exclusively infected with *E. vermicularis*. These metabolites are known to inhibit the function of NF-κB and thus higher production leads to anti-inflammation. Furthermore these metabolites are implicated in establishing gut barrier integrity and thus could be beneficial during malaria infection, as one part of malaria pathogenicity is gut barrier dysfunction and efflux of endotoxins into the system. Lower biosynthesis of LPS and peptiodoglycan imply that during infection with *E. vermicularis* these endotoxins are less abundant. No major changes in composition of fecal microbiome and associated metabolomics in children with asymptomatic malaria and co-infection was observed. The fecal microbiome of uninfected children and children exclusively infected with *E. vermicularis* was found to be highly homogeneous, unlike that of asymptomatic malaria (co-)infected. This implies that a definite assessment of the impact of the microbiome in co-infected children requires higher numbers of study participants.

Generally the biggest criticism of this study are the low number of cases. A broad spectrum of helminth diagnostic tools was used to cover detection of most helminth species. However, samples were only taken on study day 0 and 28. Since most STH infections were low intensity, false-negative results are likely. After anthelminthic treatment, no helminth diagnosis was performed and thus follow-up samples could

not be included due to unknown helminth infection status. Cases of clinical malaria are missing in the follow-up analyses of the immunological interplay and the fecal microbiome. This would be important information and would shed more light on the interaction of *E. vermicularis* and malaria, especially since there were *E. vermicularis* co-infections among uncomplicated malaria cases. The flow cytometric analysis gives information on which cell is positive for which cytokine. However, there is no information on how much cytokine a cell can produce. The gene panel for the dual-color RT-MLPA was initially designed to detect biomarkers for tuberculosis disease. Although most included genes are applicable to helminth and malaria infections, a bigger panel might reveal information more relevant to this study. The metabolites butyrate, propionate, the primary and secondary bile acids and also LPS and peptidoglycan were not directly measured in blood and/or stool and thus a physical proof of the solely computationally assessed activity of these pathways is missing. Analysis of the fecal microbiome stopped at the species level. However, as Greenblum et al. recently showed, there is extensive strain level copy number variations, which influences the functional capacity of the microbiome [355].
Summarizing, this study provides potent insights into mechanisms reducing the risk of clinical malaria. Confusing data exist in the co-morbidity of helminths and malaria and the study proves that different helminth species induce different outcomes. We draw the focus of malaria pathogenicity away from the systemic immunity to the gastro-intestinal tract and provide first evidence that eventually could lead to a efficacious intervention strategy.

5.2 Outlook

H1/IC31® will not be tested in phase IIb trials. Nonetheless, findings from this thesis provide valuable information for the H56 vaccine from the Statens Serum

Institute. H56 is constructed with the H1 backbone and an added latency associated antigen (Rv2660c) administered with the IC31® adjuvant (Ag85B-ESAT-6-Rv2660c). Currently it is tested in phaseI/IIa trials investigating the safety and immunogenicity of H56/IC31® in HIV negative adults with or without latent TB [356].

For future vaccine trials with H56/IC31® in HIV infected adults, I advice to include HIV uninfected controls for better comparison of vaccine immunogenicity and maintenance of cellular memory responses. Furthermore, screening of the TLR-8 SNP rs3764880 prior to vaccination and enrollment of enough individuals with or without the SNP would enable to confirm the role of the TLR-8 variant in induction and maintenance of cellular memory. Additional PaxGene tubes for AmpliSEQ analysis should be taken between baseline and three days post vaccinations, ideally on consecutive days (e.g day 0, day 1, day 2 and day 3). I also recommend to store serum samples to enable testing of levels of type I IFN. Since experimental conditions for detecting $CD8^+$ lymphocyte responses were possibly suboptimal, I advice to add an additional marker to the flow cytometry panel. CD107a is a marker for degranulation, which may be a surrogate for cytotoxic potential and was introduced by DeRosa et al. [357]. $CD8^+$ did not express higher levels of cytokines in response to stimulation with H1, Ag85B or ESAT-6. Nevertheless, they could react with degranulation. Long-term storage of PBMC in liquid nitrogen from HIV infected individuals proved problematic in this study due to low recovery of cells (data not shown). Hence, I recommend to continue performing the whole blood assay.

One problem in chapter 2 was that QFT results implied that the cohort consisted of a mixture of *M.tb* naïve and latently infected individuals and the number of enrolled participants was to small to enable stratification. Since the H56/IC31® contains a latency associated antigen, there is interest in investigating and comparing *M.tb* naïve and latently infected participants. Thus, stratification according

to latency status will be made and enough participants in each category will be enrolled.

Helminths have a significant impact on systemic immunity and most probably vaccination outcome [358]. Since it is not known, whether and how fast this effect diminishes after anthelminthic treatment, I advice to exclude helminth infected volunteers and inform enrolled volunteers on basic hygiene procedures to avoid helminth infection during the study period. The gut microbiome is gaining much attention also in the HIV field. Evidence suggest that HIV infection is associated with an altered gut microbiome that leads to mucosal and systemic immune activation and endotoxemia [359]. It would be interesting to investigate, whether the function of the gut microbiome correlates with vaccine induced cellular memory responses and activation of antiviral immunity at baseline. Therefore I suggest to take stool samples for analysis of the fecal microbiome and also helminth diagnosis. This information could form the basis of an intervention strategy to improve vaccination outcomes.

The observations made in Chapter 4 open a completely new perspective on the interaction of helminth and malaria in the human host and drives the focus away from the systemic immunity to the GI tract. Further research is required on the exact role of malaria parasite sequestration to the intestine, gut barrier permeability, the consequent release of endotoxins, progression to malaria disease and the mechanism by which *E. vermicularis* co-infection reduces the risk of clinical malaria. One major problem were the low numbers of study participants in each group and the lack of children with malaria disease in the immunological and fecal microbiome assessment. For further studies I advice to selectively search for children infected with *E. vermicularis* and co-infected with asymptomatic and clinical malaria with ideally a minimum of 25 children in each group aged between 2 and 9 years. An-

other issue was the schedule for helminth diagnosis and treatment. For the ancillary study, ideally helminth diagnosis should be performed with samples from 3 consecutive days to avoid false-negative cases, especially since the study population showed mainly low intensity infections. Furthermore we had to exclude follow-up samples, since helminth diagnosis was not performed after helminth treatment. I suggest to also take samples on three consecutive days following anthelminthic treatment. Since flow cytometry analysis doesn't enable quantitative analysis of cytokine concentrations, ELISA can be performed with culture supernatants measuring the cytokines IL-12, IL-6 and TNF-α. This verifies that the observations in the flow cytometry analysis do result in changes of cytokine concentration. In chapter 3 we applied AmpliSeq to analyse the transcriptome and it proved very robust and sensitive. AmpliSeq allows to analyse more genes than the dual-color RT-MLPA and the panels we established in chapter 3 would fit perfectly to this study too. A direct verification of elevated levels of butyrate, propionate, primary and secondary bile acids, LPS and peptidoglycan in blood and stool was missing and thus should be measured in the next study. We hypothesized that *E. vermicularis* reduces the risk of clinical malaria by maintaining the gut barrier and thus avoiding endotoxemia. I advice to analyse the gut barrier integrity similar to the study of Molyneux et al. [235]. They gave patients a solution of 4 test sugars to drink, which are either absorbed or diffuse through the intestine, followed by measuring the sugars in the urine. To better understand the interaction of *E. vermicularis* and the microbiome and to find out whether this is a passive process (such as competition for nutrients) or an active modulation of the composition of the microbiome, sequencing the *E. vermicularis* genome would be helpful.

References

[1] WHO. Global tuberculosis report. *Genev: Wolrd Health Organiszation*, 2013.

[2] Brennan Patrick J. and Nikaido Hiroshi. The envelope of mycobacteria. *Annu. Rev. Biochem.*, 64:29–63, 1995.

[3] Jordi B. Torrelles and Larry S. Schlesinger. Diversity in Mycobacterium tuberculosis mannosylated cell wall determinants impacts adaptation to the host . *Tuberculosis*, 90(2):84 – 93, 2010.

[4] Kleinnijenhuis Johanneke, Oosting Marije, Joosten Leo A. B., Netea Mihai G., and Reinout Van Crevel. Innate Immune Recognition of *Mycobacterium tuberculosis*. *Clinical and Developmental Immunology*, 2011.

[5] Thomas R Frieden, Timothy R Sterling, Sonal S Munsiff, Catherine J Watt, and Christopher Dye. Tuberculosis . *The Lancet*, 362(9387):887 – 899, 2003.

[6] Marc Mendelson. Diagnosing tuberculosis in HIV-infected patients: challenges and future prospects. *British Medical Bulletin*, 81-82(1):149–165, 2007.

[7] Ibrahim O Al-Orainey. Diagnosis of latent tuberculosis: Can we do better? *Annals of Thoracic Medicine*, 4(1):5–9, October 2008.

[8] Anil Koul, Eric Arnoult, Nacer Lounis, Jerome Guillemont, and Koen Andries. The challenge of new drug discovery for tuberculosis. *Nature*, 469(7331):483–490, January 2011.

[9] Centers for Disease Control and Prevention. Treatment of latent tb infection. *Atlanta, GA:Centers for Disease Control and Prevention*, assessed at 20 Dec. 2014, 2013.

[10] Niaz Banaiee, Eleanor Z. Kincaid, Ulrike Buchwald, William R. Jacobs, and Joel D. Ernst. Potent Inhibition of Macrophage Responses to IFN-γ by Live Virulent *Mycobacterium tuberculosis* Is Independent of Mature Mycobacterial Lipoproteins but Dependent on TLR2. *The Journal of Immunology*, 176(5):3019–3027, 2006.

[11] Andre Bafica, Charles A. Scanga, Carl G. Feng, Cynthia Leifer, Allen Cheever, and Alan Sher. TLR9 regulates Th1 responses and cooperates with TLR2 in mediating optimal resistance to *Mycobacterium tuberculosis*. *The Journal of Experimental Medicine*, 202(12):1715–1724, 2005.

[12] Nathalie Court, Virginie Vasseur, Rachel Vacher, Cécile Frémond, Yury Shebzukhov, Vladimir V. Yeremeev, Isabelle Maillet, Sergei A. Nedospasov, Siamon Gordon, Padraic G. Fallon, Hiroshi Suzuki, Bernhard Ryffel, and Valérie F. J. Quesniaux. Partial Redundancy of the Pattern Recognition Receptors, Scavenger Receptors, and C-Type Lectins for the Long-Term Control of *Mycobacterium tuberculosis* Infection. *The Journal of Immunology*, 184(12):7057–7070, 2010.

[13] François Coulombe, Maziar Divangahi, Frederic Veyrier, Louis de Leseleuc, James L. Gleason, Yibin Yang, Michelle A. Kelliher, Amit K. Pandey, Christopher M. Sassetti, Michael B. Reed, and Marcel A. Behr. Increased

NOD2-mediated recognition of N-glycolyl muramyl dipeptide. *The Journal of Experimental Medicine*, 206(8):1709–1716, 2009.

[14] Bibhuti B. Mishra, Pedro Moura-Alves, Avinash Sonawane, Nir Hacohen, Gareth Griffiths, Luis F. Moita, and Elsa Anes. *Mycobacterium tuberculosis* protein ESAT-6 is a potent activator of the NLRP3/ASC inflammasome. *Cellular Microbiology*, 12(8):1046–1063, 2010.

[15] Alexander S. Pym, Priscille Brodin, Roland Brosch, Michel Huerre, and Stewart T. Cole. Loss of RD1 contributed to the attenuation of the live tuberculosis vaccines *Mycobacterium bovis* BCG and *Mycobacterium microti*. *Molecular Microbiology*, 46(3):709–717, 2002.

[16] Alessandra Romagnoli, Marilena P. Etna, Elena Giacomini, Manuela Pardini, Maria Elena Remoli, Marco Corazzari, Laura Falasca, Delia Goletti, ValÃĺrie Gafa, Roxane Simeone, Giovanni Delogu, Mauro Piacentini, Roland Brosch, Gian Maria Fimia, and Eliana M. Coccia. ESX-1 dependent impairment of autophagic flux by *Mycobacterium tuberculosis* in human dendritic cells. *Autophagy*, 8(9):1357–1370, 2012.

[17] K B Urdahl, S Shafiani, and J D Ernst. Initiation and regulation of T-cell responses in tuberculosis. *Mucosal Immunol*, 4(3):288–293, May 2011.

[18] S.M. Behar, M. Divangahi, and H.G. Remold. Evasion of innate immunity by *mycobacterium tuberculosis*: Is death an exit strategy? *Nature Reviews Microbiology*, 8(9):668–674, 2010. cited By 81.

[19] C.J. Cambier, K.K. Takaki, R.P. Larson, R.E. Hernandez, D.M. Tobin, K.B. Urdahl, C.L. Cosma, and L. Ramakrishnan. Mycobacteria manipulate macrophage recruitment through coordinated use of membrane lipids. *Nature*, 505(7482):218–222, 2014. cited By 20.

[20] Smita Srivastava and JoelăD. Ernst. Cell-to-Cell Transfer of *M. tuberculosis* Antigens Optimizes CD4 T Cell Priming . *Cell Host & Microbe*, 15(6):741 – 752, 2014.

[21] Shahin Shafiani, Crystal Dinh, James M. Ertelt, Albanus O. Moguche, Imran Siddiqui, Kate S. Smigiel, Pawan Sharma, Daniel J. Campbell, Sing Sing Way, and Kevin B. Urdahl. Pathogen-Specific Treg Cells Expand Early during *Mycobacterium tuberculosis* Infection but Are Later Eliminated in Response to Interleukin-12 . *Immunity*, 38(6):1261 – 1270, 2013.

[22] P S Redford, P J Murray, and A O'Garra. The role of IL-10 in immune regulation during *M. tuberculosis* infection. *Mucosal Immunol*, 4(3):261–270, May 2011.

[23] Zahra Toossi and Jerrold J. Ellner. The Role of TGFβ in the Pathogenesis of Human Tuberculosis . *Clinical Immunology and Immunopathology*, 87(2):107 – 114, 1998.

[24] E John Wherry. T cell exhaustion. *Nat Immunol*, 12(6):492–499, June 2011.

[25] Stefan H.E. Kaufmann. Future Vaccination Strategies against Tuberculosis: Thinking outside the Box. *Immunity*, 33(4):567 – 577, 2010.

[26] David G. Russell, Clifton E. Barry, and JoAnne L. Flynn. Tuberculosis: What We Don't Know Can, and Does, Hurt Us. *Science*, 328(5980):852–856, 2010.

[27] David G. Russell. Who puts the tubercle in tuberculosis? *Nat Rev Micro*, 5(1):39–47, January 2007.

[28] Hsien-Ho Lin, Majid Ezzati, and Megan Murray. Tobacco Smoke, Indoor Air Pollution and Tuberculosis: A Systematic Review and Meta-Analysis. *PLoS Med*, 4(1):e20, 01 2007.

[29] Sungae Cho, Vijay Mehra, Sybille Thoma-Uszynski, Steffen Stenger, Natalya Serbina, Richard J. Mazzaccaro, JoAnne L. Flynn, Peter F. Barnes, Scott Southwood, Esteban Celis, Barry R. Bloom, Robert L. Modlin, and Alessandro Sette. Antimicrobial activity of MHC class I-restricted CD8+ T cells in human tuberculosis. *PNAS*, 97(22):12210–12215, 2000.

[30] Joshua S. M. Woodworth and Samuel M. Behar. *Mycobacterium tuberculosis*-Specific $CD8^+$ T Cells and Their Role in Immunity. *Critical Reviews™ in Immunology*, 26(4):317–352, 2006.

[31] J L Flynn, J Chan, K J Triebold, D K Dalton, T A Stewart, and B R Bloom. An essential role for interferon gamma in resistance to *Mycobacterium tuberculosis* infection. *J Exp Med*, 178:2249–2254, 1993.

[32] Jean-Laurent Casanova and Laurent Abel. The human model: a genetic dissection of immunity to infection in natural conditions. *Nat Rev Immunol*, 4(1):55–66, January 2004.

[33] Melanie J. Newport, Clare M. Huxley, Sara Huston, Catherine M. Hawrylowicz, Ben A. Oostra, Robert Williamson, and Michael Levin. A Mutation in the Interferon-γ-Receptor Gene and Susceptibility to Mycobacterial Infection. *New England Journal of Medicine*, 335(26):1941–1949, December 1996.

[34] S Stenger. Adverse events with biologics: Immunological control of tuberculosis: role of tumour necrosis factor and more. *Ann Rheum Dis*, 64:iv24–iv28, 2005.

[35] Shabaana A Khader, Guy K Bell, John E Pearl, Jeffrey J Fountain, Javier Rangel-Moreno, Garth E Cilley, Fang Shen, Sheri M Eaton, Sarah L Gaffen, Susan L Swain, Richard M Locksley, Laura Haynes, Troy D Randall, and Andrea M Cooper. IL-23 and IL-17 in the establishment of protective pulmonary CD4+ T cell responses after vaccination and during *Mycobacterium tuberculosis* challenge. *Nat Immunol*, 8(4):369–377, April 2007.

[36] Shunsuke Sakai, Keith D. Kauffman, Jason M. Schenkel, Cortez C. McBerry, Katrin D. Mayer-Barber, David Masopust, and Daniel L. Barber. Cutting Edge: Control of *Mycobacterium tuberculosis* Infection by a Subset of Lung Parenchyma-Homing CD4 T Cells. *The Journal of Immunology*, 192(7):2965–2969, 2014.

[37] Thomas Lindenstroem, Niels Peter Hell Knudsen, Else Marie Agger, and Peter Andersen. Control of Chronic *Mycobacterium tuberculosis* Infection by CD4 KLRG1- IL-2-Secreting Central Memory Cells. *The Journal of Immunology*, 190(12):6311–6319, 2013.

[38] Joshua S. Woodworth, Claus Sindbjerg Aagaard, Paul R. Hansen, Joseph P. Cassidy, Else Marie Agger, and Peter Andersen. Protective CD4 T Cells Targeting Cryptic Epitopes of *Mycobacterium tuberculosis* Resist Infection-Driven Terminal Differentiation. *The Journal of Immunology*, 192(7):3247–3258, 2014.

[39] Keertan Dheda, Stephan K. Schwander, Bingdong Zhu, Richard N. Van Zyl-Smit, and Ying Zhang. The immunology of tuberculosis: From bench to bedside. *Respirology*, 15(3):433–450, 2010.

[40] Elizabeth L. Corbett, Catherine J. Watt, Neff Walker, Dermot Maher, Brian G. Williams, Mario C. Raviglione, and Christopher Dye. The Grow-

ing Burden of Tuberculosis: Global Trends and Interactions With the HIV Epidemic. *Arch Intern Med*, 163(9):1009–1021, 2003.

[41] Pam Sonnenberg, Judith R. Glynn, Katherine Fielding, Jill Murray, Peter Godfrey-Faussett, and Stuart Shearer. How Soon after Infection with HIV Does the Risk of Tuberculosis Start to Increase? A Retrospective Cohort Study in South African Gold Miners. *Journal of Infectious Diseases*, 191(2):150–158, 2005.

[42] Glynn JR, Murray J, Bester A, Nelson G, Shearer S, and Sonnenberg P. Effects of duration of HIV infection and secondary tuberculosis transmission on tuberculosis incidence in the South African gold mines. *AIDS*, 22(14):1859–1867, 2008.

[43] Anthony D Harries, Rony Zachariah, Elizabeth L Corbett, Stephen D Lawn, Ezio T Santos-Filho, Rhehab Chimzizi, Mark Harrington, Dermot Maher, Brian G Williams, and Kevin M De Cock. The HIV-associated tuberculosis epidemic–when will we act? *The Lancet*, 375(9729):1906 – 1919, 2010.

[44] Tsiouris SJ El-Sadr WM. HIV-associated tuberculosis: diagnostic and treatment challenges. *Semin Respir Crit Care Med*, 29(5):525–531, 2008.

[45] Motasim Badri, Douglas Wilson, and Robin Wood. Effect of highly active antiretroviral therapy on incidence of tuberculosis in South Africa: a cohort study. *The Lancet*, 359(9323):2059 – 2064, 2002.

[46] Soraya Gaze, Henry J. McSorley, James Daveson, Di Jones, Jeffrey M. Bethony, Luciana M. Oliveira, Richard Speare, James S. McCarthy, Christian R. Engwerda, John Croese, and Alex Loukas. Characterising the Mucosal and Systemic Immune Responses to Experimental Human Hookworm Infection. *PLoS Pathog*, 8(2):e1002520, 02 2012.

[47] Wasiullaa Rafi, Rodrigob Ribeiro-Rodrigues, Jerrold J.c Ellner, and Padminia Salgame. Coinfection-helminthes and tuberculosis. *Current opinion in HIV and AIDS*, 2012.

[48] Christie Y Jeon and Megan B Murray. Diabetes Mellitus Increases the Risk of Active Tuberculosis: A Systematic Review of 13 Observational Studies. *PLoS Med*, 5(7):e152, 07 2008.

[49] Marit Eika Jorgensen and Daniel Faurholt-Jepsen. Is There an Effect of Glucose Lowering Treatment on Incidence and Prognosis of Tuberculosis? A Systematic Review. *Current Diabetes Reports*, 14(7), 2014.

[50] Therese Vallerskog, Gregory W. Martens, and Hardy Kornfeld. Diabetic Mice Display a Delayed Adaptive Immune Response to *Mycobacterium tuberculosis*. *The Journal of Immunology*, 184(11):6275–6282, 2010.

[51] WHO. Revised BCG vaccination guidelines for infants at risk for HIV infection. *Weekly Epidemiological Record*, 82:193–196, 2007.

[52] AC Hesseling, LF Johnson, H Jaspan, MF Cotton, A Whitelaw, HS Schaaf, PEM Fine, BS Eley, BJ Marais, J Nuttall, N Beyers, and P Godfrey-Faussett. Disseminated Bacille-Calmette-Guerin disease in HIV-infected South African infants. *Bulletin of the World Health Organization*, 87:505 – 511, 07 2009.

[53] Mansoor Nazma, Scriba Thomas J.,De Kock Marwou, Tameris Michele, Abel Brian, Keyser Alana, Little Francesca, Soares Andreia, Gelderbloem Sebastian, Mlenjeni Silvia, Denation Lea, Hawkridge Anthony, Boom W. Henry, Kaplan Gilla, Hussey Gregory D., HanekomWillem A. HIV-1 infection in infants severely impairs the immune response induced by Bacille Calmette-Guérin vaccine. *J Infect Dis*, 199(7):982–990, 2009.

[54] Jun Liu, Vanessa Tran, Andrea S. Leung, David C. Alexander, and Baoli Zhu. BCG Vaccines: Their mechanisms of attenuation and impact on safety and protective efficacy. *Hum Vaccine*, 5:70–78, 2009.

[55] Katie Ewer, Jonathan Deeks, Lydia Alvarez, Gerry Bryant, Sue Waller, Peter Andersen, Philip Monk, and Ajit Lalvani. Comparison of T-cell-based assay with tuberculin skin test for diagnosis of *Mycobacterium tuberculosis* infection in a school tuberculosis outbreak. *The Lancet*, 361(9364):1168–1173, April 2003.

[56] Laith J. Abu-Raddad, Lorenzo Sabatelli, Jerusha T. Achterberg, Jonathan D. Sugimoto, Ira M. Longini, Jr., Christopher Dye and M. Elizabeth Halloran. Epidemiological benefits of more-effective tuberculosis vaccines, drugs, and diagnostics. *PNAS*, 106 (33):13980–13985, 2009.

[57] Stop TB Partnership. Tb vaccine pipeline, available at `http://www.stoptb.org/wg/new_vaccines/assets/documents/Global%20TB%20Vaccine%20Pipeline_June%2`. accessed on 17 Dec 2014.

[58] Morven E M Wilkie and Helen McShane. TB vaccine development: where are we and why is it so difficult? *Thorax*, 2014.

[59] Helen McShane, Ansar A Pathan, Clare R Sander, Sheila M Keating, Sarah C Gilbert, Kris Huygen, Helen A Fletcher, and Adrian V S Hill. Recombinant modified vaccinia virus Ankara expressing antigen 85A boosts BCG-primed and naturally acquired antimycobacterial immunity in humans. *Nat Med*, 10(11):1240–1244, November 2004.

[60] Tony Hawkridge, Thomas J. Scriba, Sebastian Gelderbloem, Erica Smit, Michele Tameris, Sizulu Moyo, Trudie Lang, Ashley Veldsman, Mark Hatherill, Linda van der Merwe, Helen A. Fletcher, Hassan Mahomed, Adrian V. S.

Hill, Willem A. Hanekom, Gregory D. Hussey, and Helen McShane. Safety and Immunogenicity of a New Tuberculosis Vaccine, MVA85A, in Healthy Adults in South Africa. *Journal of Infectious Diseases*, 198(4):544–552, 2008.

[61] Michele D Tameris, Mark Hatherill, Bernard S Landry, Thomas J Scriba, Margaret Ann Snowden, Stephen Lockhart, Jacqueline E Shea, J Bruce McClain, Gregory D Hussey, Willem A Hanekom, Hassan Mahomed, and Helen McShane. Safety and efficacy of MVA85A, a new tuberculosis vaccine, in infants previously vaccinated with BCG: a randomised, placebo-controlled phase 2b trial. *Lancet*, 381(9871):1021–1028, March 2013.

[62] Carola Schellack, Karin Prinz, Alena Egyed, Jörg H. Fritz, Barbara Wittmann, Michael Ginzler, Gabriele Swatosch, Wolfgang Zauner, Constantia Kast, Shizuo Akira, Alexander von Gabain, Michael Buschle, and Karen Lingnau. IC31, a novel adjuvant signaling via TLR9, induces potent cellular and humoral immune responses . *Vaccine*, 24(26):5461 – 5472, 2006. Immunopotentiators in Modern Vaccines IMV-II, Malaga, Spain, May 18-20 2005.

[63] Karen Lingnau, Karin Riedl, and Alexander von Gabain. IC31® and IC30, novel types of vaccine adjuvant based on peptide delivery systems. *Expert Review Vaccines*, 6(5):741–746, 2007.

[64] Jaap T. van Dissel, Sandra M. Arend, Corine Prins, Peter Bang, Pernille Nyholm Tingskov, Karen Lingnau, Jan Nouta, Michèl R. Klein, Ida Rosenkrands, Tom H.M. Ottenhoff, Ingrid Kromann, T. Mark Doherty, and Peter Andersen. Ag85B-ESAT-6 adjuvanted with IC31® promotes strong and long-lived *Mycobacterium tuberculosis* specific T cell responses in naïve human volunteers. *Vaccine*, 28(20):3571 – 3581, 2010.

[65] Jaap T. van Dissel, Darius Soonawala, Simone A. Joosten, Corine Prins, Sandra M. Arend, Peter Bang, Pernille Nyholm Tingskov, Karen Lingnau, Jan Nouta, Soren T. Hoff, Ida Rosenkrands, Ingrid Kromann, Tom H.M. Ottenhoff, T. Mark Doherty, and Peter Andersen. Ag85B-ESAT-6 adjuvanted with IC31® promotes strong and long-lived *Mycobacterium tuberculosis* specific T cell responses in volunteers with previous BCG vaccination or tuberculosis infection . *Vaccine*, 29(11):2100 – 2109, 2011.

[66] Robert L. Coffman, Alan Sher, and Robert A. Seder. Vaccine Adjuvants: Putting Innate Immunity to Work . *Immunity*, 33(4):492 – 503, 2010.

[67] Steven R. Wiley, Vanitha S. Raman, Anthony Desbien, Hilton R. Bailor, Rukmini Bhardwaj, Ahmed Rushdi Shakri, Steven G. Reed, Chetan E. Chitnis, and Darrick Carter. Targeting TLRs Expands the Antibody Repertoire in Response to a Malaria Vaccine. *Science Translational Medicine*, 3(93):93ra69, 2011.

[68] Surender Khurana, Nitin Verma, Jonathan W. Yewdell, Anne Katrin Hilbert, Flora Castellino, Maria Lattanzi, Giuseppe Del Giudice, Rino Rappuoli, and Hana Golding. MF59 Adjuvant Enhances Diversity and Affinity of Antibody-Mediated Immune Response to Pandemic Influenza Vaccines. *Science Translational Medicine*, 3(85):85ra48, 2011.

[69] Sudhir Pai Kasturi, Ioanna Skountzou, Randy A. Albrecht, Dimitrios Koutsonanos, Tang Hua, Helder I. Nakaya, Rajesh Ravindran, Shelley Stewart, Munir Alam, Marcin Kwissa, Francois Villinger, Niren Murthy, John Steel, Joshy Jacob, Robert J. Hogan, Adolfo Garcia-Sastre, Richard Compans, and Bali Pulendran. Programming the magnitude and persistence of antibody responses with innate immunity. *Nature*, 470(7335):543–547, February 2011.

[70] Bali Pulendran. Learning immunology from the yellow fever vaccine: innate immunity to systems vaccinology. *Nat Rev Immunol*, 9(10):741–747, October 2009.

[71] Troy Querec, Soumaya Bennouna, Sefik Alkan, Yasmina Laouar, Keith Gorden, Richard Flavell, Shizuo Akira, Rafi Ahmed, and Bali Pulendran. Yellow fever vaccine YF-17D activates multiple dendritic cell subsets via TLR2, 7, 8, and 9 to stimulate polyvalent immunity. *The Journal of Experimental Medicine*, 203(2):413–424, 2006.

[72] Troy D Querec, Rama S Akondy, Eva K Lee, Weiping Cao, Helder I Nakaya, Dirk Teuwen, Ali Pirani, Kim Gernert, Jiusheng Deng, Bruz Marzolf, Kathleen Kennedy, Haiyan Wu, Soumaya Bennouna, Herold Oluoch, Joseph Miller, Ricardo Z Vencio, Mark Mulligan, Alan Aderem, Rafi Ahmed, and Bali Pulendran. Systems biology approach predicts immunogenicity of the yellow fever vaccine in humans. *Nat Immunol*, 10(1):116–125, January 2009.

[73] Michael C. Aichinger, Michael Ginzler, Julian Weghuber, Lars Zimmermann, Karin Riedl, Gerhard Schuetz, Eszter Nagy, Alexander von Gabain, Rudolf Schweyen, and Tamas Henics. Adjuvating the adjuvant: Facilitated delivery of an immunomodulatory oligonucleotide toTLR9 by a cationic antimicrobial peptide in dendritic cells . *Vaccine*, 29(3):426 – 436, 2011.

[74] Amanda L. Blasius and Bruce Beutler. Intracellular Toll-like Receptors . *Immunity*, 32(3):305 – 315, 2010.

[75] Taro Kawai and Takumi Kawasaki. Toll-like receptor signaling pathways. *Frontiers in Immunology*, 5(461), 2014.

[76] Martien L. Kapsenberg. Dendritic-cell control of pathogen-driven T-cell polarization. *Nat Rev Immunol*, 3(12):984–993, December 2003.

[77] Donna L. Farber, Naomi A. Yudanin, and Nicholas P. Restifo. Human memory T cells: generation, compartmentalization and homeostasis. *Nat Rev Immunol*, 14(1):24–35, January 2014.

[78] John T Chang, E John Wherry, and Ananda W Goldrath. Molecular regulation of effector and memory T cell differentiation. *Nat Immunol*, 15(12):1104–1115, December 2014.

[79] Federica Sallusto, Danielle Lenig, Reinhold Forster, Martin Lipp, and Antonio Lanzavecchia. Two subsets of memory T lymphocytes with distinct homing potentials and effector functions. *Nature*, 1999.

[80] Luca Gattinoni, Enrico Lugli, Yun Ji, Zoltan Pos, Chrystal M Paulos, Maire F Quigley, Jorge R Almeida, Emma Gostick, Zhiya Yu, Carmine Carpenito, Ena Wang, Daniel C Douek, David A Price, Carl H June, Francesco M Marincola, Mario Roederer, and Nicholas P Restifo. A human memory T cell subset with stem cell-like properties. *Nat Med*, 2011.

[81] Rahul Purwar, James Campbell, George Murphy, William G. Richards, Rachael A. Clark, and Thomas S. Kupper. Resident Memory T Cells (T_{RM}) Are Abundant in Human Lung: Diversity, Function, and Antigen Specificity. *PLoS ONE*, 6(1):e16245, 01 2011.

[82] Dietmar Herndler-Brandstetter, Katja Landgraf, Brigitte Jenewein, Alexandar Tzankov, Regina Brunauer, Stefan Brunner, Walther Parson, Frank Kloss, Robert Gassner, Günter Lepperdinger, and Beatrix Grubeck-Loebenstein. Human Bone Marrow Hosts Polyfunctional Memory CD4+ and CD8+ T Cells with Close Contact to IL-15-Producing Cells. *The Journal of Immunology*, 186(12):6965–6971, 2011.

[83] Taheri Sathaliyawala, Masaru Kubota, Naomi Yudanin, Damian Turner, Philip Camp, Joseph J C Thome, Kara L Bickham, Harvey Lerner, Michael Goldstein, Megan Sykes, Tomoaki Kato, and Donna L Farber. Distribution and compartmentalization of human circulating and tissue-resident memory T cell subsets. *Immunity*, 38(1):187–197, December 2012.

[84] Michael L. Landrum, Katherine Huppler Hullsiek, Robert J. O'Connell, Helen M. Chun, Anuradha Ganesan, Jason F. Okulicz, Tahaniyat Lalani, Amy C. Weintrob, Nancy F. Crum-Cianflone, Brian K. Agan, and Infectious Disease Clinical Research Program HIV Working Group. Hepatitis B Vaccine Antibody Response and the Risk of Clinical AIDS or Death. *PLoS ONE*, 7(3):e33488, 03 2012.

[85] Jason F. Okulicz, Octavio Mesner, Anuradha Ganesan, Thomas A. O'Bryan, Robert G. Deiss, and Brian K. Agan. Hepatitis B Vaccine Responsiveness and Clinical Outcomes in HIV Controllers. *PLoS ONE*, 9(8):e105591, 08 2014.

[86] Sharilyn K. Stanley, Mario A. Ostrowski, Jesse S. Justement, Kira Gantt, Susan Hedayati, Margaret Mannix, Kim Roche, Douglas J. Schwartzentruber, Cecil H. Fox, and Anthony S. Fauci. Effect of Immunization with a Common Recall Antigen on Viral Expression in Patients Infected with Human Immunodeficiency Virus Type 1. *New England Journal of Medicine*, 334(19):1222–1229, 1996. PMID: 8606717.

[87] Lorenzo A. Ramirez, Alexander Daniel, Ian Frank, Pablo Tebas, and Jean Boyer. Seroprotection of HIV-Infected Subjects after H1N1-vaccination is Directly Associated with Baseline frequency of Naive T-Cells. *Journal of Infectious Diseases*, 2014.

[88] Akiko Iwasaki. Innate Immune Recognition of HIV-1. *Immunity*, 37(3):389 – 398, 2012.

[89] Martin D. Hyrcza, Colin Kovacs, Mona Loutfy, Roberta Halpenny, Lawrence Heisler, Stuart Yang, Olivia Wilkins, Mario Ostrowski, and Sandy D. Der. Distinct Transcriptional Profiles in *Ex Vivo* CD4+ and CD8+ T Cells Are Established Early in Human Immunodeficiency Virus Type 1 Infection and Are Characterized by a Chronic Interferon Response as Well as Extensive Transcriptional Changes in CD8+ T Cells. *Journal of Virology*, 81(7):3477–3486, 2007.

[90] Margalida Rotger, Judith Dalmau, Andri Rauch, Paul McLaren, Steven E. Bosinger, Raquel Martinez, Netanya G. Sandler, Annelys Roque, Julia Liebner, Manuel Battegay, Enos Bernasconi, Patrick Descombes, Itziar Erkizia, Jacques Fellay, Bernard Hirschel, José M. Miro, Eduard Palou, Matthias Hoffmann, Marta Massanella, Juliàă Blanco, Matthew Woods, Huldrych F. Günthard, Paul de Bakker, Daniel C. Douek, Guido Silvestri, Javier Martinez-Picado, and Amalio Telenti. Comparative transcriptomics of extreme phenotypes of human HIV-1 infection and SIV infection in sooty mangabey and rhesus macaque. *The Journal of Clinical Investigation*, 121(6):2391–2400, 6 2011.

[91] Meagan O'Brien, Olivier Manches, Rachel Lubong Sabado, Sonia Jimenez Baranda, Yaming Wang, Isabelle Marie, Linda Rolnitzky, Martin Markowitz, David M. Margolis, David Levy, and Nina Bhardwaj. Spatiotemporal trafficking of HIV in human plasmacytoid dendritic cells defines a persistently IFN-α producing and partially matured phenotype. *The Journal of Clinical Investigation*, 121(3):1088–1101, 3 2011.

[92] Jeffrey A. Martinson, Alejandro Roman-Gonzalez, Allan R. Tenorio, Carlos J. Montoya, Carolyne N. Gichinga, Maria T. Rugeles, Mark Tomai, Arthur M. Krieg, Smita Ghanekar, Linda L. Baum, and Alan L. Landay. Dendritic cells from HIV-1 infected individuals are less responsive to toll-like receptor (TLR) ligands . *Cellular Immunology*, 250:75 – 84, 2007.

[93] Erietta Stelekati, Haina Shin, TravisăA. Doering, DouglasăV. Dolfi, CarlyăG. Ziegler, DanielăP. Beiting, Lucas Dawson, Jennifer Liboon, David Wolski, Mohammed-Alkhatim.A. Ali, PeteraD. Katsikis, Hao Shen, DavidăS. Roos, W.ăNicholas Haining, GeorgăM. Lauer, and E.ăJohn Wherry. Bystander Chronic Infection Negatively Impacts Development of CD8+ T Cell Memory. *Immunity*, 40(5):801 – 813, 2014.

[94] WHO. World Malaria Report 2013. *World Health Organization*, 2013.

[95] Louis H. Miller, Dror I. Baruch, Kevin Marsh, and Ogobara K. Doumbo. The pathogenic basis of malaria. *Nature*, 415(6872):673–679, February 2002.

[96] L. H. Bannister, J. M. Hopkins, R. E. Fowler, S. Krishna, and G. H. Mitchell. A Brief Illustrated Guide to the Ultrastructure of *Plasmodium falciparum* Asexual Blood Stages. *Parasitology Today*, 16(10):427 – 433, 2000.

[97] Brian M. Greenwood, David A. Fidock, Dennis E. Kyle, Stefan H.I. Kappe, Pedro L. Alonso, Frank H. Collins, and Patrick E. Duffy. Malaria: progress, perils, and prospects for eradication. *The Journal of Clinical Investigation*, 118(4):1266–1276, 4 2008.

[98] C Golgi. On the cycle of development of malarial parasites in tertian fever: differential diagnosis between the intracellular parasites of tertian and quartant fever. *Archivio per le Scienza Mediche*, 13:173–196, 1889. italian.

[99] Louis H Miller, Hans C Ackerman, Xin-zhuan Su, and Thomas E Wellems. Malaria biology and disease pathogenesis: insights for new treatments. *Nat Med*, 19(2):156–167, February 2013.

[100] Louis Schofield and Georges E. Grau. Immunological processes in malaria pathogenesis. *Nat Rev Immunol*, 5(9):722–735, September 2005.

[101] Ian Clark, Alison Budd, Lisa Alleva, and William Cowden. Human malarial disease: a consequence of inflammatory cytokine release. *Malaria Journal*, 5(1):85, 2006.

[102] Lucy C. Okell, Teun Bousema, Jamie T. Griffin, Andre Lin Ouedraogo, Azra C. Ghani, and Chris J. Drakeley. Factors determining the occurrence of submicroscopic malaria infections and their relevance for control. *Nat Commun*, 3:1237–, December 2012.

[103] Benjamin J Visser, Michele van Vugt, and Martin P Grobusch. Malaria: an update on current chemotherapy. *Expert Opinion on Pharmacotherapy*, 15(15):2219–2254, 2014. PMID: 25110058.

[104] S Clincal Trials Partnership The RTS. First Results of Phase 3 Trial of RTS,S/AS01 Malaria Vaccine in African Children. *New England Journal of Medicine*, 365(20):1863–1875, 2011. PMID: 22007715.

[105] S Clinical Trials Partnership (2014) The RTS. Efficacy and Safety of the RTS,S/AS01 Malaria Vaccine during 18 Months after Vaccination: A Phase 3 Randomized, Controlled Trial in Children and Young Infants at 11 African Sites. *PLoS Med*, 11(7):e1001685, 07 2014.

[106] Robert A. Seder, Lee-Jah Chang, Mary E. Enama, Kathryn L. Zephir, Uzma N. Sarwar, Ingelise J. Gordon, LaSonji A. Holman, Eric R. James, Pe-

ter F. Billingsley, Anusha Gunasekera, Adam Richman, Sumana Chakravarty, Anita Manoj, Soundarapandian Velmurugan, MingLin Li, Adam J. Ruben, Tao Li, Abraham G. Eappen, Richard E. Stafford, Sarah H. Plummer, Cynthia S. Hendel, Laura Novik, Pamela J. M. Costner, Floreliz H. Mendoza, Jamie G. Saunders, Martha C. Nason, Jason H. Richardson, Jittawadee Murphy, Silas A. Davidson, Thomas L. Richie, Martha Sedegah, Awalludin Sutamihardja, Gary A. Fahle, Kirsten E. Lyke, Matthew B. Laurens, Mario Roederer, Kavita Tewari, Judith E. Epstein, B. Kim Lee Sim, Julie E. Ledgerwood, Barney S. Graham, Stephen L. Hoffman, and the VRC 312 Study Team. Protection Against Malaria by Intravenous Immunization with a Nonreplicating Sporozoite Vaccine. *Science*, 341(6152):1359–1365, 2013.

[107] Luke A. J. O'Neill, Douglas Golenbock, and Andrew G. Bowie. The history of Toll-like receptors [mdash] redefining innate immunity. *Nat Rev Immunol*, 13(6):453–460, June 2013.

[108] Roman Barbalat, Sarah E. Ewald, Maria L. Mouchess, and Gregory M. Barton. Nucleic Acid Recognition by the Innate Immune System. *Annual Review of Immunology*, 29(1):185–214, 2011. PMID: 21219183.

[109] Kate Schroder and Jurg Tschopp. The Inflammasomes . *Cell*, 140(6):821 – 832, 2010.

[110] Peter Liehl, Vanessa Zuzarte-Luis, Jennie Chan, Thomas Zillinger, Fernanda Baptista, Daniel Carapau, Madlen Konert, Kirsten K Hanson, Celine Carret, Caroline Lassnig, Mathias Muller, Ulrich Kalinke, Mohsan Saeed, Angelo Ferreira Chora, Douglas T Golenbock, Birgit Strobl, Miguel Prudencio, Luis P Coelho, Stefan H Kappe, Giulio Superti-Furga, Andreas Pichlmair, Ana M Vigario, Charles M Rice, Katherine A Fitzgerald, Winfried Barchet, and

Maria M Mota. Host-cell sensors for Plasmodium activate innate immunity against liver-stage infection. *Nat Med*, 20(1):47–53, January 2014.

[111] Peggy Parroche, Fanny N. Lauw, Nadege Goutagny, Eicke Latz, Brian G. Monks, Alberto Visintin, Kristen A. Halmen, Marc Lamphier, Martin Olivier, Daniella C. Bartholomeu, Ricardo T. Gazzinelli, and Douglas T. Golenbock. Malaria hemozoin is immunologically inert but radically enhances innate responses by presenting malaria DNA to Toll-like receptor 9. *Proceedings of the National Academy of Sciences*, 104(6):1919–1924, 2007.

[112] Gowdahalli Krishnegowda, Adeline M. Hajjar, Jianzhong Zhu, Erika J. Douglass, Satoshi Uematsu, Shizuo Akira, Amina S. Woods, and D. Channe Gowda. Induction of Proinflammatory Responses in Macrophages by the Glycosylphosphatidylinositols of *Plasmodium falciparum*: CELL SIGNALING RECEPTORS, GLYCOSYLPHOSPHATIDYLINOSITOL (GPI) STRUCTURAL REQUIREMENT, AND REGULATION OF GPI ACTIVITY. *Journal of Biological Chemistry*, 280(9):8606–8616, 2005.

[113] Alyssa Baccarella, Mary F. Fontana, Eunice C. Chen, and Charles C. Kim. Toll-Like Receptor 7 Mediates Early Innate Immune Responses to Malaria. *Infection and Immunity*, 81(12):4431–4442, 2013.

[114] Peter Goldie, Eugene F. Roth, Joel Oppenheim, and Jerome P. Vanderberg. Biochemical Characterization of Plasmodium falciparum Hemozoin. *The American Journal of Tropical Medicine and Hygiene*, 43(6):584–596, 1990.

[115] L Schofield, S Novakovic, P Gerold, R T Schwarz, M J McConville, and S D Tachado. Glycosylphosphatidylinositol toxin of Plasmodium up-regulates intercellular adhesion molecule-1, vascular cell adhesion molecule-1, and E-selectin expression in vascular endothelial cells and increases leukocyte and

parasite cytoadherence via tyrosine kinase-dependent signal transduction. *The Journal of Immunology*, 156(5):1886–96, 1996.

[116] Ricardo T. Gazzinelli, Parisa Kalantari, Katherine A. Fitzgerald, and Douglas T. Golenbock. Innate sensing of malaria parasites. *Nat Rev Immunol*, 14(11):744–757, November 2014.

[117] Jean Langhorne, Francis M Ndungu, Anne-Marit Sponaas, and Kevin Marsh. Immunity to malaria: more questions than answers. *Nat Immunol*, 9(7):725–732, July 2008.

[118] Janine Jason, Lennox K. Archibald, Okey C. Nwanyanwu, Michael Bell, Ian Buchanan, Joshua Larned, Peter N. Kazembe, Hamish Dobbie, Bharat Parekh, Martha G. Byrd, Angelia Eick, Alison Han, and William R. Jarvis. Cytokines and Malaria Parasitemia . *Clinical Immunology*, 100(2):208 – 218, 2001.

[119] Robert A. Gramzinski, Denise L. Doolan, Martha Sedegah, Heather L. Davis, Arthur M. Krieg, and Stephen L. Hoffman. Interleukin-12- and Gamma Interferon-Dependent Protection against Malaria Conferred by CpG Oligodeoxynucleotide in Mice. *Infection and Immunity*, 69(3):1643–1649, 2001.

[120] Mary M. Stevenson and Eleanor M. Riley. Innate immunity to malaria. *Nat Rev Immunol*, 4(3):169–180, March 2004.

[121] M J Blackman, H G Heidrich, S Donachie, J S McBride, and A A Holder. A single fragment of a malaria merozoite surface protein remains on the parasite during red cell invasion and is the target of invasion-inhibiting antibodies. *The Journal of Experimental Medicine*, 172(1):379–382, 1990.

[122] H Bouharoun-Tayoun, C Oeuvray, F Lunel, and P Druilhe. Mechanisms underlying the monocyte-mediated antibody-dependent killing of Plasmodium falciparum asexual blood stages. *The Journal of Experimental Medicine*, 182(2):409–418, 1995.

[123] Ramachandra S. Naik, OraLee H. Branch, Amina S. Woods, Matam Vijaykumar, Douglas J. Perkins, Bernard L. Nahlen, Altaf A. Lal, Robert J. Cotter, Catherine E. Costello, Christian F. Ockenhouse, Eugene A. Davidson, and D. Channe Gowda. Glycosylphosphatidylinositol Anchors of Plasmodium falciparum: Molecular Characterization and Naturally Elicited Antibody Response That May Provide Immunity to Malaria Pathogenesis. *The Journal of Experimental Medicine*, 192(11):1563–1576, 2000.

[124] D. Dodoo, F. M. Omer, J. Todd, B. D. Akanmori, K. A. Koram, and E. M. Riley. Absolute Levels and Ratios of Proinflammatory and Anti-inflammatory Cytokine Production In Vitro Predict Clinical Immunity to Plasmodium falciparum Malaria. *Journal of Infectious Diseases*, 185(7):971–979, 2002.

[125] Fakhereldin M. Omer and Eleanor M. Riley. Transforming Growth Factor β Production Is Inversely Correlated with Severity of Murine Malaria Infection. *The Journal of Experimental Medicine*, 188(1):39–48, 1998.

[126] Margarida Saraiva and Anne O'Garra. The regulation of IL-10 production by immune cells. *Nat Rev Immunol*, 10(3):170–181, March 2010.

[127] Utzinger Jürg, Beckera Sören L., Knopp Stefanie, Blum Johannes, Neumayr Andreas L., Keiser Jennifer, and Hatz Christoph F. Neglected tropical diseases: diagnosis, clinical management, treatment and control. *Swiss Med Wkly.*, 142:w13727, 2012.

[128] Stefanie Knopp, Peter Steinmann, Jennifer Keiser, and Jürg Utzinger. Nematode Infections: Soil-Transmitted Helminths and Trichinella . *Infectious Disease Clinics of North America*, 26(2):341 – 358, 2012. Tropical Diseases.

[129] Jeffrey Bethony, Simon Brooker, Marco Albonico, Stefan M Geiger, Alex Loukas, David Diemert, and Peter J Hotez. Soil-transmitted helminth infections: ascariasis, trichuriasis, and hookworm . *The Lancet*, 367(9521):1521 – 1532, 2006.

[130] Rachel Pullan, Jennifer Smith, Rashmi Jasrasaria, and Simon Brooker. Global numbers of infection and disease burden of soil transmitted helminth infections in 2010. *Parasites & Vectors*, 7(1):37, 2014.

[131] Alejandro J. Krolewiecki, Patrick Lammie, Julie Jacobson, Albis-Francesco Gabrielli, Bruno Levecke, Eugenia Socias, Luis M. Arias, Nicanor Sosa, David Abraham, Ruben Cimino, Adriana Echaz, Favio Crudo, Jozef Vercruysse, and Marco Albonico. A Public Health Response against *Strongyloides stercoralis*: Time to Look at Soil-Transmitted Helminthiasis in Full. *PLoS Negl Trop Dis*, 7(5):e2165, 05 2013.

[132] Stefanie Knopp, Nahya Salim, Tobias Schindler, Dimitrios A. Karagiannis Voules, Julian Rothen, Omar Lweno, Alisa S. Mohammed, Raymond Singo, Myrna Benninghoff, Anthony A. Nsojo, Blaise Genton, and Claudia Daubenberger. Diagnostic Accuracy of Kato-Katz, FLOTAC, Baermann, and PCR Methods for the Detection of Light-Intensity Hookworm and *Strongyloides stercoralis* Infections in Tanzania. *The American Journal of Tropical Medicine and Hygiene*, 90(3):535–545, 2014.

[133] Martin Montes, Charu Sawhney, and Nicolas Barros. Strongyloides stercoralis: there but not seen. *Current Opinion in Infectious Diseases*, 23(5):–, 2010.

[134] Sören L. Becker, Benjamin Sieto, Kigbafori D. Silue, Lucas Adjossan, Siaka Kone, Christoph Hatz, Winfried V. Kern, Eliezer K. N'Goran, and Jürg Utzinger. Diagnosis, Clinical Features, and Self-Reported Morbidity of *Strongyloides stercoralis* and Hookworm Infection in a Co-Endemic Setting. *PLoS Negl Trop Dis*, 5(8):e1292, 08 2011.

[135] Karin Leder and Peter F Weller. Eosinophilia and helminthic infections . *Best Practice & Research Clinical Haematology*, 13(2):301 – 317, 2000.

[136] Virak Khieu, Sophanaroth Srey, Fabian Schar, Sinuon Muth, Hanspeter Marti, and Peter Odermatt. *Strongyloides stercoralis* is a cause of abdominal pain, diarrhea and urticaria in rural Cambodia. *BMC Research Notes*, 6(1):200, 2013.

[137] Marisel Segarra-Newnham. Manifestations, Diagnosis, and Treatment of Strongyloides stercoralis Infection. *Annals of Pharmacotherapy*, 41(12):1992–2001, 2007.

[138] Fabian Schär, Ulf Trostdorf, Federica Giardina, Virak Khieu, Sinuon Muth, Hanspeter Marti, Penelope Vounatsou, and Peter Odermatt. *Strongyloides stercoralis*: Global Distribution and Risk Factors. *PLoS Negl Trop Dis*, 7(7):e2288, 07 2013.

[139] Vassil St Georgiev. Chemotherapy of enterobiasis (oxyuriasis). *Expert Opinion on Pharmacotherapy*, 2(2):267–275, 2001. PMID: 11336585.

[140] Gary F. Fry and John G Moore. *Enterobius vermicularis*: 10,000-year-old human infection. *Science*, 166:(3913):1620, 1969.

[141] Salim Nahya, Schindler Tobias, Abdul Ummi, Rothen Julian, Genton Blaise, Lweno Omar, Mohammed Alisa S, Masimba John, Kwaba Denis, Abdulla Salim, Tanner Marcel, Daubenberger Claudia, and Knopp Stefanie. Enterobiasis and strongyloidiasis and associated co-infections and morbidity markers in infants, preschool- and school-aged children from rural coastal Tanzania: a cross-sectional study. *BMC Infectious diseases*, 14:644, 2014.

[142] Luciene Mascarini-Serra. Prevention of Soil-transmitted Helminth Infection. *Journal of Global Infectious Diseases*, 3(2):175–182, 2011.

[143] Shanthi Kappagoda, Upinder Singh, and Brian G Blackburn. Antiparasitic Therapy. *Mayo Clinic Proceedings*, 86(6):561–583, June 2011.

[144] William C. Gause, Thomas A. Wynn, and Judith E. Allen. Type 2 immunity and wound healing: evolutionary refinement of adaptive immunity by helminths. *Nat Rev Immunol*, 13(8):607–614, August 2013.

[145] M. W. Lightowlers and M. D. Rickard. Excretory-secretory products of helminth parasites: effects on host immune responses. *Parasitology*, 96:S123–S166, 1 1988.

[146] Helen S. Goodridge, Fraser A. Marshall, Kathryn J. Else, Katrina M. Houston, Caitlin Egan, Lamyaa Al-Riyami, Foo-Yew Liew, William Harnett, and Margaret M. Harnett. Immunomodulation via Novel Use of TLR4 by the Filarial Nematode Phosphorylcholine-Containing Secreted Product, ES-62. *The Journal of Immunology*, 174(1):284–293, 2005.

[147] Alex Loukas, Nicholas P. Mullin, Kevin K.A. Tetteh, Luc Moens, and Rick M. Maizels. A novel C-type lectin secreted by a tissue-dwelling parasitic nematode . *Current Biology*, 9(15):825 – 828, 1999.

[148] Nirav Patel, Wenhui Wu, Pankaj K. Mishra, Fei Chen, Ariel Millman, Balazs Csoka, Balzs Koscso, Holger K. Eltzschig, György Haskó, and William C. Gau. A2B Adenosine Receptor Induces Protective Antihelminth Type 2 Immune Responses. *Cell Host & Microbe*, 15(3):339 – 350, 2014.

[149] Thirumalai R. Ramalingam, John T. Pesce, Margaret M. Mentink-Kane, Satish Madala, Allen W. Cheever, Michael R. Comeau, Steven F. Ziegler, and Thomas A. Wynn. Regulation of Helminth-Induced Th2 Responses by Thymic Stromal Lymphopoietin. *The Journal of Immunology*, 182(10):6452–6459, 2009.

[150] Neil E. Humphreys, Damo Xu, Matthew R. Hepworth, Foo Y. Liew, and Richard K. Grencis. IL-33, a Potent Inducer of Adaptive Immunity to Intestinal Nematodes. *The Journal of Immunology*, 180(4):2443–2449, 2008.

[151] D Artis and R K Grencis. The intestinal epithelium: sensors to effectors in nematode infection. *Mucosal Immunol*, 1(4):252–264, May 2008.

[152] Nicola Harris and William C. Gause. To B or not to B: B cells and the Th2-type immune response to helminths . *Trends in Immunology*, 32(2):80 – 88, 2011.

[153] Bridget M. Ogilvie, Ann Bartlett, R.C. Godfrey, J.A. Turton, M.J. Worms, and R.A. Yeates. Antibody responses in self-infections with Necator americanus. *Transactions of The Royal Society of Tropical Medicine and Hygiene*, 72(1):66–71, 1978.

[154] Michael F. Gurish, Paul J. Bryce, Hong Tao, Alison B. Kisselgof, Elizabeth M. Thornton, Hugh R. Miller, Daniel S. Friend, and Hans C. Oettgen. IgE Enhances Parasite Clearance and Regulates Mast Cell Responses in Mice Infected with Trichinella spiralis . *The Journal of Immunology*, 172(2):1139–1145, 2004.

[155] P K Mishra, M Palma, D Bleich, P Loke, and W C Gause. Systemic impact of intestinal helminth infections. *Mucosal Immunol*, 7(4):753–762, July 2014.

[156] Ruth E. Ley, Peter J. Turnbaugh, Samuel Klein, and Jeffrey I. Gordon. Microbial ecology: Human gut microbes associated with obesity. *Nature*, 444(7122):1022–1023, December 2006.

[157] Peter J Turnbaugh, Ruth E Ley, Micah Hamady, Claire Fraser-Liggett, Rob Knight, and Jeffrey I Gordon. The human microbiome project: exploring the microbial part of ourselves in a changing world. *Nature*, 449(7164):804–810, October 2007.

[158] Mitchell L Jones, Jorge G Ganopolsky, Christopher J Martoni, Alain Labbe, and Satya Prakash. Emerging science of the human microbiome. *Gut Microbes*, 5(4):446–457, 2014.

[159] Ann M O'Hara and Fergus Shanahan. The gut flora as a forgotten organ. *EMBO reports*, 7(7):688–693, 2006.

[160] Maria G. Dominguez-Bello, Elizabeth K. Costello, Monica Contreras, Magda Magris, Glida Hidalgo, Noah Fierer, and Rob Knight. Delivery mode shapes the acquisition and structure of the initial microbiota across multiple body habitats in newborns. *Proceedings of the National Academy of Sciences*, 107(26):11971–11975, 2010.

[161] Chana Palmer, Elisabeth M Bik, Daniel B DiGiulio, David A Relman, and Patrick O Brown. Development of the Human Infant Intestinal Microbiota. *PLoS Biol*, 5(7):e177, 06 2007.

[162] Jeremy E. Koenig, Aymé Spor, Nicholas Scalfone, Ashwana D. Fricker, Jesse Stombaugh, Rob Knight, Largus T. Angenent, and Ruth E. Ley. Succession of microbial consortia in the developing infant gut microbiome. *Proceedings of the National Academy of Sciences*, 108(Supplement 1):4578–4585, 2011.

[163] L.A. David, C.F. Maurice, R.N. Carmody, D.B. Gootenberg, J.E. Button, B.E. Wolfe, A.V. Ling, A.S. Devlin, Y. Varma, M.A. Fischbach, S.B. Biddinger, R.J. Dutton, and P.J. Turnbaugh. Diet rapidly and reproducibly alters the human gut microbiome. *Nature*, 505(7484):559–563, 2014. cited By 117.

[164] Ana Elena Pérez-Cobas, María José Gosalbes, Anette Friedrichs, Henrik Knecht, Alejandro Artacho, Kathleen Eismann, Wolfgang Otto, David Rojo, Rafael Bargiela, Martin von Bergen, Sven C Neulinger, Carolin Däumer, Femke-Anouska Heinsen, Amparo Latorre, Coral Barbas, Jana Seifert, Vitor Martins dos Santos, Stephan J Ott, Manuel Ferrer, and Andrés Moya. Gut microbiota disturbance during antibiotic therapy: a multi-omic approach. *Gut*, 62(11):1591–1601, 2013.

[165] Pawel Gajer, Rebecca M. Brotman, Guoyun Bai, Joyce Sakamoto, Ursel M. E. Schütte, Xue Zhong, Sara S. K. Koenig, Li Fu, Zhanshan (Sam) Ma, Xia Zhou, Zaid Abdo, Larry J. Forney, and Jacques Ravel. Temporal Dynamics of the Human Vaginal Microbiota. *Science Translational Medicine*, 4(132):132ra52, 2012.

[166] Omry Koren, Julia K. Goodrich, Tyler C. Cullender, Ayme Spor, Kirsi Laitinen, Helene Kling Baeckhed, Antonio Gonzalez, Jeffrey J. Werner, Largus T. Angenent, Rob Knight, Fredrik Baeckhed, Erika Isolauri, Seppo Salminen, and Ruth E. Ley. Host Remodeling of the Gut Microbiome and Metabolic Changes during Pregnancy . *Cell*, 150(3):470 – 480, 2012.

[167] T. Yatsunenko, F.E. Rey, M.J. Manary, I. Trehan, M.G. Dominguez-Bello, M. Contreras, M. Magris, G. Hidalgo, R.N. Baldassano, A.P. Anokhin, A.C. Heath, B. Warner, J. Reeder, J. Kuczynski, J.G. Caporaso, C.A. Lozupone, C. Lauber, J.C. Clemente, D. Knights, R. Knight, and J.I. Gordon. Human gut microbiome viewed across age and geography. *Nature*, 486(7402):222–227, 2012. cited By 494.

[168] Jacqueline M. Leung and P'ng Loke. A role for IL-22 in the relationship between intestinal helminths, gut microbiota and mucosal immunity . *International Journal for Parasitology*, 43:253 – 257, 2013.

[169] Human Microbiome Project Consortium. Structure, function and diversity of the healthy human microbiome. *Nature*, 486:(7402):207–14, 2011.

[170] The Human Microbiome Project Consortium. A framework for human microbiome research. *Nature*, 486:215–221, 2012.

[171] Manimozhiyan Arumugam, Jeroen Raes, Eric Pelletier, Denis Le Paslier, Takuji Yamada, Daniel R. Mende, Gabriel R. Fernandes, Julien Tap, Thomas Bruls, Jean-Michel Batto, Marcelo Bertalan, Natalia Borruel, Francesc Casellas, Leyden Fernandez, Laurent Gautier, Torben Hansen, Masahira Hattori, Tetsuya Hayashi, Michiel Kleerebezem, Ken Kurokawa, Marion Leclerc, Florence Levenez, Chaysavanh Manichanh, H. Bjorn Nielsen, Trine Nielsen, Nicolas Pons, Julie Poulain, Junjie Qin, Thomas Sicheritz-Ponten, Sebas-

tian Tims, David Torrents, Edgardo Ugarte, Erwin G. Zoetendal, Jun Wang, Francisco Guarner, Oluf Pedersen, Willem M. de Vos, Soren Brunak, Joel Dore, Jean Weissenbach, S. Dusko Ehrlich, and Peer Bork. Enterotypes of the human gut microbiome. *Nature*, 473(7346):174–180, May 2011.

[172] Martin J. Blaser and Stanley Falkow. What are the consequences of the disappearing human microbiota? *Nat Rev Micro*, 7(12):887–894, December 2009.

[173] Mirjana Rajilic-Stojanovic. Function of the microbiota . *Best Practice & Research Clinical Gastroenterology*, 27(1):5 – 16, 2013. The Gut Microbiome.

[174] K. Vipperla and S.J. O'Keefe. The microbiota and its metabolites in colonic mucosal health and cancer risk. *Nutrition in Clinical Practice*, 27(5):624–635, 2012. cited By 21.

[175] S. Tedelind, F. Westberg, M. Kjerrulf, and A. Vidal. Anti-inflammatory properties of the short-chain fatty acids acetate and propionate: A study with relevance to inflammatory bowel disease. *World Journal of Gastroenterology*, 13(20):2826–2832, 2007. cited By 120.

[176] L.B. Bindels, P. Porporato, E.M. Dewulf, J. Verrax, A.M. Neyrinck, J.C. Martin, K.P. Scott, P. Buc Calderon, O. Feron, G.G. Muccioli, P. Sonveaux, P.D. Cani, and N.M. Delzenne. Gut microbiota-derived propionate reduces cancer cell proliferation in the liver. *British Journal of Cancer*, 107(8):1337–1344, 2012. cited By 17.

[177] E.A. Smith and G.T. Macfarlane. Dissimilatory amino acid metabolism in human colonic bacteria. *Anaerobe*, 3(5):327–337, 1997. cited By 61.

[178] W.R. Russell, S.W. Gratz, S.H. Duncan, G. Holtrop, J. Ince, L. Scobbie, G. Duncan, A.M. Johnstone, G.E. Lobley, R.J. Wallace, G.G. Duthie, and H.J. Flint. High-protein, reduced-carbohydrate weight-loss diets promote metabolite profiles likely to be detrimental to colonic health. *American Journal of Clinical Nutrition*, 93(5):1062–1072, 2011. cited By 70.

[179] Dennis H Stamp. Three hypotheses linking bile to carcinogenesis in the gastrointestinal tract: certain bile salts have properties that may be used to complement chemotherapy. *Medical Hypotheses*, 59(4):398–405, 2002.

[180] Phillip B. Hylemon, Huiping Zhou, William M. Pandak, Shunlin Ren, Gregorio Gil, and Paul Dent. Bile acids as regulatory molecules. *Journal of Lipid Research*, 50(8):1509–1520, 2009.

[181] Henri Duboc, Sylvie Rajca, Dominique Rainteau, David Benarous, Marie-Anne Maubert, Elodie Quervain, Ginette Thomas, Véronique Barbu, Lydie Humbert, Guillaume Despras, Chantal Bridonneau, Fabien Dumetz, Jean-Pierre Grill, Joëlle Masliah, Laurent Beaugerie, Jacques Cosnes, Olivier Chazouillères, Raoul Poupon, Claude Wolf, Jean-Maurice Mallet, Philippe Langella, Germain Trugnan, Harry Sokol, and Philippe Seksik. Connecting dysbiosis, bile-acid dysmetabolism and gut inflammation in inflammatory bowel diseases. *Gut*, 62(4):531–539, 2013.

[182] Jean Guy LeBlanc, Christian Milani, Graciela Savoy de Giori, Fernando Sesma, Douwe van Sinderen, and Marco Ventura. Bacteria as vitamin suppliers to their host: a gut microbiota perspective . *Current Opinion in Biotechnology*, 24(2):160 – 168, 2013.

[183] Dan R Littman and Eric G Pamer. Role of the commensal microbiota in normal and pathogenic host immune responses. *Cell host & microbe*, 10(4):311–323, October 2011.

[184] Holly Hardy, Jennifer Harris, Eleanor Lyon, Jane Beal, and Andrew D Foey. Probiotics, Prebiotics and Immunomodulation of Gut Mucosal Defences: Homeostasis and Immunopathology. *Nutrients*, 5(6):1869–1912, May 2013.

[185] David Artis. Epithelial-cell recognition of commensal bacteria and maintenance of immune homeostasis in the gut. *Nat Rev Immunol*, 8(6):411–420, June 2008.

[186] Erik Larsson, Valentina Tremaroli, Ying Shiuan Lee, Omry Koren, Intawat Nookaew, Ashwana Fricker, Jens Nielsen, Ruth E Ley, and Fredrik Bäckhed. Analysis of gut microbial regulation of host gene expression along the length of the gut and regulation of gut microbial ecology through MyD88. *Gut*, 61(8):1124–1131, 2012.

[187] Andrew J. Macpherson and Therese Uhr. Induction of Protective IgA by Intestinal Dendritic Cells Carrying Commensal Bacteria. *Science*, 303(5664):1662–1665, 2004.

[188] Harsh Mathur, Mary C. Rea, Paul D. Cotter, R. Paul Ross, and Colin Hill. The potential for emerging therapeutic options for Clostridium difficile infection. *Gut Microbes*, 0(ja):00–00, 2015. PMID: 25564777.

[189] Jonathan R Brestoff and David Artis. Commensal bacteria at the interface of host metabolism and the immune system. *Nat Immunol*, 14(7):676–684, July 2013.

[190] Stefano Fiorucci, Andrea Mencarelli, Giuseppe Palladino, and Sabrina Cipriani. Bile-acid-activated receptors: targeting TGR5 and farnesoid-X-receptor in lipid and glucose disorders. *Trends in Pharmacological Sciences*, 30(11):570–580, 2009.

[191] Jason M. Ridlon, Dae-Joong Kang, and Phillip B. Hylemon. Bile salt biotransformations by human intestinal bacteria. *Journal of Lipid Research*, 47(2):241–259, 2006.

[192] Piero Vavassori, Andrea Mencarelli, Barbara Renga, Eleonora Distrutti, and Stefano Fiorucci. The Bile Acid Receptor FXR Is a Modulator of Intestinal Innate Immunity. *The Journal of Immunology*, 183(10):6251–6261, 2009.

[193] Yan-Dong Wang, Wei-Dong Chen, Donna Yu, Barry M. Forman, and Wendong Huang. The G-Protein-coupled bile acid receptor, Gpbar1 (TGR5), negatively regulates hepatic inflammatory response through antagonizing nuclear factor kappa light-chain enhancer of activated B cells (NF-κB) in mice. *Hepatology*, 54(4):1421–1432, 2011.

[194] Thijs WH Pols, Mitsunori Nomura, Taoufiq Harach, Giuseppe Lo Sasso, Maaike H Oosterveer, Charles Thomas, Giovanni Rizzo, Antimo Gioiello, Luciano Adorini, Roberto Pellicciari, Johan Auwerx, and Kristina Schoonjans. TGR5 activation inhibits atherosclerosis by reducing macrophage inflammation and lipid loading. *Cell metabolism*, 14(6):747–757, December 2011.

[195] Andrew J. Brown, Susan M. Goldsworthy, Ashley A. Barnes, Michelle M. Eilert, Lili Tcheang, Dion Daniels, Alison I. Muir, Mark J. Wigglesworth, Ian Kinghorn, Neil J. Fraser, Nicholas B. Pike, Jay C. Strum, Klaudia M. Steplewski, Paul R. Murdock, Julie C. Holder, Fiona H. Marshall, Philip G. Szekeres, Shelagh Wilson, Diane M. Ignar, Steve M. Foord, Alan Wise, and

Simon J. Dowell. The Orphan G Protein-coupled Receptors GPR41 and GPR43 Are Activated by Propionate and Other Short Chain Carboxylic Acids. *Journal of Biological Chemistry*, 278(13):11312–11319, 2003.

[196] Markus Waldecker, Tanja Kautenburger, Heike Daumann, Cordula Busch, and Dieter Schrenk. Inhibition of histone-deacetylase activity by short-chain fatty acids and some polyphenol metabolites formed in the colon. *Journal of Nutritional Biochemistry*, 19(9):587–593, 2008.

[197] Dallas R Donohoe, Nikhil Garge, Xinxin Zhang, Wei Sun, Thomas M O'Connell, Maureen K Bunger, and Scott J Bultman. The Microbiome and Butyrate Regulate Energy Metabolism and Autophagy in the Mammalian Colon. *Cell metabolism*, 13(5):517–526, May 2011.

[198] Cox Mary Ann, Jackson James, Stanton Michaela, Rojas-Triana Alberto, Bober Loretta, Laverty Maureen, Yang Xiaoxin, Zhu Feng, Liu Jianjun, Wang Suke, Monsma Frederick, Vassileva Galya, Maguire Maureen, Gustafson Eric, Bayne Marvin, Chou Chuan-Chu, Lundell Daniel, and Jenh. Chung-Her. Short-chain fatty acids act as antiinflammatory mediators by regulating prostaglandin e2 and cytokines. *World J. Gastroenterol*, 28(15(44)):5549:5557, 2009.

[199] Lu Liu, Lin Li, Jun Min, Jie Wang, Heng Wu, Yujie Zeng, Shuang Chen, and Zhonghua Chu. Butyrate interferes with the differentiation and function of human monocyte-derived dendritic cells. *Cellular Immunology*, 277:66 – 73, 2012.

[200] Bradford E. Berndt, Min Zhang, Stephanie Y. Owyang, Tyler S. Cole, Teresa W. Wang, Jay Luther, Natalia A. Veniaminova, Juanita L. Merchant, Chun-Chia Chen, Gary B. Huffnagle, and John Y. Kao. Butyrate increases

IL-23 production by stimulated dendritic cells. *American Journal of Physiology - Gastrointestinal and Liver Physiology*, 303(12):G1384–G1392, 2012.

[201] Ning Huang, Jonathan P. Katz, Douglas R. Martin, and Gary D. Wu. INHIBITION OF IL-8 GENE EXPRESSION IN CACO-2 CELLS BY COMPOUNDS WHICH INDUCE HISTONE HYPERACETYLATION. *Cytokine*, 9(1):27 – 36, 1997.

[202] Luying Peng, Zhong-Rong Li, Robert S. Green, Ian R. Holzman, and Jing Lin. Butyrate Enhances the Intestinal Barrier by Facilitating Tight Junction Assembly via Activation of AMP-Activated Protein Kinase in Caco-2 Cell Monolayers. *The Journal of Nutrition*, 139(9):1619–1625, 2009.

[203] Padbidri Bhaskaram. Micronutrient Malnutrition, Infection, and Immunity: an Overview. *Nutrition Reviews*, 60(suppl 5):S40–S45, 2002.

[204] Lars Kjer-Nielsen, Onisha Patel, Alexandra J. Corbett, Jerome Le Nours, Bronwyn Meehan, Ligong Liu, Mugdha Bhati, Zhenjun Chen, Lyudmila Kostenko, Rangsima Reantragoon, Nicholas A. Williamson, Anthony W. Purcell, Nadine L. Dudek, Malcolm J. McConville, Richard A. J. O/'Hair, George N. Khairallah, Dale I. Godfrey, David P. Fairlie, Jamie Rossjohn, and James McCluskey. MR1 presents microbial vitamin B metabolites to MAIT cells. *Nature*, 491(7426):717–723, November 2012.

[205] Lionel Le Bourhis, Emmanuel Martin, Isabelle Peguillet, Amelie Guihot, Nathalie Froux, Maxime Core, Eva Levy, Mathilde Dusseaux, Vanina Meyssonnier, Virginie Premel, Charlotte Ngo, Beatrice Riteau, Livine Duban, Delphine Robert, Martin Rottman, Claire Soudais, and Olivier Lantz. Antimicrobial activity of mucosal-associated invariant T cells. *Nat Immunol*, 11(8):701–708, August 2010.

[206] Lionel Le Bourhis, Yvonne K Mburu, and Olivier Lantz. MAIT cells, surveyors of a new class of antigen: development and functions. *Current Opinion in Immunology*, 25(2):174 – 180, 2013. Lymphocyte development / Tumour immunology / Cancer immunology: Clinical translation.

[207] Gil Sharon, Neha Garg, Justine Debelius, Rob Knight, PieterăC. Dorrestein, and SarkisăK. Mazmanian. Specialized Metabolites from the Microbiome in Health and Disease. *Cell Metabolism*, 20(5):719–730, 2014.

[208] Milan K. Piya, Alison L. Harte, and Philip G. McTernan. Metabolic endotoxaemia: is it more than just a gut feeling? *Current Opinion in Lipidology*, 24(1):78–85, 2013.

[209] Elhaseen E. Elamin, Ad A. Masclee, Jan Dekker, Harm-Jan Pieters, and Daisy M. Jonkers. Short-Chain Fatty Acids Activate AMP-Activated Protein Kinase and Ameliorate Ethanol-Induced Intestinal Barrier Dysfunction in Caco-2 Cell Monolayers. *The Journal of Nutrition*, 143(12):1872–1881, 2013.

[210] Peter J Hotez, David H Molyneux, Alan Fenwick, Eric Ottesen, Sonia Ehrlich Sachs, and Jeffrey D Sachs. Incorporating a Rapid-Impact Package for Neglected Tropical Diseases with Programs for HIV/AIDS, Tuberculosis, and Malaria. *PLoS Med*, 3(5):e102, 01 2006.

[211] T. W. Mwangi, J. M. Bethony, and S. Brooker. Malaria and helminth interactions in humans: an epidemiological viewpoint. *Annals of Tropical Medicine and Parasitology*, 100(7):551–570, 2006-10-01T00:00:00.

[212] Padmini Salgame, George S Yap, and William C Gause. Effect of helminth-induced immunity on infections with microbial pathogens. *Nat Immunol*, 14(11):1118–1126, November 2013.

[213] T. Resende Co, C. S. Hirsch, Z. Toossi, R. Dietze, and R. Ribeiro-Rodrigues. Intestinal helminth co-infection has a negative impact on both anti-*Mycobacterium tuberculosis* immunity and clinical response to tuberculosis therapy. *Clinical & Experimental Immunology*, 147(1):45–52, 2007.

[214] Zhong Su, Mariela Segura, Kenneth Morgan, J. Concepcion Loredo-Osti, and Mary M. Stevenson. Impairment of Protective Immunity to Blood-Stage Malaria by Concurrent Nematode Infection. *Infection and Immunity*, 73(6):3531–3539, 2005.

[215] Aprilianto Wiria, Margaretta Prasetyani, Firdaus Hamid, Linda Wammes, Bertrand Lell, Iwan Ariawan, Hae Uh, Heri Wibowo, Yenny Djuardi, Sitti Wahyuni, Inge Sutanto, Linda May, Adrian Luty, Jaco Verweij, Erliyani Sartono, Maria Yazdanbakhsh, and Taniawati Supali. Does treatment of intestinal helminth infections influence malaria? Background and methodology of a longitudinal study of clinical, parasitological and immunological parameters in Nangapanda, Flores, Indonesia (ImmunoSPIN Study). *BMC Infectious Diseases*, 10(1):77, 2010.

[216] Mathieu Nacher. Interactions between worms and malaria: Good worms or bad worms? *Malar J*, 10:259, 2011.

[217] Aurelie A. Righetti, Dominik Glinz, Lukas G. Adiossan, Ahou-Yah G. Koua, Sebastien Niamke, Richard F. Hurrell, Rita Wegmueller, Eliezer K. N'Goran, and Juerg Utzinger. Interactions and Potential Implications of *Plasmodium falciparum*-Hookworm Coinfection in Different Age Groups in South-Central Cote d'Ivoire. *PLoS Negl Trop Dis*, 6(11):e1889, 11 2012.

[218] Rachel L. Pullan, Narcis B. Kabatereine, Hasifa Bukirwa, Sarah G. Staedke, and Simon Brooker. Heterogeneities and Consequences of Plasmodium

Species and Hookworm Coinfection: A Population Based Study in Uganda. *Journal of Infectious Diseases*, 203(3):406–417, 2011.

[219] Theresa K. Nkuo-Akenji, Primus C. Chi, Jerome F. Cho, Kenneth K. J. Ndamukong, and Irene Sumbele. Malaria and helminth co-infection in children living in a malaria endemic setting of Mount Cameroon and predictors of anemia. *Journal of Parasitology*, 92(6):1191–1195, December 2006.

[220] R. Kidenya Humphrey, D. Mazigo a d Benson, E. Ambrose Emmanuela, Zinga Maria, and Waihenya Rebecca. Association of intestinal helminths and *P. falciparum* infections in co-infected school children in northwest Tanzania. *Tanzania Journal of Health Research*, 12:283–285, 2010.

[221] Anna G.C. Boef, Linda May, David van Bodegom, Lisette van Lieshout, Jaco J. Verweij, Andrea B. Maier, Rudi G.J. Westendorp, and Ulrika K. Eriksson. Parasitic infections and immune function: Effect of helminth infections in a malaria endemic area. *Immunobiology*, 218(5):706–711, May 2013.

[222] Stephen D. Hillier, Mark Booth, Lawrence Muhangi, Peter Nkurunziza, Macklyn Khihembo, Muhammad Kakande, Moses Sewankambo, Robert Kizindo, Moses Kizza, Moses Muwanga, and Alison M. Elliott. *Plasmodium falciparum* and Helminth Coinfection in a Semiurban Population of Pregnant Women in Uganda. *Journal of Infectious Diseases*, 198(6):920–927, 2008.

[223] Laura Glendinning, Norman Nausch, Andrew Free, David W. Taylor, and Francisca Mutapi. The microbiota and helminths: sharing the same niche in the human host. *Parasitology*, 141:1255–1271, 9 2014.

[224] Lisa A Reynolds, Katherine A Smith, Kara J Filbey, Yvonne Harcus, James P Hewitson, Stephen A Redpath, Yanet Valdez, MarÃŋa J Yebra, B Brett Fin-

lay, and Rick M Maizels. Commensal-pathogen interactions in the intestinal tract. *Gut Microbes*, 5(4):522–532, 2014.

[225] K. S. Hayes, A. J. Bancroft, M. Goldrick, C. Portsmouth, I. S. Roberts, and R. K. Grencis. Exploitation of the Intestinal Microflora by the Parasitic Nematode Trichuris muris. *Science*, 328(5984):1391–1394, 2010.

[226] Robert W. Li, Sitao Wu, Weizhong Li, Karl Navarro, Robin D. Couch, Dolores Hill, and Joseph F. Urban. Alterations in the Porcine Colon Microbiota Induced by the Gastrointestinal Nematode *Trichuris suis*. *Infection and Immunity*, 80(6):2150–2157, 2012.

[227] Philip Cooper, Alan W. Walker, Jorge Reyes, Martha Chico, Susannah J. Salter, Maritza Vaca, and Julian Parkhill. Patent Human Infections with the Whipworm, *Trichuris trichiura*, Are Not Associated with Alterations in the Faecal Microbiota. *PLoS ONE*, 8(10):e76573, 10 2013.

[228] Soo Ching Lee, Mei San Tang, Yvonne A. L. Lim, Seow Huey Choy, Zachary D. Kurtz, Laura M. Cox, Uma Mahesh Gundra, Ilseung Cho, Richard Bonneau, Martin J. Blaser, Kek Heng Chua, and P'ng Loke. Helminth Colonization Is Associated with Increased Diversity of the Gut Microbiota. *PLoS Negl Trop Dis*, 8(5):e2880, 05 2014.

[229] Cinzia Cantacessi, Paul Giacomin, John Croese, Martha Zakrzewski, Javier Sotillo, Leisa McCann, Matthew J Nolan, Makedonka Mitreva, Lutz Krause, and Alex Loukas. Impact of Experimental Hookworm Infection on the Human Gut Microbiota. *Journal of Infectious Diseases*, 2014.

[230] Mara Jana Broadhurst, Amir Ardeshir, Bittoo Kanwar, Julie Mirpuri, Uma Mahesh Gundra, Jacqueline M. Leung, Kirsten E. Wiens, Ivan Vujkovic-Cvijin, Charlie C. Kim, Felix Yarovinsky, Nicholas W. Lerche, Joseph M.

McCune, and P'ng Loke. Therapeutic Helminth Infection of Macaques with Idiopathic Chronic Diarrhea Alters the Inflammatory Signature and Mucosal Microbiota of the Colon. *PLoS Pathog*, 8(11):e1003000, 11 2012.

[231] Sitao Wu, Robert W. Li, Weizhong Li, Ethiopia Beshah, Harry D. Dawson, and Joseph F. Urban, Jr. Worm Burden-Dependent Disruption of the Porcine Colon Microbiota by *Trichuris suis* Infection. *PLoS ONE*, 7(4):e35470, 04 2012.

[232] Bahtiyar Yilmaz, Portugal Silvia, Tran Tuan M., Gozzelino Raffaella, Ramos Susana, Gomes Joana, Regalado Ana, Cowan Peter J., d'Apice Anthony J.F., Chong Anita S., Doumbo Ogobara K., Traore Boubacar, Crompton Peter D., Silveira Henrique, and Soares Miguel P. Gut Microbiota Elicits a Protective Immune Response against Malaria Transmission. *Cell*, 159(6):1277–1289, 2014.

[233] Emsri Pongponratn, Mario Riganti, Benjanee Punpoowong, and Masamichi Aikawa. Microvascular Sequestration of Parasitized Erythrocytes in Human *Falciparum* Malaria: a Pathological Study. *The American Journal of Tropical Medicine and Hygiene*, 44(2):168–175, 1991.

[234] Winkler Weinberg, Polrat Wilairatana, Jon B. Meddings, May Ho, Suparb Vannaphan, and Sornchi Looareesuwan. Increased Gastrointestinal Permeability in Patients with *Plasmodium falciparum* Malaria. *Clinical Infectious Diseases*, 24(3):430–435, 1997.

[235] Malcolm E. Molyneux, Sornchai Looareesuwan, Ian S. Menzies, Stephen L. Grainger, Rodney E. Phillips, Yupaporn Wattanagoon, Richard P. H. Thompson, and David A. Warrell. Reduced Hepatic Blood Flow and Intesti-

nal Malabsorption in Severe *Falciparum* Malaria. *The American Journal of Tropical Medicine and Hygiene*, 40(5):470–476, 1989.

[236] Peter Olupot-Olupot, Britta Urban, Julie Jemutai, Julius Nteziyaremye, Harry Fanjo, Henry Karanja, Japhet Karisa, Paul Ongodia, Patrick Bwonyo, Evelyn Gitau, Alison Talbert, Samuel Akech, and Kathryn Maitland. Endotoxaemia is common in children with *Plasmodium falciparum* malaria. *BMC Infectious Diseases*, 13(1):117, 2013.

[237] WHO. Global tuberculosis report 2013. Available at *http* : *//www.who.int/tb/publications/global*$_r$*eport/en/*. Accessed 22 May 2014. *WHO*, 2013.

[238] Colditz GA, Brewer TF, Berkey CS, and et al. Efficacy of bcg vaccine in the prevention of tuberculosis: Meta-analysis of the published literature. *JAMA*, 271(9):698–702, 1994.

[239] Tom H. M. Ottenhoff and Stefan H. E. Kaufmann. Vaccines against Tuberculosis: Where Are We and Where Do We Need to Go? *PLoS Pathog*, 8(5):e1002607, 05 2012.

[240] Thomas J. Scriba, Michele Tameris, Erica Smit, Linda van der Merwe, E. Jane Hughes, Blessing Kadira, Katya Mauff, Sizulu Moyo, Nathaniel Brittain, Alison Lawrie, Humphrey Mulenga, Marwou de Kock, Lebohang Makhethe, Esme Janse van Rensburg, Sebastian Gelderbloem, Ashley Veldsman, Mark Hatherill, Hendrik Geldenhuys, Adrian V. S. Hill, Anthony Hawkridge, Gregory D. Hussey, Willem A. Hanekom, Helen McShane, and Hassan Mahomed. A Phase IIa Trial of the New Tuberculosis Vaccine, MVA85A, in HIV- and/or *Mycobacterium tuberculosis*-infected Adults. *Am J Respir Crit Care Med*, 185(7):769–778, April 2012.

[241] Angela M Minassian, Rosalind Rowland, Natalie E R Beveridge, Ian D Poulton, Iman Satti, Stephanie Harris, Hazel Poyntz, Matthew Hamill, Kristin Griffiths, Clare R Sander, David R Ambrozak, David A Price, Brenna J Hill, Joseph P Casazza, Daniel C Douek, Richard A Koup, Mario Roederer, Alan Winston, Jonathan Ross, Jackie Sherrard, Guy Rooney, Nicola Williams, Alison M Lawrie, Helen A Fletcher, Ansar A Pathan, and Helen McShane. A Phase I study evaluating the safety and immunogenicity of MVA85A, a candidate TB vaccine, in HIV-infected adults. *BMJ Open*, 1(2), 2011.

[242] Tandakha N. Dieye, Birahim P. NDiaye, Alle B. Dieng, Marema Fall, Nathaniel Britain, Samantha Vermaak, Makhtar Camara, Halimatou Diop-Ndiaye, Ndeye Fatou Ngom-Gueye, Papa A. Diaw, Coumba Toure-Kane, Papa S. Sow, Souleymane Mboup, and Helen McShane. Two Doses of Candidate TB Vaccine MVA85A in Antiretroviral Therapy (ART) Naive Subjects Gives Comparable Immunogenicity to One Dose in ART+ Subjects. *PLoS ONE*, 8(6):e67177, 06 2013.

[243] Charles F von Reyn, Lillian Mtei, Robert D Arbeit, Richard Waddell, Bernard Cole, Todd Mackenzie, Mecky Matee, Muhammad Bakari, Susan Tvaroha, Lisa V Adams, Charles R Horsburgh, Kisali Pallangyo, and the DarDar Study Group. Prevention of tuberculosis in Bacille Calmette-Guerin-primed, HIV-infected adults boosted with an inactivated whole-cell *mycobacterial* vaccine. *AIDS*, 24(5):–, 2010.

[244] Alwyn Mwinga, Andrew Nunn, Bagrey Ngwira, Chifumbe Chintu, David Warndorff, Paul Fine, Janet Darbyshire, and Alimuddin Zumla. *Mycobacterium vaccae* (SRL172) immunotherapy as an adjunct to standard antituberculosis treatment in HIV-infected adults with pulmonary tuberculosis: a

randomised placebo-controlled trial . *The Lancet*, 360(9339):1050 – 1055, 2002.

[245] Andre S. Nell, Eva D'lom, Patrick Bouic, Montserrat Sabate, Ramon Bosser, Jordi Picas, Merce Amat, Gavin Churchyard, and Pere-Joan Cardona. Safety, Tolerability, and Immunogenicity of the Novel Antituberculous Vaccine RUTI: Randomized, Placebo-Controlled Phase II Clinical Trial in Patients with Latent Tuberculosis Infection. *PLoS ONE*, 9(2):e89612, 02 2014.

[246] GJ Churchyard, B Landry, MA Snowden, R Pandian, and et al. (n.d.) Douoguih, M. Safety and Immunogenicity of AERAS-402 in HIV-infected, BCG-vaccinated Adults With CD4+ Lymphocyte Counts Greater Than 350 Cells/mm3. In *CROI*, 2013.

[247] Yolanda D. Mahnke, Tess M. Brodie, Federica Sallusto, Mario Roederer, and Enrico Lugli. The who's who of T-cell differentiation: Human memory T-cell subsets. *European Journal of Immunology*, 43(11):2797–2809, 2013.

[248] Patricia A Darrah, Dipti T Patel, Paula M De Luca, Ross W B Lindsay, Dylan F Davey, Barbara J Flynn, Soren T Hoff, Peter Andersen, Steven G Reed, Sheldon L Morris, Mario Roederer, and Robert A Seder. Multifunctional TH1 cells define a correlate of vaccine-mediated protection against *Leishmania major*. *Nat Med*, 13(7):843–850, July 2007.

[249] Joseph P. Casazza, Michael R. Betts, David A. Price, Melissa L. Precopio, Laura E. Ruff, Jason M. Brenchley, Brenna J. Hill, Mario Roederer, Daniel C. Douek, and Richard A. Koup. Acquisition of direct antiviral effector functions by CMV-specific CD4+ T lymphocytes with cellular maturation. *The Journal of Experimental Medicine*, 203(13):2865–2877, 2006.

[250] Victor Appay, Rene A. W. van Lier, Federica Sallusto, and Mario Roederer. Phenotype and function of human T lymphocyte subsets: Consensus and issues. *Cytometry Part A*, 73A(11):975–983, 2008.

[251] Thomas Lindenstroem, Else Marie Agger, Karen S. Korsholm, Patricia A. Darrah, Claus Aagaard, Robert A. Seder, Ida Rosenkrands, and Peter Andersen. Tuberculosis Subunit Vaccination Provides Long-Term Protective Immunity Characterized by Multifunctional CD4 Memory T Cells. *The Journal of Immunology*, 182(12):8047–8055, 2009.

[252] Sunil Kannanganat, Chris Ibegbu, Lakshmi Chennareddi, Harriet L. Robinson, and Rama Rao Amara. Multiple-Cytokine-Producing Antiviral CD4 T Cells Are Functionally Superior to Single-Cytokine-Producing Cells. *Journal of Virology*, 81(16):8468–8476, 2007.

[253] Cheryl L. Day, Deborah A. Abrahams, Lesedi Lerumo, Esme Janse van Rensburg, Lynnett Stone, Terrence O'rie, Bernadette Pienaar, Marwou de Kock, Gilla Kaplan, Hassan Mahomed, Keertan Dheda, and Willem A. Hanekom. Functional Capacity of *Mycobacterium tuberculosis*-Specific T Cell Responses in Humans Is Associated with Mycobacterial Load. *The Journal of Immunology*, 187(5):2222–2232, 2011.

[254] Rolf Billeskov, Tara T. Elvang, Peter L. Andersen, and Jes Dietrich. The HyVac4 Subunit Vaccine Efficiently Boosts BCG-Primed Anti-Mycobacterial Protective Immunity. *PLoS ONE*, 7(6):e39909, 06 2012.

[255] Emily K. Forbes, Clare Sander, Edward O. Ronan, Helen McShane, Adrian V. S. Hill, Peter C. L. Beverley, and Elma Z. Tchilian. Multifunctional, High-Level Cytokine-Producing Th1 Cells in the Lung, but Not Spleen, Cor-

relate with Protection against *Mycobacterium tuberculosis* Aerosol Challenge in Mice. *The Journal of Immunology*, 181(7):4955–4964, 2008.

[256] Isabel Leroux-Roels, Sheron Forgus, Fien De Boever, Frédéric Clement, Marie-Ange Demoitié, Pascal Mettens, Philippe Moris, Edouard Ledent, Geert Leroux-Roels, and Opokua Ofori-Anyinam. Improved CD4+ T cell responses to *Mycobacterium tuberculosis*in PPD-negative adults by M72/AS01 as compared to the M72/AS02 and Mtb72F/AS02 tuberculosis candidate vaccine formulations: A randomized trial . *Vaccine*, 31(17):2196 – 2206, 2013.

[257] Thomas J. Scriba, Michele Tameris, Nazma Mansoor, Erica Smit, Linda van der Merwe, Fatima Isaacs, Alana Keyser, Sizulu Moyo, Nathaniel Brittain, Alison Lawrie, Sebastian Gelderbloem, Ashley Veldsman, Mark Hatherill, Anthony Hawkridge, Adrian V. S. Hill, Gregory D. Hussey, Hassan Mahomed, Helen McShane, and Willem A. Hanekom. Modified vaccinia Ankara-expressing Ag85A, a novel tuberculosis vaccine, is safe in adolescents and children, and induces polyfunctional CD4+ T cells. *European Journal of Immunology*, 40(1):279–290, 2010.

[258] Brian Abel, Michele Tameris, Nazma Mansoor, Sebastian Gelderbloem, Jane Hughes, Deborah Abrahams, Lebohang Makhethe, Mzwandile Erasmus, Marwou de Kock, Linda van der Merwe, Anthony Hawkridge, Ashley Veldsman, Mark Hatherill, Giulia Schirru, Maria Grazia Pau, Jenny Hendriks, Gerrit Jan Weverling, Jaap Goudsmit, Donata Sizemore, J. Bruce McClain, Margaret Goetz, Jacqueline Gearhart, Hassan Mahomed, Gregory D. Hussey, Jerald C. Sadoff, and Willem A. Hanekom. The Novel Tuberculosis Vaccine, AERAS-402, Induces Robust and Polyfunctional CD4+ and CD8+ T Cells in Adults. *Am J Respir Crit Care Med*, 181(12):1407–1417, June 2010.

[259] Shabaana A. Khader and Radha Gopal. IL-17 in protective immunity to intracellular pathogens. *Virulence*, 1(5):423–427, 2010.

[260] Richard N. van Zyl-Smit, Madhukar Pai, Kwaku Peprah, Richard Meldau, Jackie Kieck, June Juritz, Motasim Badri, Alimuddin Zumla, Leonardo A. Sechi, Eric D. Bateman, and Keertan Dheda. Within-Subject Variability and Boosting of T-Cell Interferon-γ Responses after Tuberculin Skin Testing. *Am J Respir Crit Care Med*, 180(1):49–58, July 2009.

[261] WHO. New WHO recommendations on use of commercial TB Interferon-Gamma Release Assays (IGRAs) in low- and middle-income countries (n.d.). $Available : http : //www.who.int/tb/features_archive/igra_policy24oct/en/$, Accessed 10 January 2014.

[262] Kerry A. Millington, Sarah M. Fortune, Jeffrey Low, Alejandra Garces, Suzanne M. Hingley-Wilson, Melissa Wickremasinghe, Onn M. Kon, and Ajit Lalvani. Rv3615c is a highly immunodominant RD1 (Region of Difference 1)-dependent secreted antigen specific for *Mycobacterium tuberculosis* infection. *Proceedings of the National Academy of Sciences*, 108(14):5730–5735, 2011.

[263] Claus Aagaard, Truc Hoang, Jes Dietrich, Pere-Joan Cardona, Angelo Izzo, Gregory Dolganov, Gary K Schoolnik, Joseph P Cassidy, Rolf Billeskov, and Peter Andersen. A multistage tuberculosis vaccine that confers efficient protection before and after exposure. *Nat Med*, 17(2):189–194, February 2011.

[264] Saad B. Omer, Walter A. Orenstein, and Jeffrey P. Koplan. Go Big and Go Fast - Vaccine Refusal and Disease Eradication. *New England Journal of Medicine*, 368(15):1374–1376, 2013. PMID: 23574116.

[265] Charles L. Daley, Peter M. Small, Gisela F. Schecter, Gary K. Schoolnik, Ruth A. McAdam, William R. Jacobs, and Philip C. Hopewell. An Outbreak of Tuberculosis with Accelerated Progression among Persons Infected with the Human Immunodeficiency Virus. *New England Journal of Medicine*, 326(4):231–235, 1992. PMID: 1345800.

[266] Jaap T. van Dissel, Sandra M. Arend, Corine Prins, Peter Bang, Pernille Nyholm Tingskov, Karen Lingnau, Jan Nouta, Michèl R. Klein, Ida Rosenkrands, Tom H.M. Ottenhoff, Ingrid Kromann, T. Mark Doherty, and Peter Andersen. Ag85B-ESAT-6 adjuvanted with IC31® promotes strong and long-lived *Mycobacterium tuberculosis* specific T cell responses in naive human volunteers . *Vaccine*, 28(20):3571 – 3581, 2010.

[267] K Reither, L Katsoulis, T Beattie, N Gardiner, N Lenz, K Said, E Mfinanga, C Pohl, KL Fielding, H Jeffrey, BM Kagina, EJ Hughes, TJ Scriba, WA Hanekom, ST Hoff, P Bang, I Kromann, C Daubenberger, P Andersen, and GJ Churchyard. Safety and Immunogenicity of H1/IC31®, an Adjuvanted TB Subunit Vaccine, in HIV-Infected Adults with CD4+ Lymphocyte Counts Greater than 350cells/mm^3: A Phase II, Multi-Centre, Double-Blind, Randomized, Placebo-Controlled Trial. *Plos One*, 2014.

[268] Jitao Zhang, Tobias Schindler, Erich Küng, Martin Ebeling, and Ulrich Certa. Highly sensitive amplicon-based transcript quantification by semiconductor sequencing. *BMC Genomics*, 15(1):565, 2014.

[269] Jamie A. Lee, Josef Spidlen, Keith Boyce, Jennifer Cai, Nicholas Crosbie, Mark Dalphin, Jeff Furlong, Maura Gasparetto, Michael Goldberg, Elizabeth M. Goralczyk, Bill Hyun, Kirstin Jansen, Tobias Kollmann, Megan Kong, Robert Leif, Shannon McWeeney, Thomas D. Moloshok, Wayne

Moore, Garry Nolan, John Nolan, Janko Nikolich-Zugich, David Parrish, Barclay Purcell, Yu Qian, Biruntha Selvaraj, Clayton Smith, Olga Tchuvatkina, Anne Wertheimer, Peter Wilkinson, Christopher Wilson, James Wood, Robert Zigon, Richard H. Scheuermann, and Ryan R. Brinkman. MIFlowCyt: The minimum information about a flow cytometry experiment. *Cytometry Part A*, 73A(10):926–930, 2008.

[270] Greg Finak, Andrew McDavid, Pratip Chattopadhyay, Maria Dominguez, Stephen C De Rosa, Mario Roederer, and Raphael Gottardo. Mixture models for single-cell assays with applications to vaccine studies. *Biostatistics*, 2013.

[271] R Core Team. *R: A Language and Environment for Statistical Computing*. R Foundation for Statistical Computing, Vienna, Austria, 2014.

[272] Michael Reich, Ted Liefeld, Joshua Gould, Jim Lerner, Pablo Tamayo, and Jill P Mesirov. GenePattern 2.0. *Nat Genet*, 38(5):500–501, May 2006.

[273] Shuzhao Li, Nadine Rouphael, Sai Duraisingham, Sandra Romero-Steiner, Scott Presnell, Carl Davis, Daniel S Schmidt, Scott E Johnson, Andrea Milton, Gowrisankar Rajam, Sudhir Kasturi, George M Carlone, Charlie Quinn, Damien Chaussabel, A Karolina Palucka, Mark J Mulligan, Rafi Ahmed, David S Stephens, Helder I Nakaya, and Bali Pulendran. Molecular signatures of antibody responses derived from a systems biology study of five human vaccines. *Nat Immunol*, 15(2):195–204, February 2014.

[274] Diletta Di Mitri, Rita I. Azevedo, Sian M. Henson, Valentina Libri, Natalie E. Riddell, Richard Macaulay, David Kipling, Maria V. D. Soares, Luca Battistini, and Arne N. Akbar. Reversible Senescence in Human CD4+CD45RA+CD27- Memory T Cells. *The Journal of Immunology*, 187(5):2093–2100, 2011.

[275] A Amendola, M L Gougeon, F Poccia, A Bondurand, L Fesus, and M Piacentini. Induction of "tissue" transglutaminase in HIV pathogenesis: evidence for high rate of apoptosis of CD4+ T lymphocytes and accessory cells in lymphoid tissues. *Proceedings of the National Academy of Sciences of the United States of America*, 93(20):11057–11062, October 1996.

[276] Weifeng Xu, Paul A Santini, John S Sullivan, Bing He, Meimei Shan, Susan C Ball, Wayne B Dyer, Thomas J Ketas, Amy Chadburn, Leona Cohen-Gould, Daniel M Knowles, April Chiu, Rogier W Sanders, Kang Chen, and Andrea Cerutti. HIV-1 evades virus-specific IgG2 and IgA class switching by targeting systemic and intestinal B cells via long-range intercellular conduits. *Nature immunology*, 10(9):1008–1017, August 2009.

[277] Melissa A. Farrow, Eun-Young Kim, Steven M. Wolinsky, and Ann M. Sheehy. NFAT and IRF Proteins Regulate Transcription of the Anti-HIV Gene, APOBEC3G. *Journal of Biological Chemistry*, 286(4):2567–2577, 2011.

[278] D.-Y. Oh, S. Taube, O. Hamouda, C. Kücherer, G. Poggensee, H. Jessen, J. K. Eckert, K. Neumann, A. Storek, M. Pouliot, P. Borgeat, N. Oh, E. Schreier, A. Pruss, K. Hattermann, and R. R. Schumann. A Functional Toll-Like Receptor 8 Variant Is Associated with HIV Disease Restriction. *Journal of Infectious Diseases*, 198(5):701–709, 2008.

[279] Solen Kerneis, Odile Launay, Clément Turbelin, Frédéric Batteux, Thomas Hanslik, and Pierre-Yves Boëlle. Long-term Immune Responses to Vaccination in HIV-Infected Patients: A Systematic Review and Meta-Analysis. *Clinical Infectious Diseases*, 58(8):1130–1139, 2014.

[280] Robert A. Seder and Adrian V. S. Hill. Vaccines against intracellular infections requiring cellular immunity. *Nature*, 406(6797):793–798, August 2000.

[281] Alberto Mantovani, Subhra K Biswas, Maria Rosaria Galdiero, Antonio Sica, and Massimo Locati. Macrophage plasticity and polarization in tissue repair and remodelling. *The Journal of Pathology*, 229(2):176–185, 2013.

[282] Noriyuki Seta and Masataka Kuwana. Derivation of multipotent progenitors from human circulating CD14+ monocytes . *Experimental Hematology*, 38(7):557 – 563, 2010.

[283] Jinqing Li, Hong Tan, Xiaolin Wang, Yuejun Li, Lisa Samuelson, Xueyong Li, Caibin Cui, and David A. Gerber. Circulating Fibrocytes Stabilize Blood Vessels during Angiogenesis in a Paracrine Manner . *The American Journal of Pathology*, 184(2):556 – 571, 2014.

[284] Bas W.M. van Balkom Hendrik Gremmels, Joost O. Fledderus and Marianne C. Verhaar. Transcriptome Analysis in Endothelial Progenitor Cell Biology. *Antioxidants & Redox Signaling*, 15(4):1092–1042, August 2011.

[285] Enoch Muyanja, Aloysius Ssemaganda, Pearline Ngauv, Rafael Cubas, Helene Perrin, Divya Srinivasan, Glenda Canderan, Benton Lawson, Jakub Kopycinski, Amanda S. Graham, Dawne K. Rowe, Michaela J. Smith, Sharon Isern, Scott Michael, Guido Silvestri, Thomas H. Vanderford, Erika Castro, Giuseppe Pantaleo, Joel Singer, Jill Gillmour, Noah Kiwanuka, Annet Nanvubya, Claudia Schmidt, Josephine Birungi, Josephine Cox, Elias K. Haddad, Pontiano Kaleebu, Patricia Fast, Rafick-Pierre Sekaly, and Lydie Trautmann. Immune activation alters cellular and humoral responses to yellow fever 17D vaccine. *The Journal of Clinical Investigation*, 124(7):3147–3158, 7 2014.

[286] G C Cook. Enterobius vermicularis infection. *Gut*, 35(9):1159–1162, September 1994.

[287] Utzinger Juŕg, Beckera Sören L., Knopp Stefanie, Blum Johannes, Neumayr Andreas L., Keiser Jennifer, and Hatz Christoph F. Neglected tropical diseases: diagnosis, clinical management, treatment and control. *Swiss Med Wkly.*, 142:w13727, 2012.

[288] Nagar H. Surgical aspects of parasitic diseas in childhood. *J Pediat Surg*, 22:325–31, 1987.

[289] Julius Lukes, Ales Horak, and Tomas Scholz. Helminth genome projects: all or nothing. *Trends in Parasitology*, 21(6):265 – 266, 2005.

[290] E. Gale. A missing link in the hygiene hypothesis? *Diabetologia*, 45(4):588–594, 2002.

[291] Edy Stermer, Igor Sukhotnic, and Ron Shaoul. Pruritus Ani: An Approach to an Itching Condition. *Journal of Pediatric Gastroenterology and Nutrition*, 48(5):513–516 10.1097/MPG.0b013e31818080c0, 2009.

[292] Severe Malaria. *Tropical Medicine & International Health*, 19:7–131, 2014.

[293] Majed Odeh. The role of Tumour Necrosis Factor alpha in the pathogenesis of complicated *Falciparum* malaria. *Cytokine*, 14(1):11 – 18, 2001.

[294] S J Dunstan, K A Rockett, N T N Quyen, Y Y Teo, C Q Thai, N T Hang, A Jeffreys, T G Clark, K S Small, C P Simmons, N Day, S E O'Riordan, D P Kwiatkowski, J Farrar, N H Phu, and T T Hien. Variation in human genes encoding adhesion and proinflammatory molecules are associated with severe malaria in the Vietnamese. *Genes Immun*, 13(6):503–508, September 2012.

[295] Robert M. Anthony, Laura I. Rutitzky, Joseph F. Urban, Miguel J. Stadecker, and William C. Gause. Protective immune mechanisms in helminth infection. *Nat Rev Immunol*, 7(12):975–987, *December* 2007.

[296] Henry J. McSorley, Mary T. O'Gorman, Natalie Blair, Tara E. Sutherland, Kara J. Filbey, and Rick M. Maizels. Suppression of type 2 immunity and allergic airway inflammation by secreted products of the helminth *Heligmosomoides polygyrus*. *European Journal of Immunology*, 42(10):2667–2682, 2012.

[297] Ayola A. Adegnika and Peter G. Kremser. Epidemiology of malaria and helminth interaction: a review from 2001 to 2011. *Current Opinion in HIV& AIDS*, 7:221–224, 2012.

[298] Harry J. Flint, Karen P. Scott, Petra Louis, and Sylvia H. Duncan. The role of the gut microbiota in nutrition and health. *Nat Rev Gastroenterol Hepatol*, 9(10):577–589, October 2012.

[299] Brittan S Scales and Gary B Huffnagle. The microbiome in wound repair and tissue fibrosis. *The Journal of Pathology*, 229(2):323–331, 2013.

[300] Sangyeon Cho, Soomin Kim, Youngchan Kim, and YongKeun Park. Optical imaging techniques for the study of malaria. *Trends in Biotechnology*, 30(2):71–79, 2012.

[301] Seth T. Walk, Arthur M. Blum, Sarah Ang-Sheng Ewing, Joel V. Weinstock, and Vincent B. Young. Alteration of the murine gut microbiota during infection with the parasitic helminth *Heligmosomoides polygyrus*. *Inflammatory Bowel Diseases*, 16(11):1841–1849 10.1002/ibd.21299, 2010.

[302] Chesney Michels, Prem Goyal, Natalie Nieuwenhuizen, and Frank Brombacher. Infection with Syphacia obvelata (Pinworm) Induces Protective Th2 Immune Responses and Influences Ovalbumin-Induced Allergic Reactions. *Infection and Immunity*, 74(10):5926–5932, 2006.

[303] F.L. Dunn. Patterns of parasitism in primates: Phylogenetic and ecological interpretations, with particular reference to the hominoidea, 1966.

[304] Paul B. Eckburg, Elisabeth M. Bik, Charles N. Bernstein, Elizabeth Purdom, Les Dethlefsen, Michael Sargent, Steven R. Gill, Karen E. Nelson, and David A. Relman. Diversity of the Human Intestinal Microbial Flora. *Science*, 308(5728):1635–1638, 2005.

[305] Nadja Larsen, Finn K. Vogensen, Frans W. J. van den Berg, Dennis Sandris Nielsen, Anne Sofie Andreasen, Bente K. Pedersen, Waleed Abu Al-Soud, SÃÿren J. SÃÿrensen, Lars H. Hansen, and Mogens Jakobsen. Gut Microbiota in Human Adults with Type 2 Diabetes Differs from Non-Diabetic Adults. *PLoS ONE*, 5(2):e9085, 02 2010.

[306] John H. Cummings. FERMENTATION IN THE HUMAN LARGE INTESTINE: EVIDENCE AND IMPLICATIONS FOR HEALTH. *The Lancet*, 321(8335):1206 – 1209, 1983. Originally published as Volume 1, Issue 8335.

[307] Fukuda Masanobu, Komiyama Yutaka, Keiichi Mitsuyama, Akira Andoh, Takahiko Aoyama, Yoshiaki Matsumoto, and Osamu Kanauchi. Prebiotic treatment reduced preneoplastic lesions through the downregulation of toll like receptor 4 in a chemo-induced carcinogenic model. *Journal of Clinical Biochemistry and Nutrition*, 49(1):57–61, 2011.

[308] Myung H. Kim, Seung G. Kang, Jeong H. Park, Masashi Yanagisawa, and Chang H. Kim. Short-Chain Fatty Acids Activate GPR41 and GPR43 on

Intestinal Epithelial Cells to Promote Inflammatory Responses in Mice. *Gastroenterology*, 145(2):396 – 406.e10, 2013.

[309] Nicholas Arpaia, Clarissa Campbell, Xiying Fan, Stanislav Dikiy, Joris van der Veeken, Paul deRoos, Hui Liu, Justin R. Cross, Klaus Pfeffer, Paul J. Coffer, and Alexander Y. Rudensky. Metabolites produced by commensal bacteria promote peripheral regulatory T-cell generation. *Nature*, 504(7480):451–455, December 2013.

[310] Christian Sina, Olga Gavrilova, Matti Förster, Andreas Till, Stefanie Derer, Friederike Hildebrand, Björn Raabe, Athena Chalaris, Jürgen Scheller, Ateequr Rehmann, Andre Franke, Stephan Ott, Robert Häsler, Susanna Nikolaus, Ulrich R. Fölsch, Stefan Rose-John, Hui-Ping Jiang, Jun Li, Stefan Schreiber, and Philip Rosenstiel. G Protein-Coupled Receptor 43 Is Essential for Neutrophil Recruitment during Intestinal Inflammation. *The Journal of Immunology*, 183(11):7514–7522, 2009.

[311] Mohamed Bellahcene, Jacqueline F. O'Dowd, Ed T. Wargent, Mohamed S. Zaibi, David C. Hislop, Robert A. Ngala, David M. Smith, Michael A. Cawthorne, Claire J. Stocker, and Jonathan R. S. Arch. Male mice that lack the G-protein-coupled receptor GPR41 have low energy expenditure and increased body fat content. *British Journal of Nutrition*, 109:1755–1764, 5 2013.

[312] Andrew Duncan Urquhart. Putative Pathophysiological Interactions of Cytokines and Phagocytic Cells in Severe Human Falciparum Malaria. *Clinical Infectious Diseases*, 19(1):117–131, 1994.

[313] Allen L. Richards. Tumour Necrosis Factor and Associated Cytokines in the host's response to malaria. *International Journal for Parasitology*, 27(10):1251 – 1263, 1997.

[314] Samuel Crocodile Wassmer, Christopher Alan Moxon, Terrie Taylor, Georges Emile Grau, Malcolm Edward Molyneux, and Alister Gordon Craig. Vascular endothelial cells cultured from patients with cerebral or uncomplicated malaria exhibit differential reactivity to TNF. *Cellular Microbiology*, 13(2):198–209, 2011.

[315] Gareth D H Turner, Heather Morrison, Margaret Jones, Timothy M E Davis, Sornchai Looareesuwan, Ian D Buley, Kevin C Gatter, Christopher I Newbold, Sasithon Pukritayakamee, Bussarin Nagachinta, Nicholas J White, and Anthony R Berendt. An Immunohistochemical Study of the Pathology of Fatal Malaria: Evidence for Widespread Endothelial Activation and a Potential Role for Intercellular Adhesion Molecule-1 in Cerebral Sequestration. *The American Journal of Pathology*, 145(5):1057–1069, November 1994.

[316] Lucia Malaguarnera and Salvatore Musumeci. The immune response to Plasmodium falciparum malaria. *The Lancet Infectious Diseases*, 2(8):472 – 478, 2002.

[317] Peter Kern, Christoph Josef Hemmer, Jo Van Damme, Hans-Jürgen Gruss, and Manfred Dietrich. Elevated tumor necrosis factor alpha and interleukin-6 serum levels as markers for complicated *plasmodium falciparum* malaria. *The American Journal of Medicine*, 87(2):139 – 143, 1989.

[318] Georges E. Grau, Terrie E. Taylor, Malcolm E. Molyneux, Jack J. Wirima, Pierre Vassalli, Marcel Hommel, and Paul-Henri Lambert. Tumor Necro-

sis Factor and Disease Severity in Children with Falciparum Malaria. *New England Journal of Medicine*, 320(24):1586–1591, 1989. PMID: 2657427.

[319] Estelle Bettelli, Yijun Carrier, Wenda Gao, Thomas Korn, Terry B. Strom, Mohamed Oukka, Howard L. Weiner, and Vijay K. Kuchroo. Reciprocal developmental pathways for the generation of pathogenic effector TH17 and regulatory T cells. *Nature*, 441(7090):235–238, May 2006.

[320] Chandrashekhar Pasare and Ruslan Medzhitov. Toll Pathway-Dependent Blockade of CD4+CD25+ T Cell-Mediated Suppression by Dendritic Cells. *Science*, 299(5609):1033–1036, 2003.

[321] Etienne Meunier, Pierre Wallet, Roland F Dreier, Stephanie Costanzo, Leonie Anton, Sebastian Ruhl, Sebastien Dussurgey, Mathias S Dick, Anne Kistner, Melanie Rigard, Daniel Degrandi, Klaus Pfeffer, Masahiro Yamamoto, Thomas Henry, and Petr Broz. Guanylate-binding proteins promote activation of the AIM2 inflammasome during infection with *Francisella novicida*. *Nat Immunol*, advance online publication:–, March 2015.

[322] Avinash R. Shenoy, David A. Wellington, Pradeep Kumar, Hilina Kassa, Carmen J. Booth, Peter Cresswell, and John D. MacMicking. GBP5 Promotes NLRP3 Inflammasome Assembly and Immunity in Mammals. *Science*, 336(6080):481–485, 2012.

[323] Mandar Bawadekar, Marco De Andrea, Irene Lo Cigno, Gianluca Baldanzi, Valeria Caneparo, Andrea Graziani, Santo Landolfo, and Marisa Gariglio. The Extracellular IFI16 Protein Propagates Inflammation in Endothelial Cells Via p38 MAPK and NF-κB p65 Activation. *Journal of Interferon & Cytokine Research*, pages –, February 2015.

[324] Anshuman Das, Phat X. Dinh, Debasis Panda, and Asit K. Pattnaik. Interferon-Inducible Protein IFI35 Negatively Regulates RIG-I Antiviral Signaling and Supports Vesicular Stomatitis Virus Replication. *Journal of Virology*, 88(6):3103–3113, 2014.

[325] Venugopalan Cheriyath, Keith B. Glaser, Jeffrey F. Waring, Rachid Baz, Mohamad A. Hussein, and Ernest C. Borden. G1P3, an IFN-induced survival factor, antagonizes TRAIL-induced apoptosis in human myeloma cells. *The Journal of Clinical Investigation*, 117(10):3107–3117, 10 2007.

[326] L.C. Hallen, Y. Burki, M. Ebeling, C. Broger, F. Siegrist, K. Oroszlan-Szovik, B. Bohrmann, U. Certa, and S. Foser. Antiproliferative Activity of the Human IFN-α-Inducible Protein IFI44. *Journal of Interferon & Cytokine Research*, 27(8):675–680, August 2007.

[327] GeorgeăR. Stark and JamesăE. Darnell Jr. The JAK-STAT Pathway at Twenty. *Immunity*, 36(4):503 – 514, 2012.

[328] Florian Forster, Wolfgang Paster, Verena Supper, Philipp Schatzlmaier, Stefan Sunzenauer, Nicole Ostler, Anna Saliba, Paul Eckerstorfer, Nathalie Britzen-Laurent, Gerhard Schütz, Johannes A. Schmid, Gerhard J. Zlabinger, Elisabeth Naschberger, Michael Stürzl, and Hannes Stockinger. Guanylate Binding Protein 1ŰMediated Interaction of T Cell Antigen Receptor Signaling with the Cytoskeleton. *The Journal of Immunology*, 192(2):771–781, 2014.

[329] Jim Kaufman. What chickens would tell you about the evolution of antigen processing and presentation. *Current Opinion in Immunology*, 34(0):35 – 42, 2015.

[330] Jonathan J Miner and Michael S Diamond. MDA5 and autoimmune disease. *Nat Genet*, 46(5):418–419, May 2014.

[331] Mariela Granero Farias, Natalia Pieruccini de Lucena, Suzane Dal Bo, and Simone Martins de Castro. Neutrophil CD64 expression as an important diagnostic marker of infection and sepsis in hospital patients. *Journal of Immunological Methods*, 414(0):65 – 68, 2014.

[332] Parisa Kalantari, Rosane B. DeOliveira, Jennie Chan, Yolanda Corbett, Vijay Rathinam, Andrea Stutz, Eicke Latz, Ricardo T. Gazzinelli, Douglas T. Golenbock, and Katherine A. Fitzgerald. Dual Engagement of the NLRP3 and AIM2 Inflammasomes by Plasmodium-Derived Hemozoin and DNA during Malaria. *Cell Reports*, 6(1):196 – 210, 2014.

[333] Marco A. Ataide, Warrison A. Andrade, Dario S. Zamboni, Donghai Wang, Maria do Carmo Souza, Bernardo S. Franklin, Samir Elian, Flaviano S. Martins, Dhelio Pereira, George Reed, Katherine A. Fitzgerald, Douglas T. Golenbock, and Ricardo T. Gazzinelli. Malaria-Induced NLRP12/NLRP3-Dependent Caspase-1 Activation Mediates Inflammation and Hypersensitivity to Bacterial Superinfection. *PLoS Pathog*, 10(1):e1003885, 01 2014.

[334] Jessica L. Miller, Brandon K. Sack, Michael Baldwin, Ashley M. Vaughan, and Stefan H.I. Kappe. Interferon-Mediated Innate Immune Responses against Malaria Parasite Liver Stages. *Cell Reports*, 7(2):436 – 447, 2014.

[335] Chelsea L. Edwards, Shannon E. Best, Sin Yee Gun, Carla Claser, Kylie R. James, Marcela Montes de Oca, Ismail Sebina, Fabian de Labastida Rivera, Fiona H. Amante, Paul J. Hertzog, Christian R. Engwerda, Laurent Renia, and Ashraful Haque. Spatiotemporal requirements for IRF7 in mediating

type I IFN-dependent susceptibility to blood-stage Plasmodium infection. *European Journal of Immunology*, 45(1):130–141, 2015.

[336] Lidija Klampfer, Jie Huang, Laurie-Anne Swaby, and Leonard Augenlicht. Requirement of Histone Deacetylase Activity for Signaling by STAT1. *Journal of Biological Chemistry*, 279(29):30358–30368, 2004.

[337] A. DI SABATINO, R. MORERA, R. CICCOCIOPPO, P. CAZZOLA, S. GOTTI, F. P. TINOZZI, S. TINOZZI, and G. R. CORAZZA. Oral butyrate for mildly to moderately active Crohn's disease. *Alimentary Pharmacology & Therapeutics*, 22(9):789–794, 2005.

[338] Lei Yin, Gary Laevsky, and Charles Giardina. Butyrate Suppression of Colonocyte NF-κB Activation and Cellular Proteasome Activity. *Journal of Biological Chemistry*, 276(48):44641–44646, 2001.

[339] Herbert F Helander and Lars Fändriks. Surface area of the digestive tract - revisited. *Scandinavian Journal of Gastroenterology*, 49(6):681–689, 2014. PMID: 24694282.

[340] Leanne J. Robinson, Marthe C. D'Ombrain, Danielle I. Stanisic, Jack Taraika, Nicholas Bernard, Jack S. Richards, James G. Beeson, Livingstone Tavul, Pascal Michon, Ivo Mueller, and Louis Schofield. Cellular Tumor Necrosis Factor, Gamma Interferon, and Interleukin-6 Responses as Correlates of Immunity and Risk of Clinical Plasmodium falciparum Malaria in Children from Papua New Guinea. *Infection and Immunity*, 77(7):3033–3043, 2009.

[341] Christoph Wenisch, Ken F. Linnau, Sornchai Looaresuwan, and Helmut Rumpold. Plasma Levels of the Interleukin-6 Cytokine Family in Persons

with Severe *Plasmodium falciparum* Malaria. *Journal of Infectious Diseases*, 179(3):747–750, 1999.

[342] Cassandra Willyard. Large trial to examine parasites' influence on global killers. *Nat Med*, 15(10):1097–1097, October 2009.

[343] Darren Blimkie, Edgardo S. Fortuno III, Howard Yan, Patricia Cho, Kevin Ho, Stuart E. Turvey, Arnaud Marchant, Stanislas Goriely, and Tobias R. Kollmann. Variables to be controlled in the assessment of blood innate immune responses to Toll-like receptor stimulation. *Journal of Immunological Methods*, 366:89 – 99, 2011.

[344] Kinga K. Smolen, Candice E. Ruck, Edgardo S. Fortuno III, Kevin Ho, Pedro Dimitriu, William W. Mohn, David P. Speert, Philip J. Cooper, Monika Esser, Tessa Goetghebuer, Arnaud Marchant, and Tobias R. Kollmann. Pattern recognition receptor-mediated cytokine response in infants across 4 continents. *Journal of Allergy and Clinical Immunology*, 133(3):818 – 826.e4, 2014.

[345] Nathan P. Corbett, Darren Blimkie, Kevin C. Ho, Bing Cai, Darren P. Sutherland, Arlene Kallos, Juliet Crabtree, Annie Rein-Weston, Pascal M. Lavoie, Stuart E. Turvey, Natalie R. Hawkins, Steven G. Self, Christopher B. Wilson, Adeline M. Hajjar, Edgardo S. Fortuno, III, and Tobias R. Kollmann. Ontogeny of Toll-Like Receptor Mediated Cytokine Responses of Human Blood Mononuclear Cells. *PLoS ONE*, 5(11):e15041, 11 2010.

[346] S A Joosten, J J Goeman, J S Sutherland, L Opmeer, K G de Boer, M Jacobsen, S H E Kaufmann, L Finos, C Magis-Escurra, M O C Ota, T H M Ottenhoff, and M C Haks. Identification of biomarkers for tuberculosis dis-

ease using a novel dual-color RT-MLPA assay. *Genes Immun*, 13(1):71–82, January 2012.

[347] Christian Milani, Arancha Hevia, Elena Foroni, Sabrina Duranti, Francesca Turroni, Gabriele Andrea Lugli, Borja Sanchez, Rebeca Martŋn, Miguel Gueimonde, Douwe van Sinderen, Abelardo Margolles, and Marco Ventura. Assessing the Fecal Microbiota: An Optimized Ion Torrent 16S rRNA Gene-Based Analysis Protocol. *PLoS ONE*, 8(7):e68739, 07 2013.

[348] Erik Dassi, Annalisa Ballarini, Giuseppina Covello, Alessandro Quattrone, Olivier Jousson, Veronica De Sanctis, Roberto Bertorelli, Michela Alessandra Denti, and Nicola Segata. Enhanced microbial diversity in the saliva microbiome induced by short-term probiotic intake revealed by 16S rRNA sequencing on the IonTorrent **PGM** platform. *Journal of Biotechnology*, 190(0):30 – 39, 2014. The Genomics Revolution and its Impact on Future Biotechnology.

[349] Victor S. Pylro, Luiz Fernando W. Roesch, Daniel K. Morais, Ian M. Clark, Penny R. Hirsch, and Marcos R. Totola. Data analysis for 16S microbial profiling from different benchtop sequencing platforms. *Journal of Microbiological Methods*, 107(0):30 – 37, 2014.

[350] Robert C Edgar. UPARSE: highly accurate OTU sequences from microbial amplicon reads. *Nat Meth*, 10(10):996–998, October 2013.

[351] J Gregory Caporaso, Justin Kuczynski, Jesse Stombaugh, Kyle Bittinger, Frederic D Bushman, Elizabeth K Costello, Noah Fierer, Antonio Gonzalez Pena, Julia K Goodrich, Jeffrey I Gordon, Gavin A Huttley, Scott T Kelley, Dan Knights, Jeremy E Koenig, Ruth E Ley, Catherine A Lozupone, Daniel McDonald, Brian D Muegge, Meg Pirrung, Jens Reeder, Joel R Sevinsky, Pe-

ter J Turnbaugh, William A Walters, Jeremy Widmann, Tanya Yatsunenko, Jesse Zaneveld, and Rob Knight. QIIME allows analysis of high-throughput community sequencing data. *Nat Meth*, 7(5):335–336, May 2010.

[352] T. Z. DeSantis, P. Hugenholtz, N. Larsen, M. Rojas, E. L. Brodie, K. Keller, T. Huber, D. Dalevi, P. Hu, and G. L. Andersen. Greengenes, a Chimera-Checked 16S rRNA Gene Database and Workbench Compatible with ARB. *Applied and Environmental Microbiology*, 72(7):5069–5072, 2006.

[353] Nicola Segata, Jacques Izard, Levi Waldron, Dirk Gevers, Larisa Miropolsky, Wendy Garrett, and Curtis Huttenhower. Metagenomic biomarker discovery and explanation. *Genome Biology*, 12(6):R60, 2011.

[354] Morgan G I Langille, Jesse Zaneveld, J Gregory Caporaso, Daniel McDonald, Dan Knights, Joshua A Reyes, Jose C Clemente, Deron E Burkepile, Rebecca L Vega Thurber, Rob Knight, Robert G Beiko, and Curtis Huttenhower. Predictive functional profiling of microbial communities using 16S rRNA marker gene sequences. *Nat Biotech*, 31(9):814–821, September 2013.

[355] Sharon Greenblum, Rogan Carr, and Elhanan Borenstein. Extensive Strain-Level Copy-Number Variation across Human Gut Microbiome Species. *Cell*, 160(4):583–594, 2015.

[356] A Phase I/IIa Safety & Immunogenicity of AERAS-456 in HIV-Negative Adults With & Without Latent Tuberculosis Infection. *https://clinicaltrials.gov/ct2/show/NCT01865487?term=h56+ic31&rank=1*, accessed 09.03.2015.

[357] Stephen C. De Rosa, Donald K. Carter, and M. Juliana McElrath. OMIP-014: Validated multifunctional characterization of antigen-specific human T

cells by intracellular cytokine staining. *Cytometry Part A*, 81A(12):1019–1021, 2012.

[358] Nopporn Apiwattanakul, Paul G. Thomas, Amy R. Iverson, and Jonathan A. McCullers. Chronic helminth infections impair pneumococcal vaccine responses. *Vaccine*, 32(42):5405 – 5410, 2014.

[359] S M Dillon, E J Lee, C V Kotter, G L Austin, Z Dong, D K Hecht, S Gianella, B Siewe, D M Smith, A L Landay, C E Robertson, D N Frank, and C C Wilson. An altered intestinal mucosal microbiome in HIV-1 infection is associated with mucosal and systemic immune activation and endotoxemia. *Mucosal Immunol*, 7(4):983–994, July 2014.

Chapter 6

Appendix

6.1 MyFlowCyt Reporting standard for chapter 3

6.1.1 Experiment Overview

Purpose

The purpose of this experiment was to document the cytokine responses of $CD4^+$ memory T cells of HIV infected volunteers vaccinated with the *Mycobacterium tuberculosis* vaccine H1/IC31®.

Keywords

Tuberculosis, memory $CD4^+$ T cells, H1/IC31® vaccination

Experimental Variables

4 volunteers received a placebo, while 20 volunteers received the H1/IC31® vaccine. They were vaccinated on study day 0 and 56. Peripheral blood was collected on study day 0, 14, 56, 70 and 182. Whole blood was stimulated with the H1

fusion protein (Statens Serum Institute at 5μg/ml), phytohaemagglutinin (PHA) (Bioweb at 5μg/ml) or left unstimulated. Anti-CD28 and anti-CD49d antibodies (BD Biosciences at 0.5μg/ml) were included in all assay conditions. 4 different subsets of $CD4^+$ memory T cells were measured in peripheral blood, namely stem cell memory T cells (T_{SCM}), central memory T cells (T_{CM}) effector memory T cells (T_{EM}) and effector memory T cells expressing CD45-RA (T_{EMRA}). Of each subset, the cytokine expression of IL-2, IFN-γ, TNF-α and IL-17 was assessed.

Organization

Name

Swiss Tropical and Public Health Institute, University of Basel, Switzerland.

Bagamoyo Reasearch and Training Center, Ifakara Health Institute, Tanzania.

South African Tuberculosis Vaccine Initiative, University of Cape Town, South Africa

Address

Socinstrasse 57, 4051 Basel, Switzerland

Bagamoyo District Hospital, PO Box 74, Bagamoyo, Tanzania

Anzio Road, Observatory, Cape Town, South Africa 7925

Primary Contact

Name: Claudia Daubenberger

Email: claudia.daubenberger@unibas.ch

Date

The blood collection and whole blood stimulation assays were performed between January 2012 and August 2012. The flow cytometry analysis was conducted be-

tween December 2012 and March 2013.

Conclusions

Vaccination with H1/IC31® mainly induces T_{CM} and T_{EM} producing IL-2, IFN-γ and TNF-α altogether or IL-2 in combination with TNF-α. Cytokine producing T_{SCM} and T_{EMRA} were not significantly elevated in vaccinated controls compared to placebo controls (apart from study day 70). Reither et al. detected no significant change in IL-17 expression by $CD4^+$ T cells. Therefore only IL-2, IFN-γ and TNF-α were included in the manuscript.

Quality Control Measures

1 peak beads (BD Biosciences) were run in each experiment to track cytometer performance and to standardize voltage settings across all samples.

Other Relevant Experiment Information

Not applicable.

6.1.2 Flow Sample/Specimen Description

Sample/Specimen Material Description

Biological Samples

- Biological Sample Description

  Blood was collected via sterile venipuncture into sodium-heparin vacutainers (Vacuette; catalog no. 455051). Red blood cells were lysed and the white blood cells were stored as described in section 6.1.2.

- Biological Sample Source Description

  Human peripheral blood.

- Biological Sample Source Organism Description

  Tanzanian adults infected with HIV (antiretroviral naïve) and BCG vaccinated with a $CD4^+$ T cell count greater than 350 cells/mm^3 and no sign of active tuberculosis.

- Other Relevant Biological Sample Information

  Ethical approval was obtained from the Medical Research Coordination Committee of Tanzania, Institutional Review Board Committee of the Ifakara Health Institute, Tanzanian Food and Drug Authority, South African Medicines Control Council and the Human Research Ethics Committee, University of Witwatersrand. The study was conducted in accordance with the Helsinki Declaration and Good Clinical Practice Guidelines.

Environmental Samples

Not applicable.

Other Samples

Compensation beads anti-mouse Ig (BD Biosciences).

Cytometer setup and tracking beads (BD Biosciences).

1 peak beads (BD Biosciences).

Sample Characteristics

Analyzed types of cells: T_{SCM} T_{CM}, T_{EM}, T_{EMRA}, Red blood cells were lysed when treated with FACSlysing solution.

Sample Treatment Description

Before phlebotomy, 3 2ml Sarstedt tubes were filled with 0.5μg of anti-CD28 and anti-CD49d antibodies and 2 of these were filled additionally with either 5μg of H1 fusion protein or 5μg of PHA respectively. 1ml of whole blood was added to each tube, the tubes were vortexed on low and incubated at 37°C and 5% CO_2 for 7 hours. 10μg Brefeldin-A was added and the tubes were incubated in a waterbath at 37°C for the next 5 hours. The waterbath was switched off and allowed to reach room temperature. The samples were cryopreserved within maximally 10 hours. To harvest, the cells were treated with 1.8mM EDTA and transferred to tubes containing 9ml of FACSlysing solution (BD Biosciences). The white cells were pelleted and resuspended with 1ml of cryosolution containing 50% RPMI (Lonza), 40% fetal calf serum (BioWest) and 10% DMSO (Sigma Aldrich). The samples were placed in a Mr Frosty (Merck) at -80°C overnight to allow stepwise freezing. The cells were transferred to liquid nitrogen the next day. Upon finalization of all stimulations, the cells were shipped to SATVI in a dry shipper with World Courier. The dry shipper was equipped with a data logger to ensure maintenance of the desired temperature. All samples of each study day of one volunteer were stained at the same time. The cryopreserved and fixed cells were thawed in a waterbath at 37°C. They were transferred to tubes containing PBS (BioWhittaker) and washed. The cells were stained with the panel shown in section 6.1. In parallel, kappa mouse compensation beads (BD Biosciences) were stained with each antibody separately.

Table 6.1: Fluorescence Reagent Description

	Characteristic being measured	Antibody name clone name	Vendor / cat nr dilution used
Violet			
BV421	Cell surface protein	CD3 UCHT1	BD 562426 1:400
BV570	Cell surface protein	CD45-RA HI100	eBio 304131 1:400
Qdot605	Cell surface protein	CD4 S3.5	Invitrogen Q10008 1/333
Red			
Alexa Fluor 647	Intracellular protein	IL-17 SCPL1362	BD 560439 1:50
Alexa Fluor 700	Intracellular protein	IFN-γ B27	BD 557995 1:20
Blue			
FITC	Intracellular protein	IL-2 5344.111	BD 340448 1:40
PerCP-Cy5.5	Cell surface protein	CD8 SK1	BD 341050 1:333
Green			
PE	Cell surface protein	CCR7 150503	BD 560765 1:7700
PE-Cy7	Intracellular protein	TNF-α MAb11	eBio 25-7349-82 1:1670

6.1.3 Instrument Details

Instrument Manufacturer

Becton Dickinson, `www.bdbiosciences.com`

Instrument Model

BD LSR II Flow Cytometer; manufactured in August 2007 (it was upgraded to a 4 laser and 16 PMT configuration)

Instrument Configuration and Settings

The detector voltages described in Table 6.2 were taken from one representative sample. The voltages were adjusted as described in section 1.8.

Other Relevant Instrument Details

Not applicable.

6.1.4 Data Analysis Details

List-mode Data Files

FCS data file can be obtained by contacting Nicole Lenz (nicole.lenz@unibas.ch) or Claudia Daubenberger.

Compensation Details

Data from subjects were compensated in FlowJo (version 10.0.7 under Microsoft Windows 7) using the spillover matrices demonstrated in Table 6.3. This Matrix corresponds to one representative sample.

Table 6.2: Instument and Configuration Settings

Laser	PMT Detector Name	LP mirror	BP filter	Detected Parameter	Detector Voltage	Ampli-fication type
532nm Green Laser	A	740	780/40	PE-Cy7	630	Log
	B	690	695/40	PE-Cy5.5	NA	Log
	C	635	660/20	PE-Cy5	NA	Log
	D	595	610/20	TexasRed-PE	NA	Log
	E	blank	575/25	PE	460	Log
	F				NA	Log
	G				NA	Log
	H				NA	Log
640nm Red Laser	A	740	780/60	APC-Cy7	NA	Log
	B	685	710/50	Alexa Fluor700/	580	Log
	C	blank	660/20	Alexa Fluor647 APC	580	Log
405nm Violet Laser	A	670	705/70	Qdot705	NA	Log
	B	630	660/20	Qdot655	NA	Log
	C	595	605/40	Qdot605	600	Log
	D	570	585/42	Qdot585	NA	Log
	E	557	560/40	BV570/Qdot565	608	Log
	F	535	559/40	Qdot545	NA	Log
	G	505	515/20	AmCyan/BV510	NA	Log
	H	blank	450/50	BV421/PacificBlue	380	Log
488nm Blue Laser	A	550	575/25	PerCP-Cy5.5	650	Log
	B	505	525/20	FITC	500	Log
	C	488	blank	SSC	520	Linear

PMT=Photomultiplier tube, LP=long pass, BP= band pass, NA= not applicable. The first number of the BP filters describes the wavelength of the center of the interval, while the second number describes the width of the interval. The dichroic LP filters reflect at an angle of 11.25 (FSC not included in the configuration but detector voltage of 480V was used.)

Table 6.3: Spillover Matrix

	FITC A	PerCP -Cy5.5-A	BV421 A	BV570 -A	Qdot 605-A	PE -A	PE -Cy7-A	Alexa 647-A	Alexa 700-A
FITC-A	1.000	0.012	0.000	0.013	0.005	0.007	0.000	0.000	0.000
PerCP Cy5.5-A	0.000	1.000	0.000	0.000	0.000	0.000	0.065	0.084	0.194
BV421-A	0.003	0.000	1.000	0.048	0.018	0.000	0.000	0.000	0.000
BV570-A	0.001	0.027	0.084	1.000	0.970	0.322	0.008	0.011	0.006
Qdot 605-A	0.000	0.001	0.000	0.009	1.000	0.013	0.000	0.000	0.000
PE-A	0.002	0.073	0.001	0.061	0.060	1.000	0.010	0.013	0.009
PE-Cy7-A	0.000	0.011	0.000	0.001	0.001	0.025	1.000	0.000	0.001
Alexa 647-A	0.000	0.005	0.000	0.001	0.001	0.000	0.006	1.000	0.565
Alexa 700-A	0.001	0.051	0.000	0.000	0.000	0.000	0.045	0.023	1.000

Data Transformation Details

The bi-exponential transformation was used to visualize events using the default parameter settings in FlowJo (version 10.0.7 under Microsoft Windows 7).

Gating (Data Filtering) Details

Similar gating strategy was used for all data files to identify the following $CD4^+$ memory T cell populations: T_{SCM}, T_{CM}, T_{EM}, T_{EMRA} producing the following cytokines: IL-2, IFN-γ, TNF-α and IL-17. After drawing the gates to define each cell population and each cytokine producing cell on a single sample, a template in FlowJo was constructed and was applied to all following samples. Each gate of each sample was manually adjusted. Using the Boolean gating feature on FlowJo, all possible combinations of the three measured cytokines was computed.

Gate Description

CD3 positive cells were gated plotting CD3-BV421 versus SSC. The singlets were selected plotting FSC-A versus FSC-H and the lymphocytes were gated with FSC-

Table 6.4: Gate Statistics

	Parameters compared	Cell subtype	Percentage of parent
Gate 1	CD3 vs SSC-A	CD3 positive	32.1
Gate 2	FSC-A vs FSC-H	Singlets	99.0
Gate 3	FSC-A vs. SSC-A	Lymphocytes	99.6
Gate 4	Time vs FITC-A		99.9
Gate 5	Alexa Fluor 700-A vs PerCP-Cy5.5-A	CD8 negative	42.2
Gate 6	Alexa Fluor 700-A vs Qdot605-A	CD4 positive	84.0
Gate 7	PE-A vs BV570-A	T_{SCM},T_{CM}, T_{EM}, T_{EMRA}	14.5; 38.9; 46.1; 0.5
Gate 8.1	Qdot605-A vs FITC-A	IL-2 positive cells	0.66 (of T_{EM})
Gate 8.2	Qdot605-A vs Alexa Fluor 647-A	IL-17 positive cells	0 (of T_{EM})
Gate 8.3	Qdot605-A vs Alexa Fluor 700-A	IFN-γ positive cells	0.33 (of T_{EM})
Gate 8.4	Qdot605-A vs PE-Cy7-A	TNF-α positive cells	0.33 (of T_{EM})

A versus SSC-A. Time versus IL-2-FITC was gated to exclude bubbles and varying fluidics pressure. The IFN-γ-Alexa 700 versus CD8-PerCp-Cy5.5 plot was used to gate the CD8 negative cells. The CD4 positive cells were selected plotting IFN-γ-Alexa 700 versus CD4-Qdot 605. The memory subsets were defined using the CD45-RA-BV570 versus CCR7-PE plot. To identify cytokine positive cells, each cytokine was plotted against CD4-Qdot605.

Gate Statistics

The Table 6.4 shows percentages [%] of the parent population of each gate. The data is extracted from a representative sample.

Gate Boundaries

An example of the gate boundaries is given in Figure 1 of the manuscript. Gate boundaries of each individual samples can be requested.

Other relevant gate information

Not applicable.

6.2 MyFlowCyt Reporting standard for chapter 4

6.2.1 Experiment Overview

Purpose

The purpose of this experiment was to document the cytokine responses to known toll-like receptor (TLR) agonists of three major antigen presenting cells in peripheral blood and compare these among Tanzanian children with following infections: i) helminth and malaria uninfected, ii) infected with *Enterobius vermicularis* (*E. vermicularis*), iii) infected with asymptomatic *P. falciparum*-malaria and iv) co-infected with *E. vermicularis* and asymptomatic *P. falciparum*-malaria. The overall aim was to assess whether an infection with *E. vermicularis* - a strictly enteric nematode - influenced the systemic immunity and whether this effect was observed in co-infected children as well.

Keywords

Systemic Immune Response; Toll-like receptors; asymptomatic *P. falciparum*-malaria; *Enterobius vermicularis*

Experimental Variables

Within 30 minutes from phlebotomy, whole blood was stimulated with TLR agonists PAM3CSK (PAM), lipopolysaccharide (LPS) or resiquimod (R848). Expression of IFN-α2, IL-12, IL-6 and TNF-α by monocytes, conventional dendritic cells (cDC) and plasmacytoid denritic cells (pDC) was measured by flow cytometry. Tanzanian children between 2 and 9 years of age with aforementioned infections were enrolled in the study.

Organization

Name

Swiss Tropical and Public Health Institute, University of Basel, Switzerland.

Bagamoyo Reasearch and Training Center, Ifakara Health Institute, Tanzania.

Address

Socinstrasse 57, 4051 Basel, Switzerland

Bagamoyo Dsitrict Hospital, PO Box 74, Bagamoyo, Tanzania

Primary Contact

Name: Claudia Daubenberger

Email: claudia.daubenberger@unibas.ch

Date

Phlebotomy and TLR stimulations were performed between the 13th of October 2011 and 18th of July 2013. The flow cytometry analyses were conducted between the 29th of April and 20th of December 2013.

Conclusions

Lower expression of IL-6 and TNF-α is observed in monocytes and cDC from children infected with *E. vermicularis*, asymptomatic *P. falciparum*-malaria or both.

Quality Control Measures

To standardize voltage settings across all samples, optimal application settings were defined at the beginning of the analysis and was applied in each experiment after

automatic voltage optimization using the cytometer setup and tracking beads. A biological standard was included in all experiments to track cytometer performance.

Other Relevant Experiment Information

Not applicable.

6.2.2 Flow Sample/Specimen Description

Sample/Specimen Material Description

Biological Samples

- Biological Sample Description

  Blood was withdrawn via sterile venipuncture into lithium-heparin vacutainers (Greiner Bio One; catalog no. 454082). Red blood cells were lysed and the white blood cells were stored as described by Blimkie et al, Journal of Immunological Methods, 2011.

- Biological Sample Source Description

  Human peripheral blood.

- Biological Sample Source Organism Description

  Tanzanian children between 2 and 9 years of age.

- Other Relevant Biological Sample Information

  Ethical approval was obtained from the Ethikkomission beider Basel (EKBB; Basel, Switzerland; reference number: 257/08) and the National Institution for Medical Research of Tanzania (NIMR; Dar es Salaam, United Republic of Tanzania; reference number NIMR/HQ/R.8a/Vol.IX/1098). Parents or legal guardians of all subjects gave informed consent.

Environmental Samples

Not applicable.

Other Samples

Compensation beads anti-mouse Ig and anti-rat ig (BD catalog no. 552843 and 552844 respectively). Cytometer setup and tracking beads (BD catalog no. 642412).

Sample Characteristics

Analyzed types of cells: monocytes, cDC, pDC. Red blood cells were lysed when samples were frozen in FACSLyse solution.

Sample Treatment Description

For this study the following TLR ligands were used at specifed concentrations: PAM3CSK4 (PAM; TLR1/2; EMC Microcollections) at 1μg/ml, Lipopolysaccharide (LPS; TLR4; InvivoGen) at 100ng/ml, resiquimod (R848; TLR7/8, InvivoGen) at 100μM and phytohemagglutinin (PHA, positive control, Oxoid) at 10 μg/ml. Whole blood was diluted 1:1 in sterile, pre-warmed RPMI 1640 (Gibco) and was incubated with the TLR agonists for 6h with Brefeldin-A at 10 μg/ml, Sigma-Aldrich. The cells were detached by adding EDTA at a concentration of 2mM and incubated for 10min. The cells were lysed in 1.4ml of FACSlysing solution (BD) and stored at -80°C. For the antibody staining the cells were thawed in a water-bath at 37°C for approximately 5min and spun down. They were washed twice in PBSAN (PBS (GIBCO) with 0.1% sodium azide (Sigma-Aldrich) and 1% bovine serum albumin). The cells were permeabilized in FACSPerm (BD) and incubated for 10min. They were washed three times and resuspended in the antibody mix (detailed description in section 6.5). The cells were incubated at room temperature for 45min. They were washed three times in PBSAN and transferred to FACS

Table 6.5: Fluorescence Reagent Description

	Characteristic being measured	Antibody name clone name	Vendor / cat nr dilution used
Violet			
eF450	Intracellular protein	IL-12 C8.6	eBio 48-7129-42 1:100
V500	Cell surface protein	CD14 M5E2	BD 561391 1:100
eF605	Cell surface protein	HLA-DR LN3	eBio 93-9956-42 1:100
Red			
APC	Cell surface protein	CD11c S-HCL-3	BD 340544 1:50
Alexa Fluor 700	Intracellular protein	TNF-α MAb11	BD 557996 1:100
Blue			
FITC	Intracellular protein	IL-6 MQ2-13A5	BD 554696 1:100
PE	Intracellular protein	IFN-α2 7N4-1	BD 560097 1:100
PE-Cy7	Cell surface protein	CD123 6H6	eBio 25-1239-42 1:100

round bottom tubes (BD) for immediately analysis by flow cytometry.

6.2.3 Instrument Details

Instrument Manufacturer

Beckton Dickinson `www.bdbiosciences.com`

Instrument Model

BD LSR Fortessa flow Cytometer; manufactured January 2011.

Table 6.6: Instument Configuration and Settings

Laser	PMT Detector Name	LP mirror	BP filter	Detected Parameter	Detector Voltage	Amplification Type
488nm Blue Laser	FSC	NA	488/10	FSC	368	linear
	A	750	780/60	PE-Cy7	584	Log
	B	685	695/40	PerCP-Cy5.5	NA	Log
	C	655	670/30	PE-Cy5	NA	Log
	D	600	610/20	PE-Texas Red	NA	Log
	E	550	575/26	PE	500	Log
	F	505	530/30	FITC	411	Log
	G	blank	488/10	SSC	232	Linear
640nm Red Laser	A	750	780/60	APC-Cy7	NA	Log
	B	710	730/45	Alexa Fluor700	503	Log
	C	blank	670/14	APC	528	Log
405nm Violet Laser	A	595	605/12	eF605	420	Log
	B	475	525/50	V500	449	Log
	C	blank	450/50	eF450	383	Log

PMT=Photomultiplier tube, LP=long pass, BP= band pass, NA= not applicable. The first number of the BP filters describes the wavelength of the center of the interval, while the second number describes the width of the interval. The dichroic LP filters reflect at an angle of 11.25.

Table 6.7: Spillover Matrix

	FITC -A	PE -A	PE -Cy7-A	APC -A	Alexa Fluor 700-A	V450 -A	V500 -A	Qdot 605-A
FITC-A	1.000	0.091	0.002	0.000	0.000	0.000	0.030	0.002
PE-A	0.018	1.000	0.022	0.000	0.000	0.000	0.004	0.066
PE-Cy7-A	0.001	0.009	1.000	0.000	0.003	0.000	0.000	0.001
APC-A	0.000	0.000	0.001	1.000	0.120	0.000	0.000	0.000
Alexa Fluor 700-A	0.001	0.000	0.016	0.059	1.000	0.001	0.001	0.000
V450-A	0.000	0.000	0.000	0.000	0.000	1.000	0.106	0.004
V500-A	0.038	0.005	0.000	0.000	0.000	0.129	1.000	0.111
Qdot 605-A	0.000	0.031	0.000	0.004	0.000	0.001	0.001	1.000

Instrument Configuration and Settings

The detector voltages described in Table 6.6 were taken from one representative sample. The voltages were adjusted as described in section 6.2.1. After purchasing the instrument, alterations were only performed by trained BD engineers. The LSR Fortessa came with the blue and red laser and stated mirrors and filters and was later on equipped with the violet laser and stated mirrors and filters.

Other Relevant Instrument Details

Not applicable.

6.2.4 Data Analysis Details

List-mode Data Files

FCS data file can be obtained by contacting Nicole Lenz (nicole.lenz@unibas.ch) or Claudia Daubenberger.

Compensation Details

Data from subjects were compensated in FlowJo (version 10.0.7 using Microsoft Windows 7) with the spillover matrices demonstrated in Table 6.7. This Matrix corresponds to one representative subject.

Data Transformation Details

The bi-exponential transformation was used to visualize events using the default parameter settings in FlowJo (version 10.0.7 using Microsoft Windows 7).

Gating (Data Filtering) Details

Similar gating strategy was used for all the data files to identify the following antigen-presenting cell populations: Monocytes, cDC and pDC and production of the following cytokines: IFN-α2, IL-6, Il-12 and TNF-α. After drawing the gates to define each cell population and each cytokine producing cell on a single sample, a template in FlowJo was constructed that was applied to all following samples. Each gate of each sample was manually adjusted. Using the Boolean gating feature in FlowJo, all possible combinations of the four measured cytokines were computed.

Gate Description

After gating on the time parameter, the singlets were gated in the FSC-A vs. FSC-H plot. Eventual bead contamination were excluded by plotting FSC-A vs. FITC. White bloods cells were gated using the FSC-A vs. SSC-A plot. The CD123 vs. HLA-DR plot was used to identifiy HLA-DR+ cells, which were further divided into CD123high and CD123neg-low . HLA-DR+ and CD123- were further divided in monocytes and cDC using the CD11c vs. CD14 plot. Monocytes were defined as CD14high and cDC were defined as CD11chigh and CD14neg-low. The pDC were extracted by negatively gating the HLA-DR+ and CD123+ in a CD14 vs. CD11c

Table 6.8: Gate Statistics

	Parameters compared	Cell subtype	Percentage of parent
Gate 1	Time vs. Alexa Fluor 700		98.60%
Gate 2	FSC-A vs FSC-H	Singlets	90.30%
Gate 3	FSC-A vs. FITC	Bead exclusion	100%
Gate 4	FSC-A vs. SSC-A	white blood cells	93.30%
Gate 4.1	Qdot605 vs. PE-Cy7	'pre'pDC	0.26%
Gate 4.2	Qdot605 vs. PE-Cy7	'pre' Monocytes and 'pre' cDC	15%
Gate 5.1	APC vs. V500	Monocytes	45%
Gate 5.2	APC vs. V500	cDC	4.49%
Gate 5.3	APC vs. V500	pDC	94.10%
Gate 6	PE	IFN-α2 producing cDC	1.84%
Gate 7	FITC	IL-6 producing cDC	53.40%
Gate 8	V450	IL-12 producing cDC	21.60%
Gate 9	Alexa Fluor700	TNF-α producing cDC	82.90%

plot.

Gate Statistics

Table 6.8 shows percentages [%] of the parent population of each gate. The data is extracted from a representative sample.

Gate Boundaries

An example of the gate boundaries can be found in Figure 6.1. Gate boundaries of each individual samples can be requested.

Other relevant gate information

Not applicable.

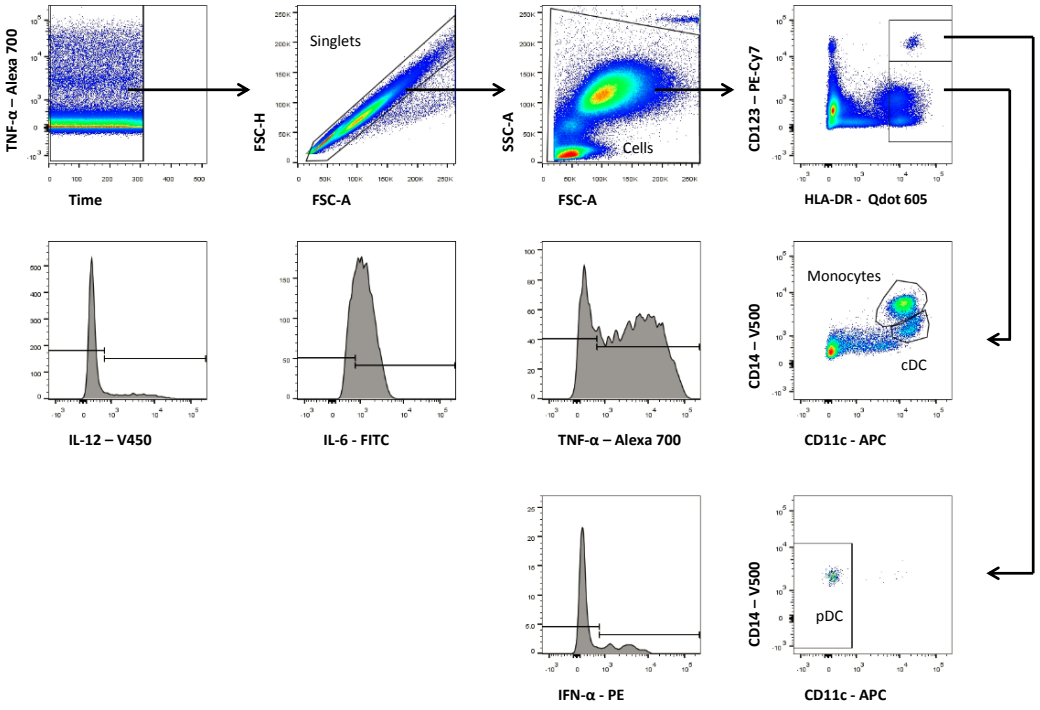

Figure 6.1: Gating strategy of one representative sample stimulated with TLR-7/8 agonist R848.

Acknowledgments

I owe deepest gratitude to

... my supervisor Claudia Daubenberger for giving me this absolutely amazing opportunity and for sharing her ideas and listening to mine.

... my co-refree Ulrich Certa for making a lot of experiments possible.

... Marcel Tanner for his great support and willingness to evaluate my thesis.

... Hermelijn Smits for being my external expert.

... the entire immuno-team with a special thanks to Max for forcing me to speak swahili although his german was terrible, Tedson and Anneth for their help with labwork, Damien for always asking the right questions, to Julian for his help with the flow and his willingness to go for a beer after work and to Tobi for a great time and making paper-writing easier.

... all my friends for always being there and listening

... my family for not really knowing what I was doing but just caring for when I was coming back.

... Elvis Ajuh for his great support.

... Marta Maia for feeding me.

Curriculum vitae

Personal Data

Name:	Nicole Lenz
Date of birth:	25th of April, 1986
Place of birth:	Olten SO
Place of citizenship:	Uesslingen-Buch TG
Current Address:	Pestalozzistrasse 17, 4600 Olten

Education

Jan. 2011 - Feb. 2015:	PhD in medical-biological research
	University of Basel
	Supervisor: PD Dr. Claudia Daubenberger
Sept. 2008 - Feb. 2010:	Master of Infection Biology and Epidemiology
	University of Basel
	Supervisor: PD Dr. Claudia Daubenberger
Sep. 2005 - Sep. 2008:	Bachelor of Integrative Biology
	University of Basel
Aug. 1998 - Sept. 2005:	Grammar school Olten SO
	Higher education entrance qualification
	Main subject: classical languages